

AN ABSTRACT OF THE THESIS OF

Charles William Payne for the degree of Master of Science in Geology presented on March 9, 1998. Title: Lithofacies, Stratigraphy, and Geology of the Middle Eocene Type Cowlitz Formation and Associated Volcanic and Sedimentary Units, Eastern Willapa Hills, Southwest Washington.

Abstract approved: _____
Signature redacted for privacy.

Alan R. Niem

Stratigraphic measurement of the 1,238-m thick Cowlitz Formation in the southwest Washington type section along Olequa and Stillwater creeks reveals complex facies succession of wave- to tide-dominated deltaic sequences. The underlying, 625-m thick upper member of the McIntosh Formation (as mapped by Wells, 1981) is composed of two units: a basal 130-m thick prograding offshore to marginal marine coal-bearing, lithic-arkosic sandstone facies succession (upper McIntosh sandstone) and a thicker, 500-m thick bathyal foraminifera-rich siltstone facies that is, in part, in fault contact with the overlying Cowlitz Formation. The lower member of the McIntosh Formation is 375 m thick in Stillwater Creek, with the base not exposed in the study area.

The Cowlitz Formation is subdivided into five informal units. The basal 558-m thick unit consists of (1) multiple prograding, wave-dominated shoreface hummocky stratified lithic arkosic sandstone successions (unit 1A) that comprise several thickening- and coarsening-upwards parasequences and (2) coal-bearing delta plain facies associations (unit 1B). The 205-m thick second unit is composed of five coarsening-up storm-dominated, hummocky-bedded shelf to delta-front arkosic sandstone parasequences. Fining-upwards subtidal, intertidal, and supratidal facies associations constitute the 170-m

thick third member. Tidal-estuarine facies in unit 3 include: (1) nested subtidal micaceous lithic-arkosic sandstone channels, (2) cross-bedded subtidal sandstone ridges with brackish water mollusc hash, (3) sandy and muddy accretionary-bank, and (4) coal-bearing marsh-swamp deposits. Thin basaltic volcanoclastic interbeds occur within units one, two, and three. A 155-m thick fourth unit, consists of wave-dominated, arkosic sandstone, shoreface to offshore bioturbated mudstone facies successions; these successions form 10 coarsening-upward parasequences that overall define a retrogradational parasequence set. Thick, transgressive, bioturbated outer shelfal mollusc-bearing sandy siltstone and glauconitic mudstone in the Big Bend type locality along the Cowlitz River can be correlated to this unit in the type section in Olequa Creek. The uppermost unit consists of 150 m of deeper marine laminated siltstone, subordinate fine-grained and thin-bedded turbidites, thick amalgamated submarine-channel sandstone and chaotic mudstone conglomerate, and slump-folded and soft-sediment deformed laminated siltstone intervals.

Petrography of lithic-arkosic micaceous sandstones of the McIntosh and Cowlitz formations indicates there was a distant eastern, extrabasinal acid plutonic-metamorphic source for the arkosic component of these sandstones. The predominant quartz, feldspar, and mica constituents of Cowlitz Formation were transported from a distant dissected arc (such as the Idaho Batholith and metamorphic core complexes to the east) through an ancestral Columbia River drainage system. A second, local and active intrabasinal basaltic source (Grays River volcanics) supplied basaltic scoria and lava rock fragments to form volcanoclastic interbeds. Some volcanoclastics were reworked and mixed with the arkosic extrabasinal sediments in the shallow marine and nonmarine environments of units 2 and 3 of the Cowlitz Formation. Explosive calc-alkaline volcanic activity (Northcraft Formation or Goble Volcanics) is also evident in the silicic and pumiceous tuff beds interbedded with coal marsh/swamp strata in units 1 and 3. Paleocurrent directions indicated by cross-

bedded tidal strata of unit 3 are to the north-northwest and south-southeast as a result of shore parallel transport and deflection around a proposed growing volcanic edifice of Grays River volcanics to the south and southwest. A very high sedimentation rate of 1.6 m/1,000 years was calculated for the upper part of the Cowlitz Formation (units 3 to 5) using thickness measurement and $^{39}\text{Ar}/^{40}\text{Ar}$ age dates from the Cowlitz Formation (i. e., from tuff in unit 3) and the easternmost locality in the unconformably overlying Grays River volcanics at Bebe Mountain. The large influx of sediment deposited over a relatively short time period was accommodated by this rapidly subsiding forearc basin.

In this study area, subaerial flows of the Grays River volcanics locally unconformably overlie the Cowlitz Formation. A 38.9 ± 0.1 Ma $^{39}\text{Ar}/^{40}\text{Ar}$ age date from a tuff bed in unit 3 of the underlying Cowlitz Formation (Irving et al., 1996) and three $^{39}\text{Ar}/^{40}\text{Ar}$ age dates of 38.64 ± 0.40 (south Abernathy Mtn.), 37.44 ± 0.45 (west Bebe Mtn.), and 36.85 ± 0.46 Ma (east Bebe Mtn.) from the overlying Grays River volcanics bracket the timing of this regional unconformity. Additionally, field mapping (this study) and drill hole data supplied by Weyerhaeuser Company (Pauli, written communications) show there is a valley-fill unit at the base of the Grays River volcanics exposed on the surface and in the subsurface, respectively. These data confirm the volcanic- and tectonically-controlled unconformable relationship of the Cowlitz Formation to the overlying the Grays River volcanics.

The Cowlitz Formation is in disconformable contact (a tectonically forced sequence boundary) with an overlying second, younger lowstand valley-fill unit (Toutle Formation unit A) recognized in this study along Olequa Creek. The 265-m thick, newly discovered, Toutle Formation in this area is subdivided into three informal units: (1) a basal incised, non-marine valley-fill sequence (unit A), (2) a marginal marine (estuarine or nearshore) sequence (unit B), and (3) an upper fluvial sequence (unit C). A 31.9 ± 0.4 Ma $^{39}\text{Ar}/^{40}\text{Ar}$ date from a hornblende-bearing pumiceous lapilli tuff in unit A indicates that

the Toutle Formation is a time equivalent of the upper fluvial member of the Oligocene type Toutle Formation and the middle part of the Lincoln Creek Formation far from the center of the forearc basin to the west. Unit C of the Toutle Formation grades upward into the overlying deeper marine tuffaceous siltstone of the Lincoln Creek Formation.

Deformation in this area resulted from two plate tectonic events: (1) latest middle Eocene highly oblique subduction that resulted in short-lived, normal faulting and intrusion of Grays River basalt dikes along small faults and (2) rapid post mid-Miocene oblique subduction that formed northeast-trending dextral and northwest-trending sinistral conjugate faults and broad regional compressional folding throughout southwest Washington. The broad open Arkansas anticline that trends northwest-southeast between Bebe and Abernathy mountains is an eastward extension of the Willapa Hills basement uplift to the west and is extensively cut by northeast and northwest trending faults (Plate I). This compressional event deformed both the Cowlitz Formation and the overlying Grays River volcanics. A similar structural pattern recognized in regional field mapping by Wells (1981) indicates this folding event also deformed mid-Miocene volcanic and sedimentary unit (i.e., Astoria Formation and Columbia River basalts).

Reservoir quality of the Cowlitz and upper McIntosh formations micaceous lithic-arkosic sandstones is good. These sandstones are clean, highly friable and porous except where carbonate and smectite clay rim cements formed in the lithic arkose. Unit 5 siltstone could act as a cap rock in the subsurface and the 1- to 10-m thick coals could be a source for natural gas. The McIntosh marine siltstone is another possible source for gas and the micaceous arkosic sandstone in the upper McIntosh is a potential reservoir. Stratigraphic pinchouts and normal and wrench fault traps are similar to the Mist gas field of northwest Oregon.

© Copyright by Charles William Payne

March 9, 1998

All Rights Reserved

Lithofacies, Stratigraphy, and Geology of the Middle Eocene Type Cowlitz Formation and
Associated Volcanic and Sedimentary Units, Eastern Willapa Hills, Southwest
Washington

by

Charles William Payne

A THESIS

submitted to

Oregon State University

in partial fulfillment of
the requirements for the
degree of

Master of Science

Completed March 9, 1998
Commencement June 1998

ACKNOWLEDGMENT

This thesis was made possible through generous grants from Weyerhaeuser Corporation and the Chevron Company. Additional funding was provided through a teaching assistantship in the Department of Geosciences, Oregon State University.

Dr. Alan Niem, my major professor, provided much encouragement through the many months spent in the field and during laboratory analysis. Many hours spent discussing the geologic relationships of southwestern Washington to that of northwest Oregon is greatly appreciated by this author. Time spent by Dr. Alan Niem, committee members Dr. Robert Yeats and Dr. Reed Glasmann, and Wendy Niem reviewing my thesis greatly improved the quality of this work.

I would like to extend special thanks to Peter Hales and Dave Pauli of Weyerhaeuser Co. for initial guidance, invaluable information, and discussion about the subsurface relationships in this area. Both Dr. Ray Wells and Dr. Samuel Johnson of the U. S. Geological Survey and Dr. Timothy Walsh of the Washington State Department of Natural Resources provided invaluable information and guidance during the initiation of this study.

Additionally, thanks are offered to Dr. Kristin McDougall of the U. S. Geological Survey who provided foraminiferal analysis of mudstones from samples collected throughout the measured sections of the McIntosh and Cowlitz formations. Macrofaunal samples identified by Dr. Elizabeth Nesbitt of the University of Washington's Thomas Burke Museum, Geology and Paleontology Division added greatly to the interpretation of the depositional environments of these sedimentary deposits. Grays River volcanics geochemical data supplied by Dr. Russell Evarts and Dr. Roger Ashley of the U. S. Geological Survey and many hours discussing the stratigraphy of the lower Cascade volcanic sequences are greatly appreciated. Dr. Paul Hammond of Portland State University analyzed numerous tuff samples collected from the Cowlitz measured section.

Former graduate students and friends of the Cowlitz, Christina Robertson of Oregon State University and Steve Kenitz of Portland State University added greatly to this effort in unraveling the complex Eocene geology of southwest Washington and northwest Oregon.

Also, I am thankful for having my trailer home and office at Volcano View, Washington and my natural friends in the field: bear, porcupine, beaver, elk, and stream. Finally, a loving acknowledgment of my parents Bill and Mary without whom I could not have lived out my dreams to be a scientist and scholar.

TABLE OF CONTENTS

	<u>Page</u>
INTRODUCTION.....	1
OBJECTIVES OF THIS INVESTIGATION.....	3
LOCATION AND ACCESS.....	3
GEOLOGIC SETTING.....	5
METHODS OF INVESTIGATION.....	9
STRATIGRAPHY AND LITHOFACIES OF THE MCINTOSH, COWLITZ, TOUTLE, AND LINCOLN CREEK FORMATIONS.....	12
NOMENCLATURE AND CORRELATION	12
AGE DETERMINATION.....	16
MCINTOSH FORMATION	20
Outcrop Distribution and Thickness.....	20
Lithofacies and Contact Relationships	22
Lower McIntosh Formation	22
Upper McIntosh Formation-Sandstone Unit.....	25
Upper McIntosh Formation-Siltstone Unit.....	29
Depositional Environments.....	32
Lower McIntosh Formation	32
Upper McIntosh Formation-Sandstone Unit.....	35
Upper McIntosh Formation-Siltstone Unit.....	37
COWLITZ FORMATION.....	39
Introduction	39
Outcrop Distribution and Thickness.....	42
Lithostratigraphy and Contact Relationships	45

TABLE OF CONTENTS (Continued)

	<u>Page</u>
Unit 1A: Lower Marine Sandstone Sequences.....	45
Unit 1B: Lower Coal-Rich Heterolithic Facies Associations...	51
Unit 2: Middle Marine Mudstone and Sandstone Sequences...	57
Unit 3: Upper Coal-Rich Tidal Facies Associations.....	67
Unit 4: Upper Shallow Marine Lithofacies Succession.	80
Unit 5: Planar-Laminated Deep Marine Siltstone	85
 Depositional Environments.....	 90
Unit 1: Prograding Shoreface and Delta/Coastal Plain	90
Unit 2: Middle Marine Shelf and Delta-Front	97
Unit 3: Upper Tide-Dominated Coal-Bearing Delta Plain....	102
Unit 4: Upper Transgressive Shallow Marine Succession....	111
Unit 5: Lowstand Prodelta Siltstone.....	114
 TOUTLE AND LINCOLN CREEK FORMATIONS.....	 119
 Outcrop Distribution and Thickness.....	 123
 Contact relationships and Lithology.....	 123
Toutle Formation	123
Tuffaceous Siltstone Member of the Lincoln Creek Formation.....	129
 Depositional Environments.....	 130
Toutle Formation.....	130
Tuffaceous Siltstone Member of the Lincoln Creek Formation.....	136
 SEQUENCE STRATIGRAPHY OF THE COWLITZ FORMATION AND ASSOCIATED UNITS	 137
 SEDIMENTARY PETROLOGY AND VOLCANICLASTIC GEOCHEMISTRY OF THE MCINTOSH, COWLITZ, AND TOUTLE FORMATIONS.....	 146
 INTRODUCTION.....	 146
 ARKOSIC-LITHIC SANDSTONES OF THE MCINTOSH AND COWLITZ FORMATIONS	 147

TABLE OF CONTENTS (Continued)

	<u>Page</u>
VOLCANIC SANDSTONE OF THE COWLITZ FORMATION.....	155
SANDSTONE OF THE TOUTLE FORMATION	161
GEOCHEMISTRY OF TUFF BEDS FROM THE COWLITZ AND TOUTLE FORMATIONS.....	163
SUMMARY.....	167
STRATIGRAPHY, PETROLOGY, AND GEOCHEMISTRY OF THE GRAYS RIVER VOLCANICS AND UNDERLYING GRAYS RIVER SEDIMENTARY SEQUENCE.....	171
NOMENCLATURE AND CORRELATION	171
AGE DETERMINATION.....	174
MAGNETIC POLARITY	177
GRAYS RIVER SEDIMENTARY SEQUENCE UNDERLYING THE GRAYS RIVER VOLCANICS.....	178
GRAYS RIVER VOLCANIC STRATIGRAPHY	181
IGNEOUS GEOCHEMISTRY AND PETROLOGY.....	188
MIDDLE EOCENE TO OLIGOCENE REGIONAL CORRELATION AND STRATIGRAPHIC RELATIONSHIPS IN SOUTHWEST WASHINGTON AND NORTHWEST OREGON.....	199
STRUCTURAL GEOLOGY.....	207
REGIONAL STRUCTURE.....	207
LOCAL STRUCTURE.....	208
SUMMARY.....	211
OIL AND GAS POTENTIAL.....	213

TABLE OF CONTENTS (Continued)

	<u>Page</u>
GEOLOGIC HISTORY	216
CONCLUSIONS.....	221
REFERENCES	228
APPENDICES.....	235
APPENDIX I: FORAMINIFERA IDENTIFICATION.....	236
APPENDIX II: MACROFAUNAL IDENTIFICATION	243
APPENDIX III: POINT COUNT DATA.....	246
APPENDIX IV: TUFF GEOCHEMISTRY.....	247
APPENDIX V: GRAYS RIVER GEOCHEMISTRY.....	249
APPENDIX VI: $^{39}\text{Ar}/^{40}\text{Ar}$ AGE DATES.....	250

LIST OF FIGURES

<u>Figure</u>	<u>Page</u>
1. Location of thesis study area, southwest Washington.....	4
2. Regional geologic map of Eocene and Oligocene sedimentary and volcanic units of southwestern Washington and northwestern Oregon (slightly modified from Walsh et al., 1987 and Robertson, 1997).....	6
3. Regional stratigraphic correlation chart for southwest Washington and northwest Oregon	7
4. Lower McIntosh Formation mudstone in Stillwater Creek (section location 3D; NW 1/4, Sec. 4, T10N, R3W; Plate II).....	23
5. Composite stratigraphic section of the lower part of the upper McIntosh Formation sandstone (section locations 2E to 3D2; NW 1/4, Sec. 4, T10N, R3W; Plates I and II).....	26
6. Coal bed in the basal sandstone unit of the upper McIntosh Formation, Stillwater Creek location 3E (NW 1/4, SE 1/4, Sec. 4, T10N, R3W, Plates I and II).....	27
7. Parallel-laminated and swaley to hummocky cross-stratified, micaceous, lithic arkose of the upper McIntosh sandstone exposed along Owens Creek (location 135L; NW 1/4, Sec. 33, T3N, R3W; Plate I)	30
8. Onshore-offshore profile of depositional environments and lateral ichnofacies of the McIntosh Formation and normal marine units of the Cowlitz Formation (slightly modified from Berkman, 1990 and Robertson, 1997).....	34
9. General stratigraphic column of the middle Eocene type Cowlitz Formation, southwest Washington	41
10. Measured-section correlation diagram for units 2 and 3 of the Cowlitz Formation showing marker beds used to construct the upper, middle, and lower Olequa Creek compilation sections (Plate III) and the master composite stratigraphic column (Plate II)	43
11. The prograding wave-dominated shoreface succession of the basal part of the Cowlitz Formation unit 1A exposed in Stillwater Creek at location 6H (interval 0 to 42 m, Plates I and II)	47

LIST OF FIGURES (Continued)

<u>Figure</u>	<u>Page</u>
12. Facies of the basal part the Cowlitz Formation unit 1A: (A) hummocky cross-stratified lower shoreface sandstone and siltstone (lithofacies 1b) and (B) bioturbated shelfal siltstone (lithofacies 1a) with burrows of the <i>Cruziana</i> ichnofacies (location 6H; SW 1/4, Sec. 26, T11N, R3W; Plates I and II).....	48
13. Micaceous, arkosic sandstone-dominated facies of the upper shoreface (lithofacies 1d) and the lowest coal-bearing heterolithic facies association (lithofacies 1f to 1h) of unit 1A of the Cowlitz Formation (locations 7B and 7C; SE 1/4, NW 1/4, Sec 26, T11N, R3W, Plates I and II).....	50
14. Highly fossiliferous, silty sandstone of lithofacies 1j (subtidal channel-bar) from unit 1B.	53
15. Stratigraphic column of the subtidal- to supratidal-flat facies associations that include: a heterolithic facies association, tidal-channel sandstone, coal, and volcanoclastic beds (lithofacies 1f, 1h, 1i, and 1j) from the uppermost 30 m of unit 1 of the Eocene Cowlitz Formation (measured section 8C, Plate II; NE 1/4, Sec 25, T11N, R3W).....	56
16. (A) Silty sandstone (lithofacies 2a) from the lower part of unit 2 of the Cowlitz Formation containing <i>Thalassinoides</i> burrows of the <i>Skolithos</i> ichnofacies at location 9E and (B) fossiliferous, volcanic sandstone bed (lithofacies 2a) from section 9C (Plate II).....	60
17. Mudstone facies succession and a normally graded, medium- to coarse-grained, framework-supported, altered volcanic sandstone from the uppermost part of unit 2 of the Cowlitz Formation (measured section O10, Plate II; NW 1/4, Sec. 29, T11N, R2W, Plate I).....	65
18. Unique characteristics of clastic tidal deposits recording tide fluctuating cycles: (A) tidal bundle sequences (schematic) and (B) vertically stacked, thinly laminated tidal rhythmites (from the recent Mont Saint-Michel Bay, France) (after Yang and Nio, 1985)	69
19. Tidal megaripple cross-bedding in the lower part of Cowlitz Formation unit 3 (section location O16, SW 1/4, Sec. 17, T11N, R2W, Plates I and II)	70
20. (A) Field sketch of tidal megaripple cross-bedded arkosic sandstone of a subtidal channel with mud-draped tidal bundle sequences bounded by wavy reactivation surfaces and (B) rose diagram of paleocurrent orientation measurements of cross-bedded tidal sandstone foresets at this location (measured section O16 in Olequa Creek, Plate II; SW 1/4, Sec. 17, T11N, R2W, Plate I)	71

LIST OF FIGURES (Continued)

<u>Figure</u>	<u>Page</u>
21. Field sketch of the cross-bedded nested subtidal channel sandstone lithofacies association at lower Olequa Creek section location 11E (SE 1/4, Sec. 32, T11N, R2W; Plates I and II)	73
22. Volcaniclastic lithofacies (3a) from coal seam A and subtidal sandstone ridge lithofacies (3c) from unit 3 (Plates III).....	75
23. Two fossiliferous intervals in unit 3 of the Cowlitz Formation (Plate III)	77
24 Stratigraphic section of the 7.5 m-thick upper coal bed in unit 3 of the Cowlitz Formation (coal seam C)	79
25. (A) Fossiliferous, shallow marine, silty sandstone with multiple shell lags (macrofaunal sample CP-95-177, 1/4 SW, 1/4 NE, Sec. 8, T11N, R2W; Plates I and II)	82
26. Massive, fine- to medium-grained channelized, micaceous, arkosic sandstone that contains cobble-sized angular mudstone rip-ups (lithofacies 5b) in unit 5 section O33 in Olequa Creek (1/4 SW, Sec. 8, T11N, R2W; Plate I).....	86
27. (A) Laminated siltstone and micro-cross-laminated sandstone and siltstone (Bouma turbidite Tcd) of unit 5 and (B) soft sediment deformed siltstone and sandstone (measured section O36; 1/4, T11N, R2W; Plates I and II).....	88
28. Paleogeography of unit 1A and B of the Cowlitz Formation showing depositional environments and the prograding Cowlitz delta.	92
29. Paleogeographic reconstruction of the tidal estuary of unit 3 showing depositional environments and relationship to underlying marine unit 2.	104
30. Paleogeographic reconstruction of the uppermost Cowlitz Formation unit 5 showing depositional environments of this deep marine prodelta sequence.....	116
31. Stratigraphic cross section showing unconformable contact relationship of the Cowlitz Formation with the overlying valley-fill Toutle Formation (from Dave Pauli, written communications, 1997)	120
32. Regional correlation of the type Toutle Formation fluvial unit and the Toutle fluvial unit A in Olequa Creek	121

LIST OF FIGURES (Continued)

<u>Figure</u>	<u>Page</u>
33. (A) Unconformable contact of the Toutle Formation (valley-fill unit A) with the underlying deep marine siltstone of the Cowlitz Formation unit 5 in Olequa Creek (top of section O37; 1/SE, Sec. 5, T11N. R2W; Plates I and II).....	125
34. Paleogeographic reconstruction of the Toutle and Lincoln Creek formations showing depositional environments and unconformable stratigraphic relationship with the underlying Cowlitz Formation	132
35. Sequence stratigraphy and local water depths of the McIntosh, Cowlitz, and Toutle formations compared to world wide eustatic sea level curves of Haq et al. (1987)	139
36. QFL ternary classification diagram (after Folk, 1974) (upper diagram) and more detailed framework grain composition bar graph (lower diagram) of the McIntosh, Cowlitz and Toutle sandstones in the study area	148
37. Photomicrograph of micaceous, lithic arkose from the upper McIntosh Formation sandstone (sample CP-94-86d2, Plates I and II)	150
38. Photomicrograph of the micaceous, lithic-arkosic sandstone of unit 1A of the Cowlitz Formation (CP-94-108, Plates I and II).	151
39. X-ray diffraction pattern and scanning electron (SEM) photograph of sample CP-94-105 from the upper shoreface lithic-arkosic sandstone of unit 1 of the Cowlitz Formation (Plates I and II)	154
40. Photomicrograph of shallow marine basaltic sandstone (sample CP-94-121) from the epiclastic (lithofacies 2a) storm-dominated middle to inner shelf sequence in unit 2	157
41. X-ray diffraction pattern and scanning electron (SEM) photograph of sample CP-95-186b from the upper fluvial sandstone unit of the Toutle Formation (Plates I and II)	164
42. Tuffs of the Cowlitz, Toutle, and Lincoln Creek formations and the Grays River volcanics from the thesis area plotted on a total alkali vs. SiO ₂ (TAS) diagram....	165
43. Paragenetic sequence of the diagenetic events in outcrop sample of sandstones in the McIntosh and Cowlitz formations.....	168

LIST OF FIGURES (Continued)

<u>Figure</u>	<u>Page</u>
44. Residual wavelength-filtered gravity anomaly map and volcanic geology map superimposed to show relationship of shallow crustal features with mapped surface volcanic units	172
45. Magnetic polarity chart and volcanic age dates of the Grays River volcanics.....	176
46. Stratigraphic and structural cross-sections from the Arkansas Creek area	179
47. (A) Subaerial, columnar-jointed, basalt flow of the Grays River volcanics and (B) interbedded carbonaceous shale, finely laminated siltstone, and thin tuff beds from a quarry east of the Cowlitz River (1/4 SE, Sec. 16, T10, R2W; Plate I)....	182
48. (A) Basalts of the Grays River volcanics from the thesis area plotted on a total alkali vs. SiO ₂ (TAS) diagram. (B) Iron enrichment diagram of part of the Grays River volcanics (CP-95-196, Plate I)	190
49. Photomicrograph of porphyritic olivine tholeiitic basalt flow from lower part of the Grays River volcanics (CP-95-196, Plate I)	192
50. Photomicrograph of plagioclase glomerophyric basalt from a Grays River dike to the west of Bebe Mountain (CP-95-198, Plate I).....	194
51. Photomicrograph of subaerial Gray River basalt displaying pilotaxitic flow texture (sample CP-94-138, Ar ³⁹ /Ar ⁴⁰ age dated at 36.8 Ma, Plate I) from the upper flows of the Grays River volcanics.....	196
52. Correlation diagram of the Eocene Cowlitz Formation units and bounding formations between northwest Oregon and southwest Washington (from Robertson, 1997 and this study).....	200
53. Two hypotheses for the unconformable relationship between the Cowlitz Formation and the Gray River volcanics and between the Cowlitz and Toutle formations in the Bebe Mountain area and in Olequa Creek.....	206

LIST OF PLATES

Plate

- I: Geologic Map of the Eocene Type Cowlitz Formation and Associated Units, Lewis and Cowlitz Co., Southwest Washington.**
- II: Stratigraphy and Lithofacies of the Eocene Type Cowlitz Formation and Associated Units, Southwest Washington.**
- III: Correlated Measured Sections of the Tide-Dominated Unit 3 of the Cowlitz Formation Showing Lateral Facies Variations.**

LITHOFACIES, STRATIGRAPHY, AND GEOLOGY OF THE MIDDLE EOCENE TYPE COWLITZ FORMATION AND ASSOCIATED VOLCANIC AND SEDIMENTARY UNITS, EASTERN WILLAPA HILLS, SOUTHWEST WASHINGTON

INTRODUCTION

Middle to upper Eocene stratigraphy in southwest Washington consists of sedimentary and volcanic units that reflect a complex geologic history of active convergent-margin events. These events include eruption and accretion of oceanic crust, plate reorganization and rotation, forearc-basin evolution, deltaic progradation, and transition from oceanic to calc-alkaline arc volcanism (Armentrout, 1987). Sequence stratigraphy (Van Wagoner et al., 1990) is an approach recently being applied to convergent margins that can help to unravel these complex depositional, tectonic, and volcanic events (Armentrout, 1987; Ryu and Niem, 1992).

For example, stratigraphic and structural relationships of the Eocene Cowlitz Formation in its type area in southwest Washington with the adjacent sedimentary and volcanic rock units were unclear (Ray Wells, personal communication 1994). Field reconnaissance by Samuel Johnson of the U. S. Geological Survey revealed the presence of a coal-bearing interval in the sandstone near the base of the upper McIntosh Formation, but the depositional environment of this sandstone-dominated unit and its stratigraphic and formational relationships were poorly understood (S. Y. Johnson, personal communication, 1994). Detailed stratigraphic measurement, description, and geologic mapping of the Cowlitz Formation in the type area were required to establish the stratigraphic relationship of this unit to adjacent units in Washington and northwest Oregon. Field reconnaissance suggests that highstand deltaic and lowstand deep-marine sandstone-channel facies occur in the type area of the Cowlitz Formation, but these facies have until now never been mapped or described (Niem, personal communication, 1994).

The stratigraphic relationships of the Eocene Grays River volcanics with the Cowlitz Formation in the type area were also in need of resolution. The Grays River Volcanics have been proposed to interfinger with, stratigraphically overlie, or be completely enclosed within the Cowlitz Formation (Henriksen, 1956; Wells, 1981; Wells, 1994, personal communication). Additionally, the relationship of the overlying late Eocene and Oligocene Lincoln Creek and Toutle formations exposed to the north and east with the Cowlitz Formation and Grays River volcanics had not been explored in detail.

The Cowlitz Formation forms the only major commercial gas reservoir (Clark and Wilson sandstone) in the Pacific Northwest. The Mist Gas Field occurs in northwest Oregon (Armentrout and Suek, 1985; Niem et al., 1992a), 50 kilometers south of the thesis area. The hydrocarbon potential of this formation in southwest Washington, however, has been largely untested. The regional stratigraphic relationships of the Cowlitz Formation with adjacent volcanic and sedimentary units in southwest Washington and northwest Oregon also needed resolution (Niem et al., 1992a; Niem, personal communication).

OBJECTIVES OF THIS INVESTIGATION

- (1) Refine the lithostratigraphy and facies of the type Cowlitz Formation and associated units in the thesis area using surface geologic mapping, measured stratigraphic sections, subsurface well data, and sequence-stratigraphic concepts.
- (2) Produce a geologic map of Eocene sedimentary and volcanic units in the type area of the Cowlitz Formation at a 1:24,000 scale.
- (3) Interpret the depositional environments, paleocurrent dispersal pattern, source areas, diagenetic history, and reservoir potential of the Cowlitz and McIntosh formations.
- (4) Determine the stratigraphic relationships of the Cowlitz Formation to the McIntosh Formation, Grays River volcanics, and Toutle and Lincoln Creek formations.
- (5) Reconstruct the paleogeographic and plate-tectonic setting of these middle to late Eocene sedimentary and volcanic units.
- (6) Resolve the regional stratigraphic relationships of the type Cowlitz Formation and adjacent units of southwest Washington with the Cowlitz Formation and associated Eocene units of northwest Oregon.

LOCATION AND ACCESS

The thesis area is located in the eastern Willapa Hills in Lewis and Cowlitz counties, southwest Washington (Figure 1). The villages of Vader and Ryderwood lie within the 130 square kilometer (53 square mile) area. Major topographic features include the Arkansas Creek valley, Abernathy and Bebe mountains, and the floodplain of Stillwater and Olequa creeks. Paved highways, numerous gravel logging roads, and streams provide access to and within this forested and hilly area. The type section of the Cowlitz Formation and McIntosh Formation are well exposed in Olequa and Stillwater creeks during low summer flow (Henriksen, 1956; Yett, 1979; Johnson, 1994 personal communication; this study) (Figure 1 and Plate I).

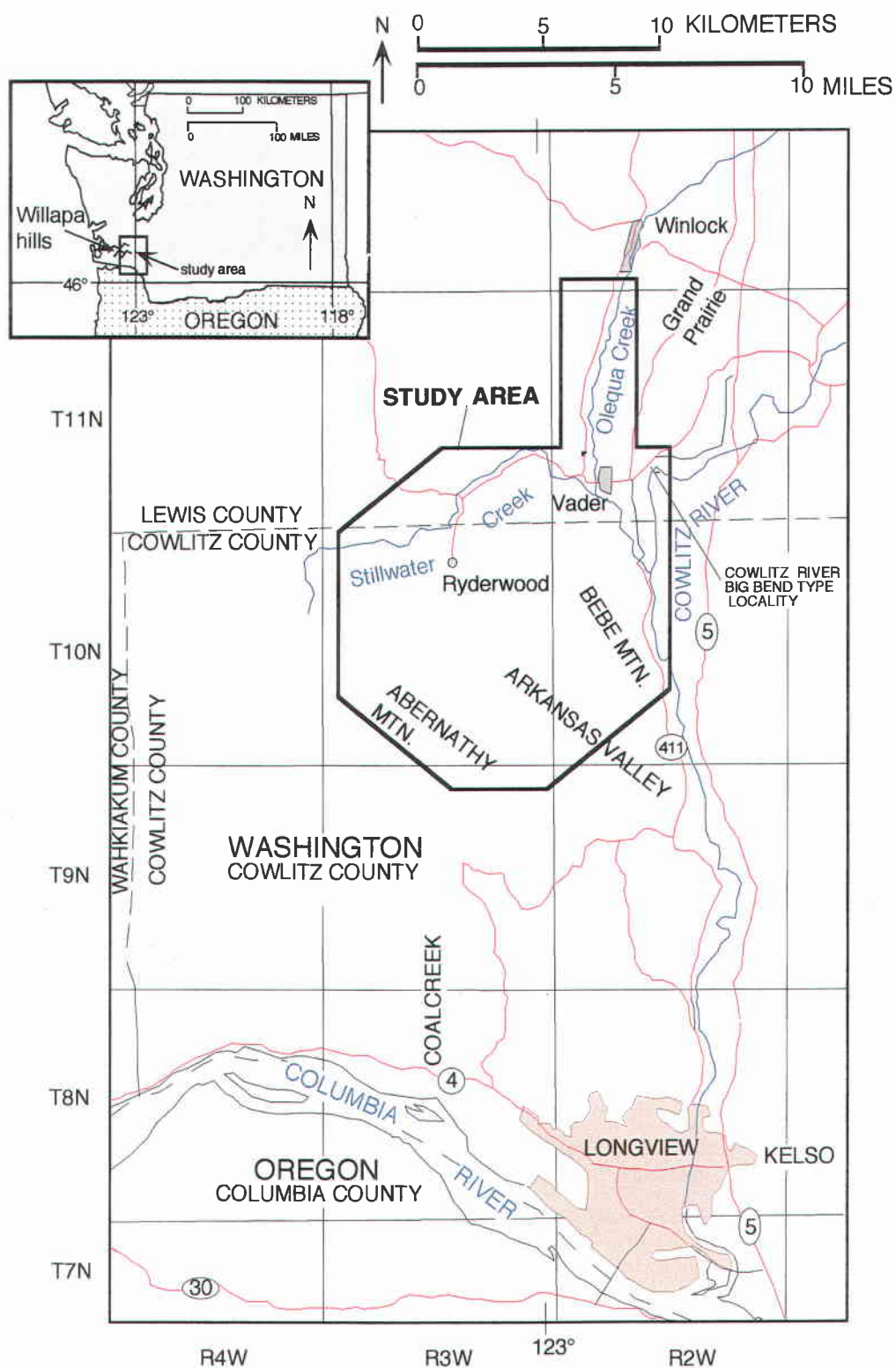


Figure 1. Location of thesis area, southwest Washington.

GEOLOGIC SETTING

The basement rocks of the Oregon and Washington Coast Ranges are composed of seamount and oceanic island basaltic crust of the lower to middle Eocene Siletz River Volcanics and Crescent Formation (Figures 2 and 3). These volcanics consist of a thick sequence of tholeiitic to alkalic pillow basalts and basaltic breccias with minor interbeds of deep-marine basaltic sandstone and siltstone (Wells, 1981). This crust was either formed from hotspot volcanism centered over a spreading oceanic ridge that was later accreted to the North American continental margin in early middle Eocene (Duncan, 1982), or was erupted *in situ* during rifting of the continental margin (Snively, 1987).

After emplacement of the oceanic crust, the rate of Farallon-North America plate convergence decreased and there was a westward migration of the subduction zone (Well, 1984; Armentrout, 1987). Changes in plate-motion and small-block tectonic rotation resulted in development of a northwest-southeast striking conjugate fault system (Wells and Coe, 1985; Armentrout, 1987). This plate-boundary relocation and shear rotation event define the first major sequence boundary (unconformity) preserved in the geologic record of southwest Washington (Armentrout, 1987).

During the middle Eocene, crustal extension caused rapid subsidence of the volcanic basement creating a 640-kilometer long forearc or marginal basin extending from the Klamath Mountains of southwestern Oregon to southern Vancouver Island, Canada (Niem and Niem, 1984; Niem et al., 1992b). Deltaic and submarine-fan facies of the Tyee Formation began filling the southern margin of this basin in Oregon (Heller and Ryberg, 1983; Ryu and others 1992; Ryu, 1995). In southwestern Washington during this time, middle to upper Eocene bathyal mudstone and sandstone (McIntosh Formation), derived from the Okanogan uplift, the North Cascades, and/or the Idaho Batholith (Heller et al., 1987), also partially filled this forearc basin (Wells, 1981).

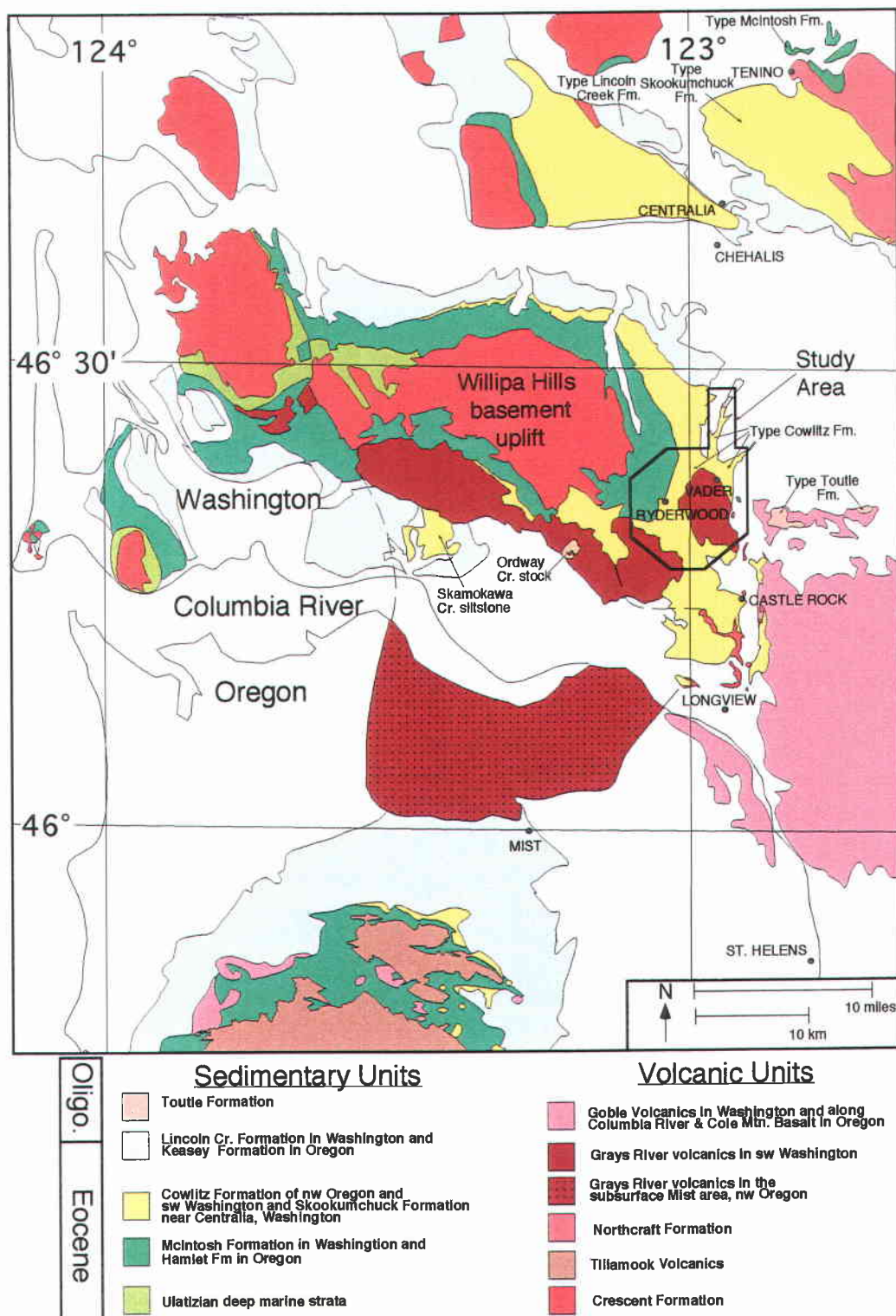


Figure 2. Regional geologic map of Eocene and Oligocene sedimentary and volcanic units of southwestern Washington and northwestern Oregon (slightly modified from Walsh et al., 1987 and Robertson, 1997).

During the late middle to late Eocene, the Tillamook Volcanics of northwest Oregon and Grays River volcanics of southwest Washington were locally erupted during a period of extension (Heller et al., 1987, Niem et al., 1992b). These mafic volcanic edifices subdivided the forearc basin into smaller marginal basins. Slope mudstone and turbidite sandstone of the McIntosh and Yamhill formations were deposited in deeper parts of these basins between growing volcanic islands and submerged eruptive volcanic centers (Niem et al., 1992b; Moothart, 1992). In northwest Oregon, the Clark and Wilson sandstone (principal reservoir at the Mist Gas Field) of the Cowlitz Formation pinches out into slope mudstone of the Hamlet formation to the west (Niem et al., 1992a). The Yamhill Formation and Hamlet Formation of northwestern Oregon correlate with the McIntosh Formation and lower Cowlitz Formation of southwestern Washington (Snively, 1987; this study) (Figure 3).

Arkosic, micaceous sandstone of the Cowlitz delta prograded westward, eventually covered some of these subsiding oceanic-island edifices, and slowly buried the underlying deep-marine mudstone dominated units. In western Washington, the Cowlitz Formation was deposited as part of an extensive deltaic system of the Eocene Puget Group that drained granitic batholiths and metamorphic core complexes of the North American continent to the east (Buckovic, 1979; Berkman, 1990).

Renewed intraplate forearc basaltic volcanism (upper part of Grays River Volcanics) and Western Cascades arc volcanism (Goble Volcanics) occurred during and after Cowlitz deposition (Phillips et al., 1989; Henriksen, 1956). Unconformity-bounded, basal basaltic conglomerate grading upward into tuffaceous marine siltstone of the overlying Lincoln Creek and Keasey formations reflects a period of renewed tectonic instability and widespread distribution of volcanic ashes in the forearc from the adjacent calc-alkaline Western Cascade volcanic arc. This unconformity represents a second, major sequence boundary in southwest Washington (Armentrout, 1987).

METHODS OF INVESTIGATION

This study involved over six months of field work from the summers of 1994 to 1996, including 65 days of stratigraphic-section measuring along a twenty-seven river-mile traverse along Stillwater and Olequa creeks (Plate I). Field work consisted of detailed geologic mapping at 1:24,000 scale (Plate I) of the thesis area using Weyerhaeuser Timber Company logging road maps, 1:6,000 scale ortho-corrected aerial photos, and the following U. S. Geological Survey 7.5' topographic maps: Winlock, Wildwood, Abernathy Mountain, and Castle Rock. Measurement and description along Stillwater Creek of the McIntosh Formation, the Cowlitz Formation type section along Olequa and Stillwater Creeks, and the Toutle and Lincoln Creek formations along upper Olequa Creek were accomplished using a Jacob staff and Abney level. Both exposed and covered intervals were measured with only a few intervals not measured due to log-jammed lakes that were traversed in a rubber raft. A total of 206 locations were sampled for further laboratory analyses of representative volcanic, sandstone, mudstone, and coal lithologies. Paleocurrent measurements of cross-bedding were collected to reconstruct the paleo-dispersal pattern of the Cowlitz deltaic sandstone facies. Lava samples of the Grays River volcanics were spatially oriented with a Brunton compass in outcrop and then collected for laboratory magnetic polarity measurements.

Interpretation of depositional environment was enhanced by fossil identification of microfossils and macrofossils that were collected for age, correlation, and paleo-environmental interpretation. Fossil samples were prepared and sent to specialists for paleobathymetry and age determination. Thirty macrofossil samples were studied by Dr. Elizabeth Nesbitt of the University of Washington (Appendix II). Forty-four samples collected along the entire measured section were submitted for foraminifera determination to Dr. Kristin McDougall, senior geologist, U. S. Geological Survey (Appendix I).

Lithostratigraphic control of measured stratigraphic sections was improved by comparison of measured sections with well data. Electric and driller's logs from the Shell-Zion #1 well, located immediately east of the study area (Plate I), were studied for subsurface correlation to the measured section of the Cowlitz Formation. In addition, Peter Hales and Dave Pauli of Weyerhaeuser Minerals Division, Tacoma, Washington were consulted for information on the subsurface stratigraphic relationships in southwest Washington.

Petrology of the sandstone facies of the Cowlitz Formation was determined using a variety of analytical techniques. Petrographic analysis involved thin section preparation and description of twenty arkosic and volcanic-rich sandstone samples including feldspar staining for point-count determination of sandstone modal compositions. Four hundred points were counted and categorized into 23 variables for nine of these samples (Appendix III). Identification of clay minerals that form the fine matrix of four sandstone samples was accomplished using a Phillips Automated X-ray diffractometer (XRD) under the direction of Dr. Reed Glasmann of the Geosciences Department, Oregon State University, Corvallis and scanning electron microscope (SEM) under the direction of Al Soeldner at the Botany Department, OSU. These analyses were performed to decipher the diagenetic history of potential reservoir sandstones in the Cowlitz and McIntosh formations.

Twenty-five tuff samples supplied to Paul Hammond at PSU were analyzed for major and trace elements using a Rigaku x-ray fluorescence unit (XRF) by Peter Hooper of Washington State University, Pullman (Appendix IV).

Three Grays River volcanics samples and one hornblende-bearing lapilli tuff from the Toutle Formation were prepared and supplied to Robert Duncan of the School of Oceanography, Oregon State University, Corvallis for $^{39}\text{Ar}/^{40}\text{Ar}$ incremental-heating age dating using a laser-fusion mass spectrometer (Appendix VI).

Nineteen thin sections of the Grays River volcanics were made commercially and then analyzed. Magnetic polarity (i.e., normal or reverse) of nineteen Grays River volcanics samples was determined by the author, using a fluxgate magnetometer. Major and trace element XRF geochemical data of Grays River volcanics samples were supplied to this author by Russ Evarts of the U. S. Geological Survey. These ten samples were from Russ Evarts's previous collection from within this study area (Appendix V).

STRATIGRAPHY AND LITHOFACIES OF THE MCINTOSH, COWLITZ, TOUTLE, AND LINCOLN CREEK FORMATIONS

NOMENCLATURE AND CORRELATION

In 1912, C. E. Weaver initially defined the type section of the Cowlitz Formation as a 500-foot long cliff of fossiliferous sandy siltstone exposed along the Big Bend of the Cowlitz River (Figure 1 and Plate I). In 1937, Weaver extended the type section to include 4,300 feet of sandstone, siltstone, and minor coal exposed in Olequa Creek. Henriksen (1956) in a mapping investigation of the area, further expanded the definition of the Cowlitz Formation to include two members, the "Olequa Creek Member" and the "Stillwater Creek Member". Deep-water mudstone and minor arkosic sandstone exposed along Stillwater Creek formed the "Stillwater Creek Member". Jan Yett (1979) in a foraminiferal study, concluded that the upper part of the Stillwater Creek Member (upper McIntosh Formation, this study) was deposited in middle-bathyal depths and the Olequa Creek Member (lower Cowlitz Formation, this study) was deposited in neritic- to marginal-marine and continental conditions.

The marine mudstone of the Stillwater Creek member of Henriksen (1956) was remapped as the McIntosh Formation in the Stillwater Creek area by Ray Wells (1981) to conform with the 1957 mapping by Pease and Hoover north of Vader, Washington. Henriksen's expansion of the type Cowlitz Formation to the Stillwater and Olequa Creek members led to correlation problems because a correlative mudstone unit had been already mapped throughout southwest Washington as the McIntosh Formation. Additionally, Wells (1981) remapped the Cowlitz Formation following Weaver's 1912 and 1937 original definition of the dominantly sandstone strata of Olequa Creek and Big Bend type locality. He restricted the Cowlitz Formation to this friable, cross-bedded micaceous

arkosic sandstone (i.e., the Olequa Creek member of Henriksen (1956)). This sandstone is interbedded with subordinate carbonaceous siltstone, volcanoclastics, and sub-bituminous coal beds (Wells, 1981).

The type McIntosh Formation was originally defined as several hundred meters of dark-gray, well indurated, tuffaceous siltstone and claystone exposed near McIntosh Lake, eight kilometers north of Tenino, Washington (Snively and others, 1951) (Figure 2). In addition, hydrocarbon exploration wells drilled in this area penetrated over 1,200 m of offshore siltstone and claystone interbedded with nearshore arkosic and basaltic sandstone in the lower and upper parts of the Formation (Snively et al., 1958). The McIntosh Formation was mapped by Pease and Hoover (1957) several kilometers to the north in the Doty-Pe Ell quadrangle. They informally subdivided the McIntosh Formation into a lower and upper member. The 275-m thick lower member consists of alternating beds of basaltic sandstone, tuffaceous siltstone, and marine mudstone interbedded with aquagene basaltic tuff and basalt breccia. The 460-m thick upper member is composed of marine tuffaceous siltstone with thin arkosic sandstone beds near the top and bottom of the unit (Pease and Hoover, 1957).

Ray Wells (1981) remapped the McIntosh Formation in the northern and eastern Willapa Hills using a modified version of Pease and Hoover's (1957) McIntosh members. The McIntosh Formation, as mapped by Wells (1981), consists of two informal members. They are: (1) a lower member of arkosic to basaltic sandstone and siltstone and (2) an upper member of siltstone and some thin-bedded sandstone. In this upper member, Wells (1981) mapped in the Ryderwood area a separate basal intercalated unit composed of massive to cross-bedded, micaceous arkosic sandstone.

Steve Moothart (1992) recently remapped the McIntosh Formation in the northern Willapa Hills area 40 kilometers to the west. On the basis of the work of Wagner (1967), Moothart informally named three members: (1) the Fort Creek member consisting of thick,

polymict pebbly, arkosic turbidite sandstone; (2) the overlying Lebam member composed of deep-marine, micaceous mudstone; and (3) the McIntosh volcanic member formed mainly of basaltic breccias.

The middle Eocene McIntosh Formation is correlative with the Yamhill and Hamlet formations of northwest Oregon (Figure 3). The arkosic to lithic arkosic basal sandstone unit of the upper McIntosh Formation (informal) may correlate with the Sunset Highway member (informal) of the Hamlet formation in northwest Oregon. Deep-water turbidite sandstone and mudstone facies in the Hamlet formation have been correlated with the shallow marine arkosic sandstone facies of the Sunset Highway member in northwestern Oregon (Mumford, 1988). Similarly, the upper McIntosh sandstone of Wells (1981) may correlate with the turbidite sandstone of the Fort Creek member (informal) of the McIntosh Formation farther west in southwest Washington (Moothart, 1992).

A 70-m thick sequence of thin-bedded mudstone and arkosic sandstone turbidites near the top of the Sweet Home Creek member (informal) of the Hamlet formation (Berkman, 1990; Robertson, 1997) may be correlated to the coarsening-upwards sandstone-rich sequences near the top of the McIntosh Formation in this study area (Plate II). To the north, over 75 m of massive to cross-bedded arkosic sandstone near the top of the type McIntosh Formation has been interpreted by Sam Johnson of U. S. Geological Survey to be fluvial in origin (Moothart, 1992).

Approximately 300 m of pyroclastics, flow breccia, subaerial basaltic andesite and andesite flows of the Northcraft Formation overlies and interfingers with the McIntosh Formation in the type area of the formation (Snively et al., 1958) (Figures 2 and 3). The Northcraft and McIntosh formations are overlain with local angular discordance by the middle to upper Eocene coal-bearing Skookumchuck Formation (Snively et al., 1951; Snively et al., 1958).

Alternating sandy, coal-bearing coastal-plain and shallow-marine facies of the Skookumchuck Formation may be correlative with the sandstone facies of the type Cowlitz Formation that crops out in southwest Washington (Flores and Johnson, 1995) (Figure 3). The Skookumchuck Formation, once well-exposed in open coal mines near Centralia, Washington, lies 40 km to the north. The middle and upper Eocene coal-bearing Skookumchuck Formation attains a maximum thickness of 1,166 m and occurs only in the Centralia-Chehalis area (Snively and others, 1958) (Figures 2 and 3). The coal-bearing deltaic Cowlitz Formation of southwest Washington appears to grade laterally into wave-dominated, micaceous, arkosic shelf sandstone and overlying deep-water mudstone in northwestern Oregon (Armentrout et al., 1983; Rarey, 1986; Berkman, 1990). The Cowlitz Formation in the subsurface at Mist, Oregon (52 km to the south-southwest of the study area) has been penetrated in numerous natural gas exploration holes. It crops out 20 km southwest of Mist, Oregon (Robertson, 1997).

The Oligocene Toutle Formation in the type area, 15 km east of the study area, is approximately 175 m thick and rests unconformably on the Hatchet Mountain Formation (Figure 2). May (1980) further subdivided the Toutle Formation into a 60-m thick lower marine member and 100-m thick upper non-marine member. The lower member was deposited in cooling subtropical shallow nearshore waters. The upper member was formed in fluvial, paludal and /or lacustrine conditions. Lithologic similarities, stratigraphic position, and age equivalence support correlation of the fluvial valley-fill strata measured along upper Olequa Creek in this study with the upper member of the type Toutle Formation of Roberts (1958).

The Lincoln Creek Formation was originally defined as massive to indistinctly bedded, concretionary, tuffaceous siltstone and minor fine-grained sandstone exposed along Lincoln Creek, west of Centralia, Washington (Snively and others, 1958) (Figure 2). This formation is over 455 m thick along Olequa Creek in the Winlock area

(Henriksen, 1956). The tuffaceous sandy siltstone facies of the Lincoln Creek Formation near the town of Winlock was interpreted by Armentrout (1973) to have been deposited in upper neritic warm-temperature waters based upon molluscan fossils. Wells (1981) mapped a basal basaltic conglomerate in the Lincoln Creek Formation in the Willapa Hills to the west.

AGE DETERMINATION

Thirteen microfaunal mudstone samples of the McIntosh Formation were sent to Kristin McDougall of the U. S. Geological Survey for foraminifera species identification, age determination, and paleoecological data. Seven samples contained foraminifers; the rest of the samples were barren. McDougall (written communication, 1997) states that the only age diagnostic assemblages occur in the lower McIntosh samples. Samples CP-94-87b and CP-94-84a (USGS numbers Mf8854 and Mf8849) from the upper part of the lower McIntosh Formation contain assemblages that suggest a middle to late Eocene age (Plate II). Based on the presence of *Cibicides elemaensis*, *C. natlandi*, and *Valvulineria jacksonensis welcomensis*, these assemblages are assigned to the late Narizian to earliest Refugian foraminiferal stages (McDougall, written communications, 1997). Foraminifera earlier identified by W. Rau (1958) from the lower McIntosh Formation (approximately 240 m below the assemblage identified by McDougall (written communications, 1997) (section locations 1B and 1D, Plate II) are assigned to the *Bulimina* Cf. *Jacksonensis* zone of the upper Ulatisian to lower Narizian stages (Figure 3). The presently accepted upper age of the *Bulimina* Cf. *Jacksonensis* zone is approximately 44 Ma (McDougall, written communication, 1997). Weldon Rau (1958) also assigned strata of the upper McIntosh Formation exposed along Stillwater Creek to the lower to middle Narizian stages. The top 180 m, he restricted to the upper Narizian stage. Additionally, Yett (1979) determined from a foraminifera study that the upper part of the upper McIntosh Formation

(Stillwater Creek Member of Henriksen, 1956) and all the lower Cowlitz Formation (Olequa Creek Member) are late Narizian in age (middle to late Eocene). These assemblages suggest the McIntosh Formation in this area ranges in age from about 44 Ma to at least 41 Ma.

Forty kilometers to the west of the study area, the lower portion of the Fort Creek member (Moothart, 1992) of the McIntosh Formation, contains an Ulatisian stage foraminiferal assemblage in siltstone interbedded with uppermost Crescent Formation pillow basalts that were $^{39}\text{Ar}/^{40}\text{Ar}$ age dated from 55 to 53 Ma. Moothart's overlying marine mudstone unit (Lebam member of the McIntosh Formation) contains foraminiferal assemblages that are mostly lower Narizian age, with upper Narizian foraminifera occurring only in the uppermost 150 m of the Lebam member (Moothart, 1992).

Foraminiferal assemblages identified by Jan Yett (1979) from Cowlitz Formation units 1, 2, and 4 defined in this study indicate strata of the lower Cowlitz Formation (Olequa Creek Member of Henriksen, 1956) are late Narizian in age (middle Eocene). A mean $^{39}\text{Ar}/^{40}\text{Ar}$ age of 38.9 ± 0.1 Ma was obtained by laser fusion of potassic oligoclase grains (Irving et. al., 1996) from a 1.5-m thick tuff (Marker 3A, Plate II) in unit 3 of the Cowlitz Formation. Calcareous nannofossils from the Big Bend locality (upper unit 4) of the Cowlitz Formation were assigned to zone CP-14 (Rarey, 1985). Macroinvertebrate fauna of the Cowlitz Formation can be correlated with the "Tejon" molluscan stage of California and the benthic Narizian foraminiferal stage (Nesbitt, 1995) (Figure 3).

Brandon and Vance (1992), using zircon fission-track analysis, determined an age of 39.2 ± 2.7 Ma for a tuff interbedded with coal deposits of the Skookumchuck Formation (Cowlitz correlative to north). Twenty km to the south, in Coal Creek near Longview (Figure 1), the Cowlitz Formation is interbedded with a basalt flow (Grays River volcanics) that has been determined to have a whole-rock plateau age of 40.3 ± 0.3 Ma (Irving et al., 1996). The volcanics in the Northcraft Formation yield whole-rock K-

Ar ages that range from 38 to 39 Ma. The Northcraft Formation underlies the upper Narizian Cowlitz Formation and overlies the McIntosh Formation (Phillips et al., 1986) (Figure 3). These age dates help restrict the "Tejon" and the Narizian stages in the Pacific Northwest to the late-middle Eocene (Irving et al., 1996) .

Sandstone at the base of the Lincoln Creek Formation contains molluscan fossil assemblages referred to the Galvinian stage of Armentrout (1973) and the Lincoln Stage of Weaver (1944) (Wells, 1981). Molluscan fauna of the Lincoln Creek Formation is also referred to the older Blakely stage of Weaver (1944) and along Olequa Creek to the middle Galvinian molluscan stage (Armentrout, 1975). Foraminiferal assemblages are referred to the Refugian and Zemorrian stages of Kleinpell (1938) of Oligocene age (Wells, 1981) (Figure 3).

Foraminiferal assemblages of the Lincoln Creek Formation from along Olequa Creek are assigned the *Sigmomorphina schencki* zone of Rau (Yett, 1979) (lower Refugian stage of Kleinpell and Weaver 1963) (Figure 3). In a sandy siltstone in the Olequa Creek section (location UW-291, Plates I and II), Armentrout (1973) identified the *Macrocallista-Nuculana* zonule that is similar to his PB III: *Turritella-Priscofus* of the Porter Bluff section. The PB III zonule ranges throughout Armentrout's *Echinophoria Fax* zone of the upper Galvinian molluscan stage (lower Oligocene) and the upper Refugian foraminiferal stage (Figure 3).

The lower member of the Toutle Formation is assigned a molluscan age within the *Echinophoria dalli* and *Echinophoria fax* zones of Armentrout (1973), within the Refugian foraminiferal stage (May, 1980) (Figure 3). An extensive Galvinian (upper Eocene to lower Oligocene) molluscan fauna is present in the lower member of the Toutle Formation (Roberts, 1958; May, 1980; and Phillips, 1987).

A two-pyroxene andesite flow that unconformably overlies the Toutle Formation has a K-Ar age of 33.9 ± 1.7 Ma (Phillips et al., 1986). The Toutle Formation exposed in

Olequa Creek in this study area contains a hornblende-bearing pumice lapilli tuff that yielded an $^{39}\text{Ar}/^{40}\text{Ar}$ age of 31.9 ± 0.44 Ma (Duncan, written communication, 1997) (Appendix VI). The source of the euhedral hornblende phenocrysts in the pumice of this tuff is unknown. However, possible vents which have erupted hornblende-bearing pyroclastics in the nearby lower western Cascade volcanics range in age from 38-32 ma. An older hornblende-bearing volcanic sequence is exposed near Hofstat Mountain in the Toutle Mountain quadrangle (Big Bend of the Toutle River near Alder Creek) (Evarts, personal communications, 1994). A younger hornblende-bearing volcanic sequence is exposed in a quarry in the Elk Rock 7.5 minute quadrangle. This younger sequence lies stratigraphically below 32 Ma age-dated basalt (Evarts, personal communications, 1994).

The Puget Group is interbedded with the base of the Ohanapecosh Formation in the western Cascades (Schasse, 1987). The Ohanapecosh consists of dacitic to basaltic-andesitic breccia, ash fall tuff, tuff breccia, and volcanoclastic siltstone, sandstone, and conglomerate. Radiometric ages of this pyroclastic unit range from 36.4 ± 3.6 Ma to 28.3 ± 2.9 Ma.

MCINTOSH FORMATION

Outcrop Distribution and Thickness

This study uses the lithostratigraphic definition of an informal lower and upper member of the McIntosh Formation as mapped by Ray Wells (1981) in the Willapa Hills area. These strata were also penetrated in the Shell-Zion #1 well (Plates I and II) northwest of Vader (Sec. 9, T11N, R2W). Electric and driller's logs from this well were used to refine field-measured stratigraphic thicknesses. Detailed section description and measurements (by this author) along Stillwater Creek were the main source of data for this discussion of the McIntosh Formation. Field mapping also added some data in limited rock exposures in the study area (Plate I). The thickness of the two McIntosh members is (1) a minimum of 375 m for the lower mudstone member (with the base not exposed) and (2) 625 m for the upper member. The upper member is further informally subdivided into a basal 128-m thick arkosic sandstone and an overlying 497-m thick tuffaceous siltstone unit.

Determination of repeated or cut-out stratigraphic section by faulting was based on geologic mapping, exploration well data, and anomalous repetition of measured lithologic sections. One fault (IP Land fault), for example, has repeated over 240 m of section (3D1 to 4A, Plate I) along Stillwater Creek. Refinement of the total thickness of the basal sandstone-rich interval of the upper member of the McIntosh Formation was based on correlation of the field measured section with a similar 128-m thick sandstone interval in the Shell-Zion Well #1 (depth interval 5,500 ft to 5,850 ft). Also, the upper McIntosh sandstone/lower McIntosh mudstone stratigraphic contact was chosen as a marker to establish stratigraphic offset along the IP Land fault (Plates I and II). This analysis revises

the geologic mapping of Ray Wells (1981). He mapped these McIntosh sandstones as interbedded with the upper McIntosh Formation mudstones. Additionally, two other faults have cut-out stratigraphic section along exposures of the upper McIntosh Formation sandstone in Stillwater Creek. (For calculations of the amount of stratigraphic offset or throw along other faults in the thesis area see the Structural Geology section.)

The following general lithologic ratios and exposure percentiles are from measured section data only. The lower member of the McIntosh Formation, with a combined total of 99 m of exposed measured stratigraphic section (25% of total measured section), has a mudstone to sandstone ratio of 9:1. However, this ratio is likely much higher (up to 40:1) if unexposed strata (i.e., covered by gravel, soil, or vegetation) are dominantly mudstone, as indicated by electric and driller's lithologic logs from the nearby Shell-Zion well #1 (Plate II). The basal arkosic sandstone unit of the Upper McIntosh Formation has a 9:1 sandstone to siltstone ratio with 40% exposure of strata along Stillwater Creek (Plate II). Rock exposures in the upper McIntosh siltstone equal a combined total of 112 m (22% of total). The siltstone unit of the upper McIntosh Formation has a siltstone to sandstone ratio of 5:1. Additional data from the work of Rau (1958) and from the Shell-Zion #1 well logs indicate there is another sandstone-rich interval in the upper part of the McIntosh Formation.

Exposures of the McIntosh Formation in the map area are significantly less frequent than along Stillwater Creek. However, numerous road cuts along logging roads allowed for adequate data collection for geologic mapping when combined with measured stratigraphic section along Stillwater Creek. For instance, geologic mapping of the McIntosh Formation southwest of Ryderwood in this study revises the published mapping of Wells (1981). He had mapped Cowlitz Formation in this area, but recent logging has exposed an extensive siltstone unit in this area similar to the McIntosh Formation exposed along Stillwater Creek (Plate I).

Lithofacies and Contact Relationships

Lower McIntosh Formation

In the thesis area, the McIntosh Formation typically forms low hills and broad, highly dissected stream valleys and is, overall, poorly exposed. The most continuous section of lower McIntosh is exposed mainly in the stream bed and rarely in the banks of Stillwater Creek west-northwest of Ryderwood, Washington (Sec. 4 and 5, T10N, R3W; Plate I). At this location, 379 m of dark medium gray mudstone, shale, and minor thin-bedded micaceous arkosic sandstone were measured (Plate II). In the lower portion of this section, marine mudstone is interbedded with thin, graded arkosic micaceous sandstone, thick channelized sandstone, and thin tuff beds while the middle and upper intervals are mainly composed of dark gray mudstone. The uppermost interval of the lower member consists of massive siltstone that is in sharp contact with the overlying sandstone of the upper McIntosh member.

The dominant lithofacies from interval 0 m to 159 m (sections 1G to 2A, Plate II) consists of (1) dark-gray and orange-stained, fissile, clay-shale and mud-shale with subordinate laminated sandy and silty mudstone, (2) muddy siltstone with very fine-grained sandstone laminations, and (3) claystone containing medium-grained tuff clasts interlaminated with mudstone. From interval 159 m to 349 m the dominant lithofacies is medium to dark gray, thinly laminated to thin-bedded mudstone (Figure 4) with minor sandstone laminae. The upper 30 m of the Lower McIntosh unit is composed of poorly bedded, medium- to dark-gray clay-rich siltstone that coarsens upward to a tuffaceous, silty, very fine-grained arkosic sandstone. The top 3 m of this member contains 10 cm-diameter calcareous concretions.

The few arkosic sandstones in this member range in thickness from 2 cm to 3 m and exhibit massive to normally graded bedding. These sandstone beds have sharp bases



Figure 4. Lower McIntosh Formation mudstone in Stillwater Creek (section location 3D; NW 1/4, Sec. 4, T10N, R3W; Plate II). Note 25 cm rock hammer for scale.

and gradational upper contacts. These beds are typically very fine- to fine-grained, moderately well-sorted, and are structureless to faintly micro-cross-bedded and parallel-laminated. Beds in erosional contact with an underlying muddy siltstone contain siltstone rip-ups and load structures. The sandstones are composed of dominantly subrounded quartz, feldspar, and lithics. Some large mica and coarse-grained volcanic (tuff or pumice) fragments are present in a few beds.

Minor, thin (1 to 5 cm-thick), buff to light gray tuff layers interbedded with dark-gray clay-shale occur in section 1E (interval 32 m to 35 m, Plate II). Multiple tuff beds interbedded with mudstone are located at 3D2 in the measured stratigraphic section. Poorly sorted, well rounded, granule-sized to coarse-grained basaltic sandstone overlies marine mudstone at stream location 3C.

A nested submarine-channel relationship composed of multiple, incised, sharp-based sandstones that each grades into mudstone is well exposed at location 1C2 (interval 77 m to 83 m, Plate II). These 3.7-m to 0.6-m thick fining-upward successions consist of medium- to coarse-grained, micaceous, arkosic sandstone mixed with granular volcanic clasts (basalt, andesite lava and tuff) that grade upward into well-sorted, fine-grained subarkosic micaceous sandstone. These 1-m-thick channel-fill deposits grade upward to intensely bioturbated sandy mudstone and lenticular to ripple-laminated carbonaceous sandy siltstone and mudstone with distinct vertical burrows filled with dark gray siltstone.

Upper McIntosh Formation-Sandstone Unit

The basal sandstone unit of the upper McIntosh Formation is 128 m thick (interval 379 m to 507 m, Plate II). This sandstone body crops out in two locations in the stream bed of Stillwater Creek with the best exposure one mile west of Ryderwood (section 2E-3D2; NE 1/4, Sec. 4, T11N, R3W; Plates I and II). Outcrops along Owens Creek also offer excellent exposure of this micaceous, arkosic to lithic-arkosic sandstone-dominated unit.

A very coarse-grained to granule-sized volcanic conglomerate bed (0.5-m thick) with a siltstone matrix is in sharp, erosional contact with the underlying lower McIntosh siltstone. This conglomerate bed grades upward into sandy siltstone and mudstone. The overlying interval is composed of 26 m of micaceous arkosic sandstone interbedded with subordinate siltstone and mudstone (upper section 2E to the lower part of section 3E; Plates I and II). These sandstones are overlain by very thin-bedded siltstone, mudstone, and basaltic sandstone (Figure 5).

Lower sandstone beds are trough cross-bedded to swaley cross-stratified and interbedded with a thin, blue-gray, fine-grained basaltic sandstone. The middle and upper parts of this interval are composed of fine- to medium-grained arkosic sandstone with planar, mica-rich laminae at base. The upper part is massive and contains carbonaceous plant material, pyrite nodules, and large calcareous concretion or nodule horizons. The highest sandstone bed displays a sharp, channelized, coarse-grained base. This sandstone contains siltstone rip-ups (up to 2.5 cm long) and internal scour structures.

A 5.5-m thick ripple-laminated siltstone facies capped by a thin coal bed is in sharp contact with the underlying sandstone (section 3E, Plate II). Bed forms include thin laminations of wavy and lenticular siltstone and (20%) very fine-grained sandstone (< 1/2 mm-thick discontinuous laminae). The upper part of this interval is composed of

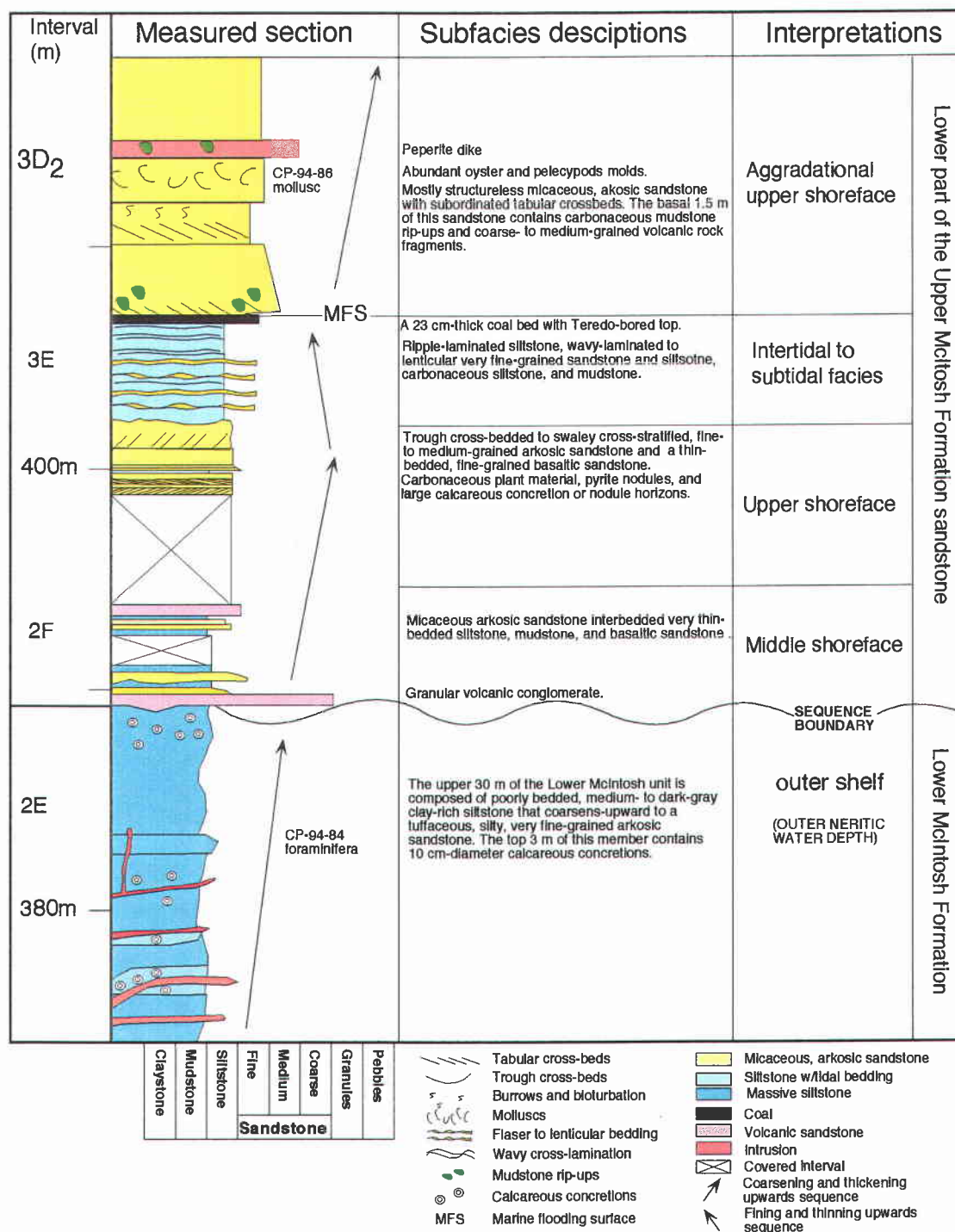


Figure 5. Composite stratigraphic section of the lower part of the upper McIntosh Formation sandstone (section locations 2E to 3D₂; NW 1/4, Sec. 4, T10N, R3W; Plates I and II).



Figure 6. Coal in the basal sandstone unit of the upper McIntosh Formation, Stillwater Creek location 3E (NW 1/4, SE 1/4, Sec. 4, T10N, R3W, Plates I and II). Note 25 cm rock hammer for scale.

bioturbated sandy siltstone that contains small-scale channel-fill sandstone horizons. The upper part of this interval consists of wavy-laminated, carbonaceous siltstone and mudstone capped by a 23 cm-thick (9 in) coal bed (Figure 6). This coal has a sharp top and contains numerous sandstone-filled *Teredo*-borings.

A mostly structureless sandstone lies with sharp contact on the coal (section 3E to 3D2, Plate II). The basal 1.5 m of this blue-gray, micaceous arkosic sandstone is faintly cross-bedded, moderately sorted, and medium-grained. The bed contains carbonaceous mudstone rip-ups and medium- to coarse-sand-sized volcanic rock fragments. Higher in the section this sandstone becomes very fine- to fine-grained, subarkosic in composition, is bioturbated, and contains large-scale planar cross-beds. A resistant, ledge-forming horizon of abundant oyster and pelecypod molds (shell-hash) in a well-indurated, calcite-cemented sandstone (macrofaunal sample CP-94-86-m) is located at interval 428 m (Figure 5). Above this shell-hash is swaley to hummocky cross-stratified and ripple-laminated arkosic-lithic sandstone (petrology sample CP-94-86d2, Appendix III). The upper interval contains multiple cut-and-fill horizons with angular coalified wood, siltstone, and mudstone rip-ups that range from cobble to pebble size. The clasts are in a fine- to medium-grained sandstone. Some imbricated clasts indicate a south-southwest paleocurrent dispersal direction.

Locally intruding this sandstone are Eocene basalt and peperite dikes that range from 0.9 to 6.1 m in width (Figure 5, Plate I). Angular clasts in the largest peperite dike include mudstone, siltstone, sandstone, and altered basalt in a sandstone groundmass. Some sedimentary clasts are baked while others are unaltered. These dikes appear to intrude a fault zone (Farm Fault in Plate I) that has cut-out 67 m of section between the mudstone rip-up sandstone facies and the underlying mostly massive sandstone facies.

Other correlative, measured stratigraphic sections are composed of massive to parallel-laminated, swaley, and hummocky cross-stratified arkosic and lithic arkosic sandstone. These sections include: (1) sandstone at 4A located along Stillwater Creek (interval 434 m, Plates I and II), (2) a mollusc-bearing tuffaceous sandstone at location CP-95-202m projected into the section at interval 455 m (Plates I and II), and (3) parallel-laminated and swaley to hummocky cross-stratified arkosic sandstone and tuffaceous-lithic sandstone with minor vertically burrowed and laminated siltstone interbeds that crop out along Owens Creek (location 135L, Plate I and Figure 7).

Upper McIntosh Formation-Siltstone Unit

The overlying 457-m thick siltstone unit of the Upper McIntosh Formation (interval 507 m to 964 m, Plate II) is exposed along the stream bed of Stillwater Creek north of Ryderwood (NW 1/4, Sec. 3, T10N, R3W and Sec. 33 and 34, T11N, R3W; Plate I). The dominant facies is siltstone and minor, thin-bedded sandstone. However, coarsening-upwards sandstone-rich intervals are present in the upper part of this member.

Sections 3D2 and 5A to 5D (interval 507 to 604 m, Plate II) are composed of parallel- to ripple-laminated siltstone beds interbedded with thinly laminated sandstone. Small (<1/4 cm in diameter) horizontal and hook-shaped *Phycosiphon*- burrows (previously called *Helminthoida*) (Niem, personal communication, 1997) in the siltstone are filled with darker mudstone. These burrowed intervals form distinctive ribs or small ledges along the creek bed. Some ripple-laminated intervals contain carbonaceous-concentration laminae. A contorted-bedded interval displays syndepositional slump folding with disorganized and chaotic-bedding. Minor channelized horizons are filled with friable, well-sorted, very fine- to -fine grained arkosic sandstone (7 cm high and 15 cm wide) overlain by bioturbated siltstone with burrows filled with fine-grained sandstone. The upper part of this interval contains micaceous, parallel-laminated sandstone interbeds.



Figure 7. Parallel-laminated and swaley to hummocky cross-stratified micaceous, lithic arkose of the upper McIntosh Formation sandstone exposed along Owens Creek (location 135L; NW 1/4, Sec. 33, T3N, R3W; Plate I). Note 25 cm hammer for scale.

Siltstone beds become generally structureless upwards (sections 5E to 6A, Plate II). Large (meters long) irregular calcareous concretions are also numerous along the creek bed. Minor thin beds of fine-grained sandstone that are normally graded and becomes ripple-laminated, grade upward into siltstone (Bouma Tabcd).

The uppermost part of the member (6B to 6F, Plate II) is composed of thin-bedded and parallel, wavy-laminated siltstone containing minor very fine-grained sandstone lenses that are locally bioturbated. Also, fine carbonaceous plant debris material is concentrated along ripple-lamination foresets and large (30 cm diameter) ellipsoidal calcareous concretions are found along the creek bed.

Rau (1951) mapped a few sandstone-rich intervals along the presently stream-gravel covered intervals between sections 6B to 6E (plates I and II). These coarsening-upwards sandstone intervals also occur in the Shell-Zion #1 well (Plate II). These sandstone intervals were visible in a landslide scarp that was exposed during the winter of 1996 (1/4 NW, Sec. 27, T11N, R3W; Plate I). That exposure revealed parallel-laminated and swaley to hummocky cross-stratified arkosic sandstone.

Minor light gray to buff tuffaceous, micaceous siltstone and thin tuff interbeds increase in frequency upwards. Multiple, very thin tuffaceous laminations in this siltstone unit are well exposed along recently graded logging roads north of Stillwater Creek (Sec. 27, T11N, R3W). Section 6B (Plate II) in Stillwater Creek contains a 1.5-m thick lenticular bed of silty, volcanic-rich, very fine-grained sandstone in bioturbated, tuffaceous siltstone with horizontal burrows (up to 10 cm long and 1 cm wide).

Depositional Environments

Lower McIntosh Formation

The middle to late Eocene lower McIntosh Formation was deposited near the shelf/slope break. Hemipelagic deposition dominated. However, minor sand-rich turbidity currents depositing thin, graded micaceous arkosic sandstone beds on the flank of this marginal marine basin. This interpretation is based on lithofacies, sedimentary structures, and microfossil data.

The organic-bearing, laminated, dark gray mudstones of this unit lacks any sedimentary features that indicate the influence of storm waves. The absence of burrows and fine laminations in this dark gray deep marine mudstone suggests this unit was deposited in anoxic bottom waters (e.g., oxygen minimum zone). This foram-bearing mudstone was most likely deposited slowly from nepheloid layers (e.g., river borne plumes of terrigenous muddy water). Volcanic sea mount(s) or island(s) of the Crescent Formation to the west resulted subdivision and restriction of this marginal-marine basin.

Four samples from the lower McIntosh Formation identified by Kris McDougall of the U. S. Geological Survey (written communication, 1996) contain foraminiferal assemblages that offer minimum water-depth of deposition (Appendix I). The lower part of the lower McIntosh mudstone contains outer neritic to upper bathyal (>50 m) foraminifera. The middle of this member was probably deposited near the shelf-slope break (+150 m). The upper mudstone contains characteristic foraminifera of slightly shallower, outer neritic water depths (50-150 m). These water-depth determinations are only minimums because re-sediment processes (e.g., nepheloid layer or dilute turbidity currents) may have brought these diagnostic benthic foraminifera into a deeper-water

environment (McDougall, written communication, 1996). These mudstones also contain some pyritized diatoms, radiolarians, and sponge spicules.

In the lower McIntosh Formation, scattered thin beds of graded, micaceous arkosic sandstone have sharp scour bases, gradational upper contacts, and parallel- and ripple-laminations, which are typical sedimentary structures of sandstones deposited by low density sand-rich turbidity currents (divisions Tabc of Bouma, 1961). Although turbidite sandstones are rare in the lower McIntosh Formation, one 6-m thick sandstone-rich interval (section location 1C, Plate II) defines small-scale nested submarine channel development in this area. This submarine channel/turbidite sequence formed a coarsening-upward sequence due to fan migration (Plate II). Turbidity currents can occur in any subaqueous environment. However, to be classified as a turbidite, these deposits must not be later reworked by other processes (such as waves or tidal currents). This limits the preservation potential of turbidites to a water-depth to below storm-wave base (Walker and Plint, 1992). In addition, the lack of distinct parasequence divisions in this unit may indicate a deep-water environment of deposition where minor sea-level fluctuations were of insufficient in magnitude to effect sedimentation (Van Wagner et al., 1990). The lower McIntosh Formation may have been deposited on the prodelta of the proto-Cowlitz delta to the east or on the upper slope to lower continental shelf (Figure 8). If foraminifera of the *Bulimina* Cf. *Jacksonensis* zone identified by Rau (1956) at section location 1D (Plate II) define the Ulatizian-Narizian boundary (44 Ma) and foraminifera from the top of the lower McIntosh Formation (location 2E, CP-94-84, Appendix I and Plate II) are upper Narizian in age (~41 Ma), then a significant amount of time may be represented in this 335-m thick interval of the lower McIntosh (sedimentation rate of 26 cm/1,000 yrs).

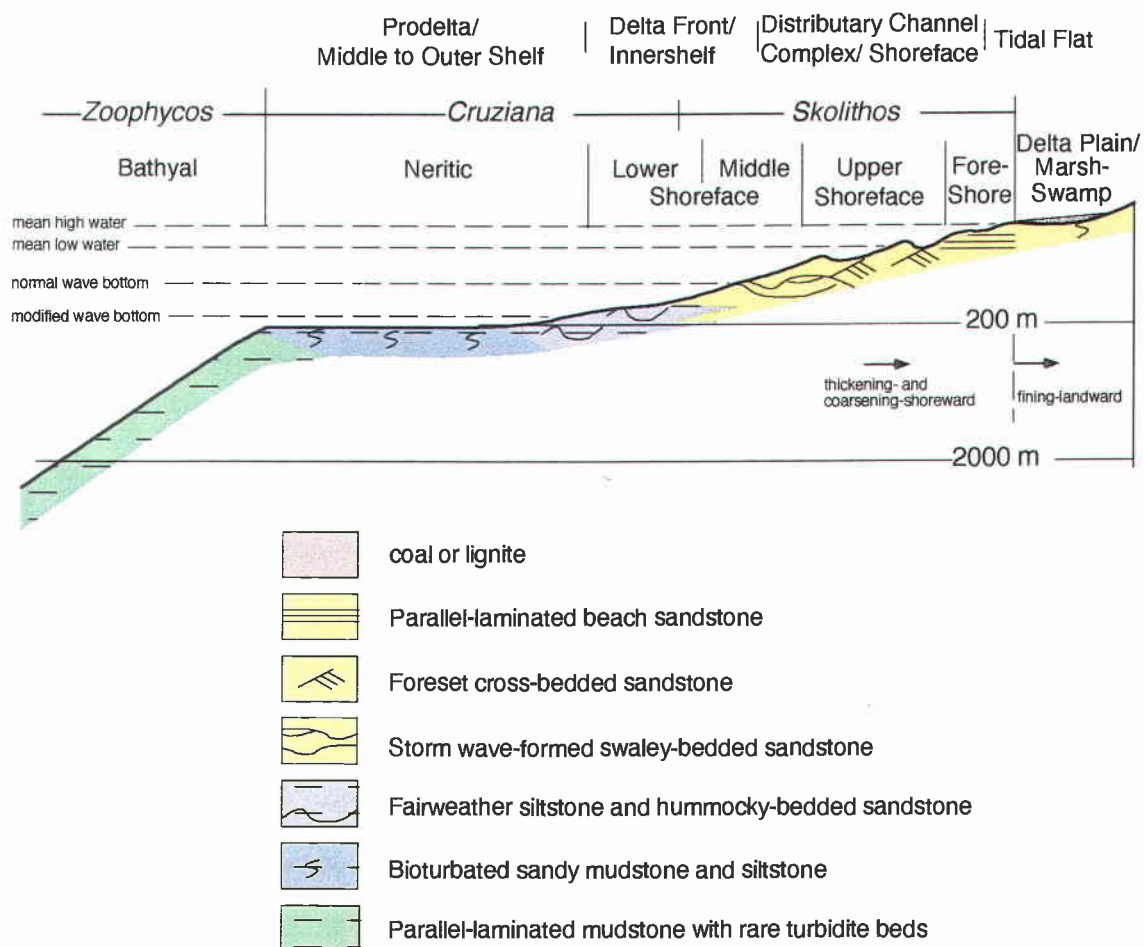


Figure 8 Onshore-offshore profile of depositional environments and lateral ichnofacies of the McIntosh Formation and normal marine units of the Cowlitz Formation (slightly modified from Berkman, 1990 and Robertson, 1997).

Upper McIntosh Formation-Sandstone Unit

The thin volcanic conglomerate (debris flow) at the base of this sandstone unit unconformably overlies outer neritic siltstone of the lower McIntosh Formation (Figure 5). Bedforms (e.g., trough cross-bedded to swaley cross-stratification) above the conglomerate indicate a middle shoreface environment of deposition. This middle shoreface facies abruptly rests on outer shelf muddy strata. The intervening shelf-to-shoreface transitional facies was probably eroded by a rapid forced regression during a reduction in accommodation space (Walker and Plint, 1992). As a result, the upper McIntosh shoreface sandstone rests on a wave-scoured erosional surface. This unconformable contact may represent a sequence boundary resulting from a third order relative sea-level fall (20 to 80 m).

Upper McIntosh sandstone is composed of a prograding upper shoreface to marginal marine facies succession and an overlying aggradational upper to middle shoreface succession (Figure 5). The lower sandstone of the upper McIntosh Formation was deposited in the middle to upper shoreface. Parallel-lamination and swaley to hummocky cross-stratification in these basal sandstones are diagnostic storm wave bedforms (Figure 8). Concretionary intervals that have abundant pyrite and mudstone rip-ups also point to deposition by storm waves and rapid burial in an anoxic, sulfide reducing shallow diagenetic environment. The uppermost sandstone of this interval contains scour surfaces with large siltstone rip-ups that may have been deposited in a distributary mouth-bar sandstone complex of a delta. These large siltstone rip-ups were probably eroded from the muddy outer shelf deposits during storm wave events and redeposited and buried in the hummocky cross-stratified middle to upper shoreface or in distributary mouth bar sands.

Bioturbated tidal-flat strata and a coastal swamp "coal" deposit overlie the upper shoreface sandstone (Figures 5 and 8). Diagnostic sedimentary structures of the tidal

flat/estuary sequence are asymmetrical ripple laminations, flaser to lenticular bedding, and vertical burrows. The distributary-bay/marsh-swamp depositional environment interpretation was based on the presence of a bioturbated carbonaceous mudstone lithofacies overlain by a thin lignitic coal bed. In sequence stratigraphic terminology, the shoreface sandstone and tidal flat strata comprise a fining-upwards parasequence that is overlain by a marine flooding surface (MFS on Figure 5) and the next parasequence. Similar parasequences have been described by Van Wagoner and others (1990) in the Cretaceous Book Cliffs of eastern Utah.

An aggradational sequence of upper shoreface sandstone, composed of micaceous, arkosic sandstone, overlies the coal and carbonaceous tidal-flat and coastal marsh interval (Figure 8). Sedimentary structures indicate rapid transgression of this sandstone over the marine flooding surface. *Teredo*-borings in the top of the coal bed indicate there was a rapid marine incursion or onlap. Large-scale foreset-bedded sandstone in the lower part of this interval indicates this was an upper shoreface or distributary mouth-bar environment of deposition. In addition, two molluscan fossil-rich intervals identified by Elizabeth Nesbitt (written communication, 1996) contain shallow-marine *Tivelina* or *Macrocallister* and brackish-water *Corbicula* pelecypods (macrofaunal samples CP-94-86 and CP-95-202m, Appendix II). These fossils are broken and disarticulated and appear to be storm wave-generated shell lags. The upper part of this sandstone is ripple-laminated and swaley to hummocky cross-stratified. This stratification formed in a storm wave-dominated middle shoreface depositional environment (similar to bedforms found by Dott and Bourgeois, 1982). Large coalified wood chunks, siltstone, and mudstone rip-ups above scour surfaces in the massive bioturbated arkosic sandstone may have been deposited into the middle shoreface by storm wave events. Imbrication of mudstone rip-ups indicates a

south-southwest paleocurrent direction approximately parallel to the presumed north-south paleoshoreline, suggesting longshore transport or geostrophic currents may have been important in the final deposition of these clasts.

Upper McIntosh Formation-Siltstone Unit

The thick, bathyal siltstone facies of the upper McIntosh Formation directly underlies the sandstone-rich Cowlitz Formation. The lower part of the upper McIntosh siltstone unit includes parallel-laminated and slump-folded siltstone, interpreted to be delta slope and delta front deposits (Figure 8). Syndepositional folding resulted from sediment loading and/or earthquake activity and subsequent submarine sliding. The presence of hooked-shaped *Phycosiphon*-burrows (*Helmenthoida*) suggests some oxygenated bottom-water conditions in these deep-marine basinal muds. Channelized and graded to massive sandstone record some abrupt emplacement and scour by low density sand-rich turbidity currents. Subsequent long-term, slow siltstone deposition is defined by extensive burrowing organisms. Hemipelagic siltstone deposition, extensive bioturbation, and numerous calcareous concretions formed diagenetically below the sea sediment/water interface are evidence of a slow sedimentation rate at the shelf-slope break. Additionally, normal-graded to massive arkosic sandstone beds with sharp erosional basal contacts that become ripple-laminated near the top are Bouma Tad turbidite beds that record minor rapid sediment emplacement.

Jan Yett (1979) identified two foraminiferal faunules in the upper part of the upper McIntosh siltstone. The siltstone from locality UWA-1988 (location 6C, Plate II) contains the *Bulimina-Lenticulina* Faunule and the sandy siltstone from locality UWA-1989 (location 6E, Plate II) (stratigraphically 30 meters above UWA-1988) is dominated by *Cibicidina cushmani* (20% of total number of specimens) and *Uvigerina garzaensis*. A few individuals of *Stilotomella adolphina*, *Plectofrondicularia searsi*, and *Cancris joaquinensis*

are also present. Yett (1979) concluded that the upper McIntosh member of Wells (1981) (previously the upper part of the Stillwater Creek member of Henriksen, 1956) was deposited in middle bathyal depths. Thus, the deepening from the middle shoreface (upper McIntosh sandstone) to the middle bathyal (upper McIntosh siltstone) resulted from tectonic or basin subsidence during deposition of the upper McIntosh Formation in this area.

COWLITZ FORMATION

Introduction

Lithofacies associations and successions, sedimentary structures, and biofacies assemblages described from detailed stratigraphic section measurement of the type Cowlitz Formation were combined with facies models (a general summary of a particular depositional system) in order to determine the different depositional environments of this formation. A lithofacies is a body of rock characterized by a particular combination of lithology, biological, and physical structures that are different from the bodies of rock above, below, and adjacent (e.g., bioturbated siltstone facies or hummocky cross-stratified sandstone facies) (Walker, 1992). Facies succession implies certain facies properties change progressively in a specific direction, either vertically or laterally (e.g., a coarsening- and thickening-upward shoreface succession) (Walker and Plint, 1992). These facies successions allow for depositional environment determination when the individual facies alone could have formed in a variety of environments (e.g., trough cross-bedded sandstone of a fluvial or upper shoreface depositional environment). Lithofacies associations consist of groups of facies genetically related to one another and which have some environmental significance (Walker, 1992). For example, a mixed intertidal facies association consists of flaser, wavy, and lenticular bedded mudstone and sandstone facies forming vertically stacked accretionary bank deposits. Lithofacies associations form the building blocks of depositional systems (e.g., point bar in a fluvial depositional environment). The depositional system is determined by combining depositional environments with processes of formation (e.g., tide-dominated deltaic depositional system) (Walker, 1992).

This study proposes an informal lithostratigraphic division of five units for the 1,238-m thick Cowlitz Formation exposed in the type section (Weaver, 1934; Henriksen, 1956) along Stillwater and Olequa creeks (Figure 9, Plates I and II). The basal unit consists of numerous prograding, wave-dominated shoreface, lithic-arkosic sandstone successions (unit 1A) and coal-bearing delta plain facies associations (unit 1B). The contact between units 1B and 2 is covered. Unit 2 is composed of coarsening-up storm-dominated, hummocky-bedded shelf to delta-front arkosic sandstone successions and outer shelf siltstone and mudstone. Unit 2 also contains multiple basaltic volcanic interbeds and thick basaltic, fossiliferous sandstone. Unit 3 is in unconformable contact (i.e., a sequence boundary) with the lower shallow marine unit 2. Fining-upwards subtidal, intertidal, and supratidal facies associations constitute the third member. These tidal-estuary facies associations of unit 3 include: (1) nested subtidal micaceous lithic-arkosic sandstone channels, (2) cross-bedded subtidal sandstone ridges with brackish water mollusc hash, (3) sandy and muddy accretionary-bank, and (4) coal-bearing marsh-swamp deposits. Thin basaltic volcanoclastic and tuff interbeds occur within the coal-bearing intervals of units one and three. A conformably overlying fourth unit, consists of wave-dominated shoreface arkosic sandstone to offshore bioturbated mudstone facies successions. These successions form 10 coarsening-upward parasequences of a retrogradational parasequence set. Thick, bioturbated outer shelfal mollusc-bearing sandy siltstone and glauconitic mudstone in the Big Bend type locality along the Cowlitz River can be correlated to this unit in the type section in Olequa Creek. The unconformably overlying, uppermost unit consists of deeper marine, (1) laminated siltstone and subordinate (2) fine-grained, thin-bedded turbidites, (3) thick, amalgamated submarine-channel sandstone, and (4) chaotic mudstone conglomerate facies, with slump-folded and soft-sediment deformed intervals.

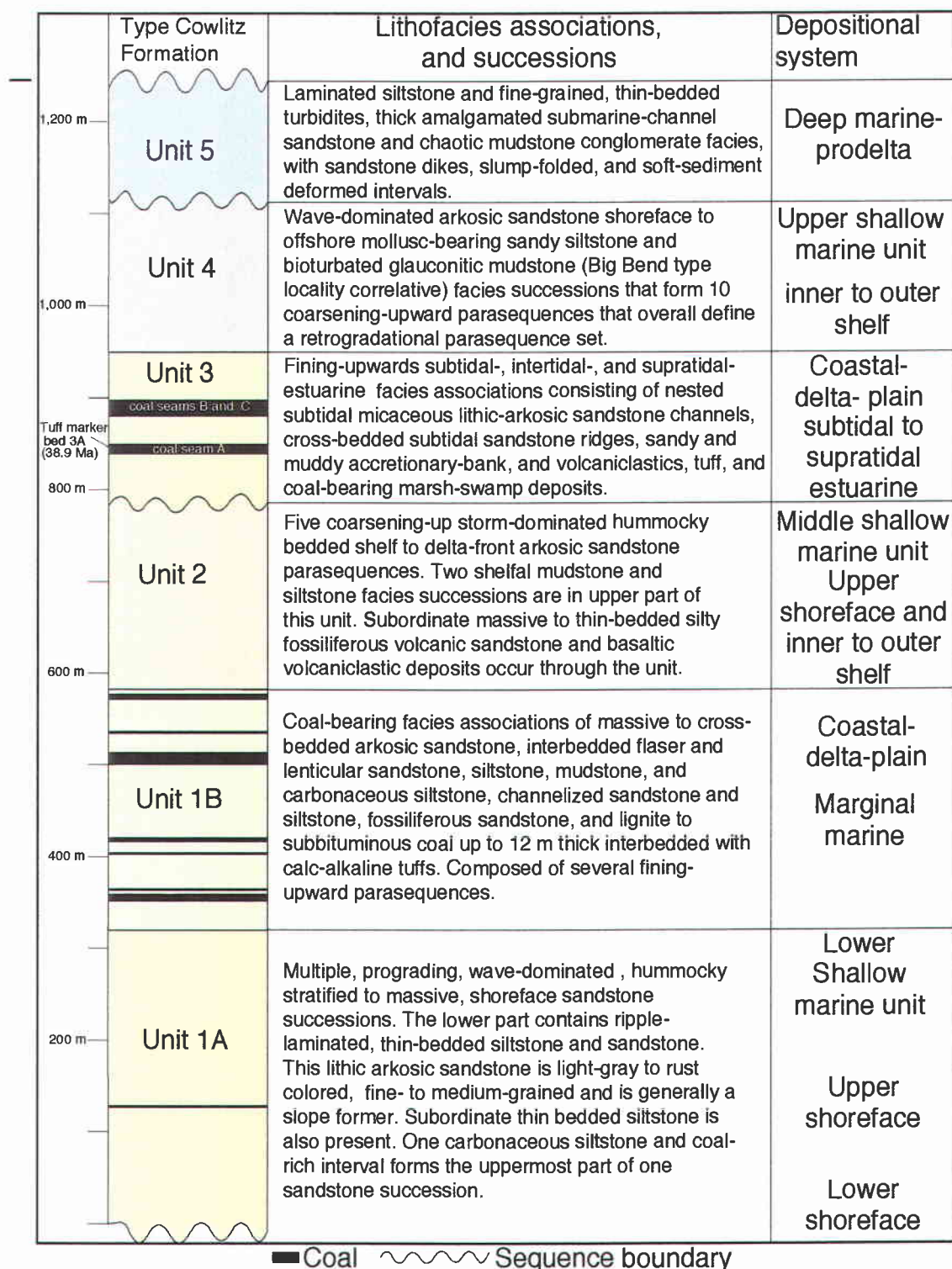


Figure 9. General stratigraphic column of the middle Eocene type Cowlitz Formation, southwest Washington.

Outcrop Distribution and Thickness

Detailed description and stratigraphic section measurement using a Jacob's staff and Abney level and mapping by this author along 27 miles of creeks were the main source of data for construction of the 1,238-m thick composite Cowlitz stratigraphic column (Plate II) and for this discussion of the Cowlitz Formation. Unit 1 is 558 m thick as determined by using field-measured stratigraphic sections and by correlation with strata penetrated in the nearby Shell-Zion #1 well (Plates I and II) northwest of Vader (Sec. 9, T11N, R2W). The well is 1 to 10 km from the measured section, which dips 10° to 15° into the well. Electric and driller's logs from this 2,150 m-deep exploration well were used to refine the stratigraphic thickness of unit one. Subunits 1A and 1B could not be mapped in detail beyond the Olequa and Stillwater creek exposures. Units 2 and 3 are 170 m and 205 m thick respectively. Stratigraphic control on these units is excellent due to normal and reverse fault repetition of numerous stratigraphic sections and the presence of distinctive marker beds for correlation (Figure 10). These marker beds include thick coal seams, volcanoclastic sandstone and tuff beds, fossil shell beds, and similar thick siltstone and mudstone lithologic packages. Correlated, field-measured sections of unit 2 are exposed along lower Stillwater and upper Olequa creeks (sections 8F2 to 8G, 9A to 10E, O1-5, O6, O7, O8, and O10).

Nine field-measured partial sections from the upper and lower parts of Olequa Creek were used to construct the composite section of unit 3 (sections 11C to 11F, O9, O11, and O14 to O22; Figure 10 and Plate III). The geographic positions of all these partial sections are shown on Plate I. The fossiliferous, mudstone-dominated unit 4 is 155 m thick along upper Olequa creek. A correlative part of unit 4 is also exposed along the well-known Big Bend fossil locality of the Cowlitz Formation along the Cowlitz River east of Vader (Plate I). At the Big Bend type locality of Weaver (1934), 65 m of strata were measured by Elizabeth Nesbitt (1979). The Big Bend section correlates with the

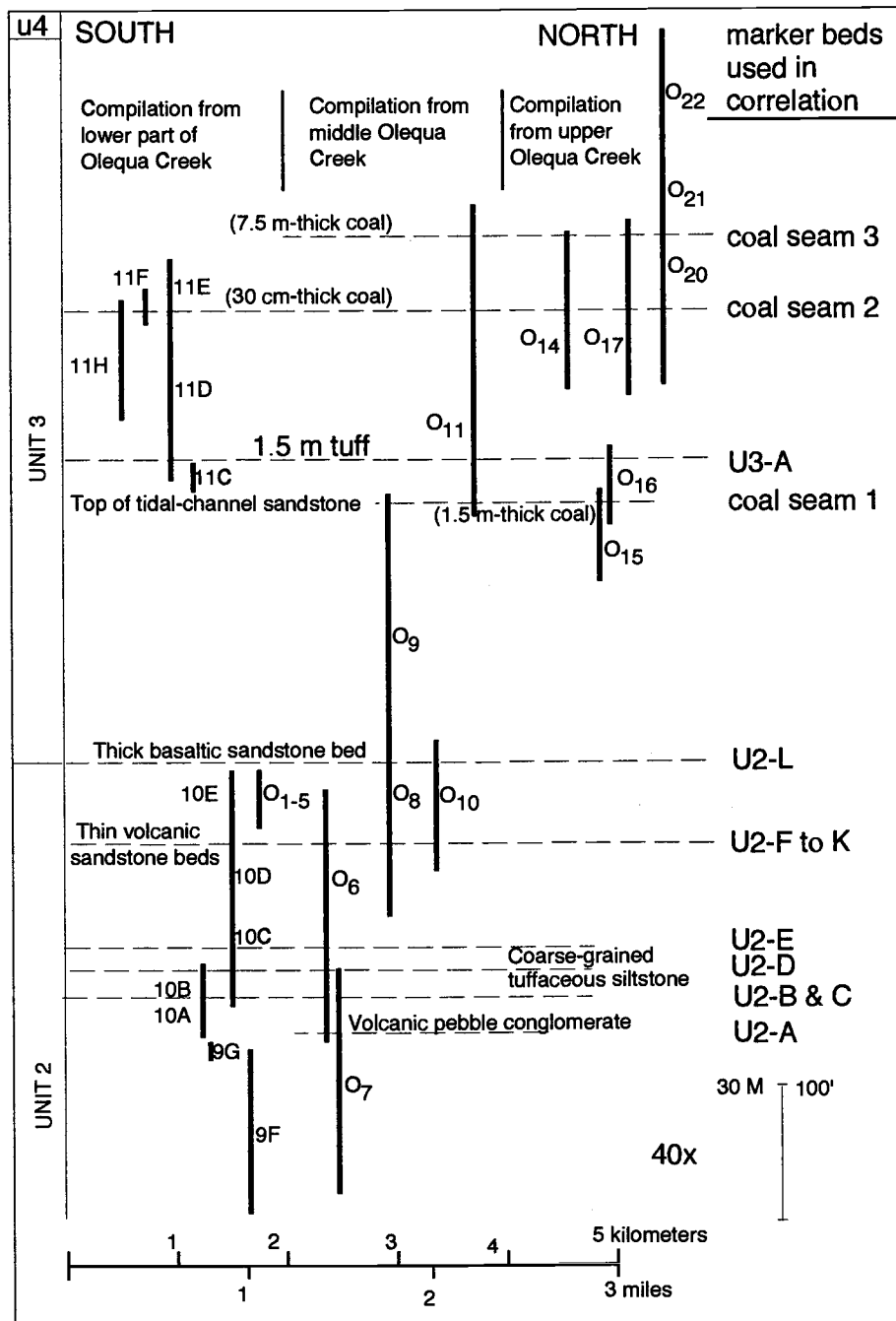


Figure 10. Measured-section correlation diagram for units 2 and 3 of the Cowlitz Formation showing marker beds used to construct the upper, middle, and lower Olequa Creek compilation sections (Plate III) and the master composite stratigraphic column (Plate II). The vertical lines represent the partial measured sections exposed in the creek bed and channel walls (see Plate I for locations).

upper part of unit 4 exposed in Olequa Creek (measured sections O29 to O32, Plates I and II) based on biofacies assemblages and lithologic similarity. The uppermost planar-laminated siltstone of unit 5 is 155-m thick and exposed along upper Olequa Creek and in a 20-m high roadcut 1.5 miles east of Vader (NW 1/4, Sec 27, T11N, R2W, Plate I).

Exposure is good along the lower reaches of Stillwater Creek and is nearly complete at the confluence with Olequa Creek (Sec. 32, T11N, R2W, Plate I). Olequa Creek is a larger creek than Stillwater Creek and has excellent exposures along much of its course. Sections were measured during late summer and fall when water level was lower, thus maximizing exposure in stream bed and channel walls. The following lithology ratios and exposure percentiles are from the composite measured section for Stillwater and Olequa creeks. Basal unit 1 of the Cowlitz Formation, with a combined total of 310 m of exposed section (55% exposure), has a sandstone/mudstone ratio of 1:1. This unit contains numerous coal seams that correlate with a lower coal-rich interval in the Shell Zion #1 well (Plate II). These coals were described in lithologic logs from this well and were identified from their characteristic, sharp resistivity spikes (Plate II). Sandstones were identified by a low resistivity response and a funnel shaped spontaneous potential curve. An 85-m thick poorly exposed beaver-dammed interval separates sections 7F to 7G2 and 7H to 8C of unit 1 (Plates I and II). Unit 2 is nearly completely exposed along Olequa Creek and is dominantly composed of volcanic and arkosic sandstone with subordinate mudstone (sandstone/mudstone ratio of 6:1). The heterolithic facies association of interbedded sandstone, siltstone, and mudstone that forms unit 3 has an overall sandstone/mudstone ratio of 1:4 and is completely exposed. Unit 3 also is a coal-bearing sandstone dominated member which correlates with an upper coal-rich interval in the Shell Zion #1 well (see lithology and electric logs, Plate II). Approximately 65% of mudstone-dominated unit 4 is exposed along Olequa Creek and has a sandstone/mudstone ratio of 1:8. The upper part of this unit is sandier in Olequa Creek than in exposures along

the Big Bend of the Cowlitz River, where the dominant lithology is sandy mudstone. The turbidite siltstone and submarine channel sandstone of unit 5 are 95% exposed along Olequa Creek. This unit has a sandstone to laminated siltstone ratio of 1:6 with most of the sandstone near the base of the member.

Other field exposures are mainly restricted to logging roadcuts and minor landslide scarps throughout the study area (outcrop localities are shown on Plate I). Unit 1 is the most extensively exposed member of the Cowlitz Formation in the study area. This unit crops out between Abernathy and Bebe mountains and north of Pumphrey Mountain to the middle part of Stillwater Creek. Scattered exposures of unit 2 were observed below Pumphrey Mountain and south of the confluence of Stillwater and Olequa creeks (Plate I). Units 3 crops out along the east side of Bebe Mountain in a limited number of exposures. Poorly exposed units 4 and 5 are observed mainly along the stream bed and cliff walls of Olequa Creek and the west banks of the Cowlitz River.

Lithostratigraphy and Contact Relationships

Unit 1A: Lower Marine Sandstone Sequences

Eight facies were recognized in unit 1A of the Cowlitz Formation. The first five are as follows: (1a) bioturbated and burrowed (middle shelf) sandy siltstone, (1b) thin-bedded, hummocky cross-stratified arkosic sandstone (storm-generated) and (fair-weather) siltstone deposits of the shelf to shoreface transition (1c) interbedded ripple laminated fine-grained sandstone and siltstone (lower to middle shoreface), (1d) thick, massive to swaley cross-stratified arkosic sandstone (middle to upper shoreface), and (1e) planar laminated sandstone (foreshore). These facies form the lowest coarsening- and thickening-upwards shoreface succession (measured section 6H, Plates I and II). Overlying this basal succession are multiple, coarsening-upwards micaceous, arkosic

sandstone shoreface successions of lithofacies 1c and 1d (sections 6I to 7E, Plate II).

Three other facies also occur in unit 1A and include: (1f) channelized arkosic sandstone, (1g) wavy-bedded, carbonaceous siltstone and fine-grained sandstone, and (1h) burrowed carbonaceous siltstone and coal. The 22-m thick heterolithic facies association of lithofacies 1f to 1h is present in the middle part of unit 1A (section 7C, Plate II).

The lowest coarsening- and thickening-upwards shoreface succession consists of lithofacies 1a to 1e (measured section 6H, Figure 11 and Plate II). The lower 10 m of section 6H is slightly laminated carbonaceous and sandy siltstone (lithofacies 1a) (Figure 11 and Plate II). Overlying the sandy siltstone is 12 m of thick-bedded, blue-gray, amalgamated, cliff-forming, massive to hummocky cross-stratified, micaceous, arkosic shoreface sandstone (lithofacies 1b) (Figure 12A). Each sandstone bed is gradationally overlain by wavy- and ripple-laminated sandy siltstone and sandstone of lithofacies 1c. Lenses of fine-grained sandstone contain micro-cross laminations defined by carbonaceous plant concentrations. Massive, ledge-forming, 40 cm-thick sandstones in lithofacies 1b are generally well-indurated and calcite-cemented. Some micro-cross laminated ripples in lithofacies 1c contain carbonaceous plant debris and coalified-wood fragments as large as 15 cm in diameter. Five intervals (average 5-m thick) of bioturbated siltstone coarsen upwards into ripple-laminated siltstone and thin-bedded sandstone in the middle of measured section 6G (lithofacies 1a and 1b) (Figure 11). The transition from the middle bioturbated siltstone facies 1a to the ripple-laminated lithofacies 1c contains vertical burrows (up to 5 cm long) of the *Cruziana* ichnofacies (Figures 11 and 12B). Sandstone beds become more common and thicker towards the top of this interval (at 32 m in measured section 6H) (Figure 11). One sandstone with bi-directional cross-bedding is overlain by rippled sandstone with siltstone drapes. The upper part of section 6H is composed of swaley cross-stratified (lithofacies 1d) and parallel-laminated (lithofacies 1e), fine-grained, micaceous, arkosic sandstone. The upper part of this shoreface sandstone is

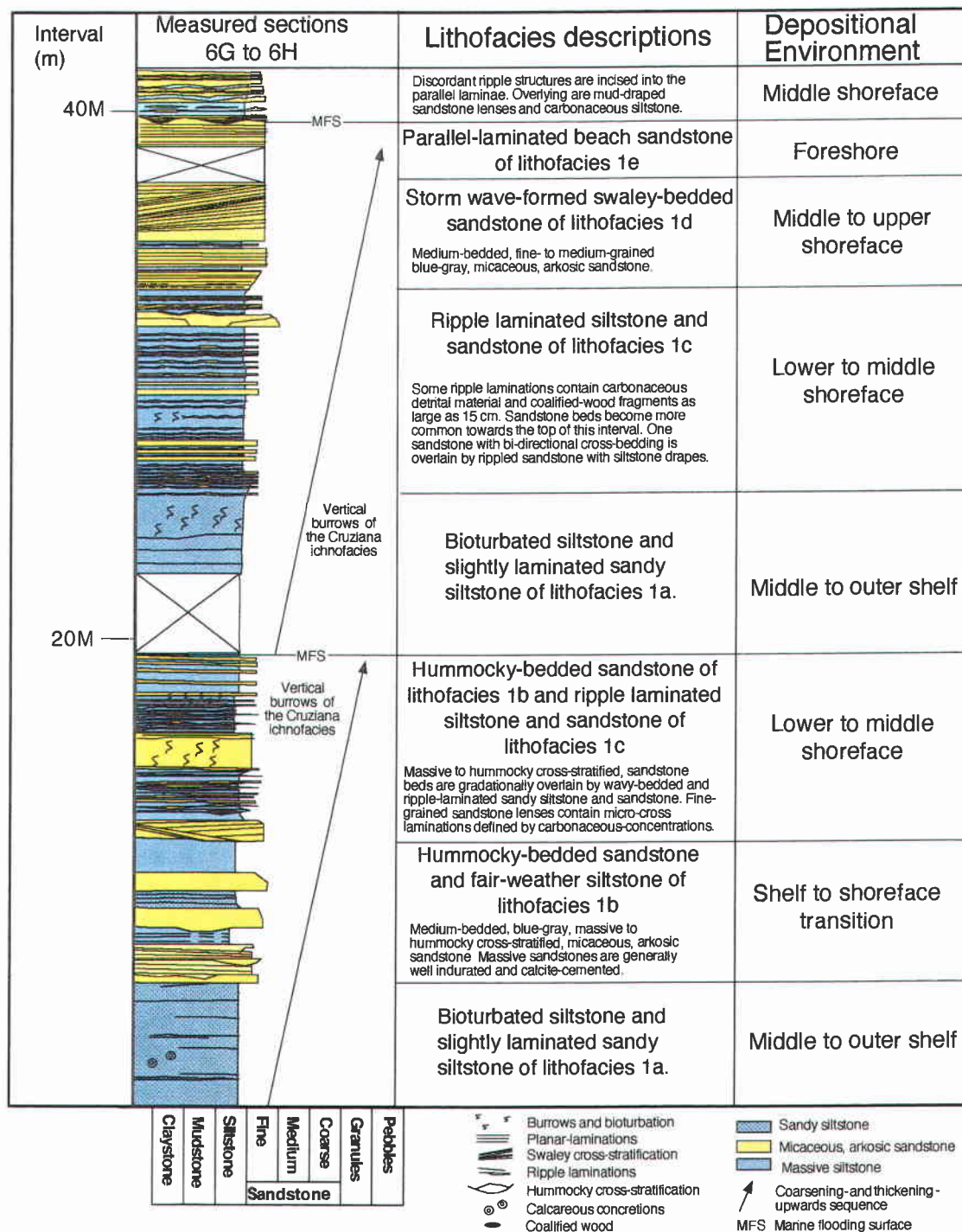


Figure 11. The prograding wave-dominated shoreface succession of the basal part of the Cowlitz Formation unit 1A exposed in Stillwater Creek at location 6H (interval 0 to 42 m, Plates I and II). This succession is composed of lithofacies 1a to 1e (SW 1/4, Sec. 26, T11N, R3W; Plates I and II).

A.



B.



Figure 12. Facies of the basal part the Cowlitz Formation unit 1A: (A) hummocky cross-stratified lower shoreface sandstone and siltstone (lithofacies 1b) and (B) bioturbated shelfal siltstone (lithofacies 1a) with burrows of the *Cruziana* ichnofacies (location 6H; SW 1/4, Sec. 26, T11N, R3W; Plates I and II). Note 25 cm rock hammer for scale.

completely planar, parallel-laminated. Discordant current ripple structures (1-3 mm high and 5 cm crest to crest) are incised into the carbonaceous parallel laminae (lithofacies 1c) (Figure 11). Overlying these current ripples are mud-draped sandstone lenses and carbonaceous siltstone.

Higher in the composite section, a 115-m thick, slope-forming interval (sections 6I to 7B, Plate II) is composed of two thickening- and coarsening-upward upper shoreface arkosic sandstone facies successions (lithofacies 1c and 1d) (Plate II). These clean, micaceous, sandstones are friable, moderately well to well-sorted, and fine- to medium-grained. Storm wave generated bedforms range from massive, parallel-laminated, to swaley and hummocky cross-stratified. Concentrations of very coarse mica and carbonaceous dark gray plant debris define finely laminated internal stratification. A moderately sorted, fine- to medium-grained, volcanic-lithic arkosic sandstone was sampled at 120 m in section 7A (petrology sample CP-94-105, Plate II). Subordinate massive, silty, very fine-grained sandstone and thin lenticular sandstone beds (sandstone lenses up to 3 cm-long) and sharp-bottomed, ripple-laminated sandy siltstone (lithofacies 1c) occur in the middle and upper part of this sandstone-dominated interval (Figure 13).

A thin, 10 cm-thick coal bed and 15-m thick carbonaceous siltstone (lithofacies 1h) in section 7C form the lowest coally interval in the Cowlitz Formation and belong to a 22-m thick heterolithic lithology facies association. This black coal is a cliff former while the carbonaceous siltstone beds are slope formers and are commonly covered. Channelized sandstone (lithofacies 1f) grades into sandy siltstone and intensively burrowed, carbonaceous siltstone overlies the thin coal seam. Sandstone of this interval is faintly cross-bedded and fine- to medium-grained. The top of this interval is composed of very thin-bedded, wavy laminated siltstone and very fine-grained sandstone with some carbonaceous laminations (lithofacies 1g) (Figure 13).

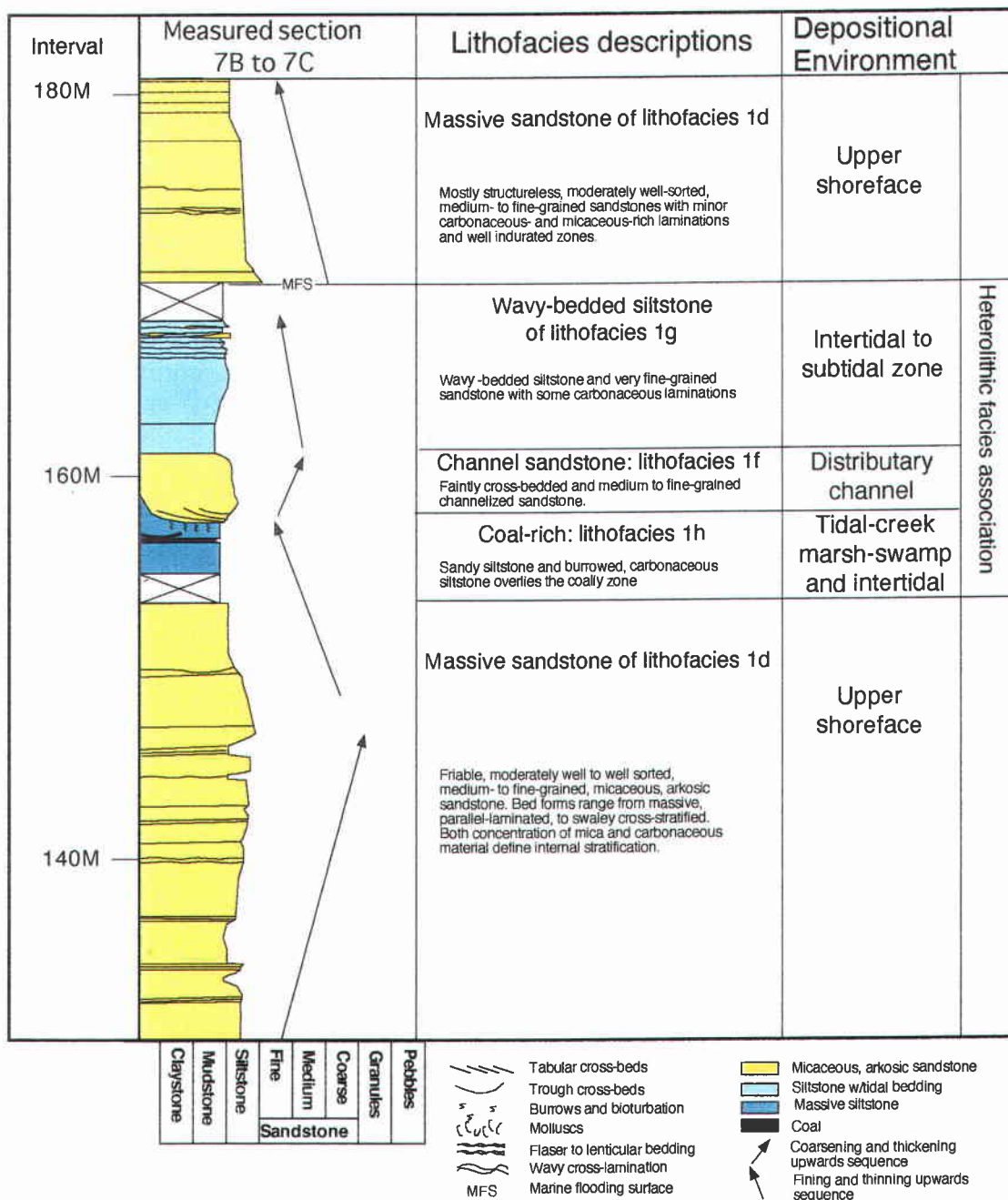


Figure 13. Micaceous, arkosic sandstone-dominated facies of the upper shoreface (lithofacies 1d) and the lowest coal-bearing heterolithic facies association (lithofacies 1f to 1h) of unit 1A of the Cowlitz Formation (locations 7B and 7C; SE 1/4, NW 1/4, Sec 26, T11N, R3W, Plates I and II).

Above this heterolithic facies association is a 103-m thick interval of multiple coarsening- and thickening-upward sandstone successions (top of 7C to base of 7F, Plate II). Dominant lithologies include silty sandstone and micaceous arkosic to arkosic-lithic sandstone (lithofacies 1d). The moderately well-sorted, fine- to medium-grained sandstones are mostly structureless (petrology sample CP-94-108). Faint carbonaceous- and micaceous-rich laminations and well indurated zones were also observed. Additionally, minor siltstone below these sandstone-rich intervals (in field-measured sections and increasing spontaneous potential response on logs from the Shell-Zion #1 well) show distinct coarsening- and thickening-upwards sandstone sequences (Plate II).

Unit 1B: Lower Coal-Rich Heterolithic Facies Associations

The upper 283 m of unit 1 (section 7F to 8C) is composed of interbedded coal and tidally influenced mudstone, siltstone, and sandstone. Five coal-rich intervals were measured, two in the lower and three in the upper interval of unit 1B. Lithofacies of unit 1B include: (1f) subtidal channel-fill sandstone and siltstone, (1g) wavy-bedded, carbonaceous siltstone and fine-grained sandstone, (1h) burrowed carbonaceous siltstone and coal, (1i) fossiliferous, subtidal channel sandstone, (1j) tuff and volcanoclastic facies and (1k) brackish-bay or estuarine siltstone. The sandy and mixed muddy intertidal-flat heterolithic facies association consists of a variety of facies and bedforms including flaser to lenticular sandstone and siltstone and the wavy-bedded siltstone of lithofacies 1g.

There is a distinct change in lithofacies associations above the sandstone-dominated lower part of unit 1 (at 275 m, Plate II). For instance, a 1-m thick indurated, mollusc-bearing, silty, lithic arkosic sandstone (lithofacies 1i) comprises the base of section 7F. This slope-forming, creek-bottom exposed, bed contains current-sorted, concave-up *Corbicula* or *Tellina* sp. bivalves (macrofaunal sample CP-94-109; Nesbitt, written communications, 1996), blue claystone layers, and up to 1 cm-in-diameter

coalified-wood fragments. Above this fossiliferous shell bed are interbedded thin siltstone, sandy siltstone, and fine- to medium-grained sandstone (intertidal facies association). This interval is wavy and flaser bedded with micro-cross laminated sandstone lenses and ripple-laminated siltstone (lithofacies 1g). Higher in the section, a medium-thick bed of massive arkosic sandstone underlies dark gray carbonaceous siltstone and a 2.1-m thick coal bed. Sharp-based, mollusc-bearing, silty, gray-green volcanic-lithic sandstone and siltstone lens (lithofacies 1f) overlie and are interbedded with this subbituminous coal (lithofacies 1h). Above the coals, a massive, micaceous, arkosic sandstone (lithofacies 1f) grades to siltstone and sandy siltstone and is capped by carbonaceous siltstone and a thin (0.5 m thick) coal bed (lithofacies 1h). A slightly indurated, moderately well-sorted, fine- to medium-grained arkosic sandstone is exposed above a 7-m thick covered interval (Plate II).

The lower 28 m of measured section 7G is composed of concretionary siltstone that is dominantly structureless (lithofacies 1a) (Plates I and II). Calcareous concretions are 1 m in diameter and are elliptical in shape. Subordinate ripple-laminated intervals with large carbonaceous plant debris fragments are also present. Overlying this massive siltstone facies is 4.5-m thick bed of fossiliferous, moderately sorted, silty, fine-grained sandstone (lithofacies 1i). This sandstone grades into bioturbated siltstone and coarsens upward to sandy siltstone with carbonaceous siltstone laminations. The top 10 cm of this bed consists of dark gray, very fossiliferous silty sandstone (lithofacies 1i) with a distinctive topmost 3 cm-thick shell-lag deposit containing *Corbicula olequahensis* and *Acutostrea idriaensis* bivalves and *Siphonalia sopenahensis* gastropods (Nesbitt, written communications, 1996) (macrofaunal sample CP-94-110; Appendix II) (Figure 14). An overlying sharp-based, lenticular thin-bedded mudstone and sandstone become flaser bedded and grade into massive siltstone upwards (lithofacies 1g). The middle and upper parts of section 7G and 7G2 (340 to 367 m on Plate II) are composed of thick-bedded



Figure 14. Highly fossiliferous, silty sandstone of lithofacies 1j (subtidal channel-bar) from unit 1B. Note distinctive 3 cm-thick shell-lag composed of a mix of 1 largely brackish water clams and a few intertidal specimens. This is interpreted as a shell lag formed by ebb/flood tidal currents concentrated in a subtidal sandstone channel in a tidal depositional system much like Willapa Bay of southwest Washington described by Clifton (1983). An overlying intertidal-flat facies consists of sharp-based, lenticular bedded mudstone and sandstone (lithofacies 1g) (location 7G, NW 1/4, Sec. 25, T11N, R3W). Five cm-wide grain-size card for scale.

massive siltstone, thin ripple-laminated carbonaceous siltstone, thin coal, and medium-bedded arkosic sandstone (lithofacies 1g, 1h, and 1k).

Measured section 7H is 29 m thick. It is composed of a basal sandstone and siltstone interval and a thick black coal with numerous light buff altered tuff partings (lithofacies 1h and 1j) (Plate II). The base of this section is 3 m of light gray-blue, micaceous, very fine-grained arkosic sandstone (lithofacies 1f). The sandstone contains thin beds with tangential foreset micaceous laminations. The overlying 1.5 m of micaceous, bioturbated siltstone grades to carbonaceous mudstone (an underclay) and underlies a 60 cm-thick coal bed (lithofacies 1h). Above this coal bed is a mollusc-rich (*Corbicula willisi*), silty very fine-grained sandstone (macrofaunal sample CP-94-111, Appendix II) and an overlying flaser-bedded siltstone and sandstone that becomes massive near the top of the section.

From 462 to 474 m, a 11.6-m thick coal (lithofacies 1h) with vitrain bands forms resistant ledge-forming, blocky-weathered medium to thin beds containing minor carbonaceous parallel laminae and nine light buff altered tuff partings (lithofacies 1j). These tuff interbeds range from 3 cm to 1.3 m in thickness. Granular (altered pumice) lapilli to fine-ash tuff beds range from white-yellow to grayish, to dark gray (organic-rich). Some volcanoclastic beds contain dark gray mudstone rip-up clasts and detrital quartz grains. Most beds are structureless but some normal graded beds are present.

The heterolithic facies association overlying the coal bed in measured sections 7I and 8A (477 to 492 m, Plate II) and the lower part of section 8C (520 to 532 m, Plate II and Figure 15) are composed of the following facies: (1) flaser, wavy, and lenticular bedded siltstone and very fine-grained sandstone, (2) thinly laminated to massive, bioturbated siltstone, (3) dark-gray ripple-laminated siltstone with minor (4 mm thick) micro-cross-laminated sandstone lenses, (4) soft-sediment contorted-bedded sandstone and siltstone, (5) carbonaceous siltstone facies, and (6) thin, trough cross-bedded

sandstone beds. Some 10 cm-thick, medium-grained, sandstone lenses and mud-draped foreset laminations (interpreted as tidal bundle sequences) are also present. A 7-m thick thickening-upwards facies association in measured section 8C (535 to 542 m, Plate II) consists of alternating thin beds of trough cross-bedded, fine-grained sandstone and contorted- to wavy-bedded siltstone and sandstone (lithofacies 1g).

Fine- to medium-grained, thin bedded, trough cross-bedded, micaceous arkosic sandstone (lithofacies 1f) that becomes thick-bedded, massive, and carbonaceous comprises the upper few meters of section 8A and most of section 8B (492 to 500 m, Plate II). A 1.5 m trough cross-bedded, moderately well-sorted, medium-grained, micaceous arkosic sandstone and laminated siltstone/sandstone (547 to 549 m, Plate II) overlies the heterolithic facies association in section 8C. Three meters of silty, moderately sorted, very fine-grained sandstone with minor carbonaceous sandstone lenses and an uppermost dark-gray sandy siltstone overlies the cross-bedded sandstone facies (Figure 15).

The top of section 8B (500 to 505 m, Plate II) contains a channel-fill lithofacies (1f) consisting of a basal dark gray carbonaceous mudstone, coal, carbonaceous siltstone, and a 3 cm reworked tuff (geochemical sample CP-94-113, Appendix IV). These strata are incised 1.5 m into the underlying strata along the 15 m-long exposure in Olequa Creek. Three fining-upwards tidal-channel deposits comprise a 3-m thick interval in section 8C (536 to 539 m on Plate II and Figure 15). The lowest channel-fill consists of dark gray, bioturbated, sandy siltstone that grades upward into discordant and lenticular- to wavy-bedded siltstone and very fine-grained sandstone. Chunks of coalified wood (up to 7 cm in diameter) are found in the base of this channel-fill. The second channelized interval is filled with orange (iron oxide stained), sandy siltstone and lenticular to massive, very fine-grained sandstone. This sandstone grades upward into sandy, micaceous

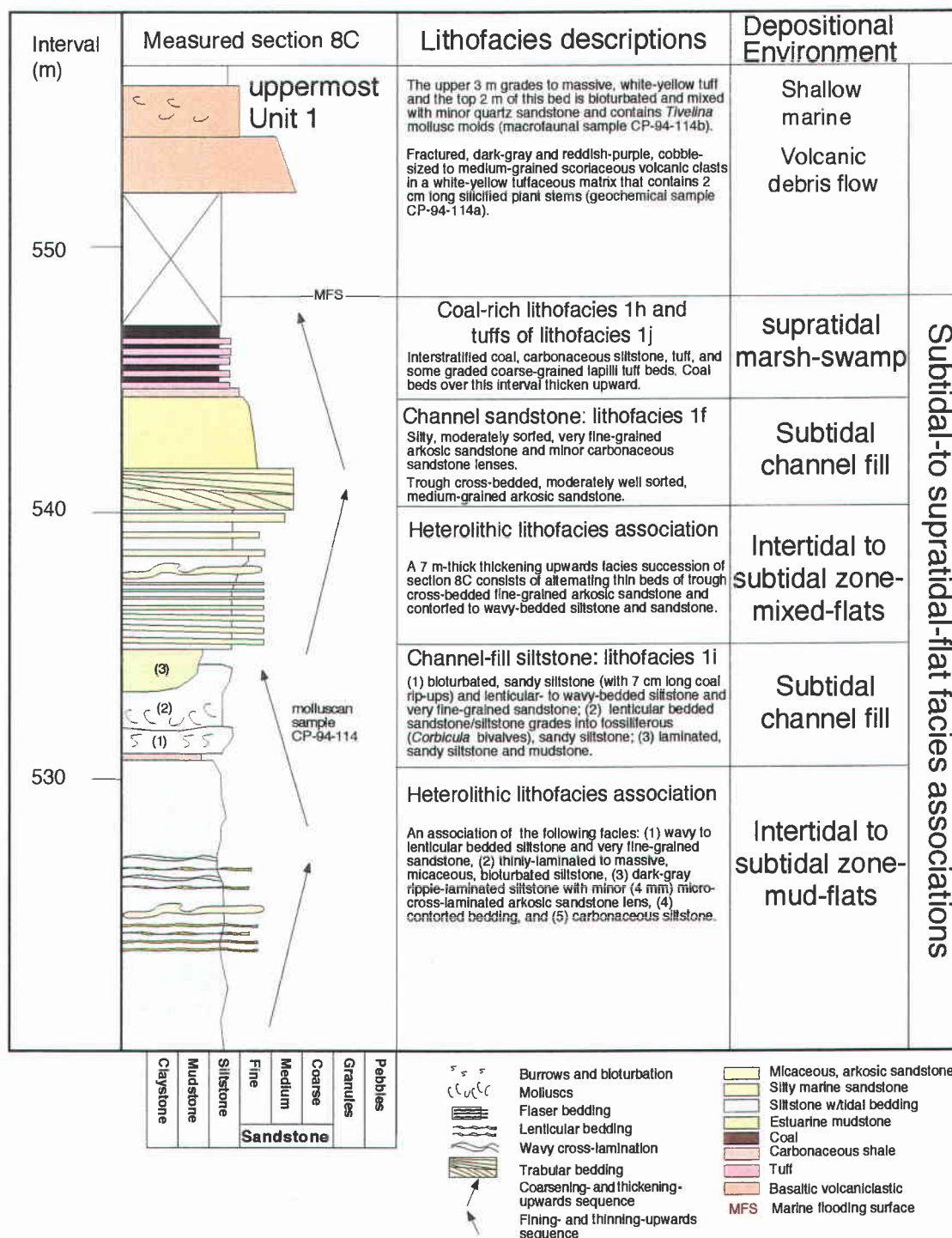


Figure 15. Stratigraphic column of the subtidal- to supratidal-flat facies associations that include: a heterolithic facies association, tidal-channel sandstone, coal, and volcanoclastic beds (lithofacies 1f, 1h, 1i, and 1j) from the uppermost 30 m of unit 1 of the Eocene Cowlitz Formation (measured section 8C, Plate II; NE 1/4, Sec 25, T11N, R3W).

siltstone containing disarticulated *Corbicula willisi* and *Acutostrea idriaensis* bivalves (Nesbitt, written communications, 1996) shell lags (macrofaunal sample CP-94-114, Appendix II). An uppermost channel-fill deposit consists of laminated sandy siltstone that grades-upward into an overlying siltstone and a fissile mudstone (Figure 15).

The top 12 m of unit 1 of the Cowlitz Formation is composed of coal and interbedded, light buff, fine-grained tuff and volcanoclastic beds. The upper part of measured section 8C consists of 2.5 m of interstratified coal, carbonaceous siltstone, light buff fine-grained tuff, and graded coarse-grained lapilli tuff beds (Plate II). Lignitic to subbituminous coal beds in this interval thicken upward. Overlying this coally interval is a 4.5-m thick pebbly volcanoclastic sandstone composed of fractured, dark-gray and reddish-purple, cobble to medium-sand-size scoriaceous volcanic fragments. Two cm long silicified plant stems are contained in a white-yellow tuffaceous siltstone matrix (geochemical sample CP-94-114a, Appendix III). The top 5 m of this section becomes tuffaceous and is bioturbated, mixed with minor micaceous arkosic sandstone, and contains shallow marine *Tivelina* sp.? mollusc molds (Nesbitt, written communications, 1996) (macrofaunal sample CP-94-114b, Appendix II).

Unit 2: Middle Marine Mudstone and Sandstone Sequences

Unit 2 differs from the other units in that it contains a significant amount of volcanic clasts intermixed with silty arkosic sandstone, contains no coals, and in the upper part contains shelfal mudstone that is quite distinct from units 1 and 3. The contact between units 1 and 2 is covered.

Lithofacies of the 205-m thick unit 2 include: (2a) molluscan bearing, coarse-grained, volcanic sandstone, (2b) marine, bioturbated silty sandstone, (2c) mudstone conglomeratic, arkosic sandstone, (2d) basaltic arkosic sandstone, (2e) mudstone to siltstone sequences, and (2f) volcanic conglomerate and thin-bedded volcanoclastic

sandstone. Exposure is nearly continuous along Olequa Creek (stream bed and channel walls) with numerous stratigraphic sections repeated by faulting (Figure 10 and Plate I).

The lower 20 m of unit 2 is poorly exposed in the stream bed of Olequa Creek but shows a coarsening upward from mudstone to arkosic sandstone (lithofacies 2e and 2d). Lithologies and bedding include graded, thin to thick, siltstone to mudstone beds, coarsening-up, fine- to very coarse-grained volcanic sandstone, and some fine-grained, moderately well-sorted, micaceous arkosic sandstone near the top of this lower interval (sections 9A-9C, 8F2 on Plate II).

This arkosic sandstone is overlain by a 12-m thick, molluscan fossil shell-rich, basaltic volcanic, silty sandstone (lithofacies 2a) in measured section 9C (578 m to 590 m, Plate II). Grain size increases from very fine- to medium- and coarse-sand-size with minor pebbly layers (petrology sample CP-94-121). Grain-size variation in this coarsening upwards volcanic sandstone is gradational. Beds are moderately poorly-sorted, thick-bedded, and massive. Minor vertical *Thalassinoides* burrows (10 cm high and 1 cm wide) of the inner neritic *Skolithos* ichnofacies (Figure 8) (Pemberton and MacEachern, 1992) are present between fossiliferous layers. Scour-and-fill structures and basal shell-lag contacts are the only discrete surfaces in this facies. Seven well indurated, graded, molluscan shell-lags occur at the base and middle of this unit (582 and 588 m, measured sections 9C and 8G, Plate II) (macrofaunal samples CP-94-121a and CP-94-121b, Appendix II). These fossiliferous zones contain disarticulated, concave-up, and current-sorted *Acutostrea idriaensis*, *Glycymeris sagittata*, *Thracia dilleri*, *Gari* sp., *Pitar eocenica*, *Tellina cowlitzensis*, and *Venericardia hornii clarki* bivalves, and high-spined *Turritella uvasana olequahensis*, and *Calyptraea diagoana* gastropods (Nesbitt, written communication, 1996).

Stratigraphically overlying this basaltic silty sandstone is a distinctive arkosic sandstone with abundant mudstone clasts (lithofacies 2c) (589 m, section 9C, Plate II).

This 90 cm-thick marker bed is composed of abundant cobble-sized angular mudstone rip-ups in a medium-grained, micaceous arkosic sandstone. This sandstone has a sharp, erosional basal contact with the underlying mollusc-bearing, volcanic sandstone.

Gradationally overlying this mudstone rip-up rich sandstone is a 31-m thick silty, fine-grained, micaceous, lithic arkosic sandstone lithofacies (2b) (590 m to 624 m, measured sections 9D and 9E, Plate II) with one mudstone (lithofacies 2e) interbed. The lower part of this interval is burrowed to intensively bioturbated and moderately-sorted. A distinctive 76 cm-thick mudstone sequence (lithofacies 2e) composed of three graded beds of fine- to coarse-grained, altered volcanic and mudstone clasts in a muddy matrix occurs at interval 609 m (marker bed in sections 9C, 9D and 9E, Plate I). The upper part of this interval consists of 9 m of blue-gray, massive, moderately well-sorted, very fine-grained arkosic sandstone (lithofacies 2b) that coarsens-upwards into a fine-grained sandstone with minor indurated calcareous zones (section 9E). Above this is 7 m of alternating sparsely fossiliferous to burrowed sandstone. These *Thalassinoides* burrows are L-shaped with a 25 cm-long vertical part and 10 cm-long horizontal lower part (Figure 16A).

A mudstone rip-up conglomeratic sandstone lithofacies 2c (storm wave-generated) is in sharp contact with the underlying silty sandstone in section 9E (Plate I). This rip-up sandstone is 7 cm- to 15 cm-thick and is composed of pebble-sized grayish green, altered volcanic sandstone rip-ups and broken bivalves in a medium gray-blue, fine-grained arkosic sandstone. Medium bedded, medium- to coarse-grained, volcanic-lithic sandstone beds contain multiple molluscan shell beds (Figure 16B). These fossil shell-lags consist of disarticulated and broken *Siphonalia sopenahensis*, *Whitneyella oregonensis*, and *Calyptraea diagoana* gastropods, *Cadulus gabbi* scaphopods, *Peteria clarki*, *Telina* sp., *Pachydesma aragoensis*, and large articulated *Venericardia hornii clarki* bivalves; a biozone typical of the *Turritella-Tivelina* shallow marine assemblage of Nesbitt (1995 and written communications, 1996) (macrofaunal sample CP-94-124, Plate II, Appendix II).

A.



B.



Figure 16. (A) Silty sandstone (lithofacies 2a) from the lower part of unit 2 of the Cowlitz Formation containing *Thalassinoides?* burrows of the *Skolithos* ichnofacies at location 9E and (B) fossiliferous, volcanic sandstone bed (lithofacies 2a) from section 9C (Plate II). Note bivalve and gastropod species in this shell lag deposit (macrofaunal sample CP-94-124, Plate II) are typical of the *Turritella-Tivelina* shallow marine inner neritic assemblage of Nesbitt (writ. comm., 1996) (NW 1/4, Sec. 30, T11N, R2W). Note 2.5 cm-diameter coin for scale.

Overlying is a sequence of very fine-grained arkosic sandstone beds that each grade into finely laminated siltstone and fractured mudstone containing white to buff volcanic clasts (altered scoria).

A distinctive 53-m thick sharp-topped arkosic sandstone (lithofacies 2d) occurs between 632 and 685 m in measured sections 9F, 9G, 10A, and lower part of section 06 (Figure 10 and Plate II). Alternating fine- to medium-grained, amalgamated, arkosic sandstone with micaceous laminations and minor interbedded very coarse-grained volcanic sandstone (petrology sample CP-94-125, Appendix II) were measured at locality 9F. Medium gray-blue (fresh) and iron oxide-stained yellow-orange (weathered), massive to slightly laminated and cross-bedded arkose is exposed along measured section location O7 (Plate II). This well-sorted, very fine- to fine-grained, mica rich sandstone interval contains minor wavy and planar laminations, calcareous concretionary horizons (45 cm wide and 15 cm thick) and coarse-grained, volcanic sand-filled vertical *Skolithos* burrows near the upper part of this interval.

Overlying this arkosic sandstone is a distinctive 2-m thick graded, volcanic clast-supported, sandy, granular to pebble volcanic conglomerate (lithofacies 2f) with a 40 cm-deep erosional, basal contact in measured section O7 (695 to 698 m, Plate II). The conglomerate consists of coarse-sand- to pebble-sized subrounded clasts of dark basalt and rounded pumice clasts up to 2 cm in diameter (petrology sample CP-94-159, Appendix IV). The clasts are mainly in clast-support and encased in a silty fine-grained lithic arkosic sandstone matrix. Grain size of the volcanic component of this conglomerate varies vertically from 50% coarse-sand- to pebble-sized clasts at the base to 20% coarse and very coarse-sand-sized clasts at the top. Sparsely fossiliferous shell lags occur near the base of this conglomerate. In the lower part of this interval are very coarse-grained silty, tuffaceous, sandstone-filled vertical *Thalassinoides*? burrows (30 cm long and 2 cm in diameter) with burrow-diameter increasing at base (flares out). This bed, 250 m along

strike, becomes 30 cm-thick and is composed of medium- to coarse-grained volcanic arkosic sandstone mixed with well-rounded dark scoriaceous basalt and altered pumice clasts and displays a sharp-basal contact in measured section O6 (Plate II). A 15-cm thick reversely graded bed of pebbly tuffaceous sandstone with a sharp basal contact in measured section 9G (757 m to 760 m) is similar to the sandy conglomerate that occurs at 749 m in section O7. Fossiliferous, volcanic-lithic, silty sandstone of lithofacies 2a appears again 0.6 m above this sandy conglomerate facies in section 9G. This 1.5-m thick bioturbated to slightly laminated silty, fossiliferous sandstone (macrofaunal sample CP-94-126, at 760 m, Plate II) contains straight and vertical shoreface *Skolithos* burrows (3 cm high and 1 cm in diameter) (petrology sample CP-94-126).

A distinct and sharp change in lithology (from sandstone to siltstone) begins at 695 m (Plate II) in Olequa Creek. A 26-m thick grayish to brown-gray, concretionary, micaceous, sandy siltstone succession (lithofacies 2e) overlies the coarse-grained sandstone and conglomerate. Strata in this succession are massive to mottled, very thinly bedded to thickly bedded, and moderately-sorted to poorly-sorted. The siltstone contains multiple, interspersed, diffuse volcanic-rich layers and minor sparsely fossiliferous layers. Microfaunal sample CP-94-158A (inner neritic water depths) from section O6 (Plate II) contains *Cibicides* spp.?, *Elphidium californium*, and *Quinqueloculina imperialis* foraminifera, pyritized diatoms, radiolarians, Ostracods, and fish debris (McDougall, written communications, 1997). Some siltstone is inter-mixed by bioturbation with granular to pebble lapilli tuff and weathered, black porphyritic basalt clasts. Indurated calcareous concretionary beds or ledges are mostly massive siltstone but some contain small channel-fill volcanic sandstone lenses composed of scoriaceous volcanic grains mixed with siltstone rip-up clasts. The upper part of this interval coarsens upward from sparsely fossiliferous siltstone to indurated, silty, very fine-grained arkosic sandstone that contains a 5-cm thick graded, granular basaltic sandstone.

Interbedded with this siltstone facies succession are four volcanic-rich sandstones (lithofacies 2f) that are marker beds (U2-A through -L) used in section correlation (Plate II and Figure 10). Marker U2-A in measured sections 10A and 10C is a 15 cm- to 30-cm thick, pebbly, medium-grained basaltic sandstone bed. A 30 cm-thick interval in measured section O6 is composed of two repeated units of reversely graded thinly laminated claystone that grade into dark gray, medium- to coarse-grained volcanic sandstone (marker beds U2-B and -C, Figure 10). In measured section 10A, a 3 cm-thick, normally graded, medium-grained basaltic sandstone forms marker interval U2-C (petrology sample CP-94-127). This marker bed varies laterally in thickness from 2 cm to 4 cm over 60 m of outcrop. Marker interval U2-D in section 10C is a 5.5-m thick coarsening-upwards light-blue to reddish-brown (weathered), burrowed, coarse-grained tuffaceous siltstone and sandy siltstone interbedded with minor micaceous siltstone. The siltstone coarsens upward into a poorly sorted, coarse-grained to pebbly, volcanic-lithic, sandy, micaceous siltstone that contains some mudstone rip-ups. In nearby measured section O6, the upper part of marker U2-D is 2.5-m thick and grades from gray, burrowed (vertical to pod-shaped burrows) siltstone to dark gray, fossiliferous sandy siltstone mixed with granular to medium-grained vesiculated basalt clasts. The upper part of marker interval U2-D in nearby section 10B is 1.5-m thick and consists of coarsening-upwards, reddish-tan, massive siltstone with interspersed pebble-sized to medium-sand-sized, light tan, volcanic (basaltic) clasts. Marker interval U2-E (sections O6 and 10C) is composed of a 15 cm-thick bed of indurated, moderately sorted, grayish blue, silty sandstone and a thin-bedded volcanic silty sandstone.

A 23-m thick friable, micaceous, lithic arkosic sandstone (lithofacies 2d) (section O6 and 10C-10D) and volcanic sandstone (lithofacies 2f) (721 to 743 m, Plate II) overlies the lower siltstone sequence. The lower part of this interval is composed of massive, very fine-grained, arkosic sandstone with numerous irregular-shaped calcareous concretions

and burrowed, fine- to medium-grained, volcanic arkosic sandstone. Shelfal *Thalassinoides* burrows are 1 m long and 3 cm in diameter and mostly horizontal with some being vertical. *Thalassinoides* burrows are characteristically found in shelfal neritic depths (Niem, written communications, 1998). One 1-m thick, sandstone bed is hummocky cross-stratified. The upper part of this sandstone sequence is composed of massive, concretionary, well-sorted, and fine- to medium-grained sandstone. Medium beds of moderately to poorly sorted, volcanic arkosic sandstone and minor cut-and-fill, coarse-grained, volcanic sandstone are more abundant towards the middle and upper part of this sequence. Interbedded with this sandstone dominated sequence is an unusual basaltic volcanoclastic sandstone (lithofacies 2f) that occurs only in measured section 10C-10D (738 to 741 m, Plates I and II). This 2.5-m thick interval is composed of two, indurated, coarse-grained to granular, scoriaceous basaltic sandstone beds (petrology sample CP-94-130a). Minor lenticular, coarse-grained, sandstone is interbedded with indurated, medium-grained, volcanic-lithic arkose.

A second distinct and sharp change in lithology (from sandstone to mudstone) begins at 743 m (Plate II) in Olequa Creek. This upper mudstone sequence (21 m thick) generally correlates between measured sections O8, O10, O1-5, and 10E (Figure 10, Plate II). This interval consists of coarsening-upwards mudstone and volcanic sandstone interbeds. The lower 2 m of this interval is composed of olive-gray, micaceous, massive mudstone that coarsens upwards to light-gray, bioturbated, silty mudstone. Foraminifera from sample CP-94-130b include inner neritic *Dentalina consobrina*, *Elphidium californium*, and *Nonionellina applini* species (McDougall, written communications, 1997).

Interbedded with this mudstone are distinctive, sharp-based and normally graded, basaltic, silty sandstone beds that contain medium- to coarse-grained, grayish green, altered volcanic clasts (marker beds U2-F to K) (Figures 10 and 17). In addition, some of



Figure 17. Mudstone facies succession and a normally graded, medium- to coarse-grained, framework-supported, altered volcanic sandstone from the uppermost part of unit 2 of the Cowlitz Formation (measured section O10, Plate II; NW 1/4, Sec. 29, T11N, R2W, Plate I). Note 2.5 cm-in-diameter coin for scale.

these sandstone beds contain coarse-grained, volcanic sandstone-filled burrows and bivalve molds. One 30-cm thick interval is composed of three thin, sharp-based, lenticular medium-grained volcanic-lithic sandstone beds that each grade into tuffaceous mudstone (2 cm-, 3 cm-, and 4 cm-thick). An overlying 11-cm thick bed of poorly sorted, fine- to coarse-grained volcanic sandstone is ripple-laminated (marker bed U2-I).

A 12-m thick mudstone to silty sandstone facies succession (lithofacies 2c and 2b) forms the top of unit 2. Dark gray, thinly bedded to massive, micaceous, silty mudstone and sandy siltstone with shell fragments and crab claws and carapaces (microfaunal sample CP-95-156, Appendix II) form the base of this sequence. This siltstone grades into 3 m of mottled (dark gray and gray) burrowed, silty sandstone. The silty sandstone is sparsely fossiliferous (macrofaunal sample CP-95-157, Appendix II) and contains *Acanthocardia brewerii* bivalves and *Turritella uvasana stewarti* gastropods (Nesbitt, written communications, 1996). Near the top of unit 2, an abundantly fossiliferous 1.5-m thick molluscan shell lag horizon is composed of very shallow marine *Pteria clarki* bivalves (Nesbitt, 1996) (macrofaunal sample CP-94-131, Appendix II).

Unit 3: Upper Coal-Rich Tidal Facies Associations

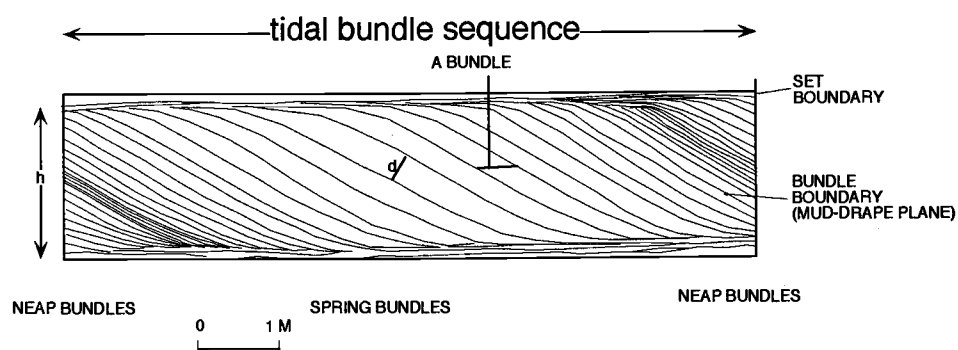
Three fining-upward heterolithic tide-dominated facies associations of unit 3 consist of the following lithofacies: (3a) coarse-grained basaltic sandstone (reworked debris flow), (3b) sigmoidal and tangential cross-bedded, mudstone-draped arkosic sandstone (subtidal-channel megaripple cross-bedding), (3c) wedge cross-bedded arkosic sandstone (sandy subtidal channel), (3d) fossiliferous silty sandstone (subtidal-channel mouth bars), (3e) vertically-stacked tidal rhythmites and flaser to lenticular bedded sandstone, siltstone and mudstone (tidal point bars and tidal-flats), (3f) massive and fossiliferous mudstone (tidal estuary mud-flat and muddy accretionary banks) (3g) numerous carbonaceous siltstone and coal-bearing intervals (supratidal marsh/swamp), including one thick coal bed (referred to as coal seam C), and (3h) basaltic and pumice lapilli volcanoclastics (pyroclastic and hyperconcentrated flows). These facies form the following three facies associations: (TC) nested, amalgamated subtidal-channel sandstone (lithofacies 3a, 3b, 3c and 3d), (TF) tidal-flat and point bar (lithofacies 3e, 3f), and (ST) supratidal marsh/swamp (lithofacies 3g and 3h) (Plates II and III).

The upper 6 m of section O10 consists of a poorly sorted, coarse-grained basaltic sandstone of lithofacies 3a (a reworked debris-flow deposit in a nested subtidal channel) that is in sharp contact with underlying shelfal, muddy siltstone at the top of unit 2. The basal 18 cm of unit 3 is composed of three, planar, thinly bedded, subangular, very coarse-grained to granule-sized volcanic sandstone beds. Clast compositions include tuff, basalt, and mudstone fragments. Minor scour-and-fill structures are apparent in the upper two beds. Above the basal 18 cm of unit 3, a 3-m thick calcite-cemented, sparsely fossiliferous, burrowed, muddy and pebbly, coarse-grained basaltic sandstone bed (subtidal channel-fill deposit) is in erosional, basal contact with the underlying planar-laminated bed (petrology sample CP-94-162b). An overlying nested, channel-fill deposit is up to 3-m thick and thins to 1.5 m. This channel deposit is composed of a basal, sandy

siltstone and an overlying sparsely mollusc-bearing granular to coarse-grained basaltic sandstone. A third, overlying 4.5 m-to 3-m thick channel-fill deposit consists of a basal, silty sandstone that grades upward into a tuffaceous silty mudstone and then into a light tan mudstone. A similar 6-m thick deposit is evident along section location O8 (Plates II and III). The lower 5 m in this section is composed of sparsely fossiliferous (*Corbicula willisi*?, molluscan sample CP-95-161, Appendix II), basaltic sandstone that contains a bluish mudstone matrix. This coarse-grained, cliff-forming basaltic sandstone fines upward into fine-grained volcanic arkosic sandstone.

The overlying 36 m of strata (lithofacies associations TC and TF) exposed along section location O9 (Plates II and III) consist of four fining- and thinning-upwards arkosic sandstone, siltstone, and mudstone sequences of lithofacies 3e, mudstone-draped megaripple arkosic sandstone of lithofacies 3b, and wedge cross-bedded arkosic sandstone of lithofacies 3c. These 6 m- to 21-m thick, fining-upwards successions consist of the following lithologies and sedimentary structures: (1) lenticular to wavy bedded very thin-bedded mudstone, siltstone and arkosic sandstone, (2) thin-bedded, planar- and ripple-laminated carbonaceous, sandstone and mudstone (3) very thin-bedded, flaser bedded sandstone and mudstone, (4) thinly bedded, cross-bedded sandstone with mud-draped foresets (Figure 19A and B) and minor herringbone cross-stratification, and (5) thick beds of megaripple sandstone consisting of sigmoidal, trough cross-bedded, medium- to coarse-grained, lithic-arkosic sandstone and micaceous arkosic arenite. The uppermost 11.5 m of this interval consists of thinly bedded, planar-laminated to sigmoidal cross-bedded, fine-grained, micaceous, arkosic-lithic sandstone (petrology sample CP-94-134a). Sedimentary structures include contorted bedding and tidal-bundle sequences (Figure 18A) consisting of dark gray mud-draped to mica-concentrated foreset laminae (Figure 19A and B) and mudstone-draped reactivation surfaces (Figure 20A). The top of section O9, the bottom of O16 and O11, 11B, and O15 (810 m, Plate III) contains

A.



B.

Vertically-stacked Sandstone And Mudstone
from Mont St. Michel Bay, France

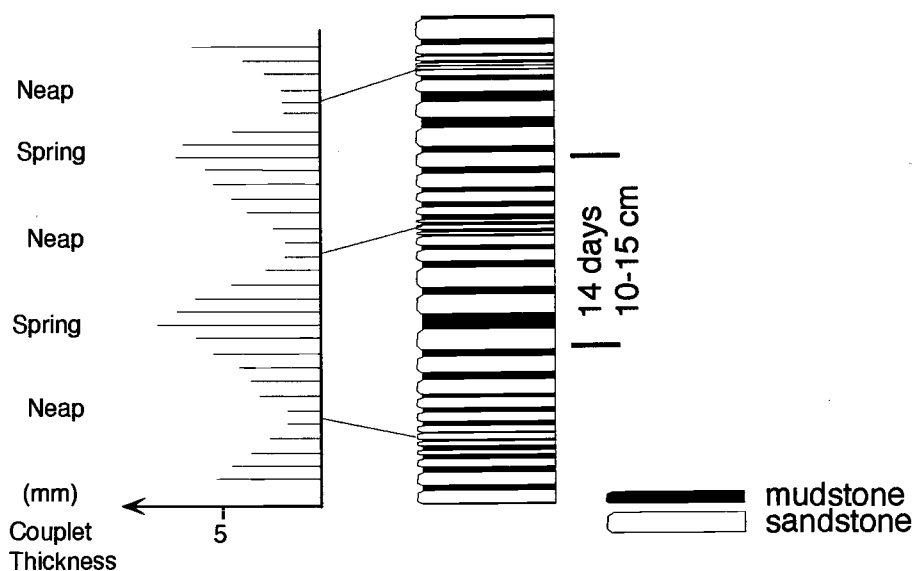


Figure 18. Unique characteristics of clastic tidal deposits recording tide fluctuation cycles: (A) tidal bundle sequences (schematic) and (B) vertically stacked, thinly laminated tidal rhythmites (from the recent Mont Saint-Michel Bay, France) (after Yang and Nio, 1985). The bundle boundaries have thin mud drapes and/or erosional reactivation surfaces. Mudstone drapes in tidal-bundle sequences and vertically-stacked tidal rhythmites were deposited during dominant and subordinate current reversals (slack-water). Variation in mudstone drape and sandstone foreset thickness record neap-spring tidal cycles (14 day cycles).

A.



B.



Figure 19. Tidal megaripple cross-bedding in the lower part of Cowlitz Formation unit 3 (section location O16, SW 1/4, Sec. 17, T11N, R2W, Plates I and II). (A) Sigmoidal cross-bedded and mudstone-draped micaceous arkosic sandstone (30 cm mark on bottom of Jacob's staff for scale). (B) Close-up of mud couplets formed after passage of dominant and subordinate currents when slack-water muds settle-out and armor foresets and bottomsets, thus preserving bedforms from later tidal current erosion (5 cm grain-size card for scale).

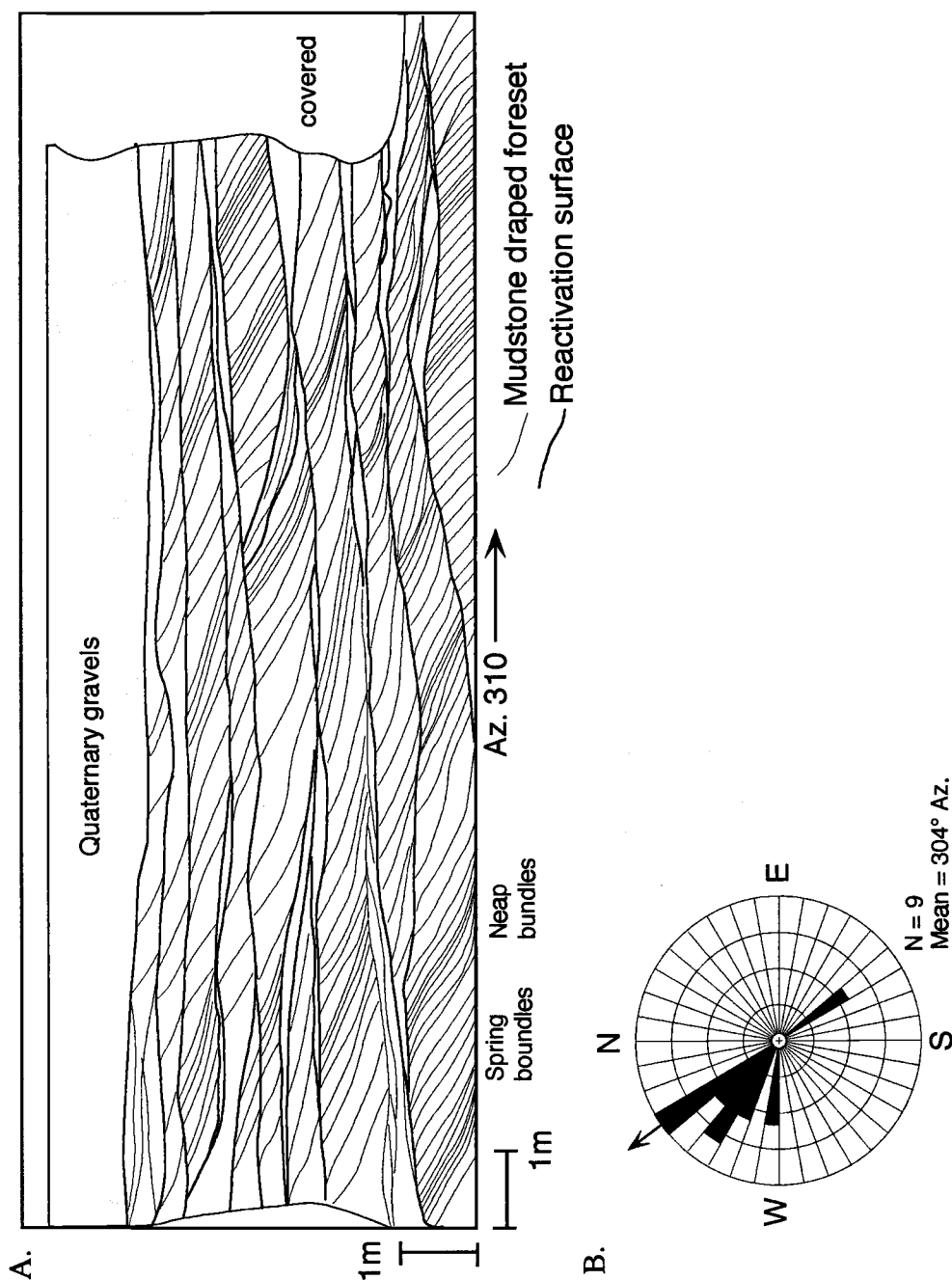


Figure 20. (A) Field sketch of tidal megaripple cross-bedded arkosic sandstone of a subtidal channel with mud-draped tidal bundle sequences bounded by wavy reactivation surfaces and (B) rose diagram of paleocurrent orientation measurements of cross-bedded tidal sandstone foresets at this location (measured section O16 in Olequa Creek, Plate II; SW 1/4, Sec. 17, T11N, R2W, Plate I). The predominately northwest trend reflects dominantly ebb flow while the southeast trend reflects a weaker flood tide in this part of the section (similar pattern occurs in modern subtidal cross-bedded sandwaves in subtidal channels of Willapa Bay (Clifton, 1983)).

an overlying correlated arkosic sandstone interval that directly underlies a thick carbonaceous-rich sandstone unit (Figure 10 and Plate III).

An excellent example of the nested subtidal channel sandstone lithofacies association (TC) occurs at section location 11E, the uppermost part of unit 3 (Figure 21). These amalgamated, lenticular channel-fill sequences overlie inclined, wavy and lenticular bedded sandstone and siltstone of lithofacies association TF. These subtidal channel deposits contain numerous discontinuous *Teredo*-bored coalified wood layers in the base of channels (Figure 21). The channel-fill above these coally layers consist of flaser and mudstone-draped tangential and sigmoidal cross-bedded arkosic sandstone and tuffaceous volcanic arkosic sandstone forming distinctive tidal bundle sequences. A correlative 13-m thick sequence (lithofacies 3c) of trough and sigmoidal cross-bedded, micaceous arkosic sandstone facies overlies coal seam C in section O21 (Plate III). Foreset and bottomset laminae are formed by concentrations of very coarse mica and carbonaceous plant debris (no mudstone-drapes in this correlative section). Cosets are generally 0.5 to 1 m thick and non-parallel or wavy planar reactivation surfaces bound these cross-bed wedges. This arkosic sandstone is, in turn, overlain by lenticular bedded mudstone (lithofacies 3e) and silty, fissile carbonaceous shale (lithofacies 3g) in sections O22 and O23 at the top of unit 3 (Plate II).

Overlying the lower subtidal channel sequence, there is a change from lithofacies associations TC and TF to ST and an overall decrease in micaceous arkosic sandstone beds (831 m, Plates II and III). This distinctive interval can be observed over 5 km in 5 measured sections correlated along Olequa Creek (Figure 10, Plates I and III). These correlated sections were hung on a cliff-forming, 1.5-m thick, well indurated, ledge-forming volcanoclastic marker bed (marker bed U3-A) of lithofacies 3h and a 7.5-m thick coal bed (coal seam C) of lithofacies 3g (Figure 10, Plates II and III). A 14 m- to 17-m thick volcanoclastic- and carbonaceous-rich mudstone interval was observed at the base

of section O11 (Figure 10 and Plate III). The lower part of this interval consists of sandy siltstone and muddy siltstone channel-fill that incises 1 m into the underlying arkosic sandstone of lithofacies 3b. This interval is overlain by a 3-m interval of dark brown volcanic sandstone, siltstone, lenticular dark gray carbonaceous shale, a 15 cm-thick coal, and three coarsening-up silty to sandy mudstone beds that contain coarse-sand-sized mudstone rip-ups. These beds are, in turn, overlain by 1.6 m of massive to laminated, very fine- to fine-grained arkosic sandstone. Strata in nearby measured sections O15 and O16 (Plate II) correlate with this coal-rich and carbonaceous mudstone horizon in measured sections O9 and O11. However, a discontinuous 15 cm-thick coal seam was found only in sections O15 and O16. This coal and carbonaceous mudstone correlated interval in measured sections O11 and O16 consists of thin-bedded carbonaceous shale, minor light tan claystone, and an upper light gray mudstone.

These strata are interbedded with twelve 5 cm- to 1.8-m thick (average 10 cm) basaltic volcanoclastic beds of lithofacies 3h that decrease in frequency upwards (petrology samples CP-94-134a and CP-94-163a). Some volcanic sandstones contain bivalve and gastropod fossil fragments. These sandstones are composed of medium- to coarse-sand-sized scoriaceous basaltic clasts. A distinctive 1 to 1.8-m thick, ledge-forming, subangular, granular to pebbly, pumice lapilli tuff forms a local correlative marker bed (marker bed U3-A, Figures 10 and 22A; interval 905 m, Plates II and III). This bed is planar-laminated to massive with some normal and reverse grading. Some minor mudstone rip-ups were also observed near the base of this interval. According to Irving et al. (1996), this pumice lapilli bed (petrology sample CP-94-163b and geochemistry sample CP-94-163b, Appendix IV) contains oligoclase feldspar crystals that indicate a western Cascade dacitic source. The crystals yield an $^{39}\text{Ar}/^{40}\text{Ar}$ age of 38.9 ± 0.1 Ma or latest middle Eocene (location 11D, Plates I, II, and III). However, geochemistry from

A.



B.



Figure 22. Volcaniclastic lithofacies (3a) from coal seam A and subtidal sandstone ridge lithofacies (3c) from unit 3 (Plates III). (A) The ledge-forming marker bed U3-A is a 1 to 1.8 m-thick, granular pumice lapilli tuff (location O16; SW 1/4, Sec. 17, T11N, R2W, Plate I). (B) Large-scale cross-bedded, fossiliferous silty sandstone in section 11C is 3 m-thick, contains the marginal marine *Erodona* molluscan faunal assemblage of Nesbitt (1995), and is inclined 15° to the nearly horizontal lower planar basaltic sandstone (Sec. 32, T11N, R2W, Plate I). Note 1.5 m Jacob's staff for scale.

Paul Hammond (written communications, 1996) indicates this tuff is andesitic in composition (Appendix IV). A more local, possible western Cascades source for this tuff is the Northcraft Formation.

One large-scale cross-bedded, fossiliferous silty sandstone (lithofacies 3d) that underlies marker tuff bed U3-A was observed only in measured sections 11C and 11D (Figure 22B). This 3-m thick interval is composed of highly fossiliferous silty arkosic sandstone, sandy siltstone and minor mudstone containing the distinctive *Erodona* molluscan faunal assemblage of Nesbitt (1982 and 1995). These beds are more steeply inclined (15°) compared to the underlying nearly horizontal basaltic sandstone (lithofacies 3a) and laterally grade into fossiliferous arkosic sandstone that loaded into the underlying softer and less dense mudstone.

The upper part of the volcanoclastic- and carbonaceous-rich mudstone interval (coal seam A) in measured sections 11D and 11E (Plates II and III) consists of a 6-m thick bioturbated, sparsely to abundantly fossiliferous silty mudstone, muddy siltstone, and siltstone unit (lithofacies 3f). Multiple, shell-rich layers are dominated by the unbroken gastropod *Viviparus washingtonianus* (Nesbitt, 1981; this study). A fossiliferous gastropod horizon containing an Unionid freshwater clam of the *Unio* assemblage (Nesbitt, written communications, 1996) was found in a correlative mudstone in measured section O17 (Figure 23A, Plates II and III).

An overlying 7-m thick fossiliferous, silty sandstone and micaceous arkosic sandstone (lithofacies 3d) are in sharp contact with the underlying dark gray mudstone facies in sections O11 and O14. This lithofacies in section 11E is stratigraphically 6 m higher (Plate III). The slightly laminated, silty sandstone facies contains multiple broken-shell lags composed of *Corbicula willisi* bivalves, *Potamides fettkei*, and *Eulima lewisiana* gastropods which are a brackish water assemblage (Nesbitt, written communications, 1996) (macrofaunal samples CP-95-163c, section O11, Appendix II). In section O14,

A.



B.



Figure 23. Two fossiliferous intervals in unit 3 of the Cowlitz Formation (Plate III). (A) *Viviparus washingtonianus* gastropod-dominated horizons in mudstone of the *Unio* assemblage (Nesbitt, written comm., 1996) (sample CP-95-170, Appendix II) (section O17, SW 1/4, Sec. 17, T11N, R2W, Plate I). (B) Silty subtidal arkosic sandstone ridge or bar (lithofacies 3c) containing multiple, brackish water *Corbicula willisi* bivalves shell lags (sample CP-95-163c, Appendix II) (section O11; NW 1/4, Sec. 20, T11N, R2W; Plate I). Note 1.5 m Jacob's staff and 25 cm rock hammer for scale.

current-sorted, disarticulated *Corbicula willisi* bivalves (Figure 23B) in discrete horizons were washed in from these brackish water mudflats (macrofaunal sample CP-94-166a) (Nesbitt, written communications, 1996). The subtidal, micaceous, arkosic sandstone is very fine- to fine-grained, massive and planar-laminated to tangential trough cross-bedded. The sandstone also contains medium-sand-sized tuffaceous mudstone rip-ups concentrated along foreset-laminations. This sandstone channel undercuts the lower muddy tidal-flat and contains shells concentrated at the base of the channel.

Coal seams B and C (lithofacies 3f) overlie these lower wavy bedded mudstone/sandstone and massive mudstone of lithofacies 3e and d (Plate III). The coal seams in section O11 are 40-m thick and consist of thinly bedded silty mudstone, lenticular microcross-laminated siltstone and very fine-grained sandstone, coal, and carbonaceous mudstone. Some claystone underlying carbonaceous shale contains coal stringers and horizontal coalified logs (10 cm long). Mudstone beds underlying carbonaceous units are rooted. The lower coal seam (B) is composed of a 3-m thick coal bed, carbonaceous shale, mudstone-draped cross-bedded sandstone, rooted mudstone, and a 70 cm-thick scoria lapilli tuff bed in section O14 (Plate III). Laminated, light gray, 8-m thick, silty mudstone lies between coal seams B and C in measured section O14.

A 7.5-m thick coal seam (C) interbedded with altered tuff beds and carbonaceous shale (lithofacies 3g and 3h) occurs in sections O14, O20, and 11E (Figure 24 and Plate III). Ten of these tuff beds were sampled in section O14 for geochemical analysis (Appendix IV). A 1.2-m thick volcanoclastic interval in this coal zone consists of graded to cross-bedded, basaltic lapilli tuff and altered andesitic tuff beds. The tuffs display scour-and-fill bases. In measured section O20, the upper part of this coal bed is soft-sediment folded. A vertically stacked, thinly laminated sequence of wavy bedded siltstone, mudstone and micro-cross-laminated sandstone (lithofacies 3e) is erosionally overlain by coal seam C in section 11E (Plate III).

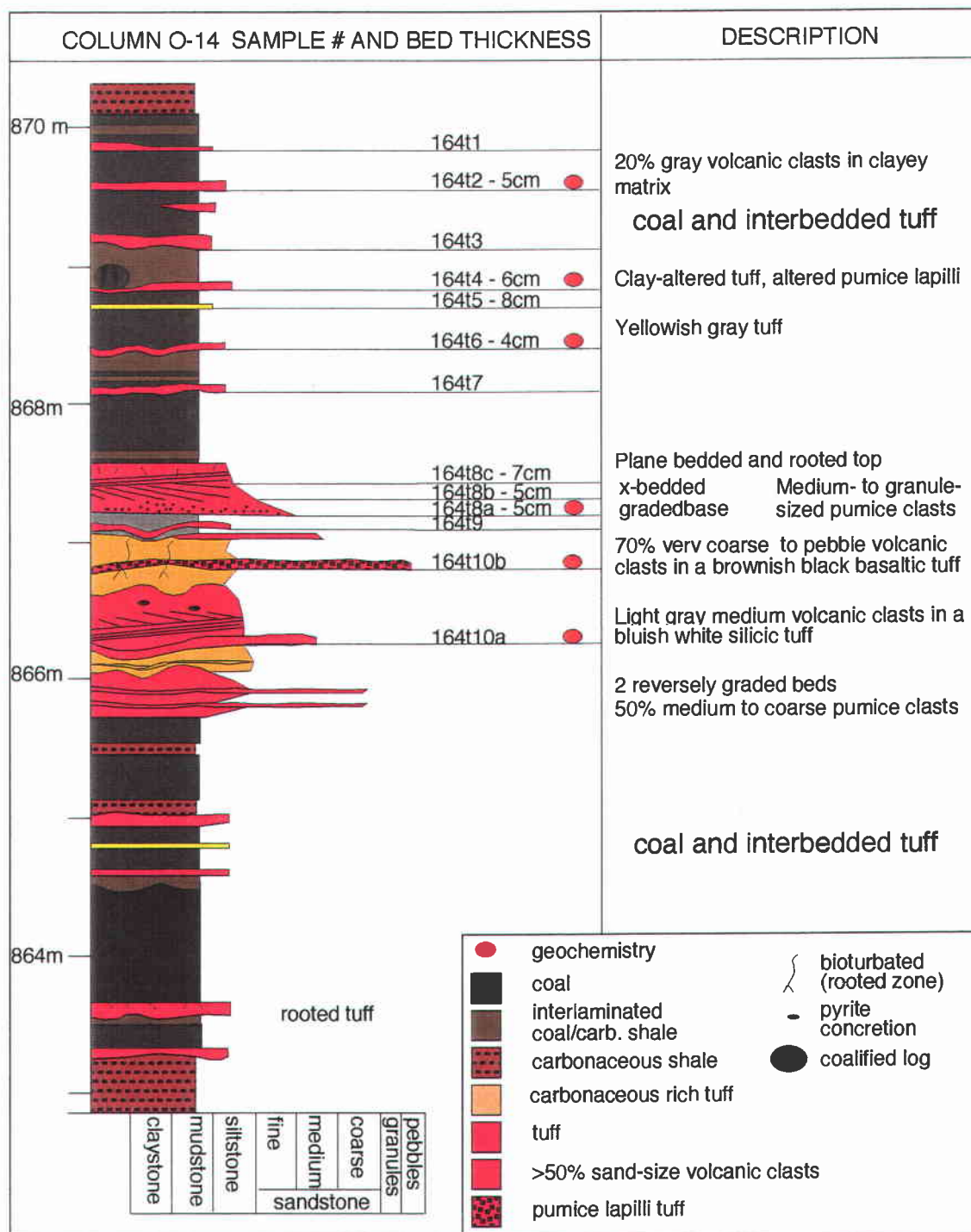


Figure 24. Stratigraphic section of the 7.5-m thick upper coal bed in unit 3 of the Cowlitz Formation (coal seam C). This coal is interbedded with altered tuff beds and carbonaceous shale and was observed in sections O14, O20, and 11E (Plate III). Ten of these tuff beds were sampled in section O14 for geochemical analysis (Appendix III). A 1.2-m thick volcanoclastic interval in this coal zone consists of graded, cross-bedded, and scour-based lapilli tuff and tuff beds (measured section location O14, NW 1/4, Sec. 20, T11N, R2W; Plate I).

Unit 4: Upper Shallow Marine Lithofacies Succession

Unit 4 consists of nearshore to inner shelf mollusc-bearing, micaceous arkosic sandstone and outer shelf to upper bathyal micaceous mudstone. They form several 5 m- to 35-m thick coarsening- and thickening-upward cycles (Plate II). Marine unit 4 differs from shallow marine units 1B and 2 and from deeper marine unit 5 in that it is mudstone-dominated, contains no basaltic sandstone interbeds, and lacks planar-laminated siltstone and slump-folded intervals. The contact with unit 3 is covered but inferred to be gradational, the upper contact with unit 5 is unconformable (i.e., submarine channel incision and arkosic sandstone in-fill).

Three lithofacies associations of this unit were identified: (1) ripple cross-laminated siltstone and sandstone (nearshore to inner shelf), (2) hummocky cross-stratified arkosic, micaceous sandstone and fair-weather mudstone (lower shoreface), and (3) bioturbated, sandy siltstone and glauconitic mudstone (outer shelf to upper bathyal).

Nearshore to inner shelf ripple cross-laminated siltstone and sandstone in the lower part of section O23 overlies carbonaceous shale at the top of unit 3 of the Cowlitz Formation (Plate II). A 14-m thick coarsening-upwards interval consists of dark medium gray sandy mudstone (with minor burrows) at the base grading up into 3 m of light-gray, laminated fine-grained sandstone with mudstone rip-ups, thinly laminated micaceous mudstone, tuff-rich lenticular arkosic sandstone and mudstone, and plane-laminated mudstone with decreasing sandstone laminations. Sections O24 through O30 are composed of interbedded wavy- to lenticular-bedded mudstone and very fine-grained, micro-cross-laminated arkosic sandstone, thin to thick beds of fine- to medium-grained sandy mudstone, mollusc-rich fossiliferous silty mudstone, clay-rich siltstone, and planar- and ripple-laminated very fine-grained sandstone. Strata in the lower part of this section contain disarticulated thick-shelled bivalves and vertical to diagonal *Skolithos* burrows (3 mm average diameter). Towards the top of these sections, finely laminated clay-rich

mudstone, arkosic micaceous sandstone and claystone are interbedded with minor thin beds of carbonaceous mudstone with large fragments of carbonized wood.

Thin to medium beds of hummocky cross-stratified micaceous, arkosic sandstone and overlying very thick beds of mudstone were measured from section location O31 to the lower part of section O32. Consistent dips and strikes and similar stratigraphic sequences allowed for correlation of measured sections (section locations O31 and O32) around two stream bends in Olequa Creek through covered intervals (Sec. 8, T11N, R2W; Plate I). The lower 4 m is composed of slightly laminated silty micaceous mudstone that is overlain by alternating arkosic micaceous sandstone and mudstone. This 5.2-m thick interval consists of five thin beds of silty sandstone, each of which is overlain by ripple-laminated siltstone and wavy- to lenticular-bedded mudstone, siltstone, and very fine-grained arkosic sandstone. Some silty sandstone beds are hummocky cross-stratified and contain minor contorted or convolute bedding intervals and calcareous concretionary horizons. An overlying 1.5-m thick medium-grained, moderately sorted, dark gray, ledge-forming, volcanic sandstone bed fines-upwards to thinly bedded, fossiliferous, fine-grained arkosic sandstone. This is, in turn, overlain by 2.1 m of slightly laminated silty mudstone and mudstone. This mudstone unit is overlain by 1 m of medium gray, abundantly fossiliferous silty arkosic sandstone containing multiple shell lags (macrofaunal sample CP-95-177, Appendix II) (Figure 25A). These sandstones, in turn, grade upwards into 10 m of sparsely fossiliferous, clay-rich, light yellow-green glauconitic sandy siltstone containing two indurated, ledge-forming beds of silty fine-grained sandstone. Shallow marine *Pitar eocenica* and *Venericardia hornii clarki* bivalves and *Turritella uvasana olequahensis*, *Calyptraea diagoana* and *Polinices nuciformis* gastropods in this fossiliferous interval belong to the *Turritella-Tivelina* assemblage of Nesbitt (written communications, 1996) (Figure 25A). Neritic foraminiferal assemblages collected and identified by Yett (1979) from this hummocky cross-stratified interval

A.



B.



Figure 25. (A) Fossiliferous, shallow marine, silty sandstone with multiple shell lags (macrofaunal sample CP-95-177, 1/4 SW, 1/4 NE, Sec. 8, T11N, R2W; Plates I and II). Molluscan fossils include *Venericardia hornii clarki* bivalves (v) and *Turritella uvasana olequahensis* (t) gastropods of the *Turritella-Tivelina* assemblage of Nesbitt (1995). Note 2.5 cm-diameter coin for scale. (B) Hummocky cross-stratified arkosic sandstone from section location 12B from the lower part of Olequa Creek (SW 1/4, Sec 32, T11N, R2W). Note 25 cm rock hammer for scale.

(UWA-3341, measured section O32) consist of the *Elphidium-Cibicides* faunule. This faunule includes the following foraminifera: *Cibicides natlandi*, *Eponides yeguaensis*, *Lenticulina inornata*, *Vaginulinopsis saundersi*, and *Quinqueloculina imperialis*.

Bioturbated, sandy siltstone and glauconitic mudstone and a distinct decrease in the abundance of sandstone beds are evident in the lower part of measured section O32. In this section, alternating beds of silty mudstone and concretionary, clay-rich siltstone comprise an 8-m thick interval. An overlying structureless, 12-m thick, silty, clay-rich glauconitic mudstone (condensed section formed during maximum flooding event) that grades upward into clay-rich micaceous siltstone is, in turn, overlain by a thin, calcareous concretionary, hummocky cross-stratified, silty arkosic sandstone bed.

In section O33 the number of hummocky cross-stratified sandstone beds increases. Five coarsening- and thickening-upward cycles are present, each starting with a 10-m thick massive to bioturbated, interstratified thin- to medium-bedded, sandy siltstone and siltstone that becomes thin-bedded, ripple-laminated, planar, and hummocky cross-stratified fine-grained arkosic sandstone (Plate II). The top 14 m of unit 4 consists of a coarsening- and thickening-upwards sequence of finely laminated clay-rich siltstone with carbonaceous flakes (up to 3 mm in diameter), thin beds of laminated sandy siltstone and silty mudstone capped by an arkosic silty sandstone. Large (3 m-wide), concave-upward, well-indurated calcareous concretions occur near the bottom of this interval. Discordant out-of-phase wave ripple micro-cross-laminations with parallel carbonaceous and micaceous laminations occur near the top of the uppermost silty sandstone. An excellent example of one of these coarsening-upwards marine sequences is exposed in the channel wall of lower Olequa Creek at section location 12B (Plate I). The lower 3 m is composed of thin beds of planar-laminated dark gray clay-rich silty micaceous mudstone and minor thinly laminated, muddy siltstone and sandy siltstone. An overlying coarsening- and thickening-upwards, thick-bedded, fossiliferous, hummocky cross-stratified, silty, very

fine-grained, arkosic sandstone is 6-m thick and has a sharp top (Figure 25B). This sandstone is abruptly overlain by fossiliferous dark gray, laminated mudstone with multiple *Turritella uvasana olequahensis* gastropod horizons and 9 m of chippy, sparsely fossiliferous gray mudstone with minor fossiliferous, calcareous concretionary horizons. The *Turritella-Tivelina* assemblage was identified by Nesbitt from this locality CP-95-189b (Appendix II and Plate I). Yett (1979) identified the *Elphidium-Cibicides* faunule from location 12B (sample UWA-1992, Plate I).

At the Big Bend locality along the Cowlitz River east of Vader (Plate I), 65 m of strata were measured by Elizabeth Nesbitt in 1979. This section is composed of siltstone, fossiliferous, bioturbated, silty mudstone, and glauconitic mudstone. The upper part of unit 4 in Olequa Creek (measured sections O31 and O32) correlates with the lower part of the Big Bend section along the Cowlitz River based on biostratigraphic correlation. The inner neritic *Turritella-Tivelina* assemblage was identified in the lower part of the Big Bend location (Nesbitt, 1995) and in Olequa Creek (Nesbitt, written communications, 1996) (section location O31, Plates I and II). Additionally, neritic foraminiferal assemblages collected and identified by Yett (1979) from the Big Bend locality consist of the *Elphidium-Cibicides* faunule and correlate with sample UWA-3341 (section location O32, Plate I).

Unit 5: Planar-Laminated Deep Marine Siltstone

Unit 5 contains distinctive very well-laminated siltstone and massive very thick-bedded channel sandstone with scattered chaotic mudstone rip-ups. The contact with unit 4 appears to be unconformable (i.e., submarine channel incision into underlying unit 4). However, the relief of this unconformity could not be determined because only one creek outcrop was observed. Unit 5 consists of the following lithofacies: (5a) deep marine laminated siltstone and fine-grained, thin-bedded arkosic turbidites, (5b) submarine-channel sandstone and chaotic mudstone rip-up conglomerate, and (5c) slump-folded and soft-sediment deformed siltstone intervals.

Friable, massive or structureless, fine- to medium-grained micaceous, arkosic sandstone that contains cobble-sized, angular, mudstone rip-ups (lithofacies 5b) is exposed in the upper 16 m of section O33 (Plate II and Figure 26). A lower 3-m thick massive friable arkosic sandstone is overlain by a channelized, medium- to coarse-grained arkosic sandstone containing large light gray mudstone rip-ups with a basal incision that cuts 1 m down into underlying sandstone bed. The bed grades into medium-grained sandstone with large ellipsoidal calcareous concretions (1.5 m by 0.3 m). The sandstone contains small ripple-laminations (10 cm crest to crest and 5 cm high). Higher in the channel-fill sandstone, lateral-accretion surfaces form large-scale avalanche cross stratification that are lined with pebble- to cobble-sized, angular to subangular, mudstone rip-ups.

A 0.6 m- to 1.5-m thick interval composed of isoclinal soft-sediment slump-folded laminated medium gray siltstone overlies this sandstone (lithofacies 5c). This interval becomes swaley-bedded (storm wave?) and is composed of laminated silty mudstone and sandstone. The top 1.5 m consists of planar, parallel-laminated siltstone (lithofacies 5a). Section O34 in Olequa Creek is composed of structureless, fine-grained sandstone (lithofacies 5a) with large concretions (1.5 m wide by 1 m high). This is overlain by a



Figure 26. Massive, fine- to medium-grained channelized, micaceous, arkosic sandstone that contains cobble-sized angular mudstone rip-ups (lithofacies 5b) in unit 5 section O33 in Olequa Creek (1/4 SW, Sec. 8, T11N, R2W; Plate I). Note 25 cm rock hammer for scale.

soft-sediment slump-folded interval consisting of large basal blocks of carbonaceous mudstone with chunks of carbonized wood, a 12-m thick recumbent, isoclinal soft-sediment fold (axial trend of 350° and plunge of 55°), and clastic arkosic sandstone dikes (lithofacies 5c). Rhythmically bedded, thinly to thickly laminated (1 cm- to 4 cm-thick), planar-parallel siltstone and minor sandstone turbidites (Tcd) (lithofacies 5a) overlie the lower slump-folded interval (Figure 27A). The basal division of these turbidites consists of planar to ripple-laminated, very fine-grained arkosic sandstone containing coarse mica flakes and carbonaceous wood fragments. Small load structures composed of arkosic sandstone have sunk into the siltstone. Siltstone laminae are planar and consist of light gray, clay-rich, very fine-grained siltstone. Minor very thin beds of medium-grained sandstone with mudstone stringers and a distinctive light green massive tuffaceous siltstone are present. Upwards, the 38-m thick interval (measured section O35, Plate II) consists of planar-parallel siltstone and 20% basal arkosic micaceous sandstone turbidites and minor massive to structureless, muddy siltstone and mudstone. Five soft-sediment slump-folded intervals (lithofacies 5c) in this section range from 3 m to 7 m in thickness. Some of these internally folded intervals contain a light green massive tuffaceous siltstone similar to the bed found in section O34 (Plate II).

A second nested submarine channel interval is evident in measured section O35, Plate II. The base of section O36 (1,177 to 1,174 m, Plate II) consists of steeply dipping thin beds of intensively bioturbated and ripple-laminated siltstone and mudstone (lithofacies 5c). Resting on the flank and top of these lower strata is basal 2.5-m thick mudstone rip-up conglomerate with an arkosic micaceous sandstone matrix (lithofacies 5a). These rip-up clasts are imbricated and indicate a down-current dispersal direction to the southwest (approximately 240° Az.). Overlying this unit is a 3 m of very thinly laminated arkosic sandstone and mudstone, ripple-laminated siltstone (lithofacies 5a) and a deep marine channelized sandstone (lithofacies 5b). Internal sedimentary features

A.



B.



Figure 27 (A) Laminated siltstone and micro-cross-laminated sandstone and siltstone (Bouma turbidite Tcd) of unit 5 and (B) soft sediment deformed siltstone and sandstone (measured section O36; NW 1/4, Sec. 8, T11N, R2W; Plates I and II). Note 2.5 cm coin and 25 cm rock hammer for scale.

include flame structures that indicate a south-southwest current direction, load casts, ball and pillow structures, and contorted or convolute bedding (Figure 27B). An overlying, 7-m thick interval consists of clay-rich, planar-laminated siltstone that contains subordinate interlaminated ripple- to planar-laminated, very fine-grained, arkosic sandstone with multiple horizons of small (15 cm in diameter) calcareous concretions. This interval grades upward into ripple-laminated silty very fine-grained sandstone and massive siltstone with a few sandy siltstone interlaminations. An overlying 12-m thick fining-upwards interval is composed of very thinly laminated, very fine-grained arkosic sandstone and sandy siltstone. These alternating laminae are planar- to ripple-laminated and interbedded with a few hummocky cross-stratified silty sandstone beds.

The uppermost 53 m of unit 5 is composed of gray, plane-laminated clay-rich siltstone with a distinctive book-pages-like outcrop pattern (O37, Plate II). These strata consist of very thin laminations of planar to micro-cross-laminated basal sandy siltstone and a clay-rich planar-parallel top. Additionally, minor micaceous laminations, a massive mudstone, and small calcareous concretions occur.

Depositional Environments

Unit 1: Prograding Shoreface and Delta/Coastal Plain

The basal 518-m thick unit 1 of the Cowlitz Formation consists of multiple prograding wave-dominated shoreface successions (unit 1A) and overlying coal-bearing coastal-delta-plain facies associations (unit 1B) (Plate II). The 275-m thick unit 1A (sections 6G to 7E, Plate II) is composed mainly of coarsening- and thickening-upward prograding upper shoreface micaceous arkosic sandstone sequences (sections 6I to 7E, Plate II). These wave-dominated hummocky-bedded sandstones in coarsening- and thickening-upwards intervals are also evident in funnel-shaped spontaneous potential and resistivity curves in the Shell-Zion #1 well (Plate II). Sedimentologic features in the coal-rich and tide-dominated upper 283 m of unit 1 (section 7F to 8C) in the Vader area indicate these lithofacies successions formed in a coastal marsh in a broad subsiding coastal plain and/or tidally influenced delta subaerial plain environment (Plate II). Within this setting, fine- to coarse-grained sands were deposited in tidal bars and/or subtidal channels. The heterolithic facies of this bedded sandstone, siltstone, and mudstone formed in tidal flats. Flaser, wavy, and lenticular bedding, mudstone drapes, bi-directional ripple laminations, and mixed molluscan fossil assemblages document fluctuating depositional energy, reversals of current direction, and shallow-marine biologic activity all characteristic of an intertidal environment. Flores and Johnson (1995) refer to these features as evidence of tidal flat deposition in the correlative Skookumchuck Formation of southwest Washington.

Unit 1A: Prograding Shoreface Parasequences

An excellent example of an offshore to lower shoreface transition facies succession and a wave-dominated shoreface succession at the base of the Cowlitz Formation in unit 1 is evident in measured-section location 6H (0 to 43 m, Plate II) (Figure 28). These thickening- and coarsening-upward successions are composed of four lithofacies (1a to 1d) formed in the following depositional environments (1) a middle to outer shelf (2) the shelf-to-shoreface transition zone, (3) lower to middle shoreface, and (5) the upper shoreface (Figure 11). Walker and Plint (1992) interpreted similar coarsening- and thickening-upward shoaling successions in the Cardium Formation of Canada. This gradation of shallow marine facies suggests there was a gradual fall in relative sea level due to eustatic changes, slowing local basin tectonics, and/or increases in sedimentation rates due to deltaic progradation during the beginning of deposition of the Cowlitz Formation (lower part of unit 1B) (Figure 28).

A series of coarsening- and thickening- upwards upper shoreface micaceous, arkosic sandstone parasequences were measured in sections 6I to 7E (Plates I and II). These lower shoreface and shelfal sandstones are mainly massive because of intensive bioturbation below storm-wave base. Some amalgamated swaley and hummocky cross-stratified sandstone indicates a middle to upper shoreface environment of deposition for these sandstone sequences under moderate to intense storm wave conditions. Minor fair-weather marine or outer shelf bioturbated siltstone below these sandstone-rich intervals observed in field-measured sections and deduced from electric-log characteristics in the Shell-Zion #1 well (Plate II) show that these sandstone sequences coarsen upwards.

**UNIT 1: PROGRADATIONAL SHOREFACE (UNIT 1A)
AND DELTA-COASTAL PLAIN (UNIT 1B)**

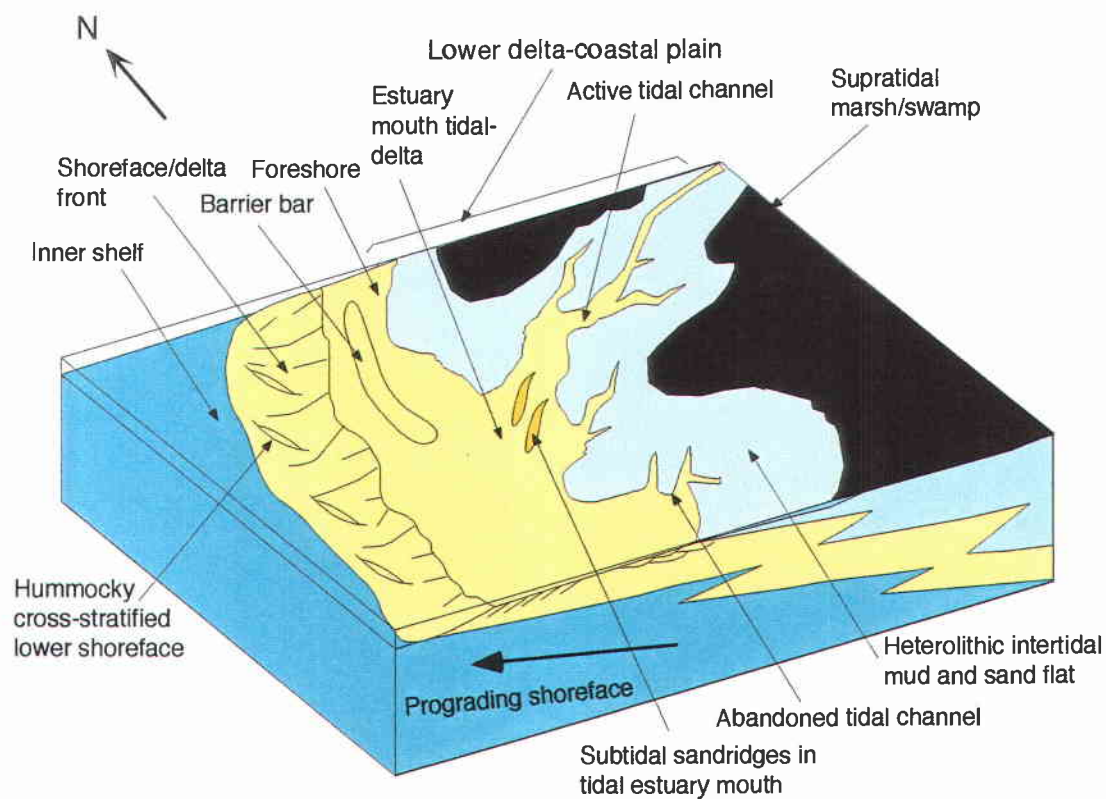


Figure 28. Paleogeography of unit 1A and B of the Cowlitz Formation showing depositional environments and the prograding Cowlitz delta.

Unit 1B: Coal-bearing Coastal-Lower Delta Plain

There is a distinct change in lithofacies association above the shoreface sandstone successions or parasequences of unit 1A (Plate II). The coal- and mudstone-dominated unit 1B (section 7F to 8C) is composed of very thin- to thick-bedded mudstone, siltstone, sandstone, and coal that comprise multiple heterolithic facies associations, reflecting a tide-dominated coastal-delta-plain depositional system (Dalrymple, 1992). These subtidal to supratidal facies associations include the following lithofacies: (1f) subtidal channel deposits, (1h) supratidal marsh/swamp deposits (coal mires), (1i) fossiliferous, subtidal sandstone ridges or bars, (1j) minor volcanoclastic, tuff, and water-laid tuff facies (1k) brackish-bay or estuarine siltstone (Figure 28). The sandy and mixed muddy intertidal-flat facies association consists of a variety of facies and bed forms including flaser to lenticular sandstone and siltstone and the wavy-bedded siltstone of lithofacies 1g.

Subtidal channel bars (sandstone) formed at the mouth of an estuary or delta distributary and associated muddy brackish-bay or estuarine facies occur in the lower interval of the unit 1B (288 m, section 7F, Plate II). A lithic arkosic sandstone bed in section 7F abruptly overlies an arkosic sandstone and contains fossil shell-lags of current-sorted, concave-up brackish-water *Corbicula* pelecypods, shallow marine *Tellina* sp. bivalves (macrofaunal sample CP-94-109, Appendix II), and up to 1 cm-in-diameter coalified wood fragments (Plates I and II). These brackish-water and normal shallow marine bivalves (Nesbitt, personal communications, 1996) and water-logged wood were mixed together and were most likely storm-generated or tidal-influenced deposits formed at the mouth of an estuary or distal mouth bar. Above this thick fossiliferous sandstone bed are intertidal very thinly bedded flaser and wavy bedded siltstone, sandy siltstone, fine- to medium-grained arkosic sandstone, and a supratidal 2.1-m thick coal bed. These strata indicate a fining-upward trend from the upper shoreface sands, an intertidal-flat, and supratidal marsh/swamp and muddy distributary bay environments. The lower part of

section 7G is composed of concretionary siltstone that is dominantly structureless due to intensive bioturbation. It contains abundant carbonaceous wood debris and was most likely deposited in a brackish-water tidal bay (Plate II). Overlying this massive siltstone is a fossiliferous, moderately sorted, silty, fine-grained subtidal cross-bedded sandstone bar or subtidal channel facies. A shell-lag deposit containing *Corbicula olequahensis* and *Acutostrea idriaensis* pelecypods and *Siphonalia sopenahensis* gastropods (Nesbitt, written communications, 1996; macrofaunal sample CP-94-110) (Figure 14). These largely brackish water clams and a few intertidal species were deposited under fluctuating storm/flood (i.e., periodic fresh water flooding of an estuary) conditions in an estuary or tidal flat/distributary bay. The fossiliferous tidal sandstone bar and brackish bay facies are transitional between the upper shoreface and intertidal environments.

Subtidal channel deposits occur at a variety of scales (e.g., from 1 m to 5 m thick). Distinct lithology changes indicate active or abandoned channel activity. Active channels are represented by scour-based, trough cross-bedded sandstone and include concentrations of intertidal mudstone rip-up clasts and coalified-wood fragments. One large abandoned channel deposit cuts down 1.5 m into siltstone at the top of section 8B (500 to 505 m, Plate II). The channel fill consists of a basal carbonaceous mudstone grading to coal and current-reworked andesitic tuff deposits. These deposits are interpreted to result from abrupt subtidal channel or creek incision and meander abandonment in this area (e.g., equivalent to oxbow lakes in fluvial environment). In measured section 7I (macrofaunal sample CP-94-111, Appendix II) brackish-water mollusc *Corbicula willisi* and carbonaceous plant debris occur in an arkosic subtidal channel fill deposit. A lower sandstone in the channel-fill is sigmoidally cross-bedded (Figure 15). Sigmoidal cross-bedding is a common feature of modern tidal channel-fill deposits such as in Willapa Bay (Clifton, 1983). Fining- and thinning-upwards, nested tidal-channel deposits are abundant in section 8C (536 to 539 m, Plate II and Figure 15).

These subtidal channel deposits contain large (7 cm in diameter) coalified logs, a mixture of brackish water *Corbicula willisi* pelecypods, and the more common broken, normal shallow marine *Acutostrea idriaensis* bivalves (macrofaunal sample CP-94-114, Nesbitt, written, communications, 1996; Appendix II). This mixture suggests tidal currents washed normal marine clams into the estuary and flood events mixed in brackish-water species at the mouth of the estuary or bay. Overlying discordant and lenticular to wavy bedded sedimentary structures in siltstone and very fine-grained arkosic sandstone suggest rapid deposition in vertically-stacked tidal-flat accretionary banks. Similar structures are found in modern accretionary bars formed inside meanders of tidal channels (such as Willapa Bay). Smaller meandering tidal channel or creek deposits include thin sets of fine- to medium-grained, moderately well-sorted, low-angle wedge to trough cross-bedded, micaceous, arkosic sandstone that become massive and carbonaceous-rich. These deposits are sharp-based and contain mud-draped foreset laminations forming distinctive tidal bundle sequences (sections 7I, 8A, and 8C, Plate II; Figures 18A).

The intertidal facies association consists of interstratified thin-bedded sandstone and mudstone deposits containing diagnostic tidal rhythmites (Figure 18B) (after Nio and Yang, 1991). Upward-fining flaser, wavy, and ripple micro-cross-laminated sandstone to lenticular bedded siltstone and very fine-grained arkosic sandstone correspond to diurnal tidal ebb and flood fluctuations in an intertidal-flat (Dalrymple, 1992). This heterolithic lithofacies association in section 7I (overlying the 11-m thick coal bed, Figure 15), sections 7I and 8A (477 to 492 m, Plate II), and the lower part of section 8C (520 to 532 m and 535 to 542 m, Figure 15 and Plate II) is composed of the following lithofacies: (1) sandstone-dominated tidal-flats preserved as thin beds of medium-grained, trough cross-bedded, micaceous, arkosic sandstone with mud-draped foreset laminations, (2) mixed mudstone and sandstone intertidal-flat deposits composed of alternating thin beds of trough cross-bedded fine-grained sandstone and contorted to wavy bedded siltstone and

sandstone, and (3) muddy intertidal flats composed of dark gray, ripple-laminated to massive, carbonaceous, intensively bioturbated siltstone and mudstone with minor 4 mm-thick ripple microcross-laminated sandstone.

Supratidal marsh/swamp (coal mires) and associated altered ash-fall and current-reworked tuffs occur throughout unit 1B and become thicker and more numerous in the upper part of the unit. In section 7H an 11.6-m thick coal seam (462 to 474 m, Plate II and Figure 15) contains nine altered tuff partings. One relatively unaltered tuff (sample CP-94-111a) from this coal seam in unit 1B (section 6H, Plates I and II) appears to be rhyolitic (73% SiO₂) in composition and has low TiO₂ (0.26%) which indicates it may have had a western Cascade silicic volcanic-arc source (Appendix IV). Some white-yellow, granular lapilli to fine-grained tuff beds show minor reworking of these pyroclastic airfall deposits. Some current-reworked beds contain mudstone rip-up clasts, detrital quartz grains, and grayish to dark gray disseminated organic material picked-up during transportation. This 11.6-m thick coal seam may be correlative with the 15-m thick Big Dirty (coal) bed of Snavely (1958) in the middle of the Skookumchuck Formation 25 km to the north. This thick bed has a minimum aerial extent of 250 square kilometers in Centralia area (Phillips, 1987) and may connect in the subsurface with this thick coal in this study area.

The top 12 m of unit 1 of the Cowlitz Formation is composed of coal, tuff beds, and an overlying water-lain tuff breccia that contains 2 cm long silicified plant stems (geochemical sample CP-94-114a, section 8C, Figure 15). This basaltic breccia is composed of reddish-purple, cobble sized scoriaceous volcanic clasts deposited as a volcanic debris flow from a proximal vent of the Grays River volcanics or Northcraft Formation. The upper 3 m consists of an altered basalt tuff that is mixed with quartz-feldspathic sandstone and contains shallow marine *Tivelina* sp.? mollusc molds

(macrofaunal sample CP-94-114b, Nesbitt, written communications, 1996), indicating this tuff was reworked by shallow-marine processes during a transgressive event at the end of unit 1B time.

Unit 2: Middle Marine Shelf and Delta-Front

The 205-m unit 2 is composed of five coarsening- and thickening-upwards storm-dominated inner shelf to shoreface/delta-front arkosic sandstone facies successions.

Lithofacies and depositional environments of unit 2 include: (1) shallow marine coarse-grained basaltic sandstone with mollusc-bearing storm wave shell lags (lithofacies 2a), (2) inner to middle shelf marine, bioturbated silty sandstone (lithofacies 2b), (3) storm-generated, shoreface mudstone conglomeratic, arkosic sandstone (lithofacies 2c), (4) storm-dominated upper shoreface/delta-front basaltic arkosic sandstone (lithofacies 2d), (5) outer to middle shelf mudstone to siltstone sequences (lithofacies 2e), and (6) shoreface volcanic conglomerate and shelfal storm-generated volcanoclastic sandstone (lithofacies 2f) (Plate II).

The coarse-grained, mollusc shell-rich, basaltic, silty sandstone (lithofacies 2a) appears in four stratigraphic locations in the lower and middle parts of unit 2 (Plate II). Two macrofaunal biozones were identified in the lowest occurrence of this lithofacies (652 and 658 m interval in section 9C, macrofaunal samples CP-94-121a and CP-94-121b, Appendix II). The lower biozone consists of current-sorted *Acutostrea idriaensis* oysters, *Glycymeris sagittata*, *Thracia dilleri*, *Gari* sp., *Pitar eocenica*, *Tellina cowlitzensis*, *Venericardia hornii clarki* bivalves, and high-spired *Turritella uvasana olequahensis*, and *Calyptraea diagoana* gastropods of the shallow marine *Turritella-Tivelina* macrofaunal assemblage of Nesbitt (1994) (Nesbitt, written communications, 1996). Four meters higher in the stratigraphic section these shallow-marine species are mixed with brackish-water *Corbicula willisi* bivalves as a result of intense storm activity that washed brackish-

water clams into the inner shelfal environment. Inner neritic *Thalassinoides* burrows of the *Skolithos* ichnofacies appear between fossiliferous layers. Fossil shell lags in section 9E also consist of disarticulated and broken specimens of the *Turritella-Tivelina* assemblage and include *Whitneyella oregonensis* gastropods and *Pachydesma aragoensis* bivalves. *Whitneyella oregonensis* gastropods were previously recorded in the Umpqua Formation and *Pachydesma aragoensis* pelecypods are common in the Coaledo and Skookumchuck formations but have not been previously recorded in the Cowlitz Formation (Nesbitt, written communications, 1996) (macrofaunal sample CP-94-124, Figure 16B). These shell-lag deposits were storm wave-generated as evidenced by bedform geometry (storm-generated scour-and-fill structures), faunal mixing, current sorting of disarticulated and broken bivalves. Additionally, nearby explosive volcanic activity appears to have increased when this facies was deposited because there is an abundance of altered basaltic scoriaceous fragments intermixed with the shell fragments.

A mudstone rip-up conglomeratic sandstone (lithofacies 2c) abruptly overlies the pebbly basaltic sandstone of lithofacies 2a in section 9C (589 m, Plate II). The sharp basal contact of this 90 cm-thick mudstone conglomeratic arkosic sandstone (lithofacies 2c) may define a marine flooding surface. Another angular pebble rip-up conglomerate sandstone is in sharp contact with the underlying silty sandstone (lithofacies 2b) in section 9E (626 m, Plate II). This rip-up lithofacies is 7 cm to 15 cm thick and composed of volcanic sandstone rip-ups and bivalves in a fine-grained arkosic sandstone. Marine flooding surfaces reflect an abrupt increase in water depth that results in minor submarine erosion or nondeposition during a relative sea level rise (Van Wagoner et al., 1990). These mudstone and volcanic sandstone rip-ups of lithofacies 2c may have been derived from the underlying strata by shoreface erosion and were concentrated as a transgressive lag on the transgressed surface (marine flooding surface) (similar relationships were described by Van Wagoner et al., 1990).

A 34-m thick, intensively bioturbated, silty, very fine- to fine-grained volcanic arkosic sandstone (lithofacies 2b), that overlies the thin rip-up conglomeratic sandstone of lithofacies 2c), formed in an inner shelf to lower shoreface/delta front environment. This interpretation is based on the presence of alternating, sparsely fossiliferous and burrowed intervals with distinctive vertical, L-shaped *Thalassinoides* burrows of the *Skolithos* ichnofacies (Figures 8 and 16A) (section 9D in Plate II). These fine-grained lower shoreface sandstones formed under low-energy conditions and laminations in these deposits were obliterated by burrowing suspension- and deposit-feeder traces (similar relationships have been described by Walker and Plint, 1992).

Silty to medium-grained, friable, micaceous, sandstone occurs at two stratigraphic intervals and formed in a middle to upper shoreface/delta front environment (sections 9F, O7, 10D, and 10C, Plate II). Bedding is massive to faintly laminated in the lower part of these interval. In the upper part of this lithofacies, trough cross-bedded and planar to wavy laminated sandstone defined by concentrations of mica contains numerous concretionary horizons. The sandstone in the upper part of these intervals could have formed in the upper shoreface to foreshore environment where breaking waves formed megaripples or sandwaves (Rarey, 1986). Clean arkosic sandstones are amalgamated and minor interbeds of very coarse-grained volcanic sandstone increase in abundance upward in section, further reflecting this shoaling event (Plate II).

A basaltic-lithic conglomerate (lithofacies 2d) overlies the upper shoreface/delta-front arkosic sandstone facies in section O7 (Plate II). This 2-m thick conglomerate is interpreted to be a distributary channel-fill. This sandy, basaltic, granular to pebbly volcanic conglomerate fines upward and has a sharp-basal contact that incised into the underlying arkosic sandstone unit. Clasts are subrounded and in framework support (petrology sample CP-95-158). The coarse volcanic conglomerate is composed mainly of basaltic to andesitic clasts that suggest a probable derivation from a minor secondary

andesitic Northcraft Formation source in the adjacent western Cascades arc. Very coarse-grained sandstone-filled vertical *Ophiomorpha* burrows (up to 30 cm long and 2 cm in diameter) occur in the lower interval of this facies. These burrows were probably formed after deposition of the basaltic conglomerate by shelfal fauna that recolonized the area during basinal deepening to shelfal water depths (Plate II).

Interbedded with the thick arkosic upper shoreface sandstone is a thinner mafic matrix-supported volcanoclastic debris-flow facies. This 2.5-m thick volcanic unit is composed of two, indurated, coarse-grained to granular, scoriaceous basaltic sandstone beds (petrology sample CP-94-130) and minor lenticular, coarse-grained, volcanic sandstone. Altered basalt clasts are subangular and moderately sorted. All these indurated, ledge-forming beds are discontinuous and coarser-grained than the adjacent lithic arkose. The scoriaceous basaltic sandstones were derived from a penecontemporaneous Coast Range basaltic eruptive source (Grays River volcanics).

Two intervals of siltstone and mudstone lithofacies 2e of the middle to outer shelf are evident in the upper part of unit 2. The lower interval is 26-m thick and consists of concretionary, micaceous, sandy siltstone that is massive to mottled and very thinly to thickly bedded (measured sections O6, O7, 10A, 10B, O1-5, and 10E; Plate II). This siltstone is inter-mixed with altered pebble to granular lapilli basaltic tuff sandstone or conglomerate that contain weathered porphyritic basalt clasts. Current reworked benthic foraminifera *Cibicides* spp.?, *Elphidium californium*, and *Quinqueloculina imperialis* from macrofaunal sample CP-95-158A have a water-depth range of 0-50 m or inner neritic (McDougall, written communications, 1997; Appendix II). These inner shelf forams were washed off the inner shelf by geostrophic currents or from storm wave surges into the middle to outer shelf.

The uppermost mudstone to siltstone lithofacies succession totals 21 m in thickness (O1-5, 11D, and 11E; Plate II). This upper coarsening-upwards succession is

composed of olive-gray, micaceous, mudstone at the base that coarsens upwards to light-gray, bioturbated, muddy siltstone. Coarse-sand-sized volcanic fragment-filled, complex-shaped burrows of the shelfal *Cruziana* ichnofacies are also present in this mudstone interval. Despite the scarcity of foraminifera, a minimum water depth can be estimated for the lower part of this upper mudstone interval at section location O3. Inner neritic (0 to 50 m) species of *Elphidium*, *Cibicides*, *Nonionellina*, and *Quinqueloculina* (sample CP-95-130 in the part of unit 2 at partial section 11E, Plate II) may have been washed off the inner shelf into the middle shelf. A more diverse foraminiferal assemblage was recovered from the upper part of unit 2 (microfaunal sample CP-95-130, section location O4, Appendix I). This assemblage (previously sampled and identified by Kris McDougall) contains benthic forams *Anomalina garzaensis*, *Pullenia salisburyi* and *Valvulineria tumeyensis* which indicate deposition at outer neritic (50-150 m) rather than inner neritic depths (McDougall, written communications, 1997). This foraminiferal assemblage indicates there was an increase in water depth of 50 to 150 m close to the end of deposition of unit 2. The uppermost part of unit 2 is composed of storm wave lags of fossiliferous silty sandstone. These very shallow (~50 m water depth) marine organisms include *Acanthocardia breweri* bivalves, *Turritella uvasana stewarti* gastropods, and crab claws and carapaces (macrofaunal sample CP-95-157, Appendix II). The abundantly fossiliferous shell lag horizons containing *Pteria clarki* bivalves (macrofaunal sample CP-94-131, Appendix II) (Nesbitt, written communications, 1996). These fauna indicate a decrease in water depth of 50 to 100 m by the end of deposition of unit 2 of the Cowlitz Formation.

Thin-bedded volcanoclastics occur in the lower and upper shelfal siltstone and mudstone intervals of unit 2 (Plate II). Some of these 3 to 30 cm-thick, granular to medium-grained basaltic beds are normally graded and contain sharp bases. These volcanic layers may be a record of a series of explosive air-fall and base-surge eruptive

events that abruptly entered the shallow marine arkosic sandstone and mudstone environments (petrology sample CP-94-127, Appendix III). Other volcanoclastic beds are normally graded, and contain mudstone rip-ups, ripple laminations, and broken or disarticulated bivalve molds that indicate the volcanic deposits were reworked after deposition, perhaps by storm waves (i.e., tempestites). A thick interval grades of gray, burrowed siltstone grading to dark gray, mollusc-bearing sandy siltstone contains some granular to medium-grained vesiculated basalt clasts. The burrowing indicates some primary volcanic detritus was extensively reworked by bioturbation and incorporated into normal shallow marine, fine-grained sediments. The thin volcanoclastic beds are continuous across the map area, suggesting uniform and widespread deposition across a broad shallow marine shelf.

Unit 3: Upper Tide-Dominated Coal-Bearing Delta Plain

The 170-m thick unit 3 of the Cowlitz Formation consists of three overall fining-upwards coal-bearing, tide-dominated coastal-lower-delta-plain facies associations (Plate II). A correlative carbonaceous and coal-rich interval also occurs in the nearby Shell-Zion #1 exploration well (Plate II) based on description of cuttings in driller's logs and spontaneous potential and resistivity logs. Based on stratigraphic position, unit 3 probably correlates with the upper coal zone of the Eocene Skookumchuck Formation (Flores and Johnson, 1995) of the Centralia area. Sedimentologic features in coal-rich unit 3 in the study area and correlative upper coal zone of the Skookumchuck Formation suggest these deposits formed on a widespread and broad tidally-influenced depositional delta and/or coastal plain (Flores and Johnson, 1995; Johnson personal communications, 1994). Within this setting, coarse-grained strata were deposited as subtidal bars, subtidal channels, intertidal-flats and supratidal coal mires. The thinly interbedded (heterolithic) sandstone, siltstone, and mudstone formed on the adjacent mud and sand flats in the

intertidal zone (Figure 29). The coals may have formed as peat in supratidal marsh deposits. Flaser, wavy, and lenticular bedding, mudstone drapes, bi-directional ripple laminations, and mixed fossil (brackish and very shallow marine) molluscan assemblages in these facies document fluctuating tidal current energy, reversal of ebb and flood tidal currents, and marginal marine biologic activity, all characteristic of a dynamic intertidal and tidal environment (Flores and Johnson, 1995; Dalrymple, 1992).

Three fining-upward facies associations of unit 3 consist of the following depositional environments and lithofacies: (3a) a tide-reworked debris flow (coarse-grained basaltic sandstone), (3b) subtidal-channel megaripple cross-bedded (sigmoidal and tangential cross-beds) mudstone-draped arkosic sandstone, (3c) sandy subtidal channel (wedge cross-bedded arkosic sandstone), (3d) subtidal-channel mouth bars (fossiliferous silty sandstone), (3e) tidal point bars and mixed lithology tidal-flats (vertically-stacked tidal rhythmites and flaser to lenticular bedded sandstone, siltstone and mudstone), (3f) tidal estuary mud-flats and muddy intertidal accretionary-banks formed on the inside of tidal channel meanders (massive and fossiliferous mudstone) (3g) supratidal marsh/swamp (coal mires) (carbonaceous siltstone and coal-bearing intervals) and (3h) pyroclastic and hyperconcentrated flow (basaltic and pumice lapilli volcanoclastics). These facies form the following three lithofacies associations: (TC) nested, amalgamated subtidal-channel sandstone (lithofacies 3a, 3b, and 3c), (TF) tidal-flat and point bar (lithofacies 3e, 3f), and (ST) supratidal marsh/swamp (lithofacies 3g and 3f) (Figure 29, Plates II and III).

A basal 7-m thick subtidal, coarse-grained, tide-reworked debris flow facies (3a) in sections O10 and O8 (Plate II) was deposited on a postulated sequence boundary that separates the underlying deeper marine (outer to middle shelfal) muddy siltstone of unit 2 from the tidal-flat and coal-bearing unit 3. Inner shelf and beach foreshore facies are missing, suggesting this contact is a sequence boundary. Unit 3 may represent an incised

**TIDE-DOMINATED ESTUARY-FILL UNIT 3
UNCONFORMABLY OVERLYING MARINE UNIT 2**

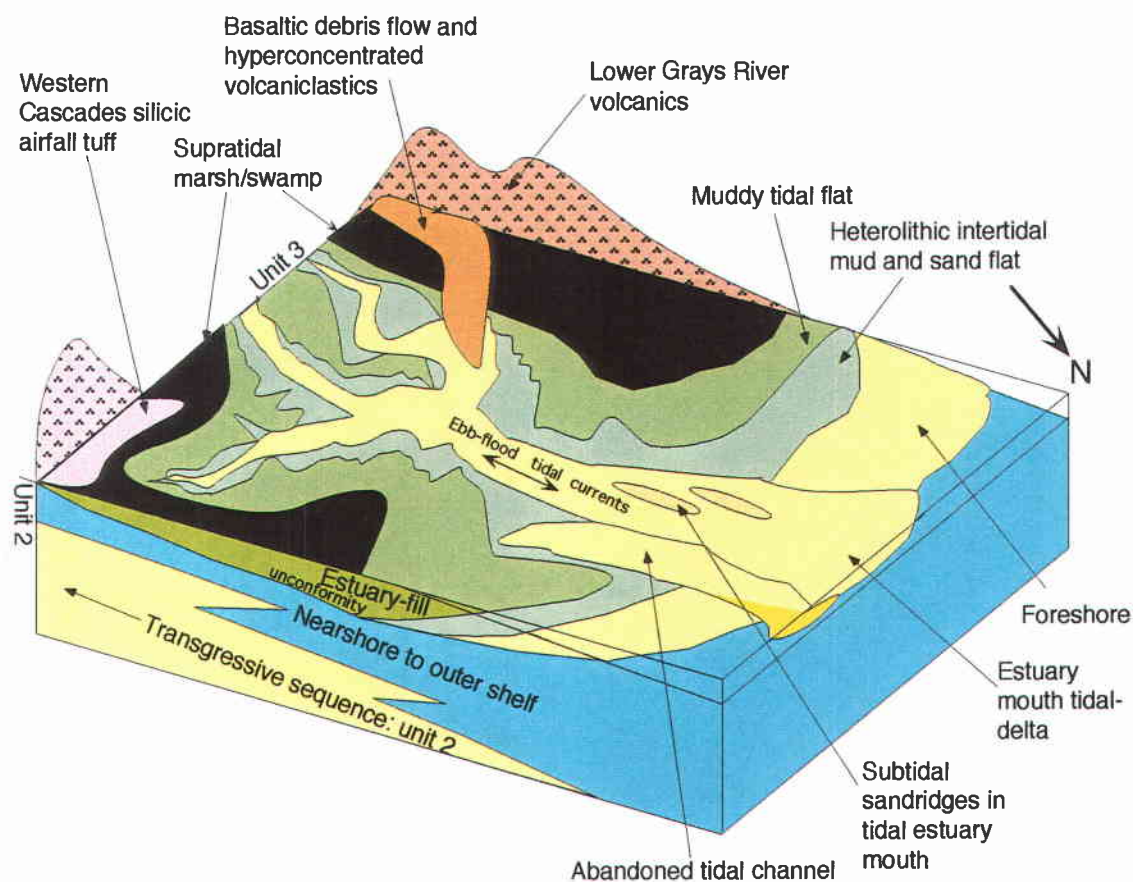


Figure 29 Paleogeographic reconstruction of the tidal estuary of unit 3 showing depositional environments and relationship to underlying marine unit 2.

estuarine valley-fill deposit formed during a lowstand followed by drowning of the valley and formation of a large estuary where the sedimentation rate kept up with rate of subsidence or accommodation space (Van Wagoner and others, 1990). Evidence for a debris flow reworked by tidal channel processes in a tidal channel environment is poor sorting, some matrix support, coarse grain size, and sharp erosive contact with unit 2. The base of this facies is composed of thin, planar beds of granular fragments of basalt lava and mudstone rip-up. The middle and upper parts of this lithofacies consist of nested channel-fill pebbly basaltic sandstone beds that are sparsely fossiliferous and bioturbated (petrology sample CP-94-162B). Broken and disarticulated *Corbicula willisi*? molluscan fossils in these volcanoclastic sandstones were scoured in a brackish bay or intertidal mud-flat environment and incorporated within these debris flow deposits (macrofaunal sample CP-95-161, Appendix II). The debris flows probably originated from nearby eruptive Grays River volcanic highlands that border the tidal flats and broad marshes (Figure 29). This volcanoclastic facies is overlain by subtidal-channel arkosic sandstones and mudstones that were deposited in this incised estuarine valley-fill after debris-flow deposition.

Subtidal sandstone ridges or bar facies occur in unit 3 in sections 11E, O8, and O14 (Plate III). One large-scale, cross-bedded, fossiliferous silty sandstone lithofacies 3d in sections 11C and 11D (Figure 22B) contains abundant disarticulated and broken bivalves and gastropods of the *Erodona* faunal assemblage of Nesbitt (1995). These shell-rich layers are inclined 15° to the regional dip and strike of the underlying planar-bedded basaltic sandstone facies, suggesting these shell beds reflect low-dipping, large-scale foresets (up to 5 m high) of a prograding tidal sand bar or ridge perhaps at the mouth of the Eocene estuary. These foresets are similar in scale and form to modern subtidal sandridges or bars (tidal delta) imaged by high resolution seismic profile, in cores, and observed in Pleistocene terrace deposits by Clifton (1983) at the mouth of Willapa Bay

estuary, southwest Washington. The *Erodona* assemblage consists of suspension feeder, brackish-water bivalves *Erodona vaderensis* and the deposit feeders *Goniobasis*, *Viviparus*, and *Hydrobia* gastropods that lived as infauna in freshwater to low-salinity (brackish water) intertidal mud-flats (Nesbitt, 1995). Another 3 m- to 7-m thick sharp-based, fossiliferous, silty arkosic sandstone contains multiple shell lags composed of *Corbicula willisi* bivalves, *Potamides fettkei*, and *Eulima lewisiana* gastropods. These molluscs were reworked in the tidal ridges or channels by erosive tidal currents of adjacent brackish-water intertidal mud-flats (macrofaunal samples CP-95-163c, Appendix II; section O11, O14, and 11E; Plates II and III) (Nesbitt, written communications, 1996). Distinct tidal current-sorting of disarticulated brackish-water *Corbicula willisi* bivalves mixed with normal marine molluscan fauna (Figure 21A) along large-scale foresets is additional evidence that these sandstone tidal ridges or bars formed at the mouth of an estuary as tidal deltas or sand bars or ridges deposited in this tidal-flat system (macrofaunal sample CP-94-166A, Plates II and III) (Nesbitt, written communications, 1996). This faunal mixing occurred during the ebb tides when shells from freshwater to mudflat habitats were washed farther seaward to the estuary mouth. Freshwater floods during periods of excessive runoff could have also flushed these brackish-water molluscs out to the mouth of the estuary after their accumulation as shell lags at the base of meandering subtidal sand channels that had undercut the adjacent intertidal shell-rich mud-flats.

A series of subtidal channel sandstones and intercalated intertidal-flat (mudstone and mixed sandstone and mudstone) deposits occur in the lower part of unit 3. A nested tidal channel facies comprises the upper part. These 7 m- to 20 m-deep subtidal channels are filled with multiple megaripple cosets consisting of tide-formed, mud-draped, sigmoidal cross-bedded sandstone. Sedimentary structures diagnostic of a subtidal channel environment include: tidal-bundle sequences, slack-water mud-draped bottomset,

double mudstone couplets (Figure 18A) (systematically formed during slack-water periods of ebb and flood tides), coset thickness variations related to monthly tidal fluctuations, contorted bedding, and mud-draped reactivation surfaces (Figure 18, sections O9, O11, O15, and O16, Plates I and III). Nio and Yang (1991) described these characteristic tide-formed sedimentary structures in the modern estuary of Mont Saint Michel Bay, France (Figure 18B). For example, 28-day neap-spring-neap tidal fluctuations can result in thin-thick-thin foreset variations in laminated foresets of sandstone and mudstone known as tidal bundle sequences (Figure 18A). During neap tide, mud-drapes deposited during slack-water cover thin sand foresets that grade into the sandstone bottomsets due to strong, yet subordinate, ebb flow. During spring tide, mud-drapes are thinner or absent due to erosion during a stronger flood current. Ideally, there are 28 tidal bundles that reflect a monthly neap to spring tidal cycle in a semidiurnal tidal system (Nio and Yang, 1991).

Nested tidal creek or channel deposits, consisting of 1 to 3-m thick multiple channelized strata, occur in the banks of Olequa Creek at location 11E (Figure 21). These channel-fill deposits are floored with layers of marine *Teredo*-bored coalified wood and are incised into the underlying strata. Higher in the channel fill are flaser bedded fine-grained sandstone, mudstone-draped tangential cross-bedded medium-grained sandstone that form tidal bundle sequences, and massive bioturbated tuffaceous arkosic sandstone. A 13-m thick micaceous, arkosic sandstone-dominated subtidal sandstone facies that directly overlies the thick coal seam C in sections O21 and O12 contains tide-formed sigmoidal and wedge cross-bedding and lack mudstone drapes. Foreset and bottomset laminae are defined by concentrations of coarse micas and disseminated black carbonaceous plant debris. These cross-bed cosets bounded by undulating or wavy non-parallel planar reactivation surfaces are 0.5 to 1 m thick. These cross-bedded subtidal sandstones were probably deposited as a series of migrating sandwaves along the main axis of a major

subtidal channel where slack-water mud deposition is insignificant or not present because strong ebb and flood currents would prevent slack water muds from settling or would erode any mud deposited during tidal slack water.

Tidal-flat and tidal point bar sediments deposited in a shallower and more landward position within the estuary-fill are associated with the subtidal channel deposits. This intertidal facies association consists of thin and thick couplets of vertically-stacked ripple micro-cross-laminated sandstone and mudstone that form diagnostic tidal rhythmites (Figure 18B) (Nio and Yang, 1991). Nio and Yang (1991) described such tidal rhythmites in a modern estuary bay in France (Figure 18B). Rhythmic sandstone-mudstone couplets result from flood-ebb tidal cycles (diurnal or semidiurnal fluctuations) (Nio and Yang, 1991). The thickness of laminae in the sand-mud couplet in these tidal rhythmites varies in a cyclic manner, indicating they resulted from neap-spring tidal variations (14-day cycles). Upward-fining of flaser, wavy, and lenticular bedded mudstone and ripple-laminated very fine-grained sandstone corresponds to a landward decrease of tidal current speed and tidal point bar or tidal flat progradation within the estuary (Dalrymple, 1992). Strata overlying subtidal megarippled cross-bedded sandstone facies in section O9 consist of tidal rhythmites (Figure 18B) possibly formed on small-scale tidal bars. Other examples of these rhythmites include: (1) a vertically-stacked, thinly laminated tidal accretionary bar sequence of thin wavy bedded siltstone, mudstone, and sandstone erosionally overlain by a coal bed in section 11E (Plate III); and (2) rhythmically laminated, fining-upward tidal flat deposits consisting of very thin-bedded sandstone and wavy to lenticular bedded mudstone and carbonaceous shale overlying an upper subtidal channel or bar sandstone in sections O22 and O23 (Plate III).

Thin-bedded, fine-grained, subtidal to intertidal accretionary banks (part of lithofacies association TF) formed on the inside of tidal channel meanders tidal channels and on the adjacent tidal flat deposits. Accretionary bank deposits are depositionally

inclined (dip 10° to regional dip) to mainly horizontal thin to thick, stratified sequences of massive mudstone, muddy siltstone, and ripple-laminated silty sandstone. These deposits occur between coal zones A and C (sections 11D, 11E, O11, O14, and O17, and O20, Plates II and III). The 6 m- to 20-m thick deposits contain a tidally mixed salinity macrofaunal assemblage of *Pteria clarki*, disarticulated and broken shallow marine pelecypods and *Viviparus washingtonianus* freshwater gastropods (macrofaunal sample CP-95-166a, Appendix II). This mixture probably formed by flood tides, storm waves, or tsunami waves moving shallow normal marine shells from the mouth of the estuary into the upper reaches of the estuary, while freshwater river floods and flood tides moved freshwater snails down into the estuary. Additionally, bi-directional imbrication of the *Viviparus washingtonianus* gastropods indicate both ebb and flood tidal currents washed over these intertidal mud flats and mud-dominated accretionary bars adjacent to the subtidal channels. A fossiliferous (gastropod) horizon containing an *Unionid* freshwater clam of the *Unio* assemblage indicates that these flats were subjected to periodic freshwater influx (i.e., river floods). When these mudflats were subaerially exposed during low tide, the *Viviparus washingtonianus* gastropods grazed on detrital organic debris in the mud (Figure 21A, section O17, Plates I and III) (Nesbitt, written communications, 1996).

Subbituminous to lignitic coals and thick carbonaceous mudstone representing coastal supratidal marsh/swamp deposits (coal mires) within the estuary-fill generally overlie the fine-grained mudstone tidal flat and accretionary bank and tidal bar deposits in unit 3. Three coal-rich intervals in unit 3 occur in this study area and in the type section in Olequa Creek (Plate II). The lower seam A contains thin coal and paper-thin carbonaceous shale intervals intercalated with numerous calc-alkaline tuff beds and locally derived basaltic and andesitic volcanoclastic deposits. Coal seams B and C occur in the upper part of unit 3, the topmost coal seam is the thickest at 7.5-m thick (sections O14, O20, and

11E, Figures 25 and 26A, Plate III). Ten light buff, fine-grained, thin, western Cascade-derived tuff beds in this thick coal seam were sampled in section O14 for geochemical analysis (Figure 24 and Appendix III). A 1.2-m thick volcanoclastic sequence in this upper coal zone contains graded to cross-bedded, and scour-based basaltic to andesitic lapilli tuff beds that indicate deposition and reworking by fluvial and possibly high spring flood tide processes (e.g., floods) in this low-lying coastal marsh/swamp (Figure 26B). These locally derived volcanoclastic tuff beds (ash fall) can be correlated across all correlated exposures of this coal interval and indicate this coastal brackish or freshwater marsh/swamp was low-lying and widespread and had minimal topographic relief (Figures 10 and 28, Plate III). In section O20 the upper part of this coal bed is soft-sediment-folded due to rapid deposition and loading of overlying siliciclastic sands and muds. The coal seams form the top of the tidally formed fining- and thinning-upward parasequences (i.e., the coals overlie the meandering subtidal channel sandstone and intertidal accretionary banks) in unit 3 (Plates II and III).

Dozens of mafic and subordinate silicic volcanoclastic deposits (lithofacies 3h) (ranging from 5 cm to 1.8 m thick and averaging 10 cm in thickness) also occur throughout the supratidal association ST (coal zones A, B, and C) of unit 3. Some basaltic sandstone beds contain mixed freshwater and normal marine bivalves and gastropod fragments indicating some tidal reworking of these volcanic sandstones. Many pebbly sandstones are composed of medium- to coarse-grained scoriaceous basaltic clasts. The nearby Grays River volcanics is the most likely intrabasinal source for the unstable scoria clasts, perhaps derived from explosive basaltic lava fountains or phreatic eruption in nearby highlands that rained pyroclastic debris onto the surrounding coastal plain or estuary fill (petrology samples CP-94-134B and CP-94-163A, Appendix IV). Streams draining these highlands flowed into the estuary or into the main trunk river that fed the estuary (Figure 29). A 1 m- to 1.8-m thick, sharp based, pumice lapilli tuff is planar-

laminated to massive and both normal and reversely graded and contains minor mudstone rip-ups near the base. These sedimentary features suggest that the reversely graded part of this deposit originated from a basal pyroclastic ash flow with subsequent ash falls forming the normally graded upper part (Cas and Wright, 1988) (marker bed U3-A, petrology sample CP-95-163b, Figure 22A). This silicic pyroclastic bed contains oligoclase feldspar crystals that indicate a more distance dacitic western Cascade calc-alkaline volcanic arc source (e.g., Northcraft Formation 25 km to the northeast) (location 11D, Plates I, II, and III). The oligoclase was $^{39}\text{Ar}/^{40}\text{Ar}$ age dated by Irving et al. (1996) at 38.9 Ma or latest middle Eocene, they believe, this bed is the earliest record of western Cascade volcanism in southwest Washington.

Unit 4: Upper Transgressive Shallow Marine Succession

Unit 4 along the type section in the upper reaches of Olequa Creek consists of nearshore to inner shelf mollusc-bearing, micaceous arkosic sandstone and outer shelf to upper bathyal micaceous mudstone. The unit represents a major transgression (i.e., a transgressive system tract TST) or onlap over the tidally dominated facies of unit 3. The wave-dominated lithofacies successions of unit 4 form 10 coarsening- and thickening-up parasequences that each becomes less thick upwards (Plate II). Each parasequence represents a gradational change from offshore marine mudstone formed below wave base to storm wave-dominated shoreface sandstones and siltstones. Individual parasequences range from 5 m to 35 m in thickness. Generally, marine mudstone abruptly overlies shoreface sandstone in each parasequence. These parasequence successions form coarsening- and thickening-upward parasequences that overall define a retrogradational parasequence set (based on the terminology of Van Wagoner et al., 1990) (Plate II). Thick transgressive, bioturbated outer shelf to upper bathyal mollusc-bearing sandy siltstone and glauconitic mudstone described and measured by Elizabeth Nesbitt (1979) at the Big Bend

locality (type Cowlitz locality of Weaver (1934)) along the Cowlitz River east of Vader (Plate I) can be lithologically and biostratigraphically correlated to unit 4 in the type section in Olequa Creek (measured sections O31 to O32, Plate II). However, the upper part of this unit is sandier in Olequa Creek than in exposures along the Big Bend locality, where the dominant lithology is massive bioturbated sandy mudstone.

Depositional environments of the three lithofacies associations of this unit include: (1) nearshore to inner shelf (ripple cross-laminated siltstone and sandstone), (2) lower shoreface (hummocky cross-stratified arkosic, micaceous sandstone), and (3) middle to outer shelf bioturbated, sandy siltstone and glauconitic mudstone.

Nearshore to inner shelf sedimentation occurred in this area during a relative sea level rise or transgression. Bioturbated sandy mudstone, wavy to lenticular bedded mudstone and very fine-grained sandstone, clay-rich siltstone, and very fine-grained micro-cross-laminated sandstone were deposited under normal wave-generated conditions (sections O23 to O30, Plate II). Some thicker sandstone beds contain mudstone rip-ups indicating that they were deposited by higher energy events (i.e., storm waves). The intervening thicker, massive mudstone and siltstone beds contain thick-shelled bivalves and small horizontal to diagonal burrows of the nearshore *Skolithos* ichnofacies. These strata are dominantly fine-grained (i.e., lack sand) and are bioturbated near the upper part of unit 4, suggesting this rise in sea level or transgression was rapid enough to starve the shelf of any significant amount of sand and the sedimentation rate was slow to allow extensive bioturbation during the initial phase of the transgression.

An overlying sequence of 2 m- to 6-m thick, sharp-bottomed, silty fine-grained, well-sorted, micaceous, arkosic sandstone beds of the lower shoreface abruptly overlies the fine-grained strata in sections 12B, O31 and in the lower part of section O32. Some sandstone beds contain storm wave-generated hummocky cross-stratification and broken molluscan fossils (Figure 25B, section 12B, Plates I and II). Minor layers of contorted

laminae and calcareous concretionary horizons also occur. A 1-m thick abundantly fossiliferous silty sandstone bed contains multiple shell lags (Figure 25A, macrofaunal sample CP-95-177, Appendix II) consisting of *Pitar eocenica* and *Venericardia hornii clarki* bivalves and *Turritella uvasana olequahensis*, *Calyptrea diagoana* and *Polinices nuciformis* gastropods of the shallow marine *Turritella-Tivelina* assemblage of Nesbitt (1995). Molluscs of the *Turritella-Tivelina* assemblage lived in a silty sand substrate and in 10 to 150 m water depths. These shallow marine benthic molluscs were reworked by storm waves to form shell lags at the base of the hummocky cross-stratified arkosic sandstone beds. These sandstones are overlain by fair-weather deposits consisting of ripple-laminated siltstone and wavy to lenticular bedded mudstone, siltstone, and very fine-grained sandstone. Neritic foraminiferal assemblages collected and identified by Yett (1979) from this hummocky cross-stratified interval (UWA-3341, measured section O32) consist of the *Elphidium-Cibicides* faunule.

Thick, massive, bioturbated, sandy siltstone and glauconitic mudstone deposited on the outer shelf to upper slope overlie the thin-bedded lower shoreface sandstone-dominated sequence near the top of unit 4 (e.g., sections O32, O33, and the upper part of section 12B, Plate II). One arkosic sandstone bed is overlain by a sharp-bottomed, fossiliferous mudstone with scattered fossil *Turritella olequahensis* gastropods and calcareous concretions (section 12B, Plate I). The sharp interface between the lower shoreface arkosic sandstone and the mudstone defines a marine flooding surface and a maximum flooding surface (Plate II). The glauconite-bearing mudstone of section O32 may be a condensed section deposited in upper bathyal water depths.

A water depth increase in the upper 65 m of unit 4 was determined from molluscan assemblages collected and identified by Nesbitt (1979, 1995) from silty, fossiliferous, and glauconitic siltstone and mudstone at the Big Bend locality along the Cowlitz River. Inner neritic *Turritella-Tivelina*, transitional *Pitar*, and upper bathyal to outer neritic *Nuculana*

assemblages record 50 m to up to 600 m water depth increase. According to Nesbitt (1995) this increase in water depth reflects a continued transgression or deepening event in the upper part of the Cowlitz Formation. Lithologic and biostratigraphic similarities were observed in the Olequa Creek section in this study.

A shoaling event (highstand system tract) is recorded in the uppermost part of unit 4. Here, clay-rich siltstone, thin beds of laminated silty mudstone, and a capping silty sandstone calcareous concretions and out-of-phase wave ripple-laminations were deposited on the middle to outer shelf. Additionally, hummocky cross-stratified sandstones were deposited by storm wave events in middle to upper shelf water depths (Plate II).

Unit 5: Lowstand Prodelta Siltstone

The uppermost unit 5 of the Cowlitz Formation is dominantly composed of planar siltstone. It forms the youngest unit in the Cowlitz Formation and is exposed along upper part of Olequa Creek (sections O33 to O37, Plate II) and in a 20 m high roadcut along the Vader Highway, 1.5 miles east of Vader (NW 1/4, Sec 27, T11N, R2W, Plate I). This prodelta and continental slope sequence represents a continued transgression or onlapping sequence over unit 4. This lowstand prodelta sequence consists of the following lithofacies: (1) deep marine fine-grained, laminated siltstone and thin-bedded arkosic turbidites, (2) submarine-channel sandstone and chaotic mudstone rip-up conglomerate, and (3) slump-folded and soft-sediment deformed siltstone intervals.

Submarine-channel sandstone occurs at the base and in the middle of unit 5 (Plate II). The 16-m thick basal channelized unit consists of very thick- to thick-bedded and amalgamated, friable, fine- to medium-grained, micaceous, arkosic sandstone and some thin siltstone interbeds. Layers of large calcareous concretions and very poorly sorted chaotic mixtures of angular, pebble- to cobble-sized mudstone rip-ups are abundant in

these sandstones (Figure 26). Many sandstone beds are massive or structureless but some are graded with sharp-bottom contacts and gradational upper contacts and contain Bouma Tcd sequences and slump-beds and clastic dikes. The nested channel facies is similar lithologically to deep marine submarine gully sequences formed seaward of delta front sands in the Eocene Coaledo Formation of southwest Oregon described by Dott and Bird (1979) and described by Niem et al. (1992) in the Miocene Astoria Formation and the Miocene Gnat Creek (Clifton formation) of northwest Oregon (Niem, written communications, 1998). This sandstone body contains multiple cross-cutting channelized layers, scour-and-fill and lateral-accretion surfaces that form large-scale epsilon and avalanche stratification lined with dark gray angular mudstone clasts. These features probably formed during migration of submarine point bars and by undercutting and collapse of siltstone levees and adjacent channel walls (Figure 30).

However, this nested channelized sandstone interval becomes hummocky and swaley cross-stratified stratigraphically higher in the section. These anomalous storm-generated features suggest an upward shallowing of depositional conditions from below storm-wave base to the lower shoreface or large storm events during which wave base temporarily reached into deeper water.

On the flank and top of a large (10 m) paleo-channel slump-block of laminated siltstone is a second mudstone and siltstone rip-up conglomerate submarine-channel sandstone deposit in section O35 along Olequa Creek (Plate II). The rip-up clasts are imbricated and indicate a paleo-current flow to the southwest. Overlying this unit is a laminated to graded sandstone and mudstone, ripple-laminated siltstone, and a third graded channelized sandstone sequence. Sedimentary features include flame structures that indicate a south-southwest paleo-slope, load casts, ball and pillow structures, and contorted bedding (Figure 27B).

**UNIT 5: LAMINATED PRODELTA SEQUENCE
SUBMARINE CHANNEL-FILL AND SLUMP-FOLDED INTERVAL**

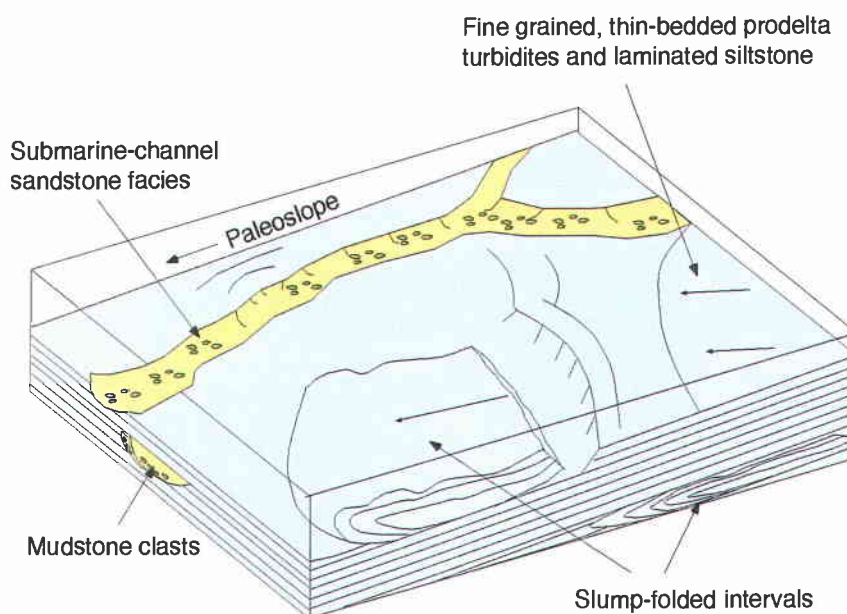


Figure 30. Paleogeographic reconstruction of the uppermost Cowlitz Formation unit 5 showing depositional environments of this deep marine prodelta sequence.

The marine fine-grained, thin-bedded turbidite facies consists of rhythmically bedded, thinly to thickly laminated, planar-parallel, clay-rich, and very fine-grained siltstone and subordinate sandstone turbidites (Bouma Tcd). The basal division of these turbidites consists of sharp-based, plane- to ripple-laminated very fine-grained arkosic sandstone. Due to rapid sand deposition over less dense soupy water-saturated silts, delicate soft sediment structures composed of thin-bedded sandstone have sunk into the underlying thinly laminated siltstone. The upper part of unit 5 is composed of very thin beds of finely laminated to micro-cross-laminated basal sandy siltstone and planar-parallel clayey siltstone. These laminations are formed by grain-size differences and minor mica and carbonaceous partings. In places, this unit is interbedded with minor hummocky cross-stratified silty sandstone, tuffaceous mudstone, and small calcareous concretionary horizons. These well-laminated turbidites formed on a prodelta slope largely below storm wave base during rapid mud sedimentation. In this possibly anoxic environment, benthic marine organisms could not live with this sediment influx, thus preserving fine laminations.

Multiple soft-sediment slump-folded and soft-sediment deformed intervals vary in thickness from 0.6 m to over 12 m and were observed throughout the lower part of the measured section (sections O33 to O35, Plates I and II). Some recumbent, east-verging to asymmetrical, and isoclinal slump folds are composed of planar-laminated siltstone with axial trends averaging 350° . These folds indicate slumping was in a north- northeasterly downslope direction. Other slump-folded intervals contain large blocks (10 m wide) of carbonaceous micaceous shale. One steeply dipping block of intensively bioturbated and ripple-laminated siltstone and mudstone underlies and forms the western margin of a submarine sandstone channel-fill (section O36, Plate II). Clastic sandstone dikes are also present near these soft-sediment slump folds.

These submarine folds and clastic dikes may have resulted from rapid sedimentation and loading of water-saturated siltstone beds in the prodelta environment. This slumping may have been triggered by earthquake activity in this active-margin depocenter.

TOUTLE AND LINCOLN CREEK FORMATIONS

Newly discovered units of the Toutle Formation are informally named in this study. These units are: (1) a 105-m thick, fluvial-dominated valley-fill unit A, (2) an overlying 85-m thick marginal marine unit B, and (3) an upper 75-m thick fluvial unit C (Plate II). The lower unit A, newly dated in this study as Oligocene (31.9 ± 0.44 Ma $^{39}\text{Ar}/^{40}\text{Ar}$ age date), disconformably overlies the Cowlitz Formation along Olequa Creek (Figure 31). Foraminifera of the *Cibicides Gyroidina* faunule identified by Yett (1979) from the Toutle Formation (as defined in this study) were assigned to the *Sigmomorphina schencki* foraminiferal zone of Rau (1958) of the Refugian stage (Yett, 1979) (Figure 3).

The Oligocene age Toutle Formation in the type area, 18 km east of Olequa, consists of a 60-m thick marine unit and a 100-m thick upper non-marine member (May, 1980) (Figure 32). In the type area, the Toutle overlies the Hatchet Mountain Formation that unconformably overlies the Cowlitz Formation (Roberts, 1958). The lower member of the Toutle was deposited in cool subtropical nearshore water based on molluscan fossils, the upper member formed in fluvial, paludal and /or lacustrine conditions (May, 1980). An extensive Galvinian (upper Eocene to lower Oligocene) molluscan fauna is present in the lower member of the Toutle Formation (Roberts, 1958; May, 1980; and Phillips, 1987). The lower member of the type Toutle Formation is assigned a molluscan age within the *Echinophia dalli* and *Echinophoria fax* zones of Armentrout (1973), within the Refugian foraminiferal stage (May, 1980) (Figure 3). The upper member may correspond with the *Echinophoria fax* zone of the Galvinian to the *Echinophoria rex* zone, within the Zemorrian foraminiferal stage (34 to 31 Ma) (May, 1980) (Figure 3).

Unit A of the Toutle Formation in this area may be correlative to the upper member of the type Toutle Formation of Roberts (1958) in the western Cascades (Figure 32).

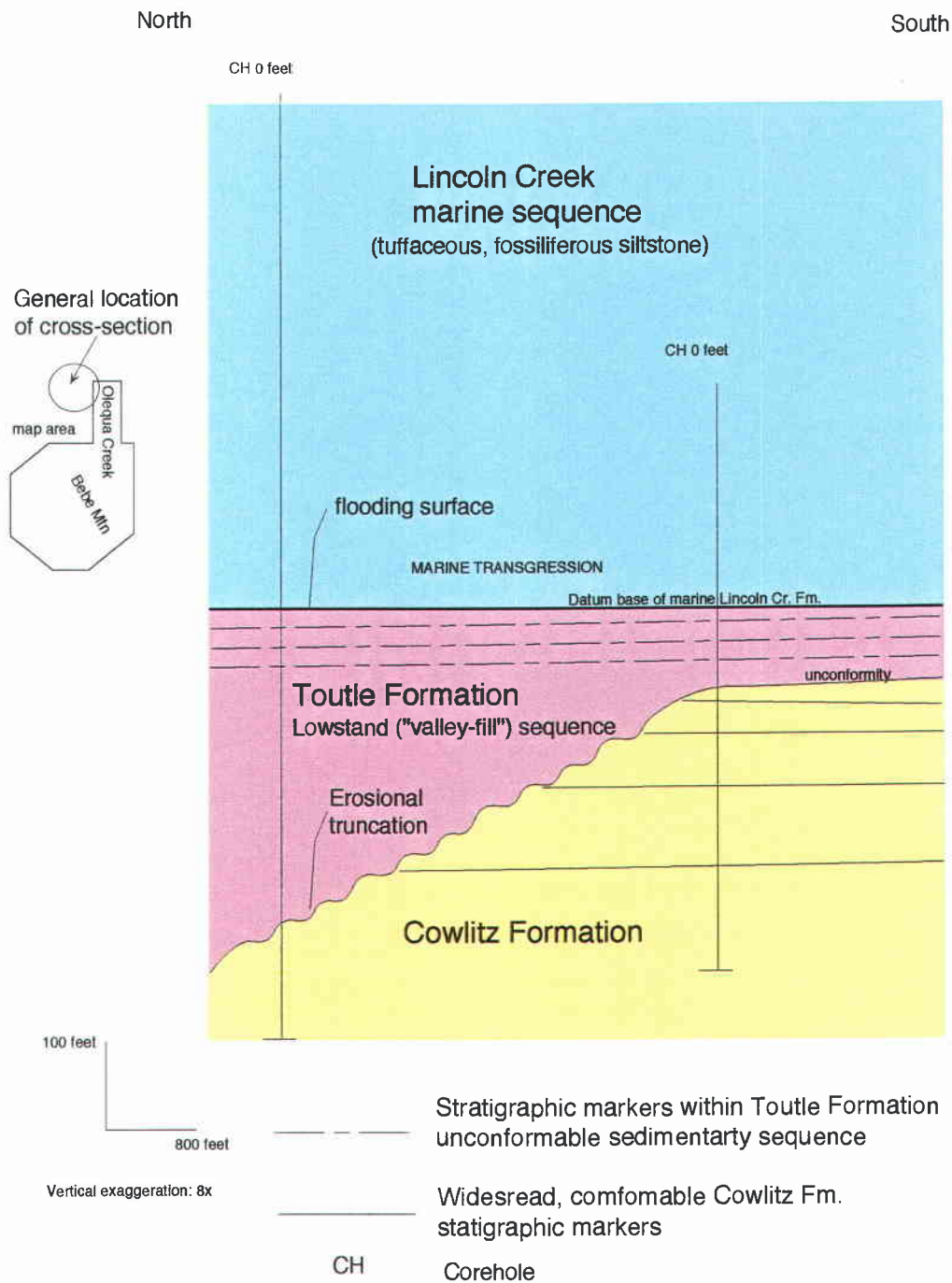


Figure 31. Stratigraphic cross section showing unconformable contact relationship of the Cowlitz Formation with the overlying valley-fill Toutle Formation (from Dave Pauli, written communications, 1997).

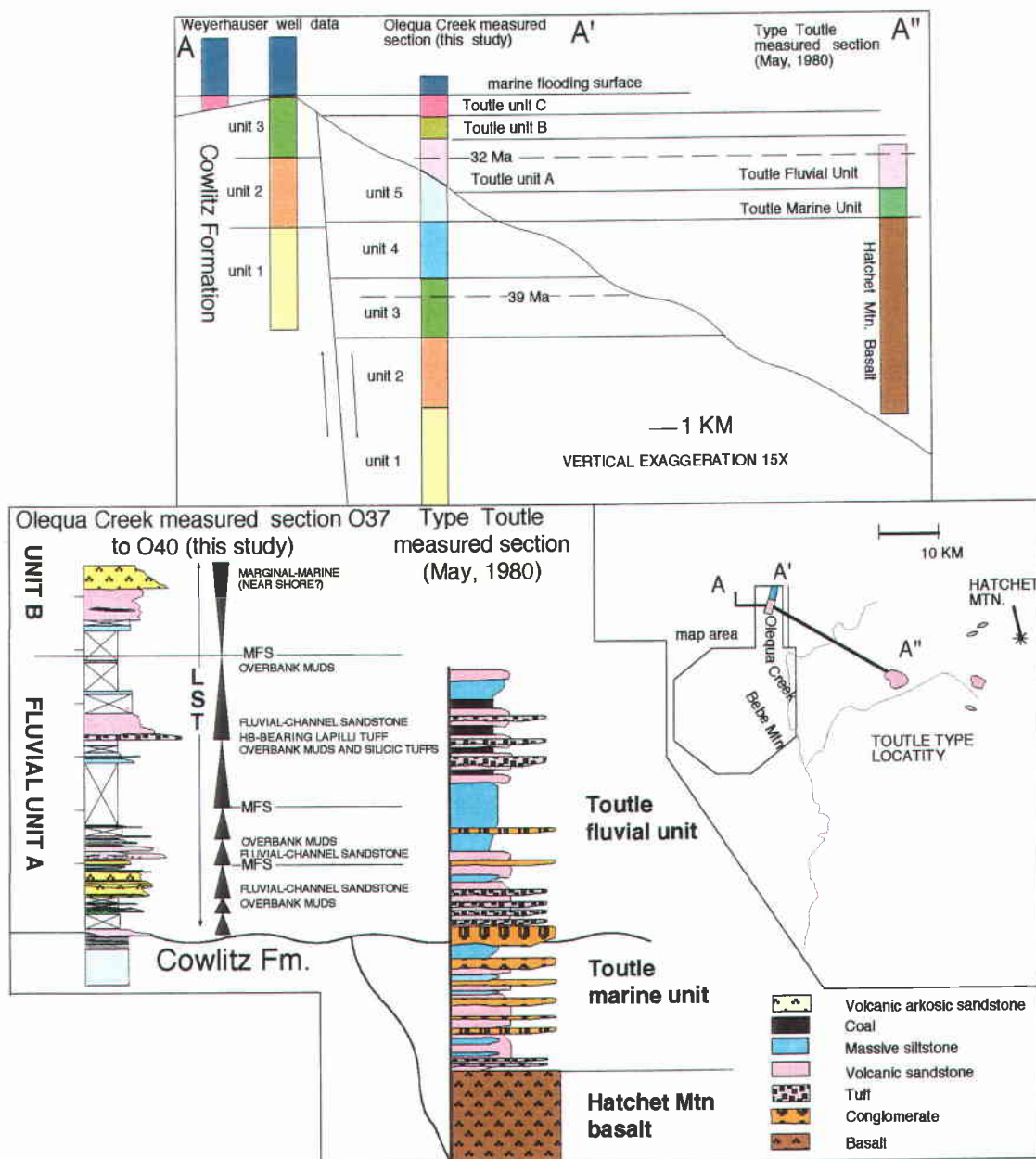


Figure 32. Regional correlation of the type Toutle Formation fluvial unit of May (1980) and the Toutle fluvial unit A (this study) in Olequa Creek.

This correlation is based on similarities in lithology, stratigraphic position, and age. The Toutle Formation may be correlative to the deeper marine Oligocene part of the Lincoln Creek Formation mapped to the west in the Willapa Hill (by Wells, 1981) and in the Gray Harbor area (by Pease and Hoover, 1957). The lower part of the type Lincoln Creek Formation in these basins is older than the Lincoln Creek in this area (i.e., upper Eocene to lower Oligocene or Refugian) based upon forams, magnetostratigraphy and molluscan fauna (i.e., 34.5 to 32 Ma) (Figure 3) (Prothero and Armentrout, 1985).

A thick sequence of massive to very thick-bedded, concretionary, and tuffaceous shelfal siltstone with minor fine-grained silty marine sandstone overlies the Toutle Formation in Olequa Creek (Plates I and II). These lithologies were mapped by Henriksen (1956) and in this study as Lincoln Creek Formation and correlate with part of the type Lincoln Formation exposed in Lincoln Creek, west of Centralia, Washington (Snively and others, 1958). According to Henriksen (1956), the Lincoln Creek Formation is over 455-m thick in Olequa Creek in the Winlock area. Armentrout (1973) using molluscan fossils, interpreted that the tuffaceous sandy siltstone facies of the Lincoln Creek Formation near the town of Winlock was deposited in warm upper neritic shelfal waters. In a fine-grained sandy siltstone at Olequa Creek section location UW-291 (Plates I and II), Armentrout (1973) identified the *Macrocallista-Nuculana* zonule that ranges throughout Armentrout's *Echinophoria Fax* zone of the upper Galvinian molluscan stage (lower Oligocene) and the upper Refugian foraminiferal stage (Figure 3). Foraminiferal assemblages in the Lincoln Creek Formation from Olequa Creek are assigned to the *Sigmomorphina schencki* zone of Rau and the lower Refugian stage (Yett, 1979).

Outcrop Distribution and Thickness

Detailed description and stratigraphic section measurement along Olequa Creek are the main source of data for this discussion and mapping the distribution of the Toutle and Lincoln Creek formations (Plates I and II). The 265-m incised valley-fill unit of the Toutle Formation consists of three units: (1) a lower fluvial-dominated section (unit A) that grades upward into (2) a marine siltstone (unit B), and overlying tuffaceous (lowstand) fluvial sequence (unit C) (Plate II). The valley-fill unit C, in turn grades up, into the thick overlying deeper marine tuffaceous siltstone of the Lincoln Creek Formation (Figure 31 and Plate II)

During low-water stage in the fall, exposure of units A and B of the Toutle Formation is good to incomplete along the Olequa Creek stream bed and banks: the upper part of the Toutle (unit C) and lower part of the Lincoln Creek formations are nearly completely exposed (Plates I and II). The Toutle Formation is 65% exposed (a total of 170 m of exposed strata) in Olequa Creek and displays a sandstone/mudstone ratio of 2:1 (Plates I and II). Exposures are restricted to the creek bed and channel walls with minor small exposures along the Winlock-Vader Highway (Plate I). Pleistocene gravels cover the Toutle and Lincoln Creek formations in the adjacent stream terrace (which were not mapped). These formations do not occur elsewhere in the map area (Plate I).

Contact relationships and Lithology

Toutle Formation

An incised basal non-marine valley-fill (unit A), the overlying (estuarine or nearshore) marginal marine sequence (unit B), and a fluvial sequence in the upper Toutle Formation (unit C) along Olequa Creek consists of the following lithofacies: (T1) a basal debris flow deposit (non-marine), (T2) volcanic-lithic arkosic channel-fill sandstone

(meandering fluvial point bar), (T3) carbonaceous mudstones (overbank floodplain), (T4) cross-bedded volcanic-arkosic sandstone (nearshore to marginal-marine estuarine), (T5) massive mudstone (shelfal), (T6) volcanic channel-fill sandstone (fluvial point bar), (T7) thin lignite and carbonaceous shale (marsh/floodplain and oxbow lakes), and (T8) thick basaltic and siliceous volcanoclastics and tuff beds.

Unit A: Lower Volcanic Arkosic Sandstone and Mudstone

In Olequa Creek, the lower contact of the non-marine Toutle Formation valley-fill unit A is sharp and erosional, with more than 3 m of relief into the underlying deep marine siltstone (unit 5) of the Cowlitz Formation (e.g., see the top of section O37 on Plate II) (Figures 31 and 33A). This contact reflects an abrupt change from deep marine siltstone to Oligocene non-marine sandstone (i.e., a sequence boundary). This sequence boundary is much younger than Armentrout's (1987) Lincoln Creek sequence boundary or regional unconformity. The basal part of valley-fill unit A is a debris flow deposit (lithofacies T1) composed of angular to subrounded rip-up clasts (up to 5 cm in diameter) of laminated siltstone (derived from the underlying Eocene Cowlitz Formation unit 5), coalified wood fragments, other volcanic sandstone, and light gray tuffaceous siltstone clasts in a mudstone matrix (CP-95-181b3, O37, Plate II).

The overlying strata in measured section O38 (Plate II) consist of 1.5 m of rooted, blue-gray mudstone and sandy mudstone with abundant carbonaceous flakes (lithofacies T3). There are shallow channels (1.5 m- to 0.6-m thick) filled with tuffaceous, moderately sorted, medium- to fine grained feldspathic volcanic-litharenite (lithofacies T2) (petrology sample CP-95-182b, Appendix III). These sandstone channels contain cross-bed foresets lined with black carbonaceous material, carbonized root traces, oriented

A.



B.



Figure 33. (A) Unconformable contact of the Toutle Formation (valley-fill unit A) with the underlying deep marine siltstone of the Cowlitz Formation unit 5 in Olequa Creek (top of section O37; 1/4 SE, Sec. 5, T11N. R2W; Plates I and II). Note head of rock hammer on Cowlitz-Toutle contact and 1.5 m Jacob's staff for scale. (B) Coalified log in fluvial volcanic arkosic channel sandstone from measured section O38 (1/4 SE, Sec. 5, T11N. R2W; Plates I and II). Note 25 cm rock hammer for scale.

coalified logs (Figure 33B), large calcareous concretions with imprints of leaves, and abundant lenses of mudstone. Four meters of indurated sandy siltstone overlies the mudstone lenses (lithofacies T3).

The overlying strata in Olequa Creek, section O39 (Plate II) consists of 10 m of blue-gray, friable, faintly trough cross-bedded, very fine- to fine-grained, clay-rich arkosic sandstone (lithofacies T2) and subordinate moderately indurated, medium-grained sandstone. These sandstones contain little or no mica. This section is overlain by medium-grained volcanic sandstone with a sharp base and an overlying mudstone sequence (lithofacies T2) that is interbedded with 5-m thick lithic arkose. The mudstone grades upward into a sandy, carbonaceous siltstone containing a few claystone layers and a fine- to medium-grained, clay-rich arkosic sandstone.

A moderately sorted, medium- to coarse-grained, volcanic-arkosic sandstone channels (lithofacies T2) into the underlying siltstone. The sandstone contains lenses of pumice lapilli tuff and large imbricated, coalified logs (70 cm long and 10 cm thick) that indicate a south paleocurrent direction. This sandstone channel grades upward into sandy mudstone. Two more lithologically similar fining-upward channel sequences are higher in this section.

In measured section O40 (Plate II), the lower valley-fill sequence is composed of 8 m of blue-gray, clay-rich siltstone, light-tan mudstone, a thin carbonaceous shale bed (lithofacies T7), a green-blue tuff (lithofacies T8), and an overlying thick blue-gray mudstone (lithofacies T3). An overlying 10-m thick partially covered interval contains a distinctive 1.5-m thick pumice-lapilli tuff (lithofacies T8). The subangular, clast-supported, pumice lapilli contain abundant euhedral hornblende crystals (up to 20%) that were $^{39}\text{Ar}/^{40}\text{Ar}$ dated by Bob Duncan of the OSU College of Oceanic and Atmospheric Sciences at 31.9 ± 0.4 Ma or Oligocene (CP-95-183B, Appendix VI). Minor subrounded, dark gray, volcanic pebbles and a west-southwest imbricated coalified log (1 m long and

0.5 m wide) suggest this hornblende pumiceous tuff was reworked by river processes. An overlying, 5.5-m thick cross-bedded, medium- to coarse-grained volcanic arkosic sandstone fines-upwards to fine-grained silty sandstone (lithofacies T4). The sandstone contains multiple, calcareous concretionary horizons towards the top and is moderately sorted and clay-rich.

Unit B: Mudstone Sequence

The lower part of section O41 along Olequa Creek (Plate II) consists of 24 m of poorly exposed, clay-rich marginal marine sandy siltstone (lithofacies T4) and mudstone (lithofacies T5) of unit B. Thick, medium-grained, moderately indurated, moderately sorted, volcanic-lithic arkosic sandstone overlies the siltstone and mudstone. The sandstone is clay-rich, silty, and moderately indurated and has up to 30% quartz and feldspar. This sandstone contains a coalified, *Teredo*-bored log. The log is 4 m long, 0.6 m wide, and 0.15 m thick and is imbricated (oriented 20°, 2°N). There are also cobble-sized mudstone and silty mudstone rip-ups (up to 10 cm in diameter) in this sandstone. The uppermost part of this sandstone is slightly trough cross-bedded. An upper 10-m thick medium- to coarse-grained sandstone that fines-upwards to fine- to medium-grained, volcanic-lithic arkosic sandstone become arkosic to subarkosic (50% quartz, feldspar, volcanics, and very little mica) in the uppermost interval.

The poorly exposed, upper part of section O41 and the lower part of section O42 (Plate II) becomes dominantly fine-grained and is 55 m thick (Plate II). This interval consists of clay-rich siltstone, medium-bedded silty very fine-grained sandstone, sandy siltstone with volcanic-rich lenses, and gray mudstone (lithofacies T5) (sample CP-95-185). A tan-gray mudstone with small carbonaceous fragments is interbedded with a blue-gray mudstone. Straight and vertical (3 cm in diameter) burrows of the *Cruziana* ichnofacies and an overlying claystone (tuff) are at the top of this interval.

Unit C: Upper Tuffaceous Volcanic Sandstone and Mudstone

A channelized volcanic sandstone (lithofacies T6) is incised into the lower mudstone (lithofacies T3) in section O42 (Plate II). This fining-upwards, tuffaceous, medium-to coarse-grained, poorly sorted, volcanic sandstone is 4.5 to 0 m thick and contains numerous coalified logs, carbonaceous wood fragments, and mudstone rip-ups. An overlying 1.5 to 3-m thick interval is composed of dark gray mudstone and contains coalified logs and carbonaceous flakes. This interval has a rooted top and is interbedded with a light tan tuff (geochemical sample CP-95-186x1, Appendix III) and a thin gray-buff tuff. A third 2 to 0-m thick channelized moderately sorted, medium-grained volcanic sandstone containing coalified wood fragments is overlain by a rooted organic-rich mudstone. This grades into carbonaceous shale to lignite and contains numerous coalified logs and trunks (lithofacies T7). A 1.5-m thick light tan to green fine-grained tuff (claystone) (geochemical sample CP-95-186x2, Appendix III) coarsens upwards into a yellow silty mudstone that is overlain by a 2.4-m thick blue-green tuff (geochemical sample CP-95-186x3, Appendix III) and mudstone with coalified logs (lithofacies T3 and T8). A 6-m thick coarse-grained volcanic sandstone with coalified woody material and mudstone interbed is at the top of section O42 (Plate II).

Above an 8 m covered interval, are 6 m of low-angle cross-bedded, fine- to medium-grained volcanic arkosic sandstone (lithofacies T2) that is interbedded with a 1.5-m thick ripple-laminated light blue-gray tuff bed (section O43). This sequence is overlain by 2.3 m of silty, tuffaceous mudstone. A 7-m thick, sharp-based, coarse-grained to granule-size volcanic conglomeritic sandstone fines upwards into medium-grained volcanic sandstone that contains pods of very coarse-grained to pebble-sized volcanic sandstone lenses and a matrix-supported lapilli tuff. A 6-m thick clast-supported, pebble-sized basaltic lapilli tuff is capped by 5 m of alternating thin beds of silty very fine-grained

sandstone, silty carbonaceous mudstone, and a brownish-gray mudstone and light tan tuff (lithofacies T3 and T8).

Near the top of measured section O43 (Plate II) is a 3-m thick, medium- to coarse-grained tuffaceous sandstone (lithofacies T6). The sandstone displays a sharp, scoured base. A cross-bedded fine-grained carbonaceous, subarkosic sandstone and some mudstone rip-ups overlie the sharp based sandstone. This unit is, in turn, overlain (in section O44) by 4.5 m of tuffaceous mudstone containing coalified plant stems, carbonaceous shale with long coal stringers, a current-reworked thin tuff bed, and mudstone with carbonized plant roots (lithofacies T7 and T8). The uppermost part of the Toutle Formation consists of 3 m of concretionary, faintly cross-bedded, friable, fine- to medium-grained, quartz-rich sandstone, fine pebble volcanic conglomerate, and a fossil shell lag composed of shallow marine *Crassellellites stillwaterensis* bivalve casts and molds (lithofacies T4) (macrofaunal sample CP-95-188a, Appendix II).

Tuffaceous Siltstone Member of the Lincoln Creek Formation

The 455-m thick Lincoln Creek Formation in the study area is dominated by uniformly massive, well-indurated shoreface to inner shelf, fossiliferous tuffaceous siltstone. A thin shoreface to inner shelf fine-grained arkosic sandstone forms the basal part of the unit. It was distinguished at the marine sandstone from the top of the underlying valley-fill Toutle Formation by the fine grain size (no conglomerates) and tuffaceous composition, and it contains a Galvinian molluscan assemblage (Armentrout, 1973). The total thickness of section measured in this study is 74 m and this siltstone was the only member of the Lincoln Creek observed (i.e., no lower Lincoln Creek basaltic sandstone member) (Plates I and II).

The upper part of measured section O44 in Olequa Creek consists of 6 m of interbedded silty fine-grained sandstone and grayish-blue sandy siltstone containing

multiple molluscan fossil shell-rich storm wave lags (sampled by Armentrout, 1973) and a *Teredo*-bored log (2 m long by 0.3 m wide). One faintly hummocky cross-stratified sandstone is interbedded with an overlying 10-m thick tuffaceous siltstone. Vertical and horizontal (*Thalassinoides*?) burrows (with some spreiten) are also present.

Measured sections O45 to O47 south of Winlock (Plates I and II) are composed of very thick-bedded, massive tuffaceous siltstone, intensively bioturbated, sandy siltstone, and minor poorly sorted sparsely fossiliferous silty tuffaceous sandstone. Additionally, large pumice lapilli, weathered casts of pelecypods, burrows filled with tuffaceous volcanic sandstone, and *Teredo*-bored coalified wood fragments are present in some beds. Silty sandstone beds are generally 1 m thick and are moderately to well indurated. Minor thin beds of graded, coarse-grained to pebbly basaltic sandstone are also present. The uppermost part of measured section O48 (Plate II) consists of 6-m thick beds of well indurated, tuffaceous sandy siltstone and subordinate thin-bedded tuffaceous arkosic sandstone. Articulated, thick-shelled bivalves and high-spined gastropods, concretionary horizons, and mudstone storm-wave rip-ups also occur near the top of this section (Plates I and II). The upper contact of the Lincoln Creek Formation with the overlying Neogene strata is not exposed in the study area.

Depositional Environments

Toutle Formation

The Toutle Formation along Olequa Creek consists of the following lithofacies from various depositional environments: (T1) a basal non-marine debris flow, (T2) fluvial point bar (volcanic-lithic arkosic sandstone channel-fill), (T3) overbank floodplain mudstones (carbonaceous mudstones), (T4) nearshore to marginal-marine estuarine (cross-bedded volcanic-arkosic sandstone), (T5) shelfal mudstone (massive mudstone),

(T6) coarse-grained, fluvial point bar (volcanic channel-fill sandstone), (T7) marsh/floodplain and oxbow lakes (thin lignite and carbonaceous shale), and (T8) thick basaltic and siliceous tuff beds (Figure 34).

Unit A: Lower Valley-Fill Fluvial Sequence

The basal debris flow (lithofacies T1) unconformably overlies the Cowlitz Formation at the top of section O37 (Plate II). At least 3 m of erosional relief is evident in this sharp contact between the deeper marine laminated siltstone of unit 5 and the basal non-marine Toutle Formation in outcrop exposure in the bank of Olequa Creek. This debris flow deposit is poorly sorted, in matrix-support, and contains angular to subrounded rip-ups clasts of planar-parallel siltstone derived from the underlying unit 5 of the Cowlitz Formation. Additionally, the debris flow deposit contains coalified wood fragments, volcanic sandstone, and tuffaceous siltstone clasts in a mudstone matrix. These clasts were derived from the surrounding hills of tectonically uplifted and subaerially exposed older Cowlitz strata and deposited in a newly formed river valley incised into the Cowlitz Formation (Figure 31 and 34).

Feldspathic litharenite (petrology sample CP-95-182b, Appendix III) and volcanic fluvial sandstone point bar lithofacies (T2) at the base and top of the Toutle Formation (units A and C) were deposited in a meandering river system. The non-marine character of sandstone beds in the lower part of the Toutle Formation is suggested by fining- and thinning-up sequences, filled channels, moderate sorting, and carbonaceous root traces in growth position (section O33 and O39, Plate II). Imbricated coalified logs at the base of many channel-fill sequences, indicate a local south-southwest paleoflow direction. Leaf imprints in calcareous concretions, lateral-accretionary bedding, and unidirectional high-angle trough cross-bedded sandstone further support a fluvial origin for these sandstones.

TOUTLE FORMATION VALLEY-FILL AND TRANSGRESSIVE MARINE LINCOLN CREEK FORMATION

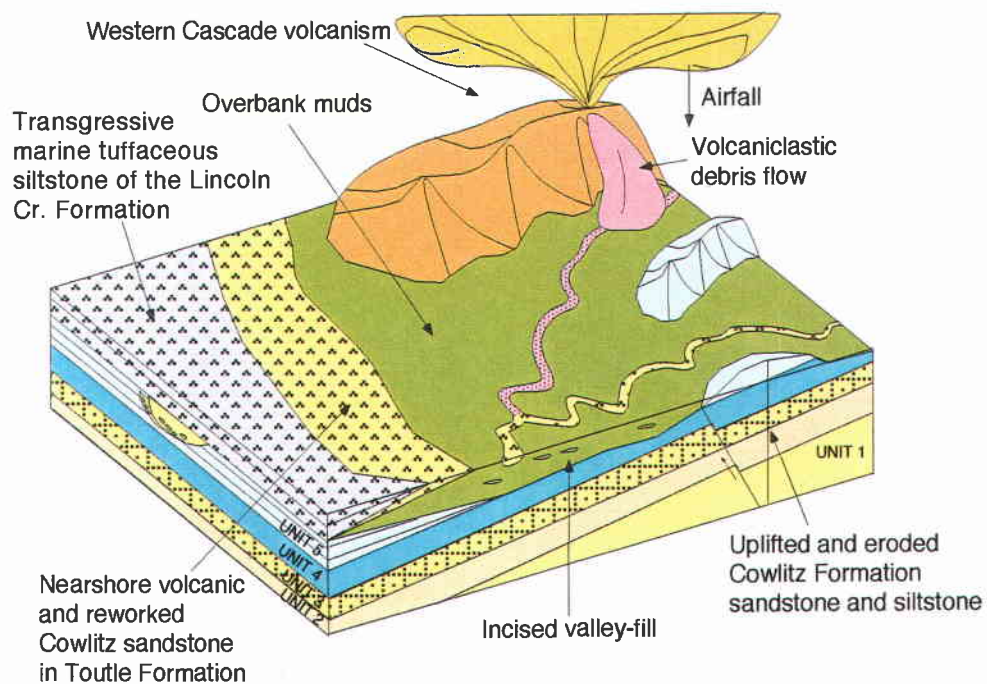


Figure 34. Paleogeographic reconstruction of the Toutle and Lincoln Creek formations showing depositional environments and unconformable stratigraphic relationship with the underlying Cowlitz Formation.

A 1.5-m thick hornblende-bearing pumice-lapilli tuff in the fluvial facies (petrology sample CP-95-183B, Ar/Ar age date of 31.9 ± 0.4 Ma) contains some subrounded volcanic pebbles, also suggesting reworking of silicic highly explosive pyroclastics derived from the nearby western Cascades volcanic arc highlands. This pumiceous clast-supported bed contains an imbricated coalified log that indicates a west-southwest current direction. The source for the euhedral hornblende phenocrysts in the pumice of this tuff is unknown. However, one possible correlative hornblende-bearing center is exposed in a quarry in the Elk Rock 7.5 minute quadrangle in the nearby lower western Cascade volcanics and stratigraphically below a 32 Ma age-dated basalt sample (Evarts, personal communications, 1994).

The mudstone, carbonaceous shale, and interbedded tuffs (lithofacies T3, T7, and T8) formed as a fluvial overbank and floodplain deposits. In section O38, these blue-gray mudstones and sandy mudstones are intermixed with sandstone lenses and abundant carbonaceous plant twigs and stems. Carbonaceous shale and interbedded tuffs contain carbonized roots in growth position. Clay-rich siltstone, carbonaceous mudstone, a thin carbonaceous shale bed, and a light green-blue tuff gradationally overlie a channelized volcanic sandstone in section O40 (Plate II). These fine-grained facies and lithologies suggest broad floodplains or oxbow meander channel-fills were the locus of swampy buildup of plant debris that was periodically inundated by volcanic ash (Figure 34).

Unit B: Mudstone-Dominated Marine Sequence

Nearshore to marginal-marine estuarine volcanic-lithic arkosic sandstone (lithofacies T4) occurs in the middle of the Toutle Formation (unit B, section O41, Plate II). This interpretation is based on the presence of massive, bioturbated, medium-grained, moderately to poorly sorted, silty, volcanic-arkosic sandstone that contains a large (1 m long) coalified *Teredo*-bored log and cobble-sized subangular mudstone rip-ups. This

structureless interval becomes arkosic to subarkosic in composition and faintly trough cross-bedded higher in the section. *Teredolite* trace fossils form when logs floating in the ocean are bored by ship worm clams, and pholad clams. The *Teredo*-bored log washed into the nearshore or estuary environment (i.e., a drowned river-mouth valley) on waves or tidal currents, the mudstones rip-ups were derived from shoreline or tidal channel erosion during high energy events. The better-sorted, cross-bedded, arkosic sandstones in the upper part of this facies were winnowed of finer silt and clay-size material by waves and/or tidal activity in the surf zone or in a tidal channel in the estuary.

A possible shelfal transgressive mudstone (lithofacies T5) occurs at the top of the lower valley-fill sequence (i.e., section O41 and the lower part of section O42). The nearshore shelfal marine origin of this 55-m thick mudstone is suggested by narrow, straight, vertical burrows of the *Cruziana* ichnofacies? A second fluvial unit (C) unconformably overlies this marine mudstone and records another period of subaerial exposure and non-marine deposition in the Toutle Formation.

Unit C: Upper Meandering Fluvial Depositional System

Fluvial volcanic sandstone and associated carbonaceous overbank mudstone (lithofacies T6 and T3) comprise the upper part of the Toutle Formation (unit C) (sections O42 to O44, Plate II). These 1 m- to 7-m thick sandstones are channelized and fine upwards; typical of point bar sequences in meandering river systems as described by Walker (1992). These sandstones are poorly sorted and are composed of granular to medium-grained volcanic clasts. They also contain numerous coalified logs, carbonaceous wood fragments, and mudstone rip-ups. The sandstone is overlain by rooted carbonaceous mudstone and thick silicic tuff beds. High-angle cross-bedded, fine- to medium-grained volcanic arkosic sandstone beds are also present and were most likely

derived and reworked from subaerial exposed, tectonically uplifted Cowlitz Formation sandstones or from more distant sources in the ancestral Columbia River drainage basin (Figure 34).

Two thin coal seams (1-m thick) composed of carbonaceous shale and coal (lignite) (lithofacies T7), are interbedded with the overbank mudstone (lithofacies T3) and are interpreted to have formed on a floodplain (section O42 and O44). These marsh/swamp floodplain deposits also contain numerous coalified logs and tree trunks in growth position. These forests on the floodplain were inundated by numerous, voluminous volcanic eruptions (lithofacies T8). Thick basaltic and siliceous tuffs interbedded with the overbank mudstone are quite numerous in the upper part of this formation (Plate II). These siliceous tuffs are light tan, green, and blue-green in color and are up to 2.5 m thick and andesitic in composition (geochemical samples CP-95-186x1, CP-95-186x2, and CP-95-186x3, Appendix III). Basaltic lapilli tuffs contain pebble-sized clasts in clast-support. These silicic and basaltic tuffs are evidence that the highly explosive active calc-alkaline Cascade volcanic arc was supplying volcanoclastic and pyroclastic sediment to this fluvial environment during deposition of the upper part of the Toutle Formation.

A concretionary faintly cross-bedded, friable, fine- to medium-grained, quartz-rich sandstone (lithofacies T4) caps the top of the Toutle Formation. This bed contains articulated *Crassellites stillwaterensis* bivalve casts and molds of a very shallow marine assemblage (Nesbitt, personal communications, 1996) (macrofaunal sample CP-95-188, Appendix II). This transgressive marine sandstone bed overlies a coal bed representing a coastal swamp and is gradational into the overlying deeper marine tuffaceous siltstone of the Lincoln Creek Formation indicating there was a rapid marine transgression or onlap and marine flooding event at the end of Toutle time during which sedimentation could not keep up with the basin accommodation rate.

Tuffaceous Siltstone Member of the Lincoln Creek Formation

The thin basal part of the Lincoln Creek Formation in the study area consists of several meters of silty fine-grained sandstone and sandy siltstone that contains multiple fossil shell lags and articulated thick-shelled bivalves and high-spired gastropods. These fossils were identified by Armentrout (1973) (UW-291, Plates I and II) as a shallow marine assemblage, most likely from the middle shoreface or inner shelf (upper part of section O44, Plate II). Minor hummocky cross-stratified sandstone is interbedded with tuffaceous sandy siltstone. These hummocky beds and shell lags indicate that storm waves periodically reworked the sea floor sediments. The overlying very thick, massive, bioturbated, concretionary tuffaceous siltstone forms the dominant lithology in this formation. The grain size, lithology, and sedimentary features indicate that the environment of deposition was mainly below wave base in a subsiding basin (i.e., middle to outer shelf) where fine hemipelagic clay could slowly settle out. *Teredo*-bored coalified wood fragments and logs, some vertical and horizontal burrows (e.g., *Thalassinoides*) of the *Cruziana* ichnofacies indicate that most of the Lincoln Creek Formation was deposited in a middle to outer shelf normal marine environment during a marine transgression in the Oligocene. Western Cascade calc-alkaline arc volcanism to the east supplied much silicic ash to this deepening marine basin. Some scattered pumice lapilli in the tuffaceous siltstone may have floated over the basin. As it slowly became water-logged, it sank to the sea floor.

SEQUENCE STRATIGRAPHY OF THE COWLITZ FORMATION AND ASSOCIATED UNITS

The study of sedimentary rock relationships within a time-stratigraphic framework is the basis of sequence stratigraphy (Armentrout, 1996; Van Wagoner et al., 1991). This is accomplished by combining sedimentary facies and depositional geometries of sedimentary rocks into time-stratigraphic units or packages that are stacked into progressively larger-scale cycles of increasing orders of durational magnitude (i.e., 5th, 4th, and 3rd order cycles). These cycles of sequence stratigraphy are constructed based on changes in sea level (or relative sea level fluctuations), in contrast to lithostratigraphy that is based only on rock type. Genetically related strata bounded by surfaces of erosion or non-deposition or their correlative conformities form the basic unit in sequence stratigraphy known as the depositional sequence (Van Wagoner et al., 1991). A depositional sequence can be further subdivided into subunits by the following stratigraphic surfaces: (1) sequence boundaries (unconformable and correlative conformable contacts), (2) a transgressive surface (first major marine flooding surface), and (3) a maximum flooding surface (maximum relative sea level) (Armentrout, 1996). Depositional sequence subunits are lowstand (LST), transgressive (TST), highstand (HST), and shelf-margin system tracts that are related to transgressive-regressive cycles (Van Wagoner et al., 1991). Each system tract is composed of a parasequence set defined as a succession of genetically related parasequences forming one of three characteristic stacking patterns (progradational, aggradational, and retrogradational parasequence sets) (Van Wagoner, 1987). For example, a retrogradational parasequence set is composed of sequential parasequences, each of which becomes thinner and finer-grained upwards. A parasequence is defined as a relatively conformable succession of genetically related beds or bedsets bounded by marine flooding surfaces and their correlative surfaces (Van

Wagoner et al., 1987). Parasequences are progradational sequences of beds and bedsets that were deposited in shoaling upwards depositional environments (e.g., shelf to beach facies) and which are abruptly overlain by deeper water deposits (e.g., outer shelf mudstone above the marine flooding surface) of the next parasequence.

These sequence stratigraphy concepts were used to characterize the stratigraphic trends of the middle Eocene McIntosh and type Cowlitz formations in the study area of southwest Washington. The following sequence stratigraphic analysis can help further work in regional stratigraphic correlation of these units in southwest Washington and northwest Oregon. This analysis, in combination with detailed studies from other parts of this depositional system, could be used in more realistic reconstruction of the regional depositional history, geometry and facies changes of these widespread Eocene deltaic and coastal depositional systems. Local relative sea level fluctuations and thickening- and coarsening-up as well as fining- and thinning-up lithologic sequences are defined in the study area based on interpretations of changing depositional environment water depths, sedimentation rates as indicated by radiometric dates, lithologies, sedimentary structures, and by using macro- (molluscan and trace fossils) and micro-faunal (foraminifera) assemblages (Figure 35 and Plate II).

Four unconformity-bounded sequences (2nd order cycles, 6 to 21 m.y. in duration) were identified in the Tertiary strata of southwest Washington by Armentrout (1987) based on major tectonically-controlled regional unconformities. The McIntosh and Cowlitz formations fit within Armentrout's (1987) sequence II, between regional unconformities 4 and 3 (~6 m.y. in duration). The 1,000-m thick middle Eocene McIntosh Formation and 1,240-m thick late middle Eocene Cowlitz Formation can be further subdivided into five 3rd order cycles consisting of complex facies successions of wave- to tide-dominated deltaic parasequence sets (Figure 35, Plate II). Using the cycle time spans determined by Van Wagoner et al. (1991), the four regional Tertiary depositional

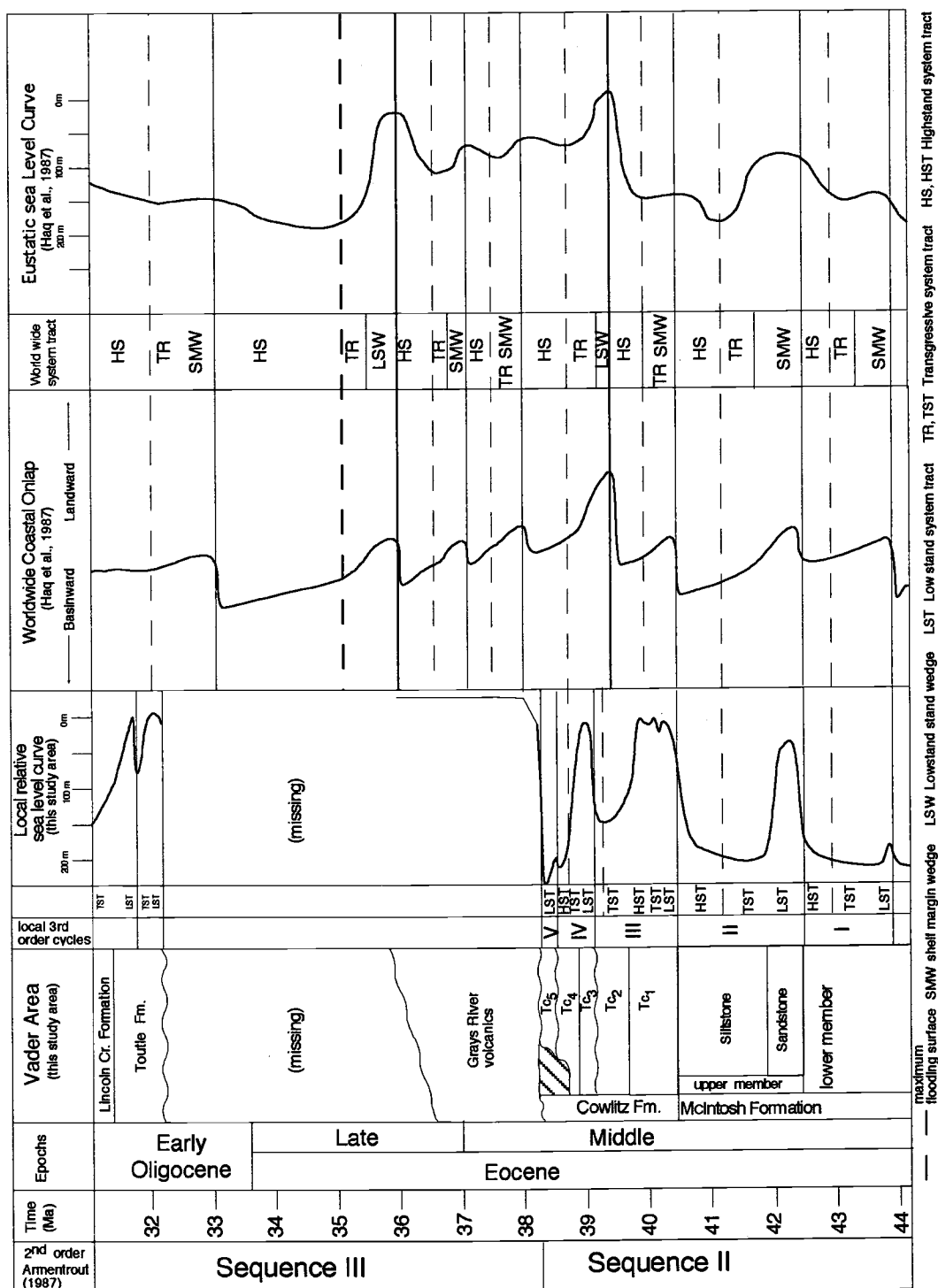


Figure 35. Sequence stratigraphy and local water depths of the McIntosh, Cowlitz, and Toutle formations compared to world-wide eustatic sea level curves of Haq et al. (1987).

sequences of southwest Washington of Armentrout's (1987) are 2nd order megacycles (5 to 50 m.y. in duration) (Figure 35). In this study, shorter-term fining- and thinning-upward and coarsening- and thickening-upward cycles comprise unconformably-bounded sequences of 4th order parasequences (100,000 yrs) to form 3rd order local depositional sequences (cycles I to V) that last only 5 to 1 m.y. (Plate II and Figure 35). This age range of 3rd order transgressive-regressive cycles was determined based on sedimentation rates calculated using $^{39}\text{Ar}/^{40}\text{Ar}$ radiometric dates and measured section thicknesses. Age dates from the upper part of the Cowlitz Formation to the overlying Toutle Formation in Olequa Creek and to the overlying Grays River volcanics at Bebe Mountain were used. The unconformable contact between the lower McIntosh deep marine mudstone with the upper McIntosh shelfal sandstone may correlate with the eustatic 42.5 Ma sequence boundary of Haq et al. (1987) (Figure 35). If this is the case, the average sedimentation rate from the top of the lower McIntosh Formation to unit 3 of the Cowlitz Formation (1400 m of section) is calculated to be 39 cm/1,000 yrs. An average sedimentation rate of 1.6 m /1000 yrs. was determined from the 420 m of section from unit 3 (38.9 ± 0.4 Ma) of the Cowlitz Formation to the overlying Grays River volcanics (36.8 ± 0.4 Ma) exposed along Olequa Creek. The average sedimentation rate calculated from the 38.9 Ma tuff dated by Irving et al. (1996) (marker bed 3A) to unit 3 (Plates I and II) and the 32 Ma hornblende-bearing pumice lapilli tuff in the Toutle Formation in this study (500 m of total section) is 7.2 cm/1,000 yrs. The low sedimentation rate of 7.2 cm/1,000 yrs is a result of including in the calculation 4 m.y., during which there was non-deposition on a surface of erosion (i.e., an unconformity), resulting in an unrealistically low value.

The lower member of the McIntosh Formation forms 3rd order cycle I and the upper member 3rd order cycle II. A sequence boundary separates the lower and upper members of the McIntosh Formation and is defined by an abrupt or rapid shoaling event and the absence of the lower to upper shoreface sandstone facies between the two

members (Plate II). The abruptly overlying 130-m thick upper McIntosh sandstone is composed of a fining-upwards parasequence first formed in an estuary environment (i.e., intertidal sandstone to subtidal channels and coal). It is followed by a coarsening upwards parasequence formed in an upper shoreface environment; these depositional facies and parasequences form a lowstand system tract (LST) of cycle II. This LST sandstone sequence is overlain by a transgressive system tract (TST) tuffaceous deep marine siltstone with *Phycosiphon*-burrows which reflects a marine flooding or onlap transgressive event (Plate II). This local transgressive-regressive cycle is also recognized on the worldwide coastal onlap and eustatic sea level curves about this time in the Eocene (Figure 35). Sandstones in the upper part of the upper McIntosh Formation form a funnel-shaped curve on the SP log (Plate II) and are coarsening- and thickening-up delta front sandstone parasequences that form a highstand system tract (HST of cycle II, Figure 35 and Plate II). The abrupt change in water depth from bathyal uppermost McIntosh HST siltstone to prograding sandy inner shelf to littoral highstand delta front depositional environments of unit 1A of the Cowlitz Formation suggests there is a sequence boundary between the two formations. This correlative conformable contact or sequence boundary with the overlying Cowlitz Formation defines the end of third order cycle II.

Units 1a, 1b, and 2 of the Cowlitz Formation form third order cycle III. A rapid decrease in water depth is evident from lithologies, sedimentary structures, and molluscan fossils in the lower part of unit 1A. The basal 558-m thick unit 1 consists of following subunits (1) multiple prograding wave-dominated shoreface coarsening- and thickening-upwards successions of the delta front/shoreface of unit 1A and (2) and fining- and thinning-upwards coal-bearing coastal-delta-plain facies associations of unit 1B. The six coarsening-upwards parasequences of the lower part of the Cowlitz Formation (unit 1A) formed a delta front lowstand wedge system tract (LST) and an overlying aggradational shoreface transgressive system tract (TST) of third order cycle III (following the

nomenclature of Van Wagoner et al., 1990) (Plate II). Unit 1B consists of ten vertically stacked coarsening- and thickening-upwards marginal marine and delta-coastal-plain marsh/swamp parasequences forming an aggradational parasequence set of a highstand system tract (HST) (Plate II). A transgression occurred at the end of Cowlitz unit 1 deposition and the beginning of Cowlitz unit 2. A mollusc-bearing tuff bed reworked by waves and currents in a shallow marine environment at the top of unit 1 (above a thick marginal or non-marine coal seam) marks the beginning of this transgression or marine flooding event. The 205-m thick Cowlitz Formation unit 2 is composed of five coarsening- and thickening-up storm-dominated shelf to delta-front arkosic sandstone parasequences. The last parasequence overlies a maximum flooding surface that defines the deepest water depths (outer neritic to upper bathyal) reached during deposition of unit 2. In this study area, a sequence boundary separates the shallow marine depositional facies of unit 2 in third order cycle of cycle III from the tide-dominated estuary facies that forms unit 3 of the third order cycle IV.

Units 3 and 4 of the Cowlitz formation form the lowstand, transgressive, and highstand system tracts of third order cycle IV (Plate II and Figure 35). The sequence boundary between units 2 and 3 formed during a lowstand that resulted in the formation of a broad river-cut valley incised into unit 2. This was followed by drowning and marine flooding of the valley and formation of a large estuary where sedimentation rate kept up with rate of subsidence or accommodation space. The several fining- and thinning-upwards parasequences of the 170-m thick unit 3 represent a subtidal to supratidal and nonmarine estuary-fill of a lowstand system tract (LST of third order cycle IV). The overlying 155-m thick unit 4 of the Cowlitz Formation consists of vertically-stacked wave-dominated shoreface to offshore mudstone facies successions that form ten coarsening- and thickening-upward parasequences (Plate II). These parasequences define a probable retrogradational parasequence set of a transgressive system tract (TST). Each

parasequence represents a gradational change in bed thickness and grain size from offshore shelfal or prodelta marine mudstone formed below wave base to storm wave-dominated delta front shoreface sandstone and siltstone. Individual parasequences range from 5 to 30 m in thickness. Marine mudstone beds generally abruptly overlie shoreface sandstone in each parasequence. The Olequa Creek section biostratigraphically correlates with highstand (HST), bioturbated mollusc-bearing sandy siltstone and glauconitic mudstone facies in the Big Bend type locality along the Cowlitz River (Plate I). Water depth gradationally increases in the upper 65 m of unit 4 from neritic to outer bathyal (maximum water depth) based on molluscan assemblages collected by Nesbitt (1994) at the Big Bend locality. This maximum flooding surface near the top of the Big Bend locality can be correlated to unit 4 in the type section in Olequa Creek (MaxFS on Plate II). According to Nesbitt (1994), this increase in water depth reflects the continued transgressive event in the upper part of the Cowlitz Formation.

The uppermost deeper marine unit 5 of the Cowlitz Formation is 150 m thick and forms a lowstand system tract of 3rd order cycle V (Figure 35). Parasequences are not well defined in deeper water sediments because fluctuations in sea level are not generally recognized in these deep water sediments that were deposited below storm wave base. Submarine channelization, muddy turbidites, grain flows and fluidized flows were formed during a relative sea level low which initiated turbidity current incision on the prodelta slope, but also sands were largely bypassed into the deeper marine environment via these channels.

The sequence boundary (this study) between the fluvial and shallow marine Toutle Formation and the underlying Cowlitz Formation (Plates I and II) is not the same regional unconformity of Armentrout (1987) that underlies the Lincoln Creek Formation in much of southwest Washington and perhaps across western North America (Armentrout, personal communications, 1997). This is because the basal basaltic sandstone of the

Lincoln Creek Formation was deposited during the late Eocene (~37 Ma) as determined by molluscs and Refugian foraminifers. However, a 31.9 ± 0.4 Ma $^{39}\text{Ar}/^{40}\text{Ar}$ radiometric date from a hornblende-bearing pumiceous lapilli tuff in the Toutle Formation lowstand valley-fill directly above this local unconformity is Oligocene in age. This incised valley-fill sequence in Olequa Creek is a time transgressive equivalent of the older Toutle and Lincoln Creek formations. The lowstand valley-fill unit grades upward into the overlying transgressive deeper marine tuffaceous siltstone of the Oligocene Lincoln Creek Formation (Figure 35).

Transgressive 3rd order cycle I of the Lower McIntosh Formation and regressive-transgressive cycle II of the upper McIntosh appear to correspond to similar regressive-transgressive 3rd order eustatic cycles of Haq et al. (1987) (3rd order cycles I and II, Figure 35). The lower sequence boundary of cycle III also correlates with a world-wide sea level fluctuation during the middle Eocene about 43 to 40.5 Ma (see coastal onlap Figure 35). The upper boundary of cycle III and the bounding surfaces of cycles IV and V appear not to match worldwide sea level fluctuation events. This discrepancy between local and eustatic sea level during the late middle Eocene indicates these upper cycles in the Cowlitz Formation were locally tectonically controlled or forced by basin subsidence and uplift events. The sudden influx of volcanic sediments in Cowlitz unit 2 may have been accomplished by thermal uplift of the basin by nearby Cascade volcanics resulting in an increase in sedimentation rate vs. accommodation rate followed by a thermal cooling event and basin subsidence of unit 4 and 5 (no volcanism) as an alternative to basin tectonics due to faulting and folding. However, the maximum flooding surface in unit 4 (third order cycle IV) does correlate with a major eustatic highstand recognized by Haq et al. (1987). The unconformity separating the Cowlitz Formation and the overlying subaerial Grays River volcanics may correspond to Armentrout's (1987) regional unconformity 3. Thermal uplift of the crust in this area preceding volcanism may also explain this

unconformity. Armentrout (personal communications, 1997) believes the regional unconformity that affected the western U. S. may have formed as a result of Farallon plate reorganization in the late Eocene. The local sea level of the Toutle Formation and the world-wide eustatic sea level do not appear to correspond, indicating the Toutle Formation was deposited under tectonically-controlled water depths. The local unconformity at the base of the Toutle Formation over the deep water Cowlitz unit 5 reflects local basin uplift. The abundance of volcanoclastics and recycled Cowlitz arkosic sands in the Toutle reflect uplift in the source area and increased silicic volcanism followed by a sea level rise or basin subsidence as the crust cooled.

SEDIMENTARY PETROLOGY AND VOLCANICLASTIC GEOCHEMISTRY OF THE MCINTOSH, COWLITZ, AND TOUTLE FORMATIONS

INTRODUCTION

Petrologic study of twenty sandstones from the upper McIntosh, Cowlitz, and Toutle formations was conducted in order to decipher the composition, provenance, and diagenetic history of these potential reservoir units. Petrographic analyses involved thin section preparation (i.e., slabbing) and textural and mineralogical description. Thin sections were point counted to determine the sandstone modal composition of the framework grains and cements. X-ray diffraction (XRD) patterns were used to identify the composition of the clay-sized mineral cements in the sandstones. Scanning electron microscopy (SEM) analyses were performed with Dr. Reed Glasmann to help identify mineral compositions, to describe the morphology of the framework mineral and intervening pores, and to interpret a sequence of diagenetic events. Several sandstone compositions in thin section were studied based on visual inspection only. The mineralogical composition of twinned plagioclase grains in some of the pebble and coarse-sand-sized volcanic clasts was estimated using the Michel-Levy technique. The plagioclase composition was used to determine the approximate volcanic composition of these fragments.

All the thin sectioned samples were collected from the measured sections of the McIntosh, Cowlitz, and Lincoln Creek formations along Stillwater and Olequa creeks (location and stratigraphic position of thin sections appear on Plates I and II). These consisted of 3 thin sections from the micaceous, lithic arkosic sandstones of the McIntosh and Cowlitz formations and 8 volcanic sandstones from units 1, 2 and 3 of the Cowlitz

into 23 components (Appendix III). Lithic arkose samples were commercially impregnated with blue epoxy before thin section preparation to help in describing pore geometries, size, and origin. Potassium feldspar grains in these samples were stained with sodium cobaltinitrate to aid in identification in point counting.

Clay-sized mineral components and cements of three arkosic sandstone samples from the McIntosh and Cowlitz formations and one volcanic sandstone from the Toutle Formation were determined from X-ray diffraction analyses. This was performed using a Phillips 3100 Automated X-ray diffractometer (XRD) unit maintained by Dr. Reed Glasmann of the Department of Geosciences at Oregon State University. Clay sample preparation and analysis were performed using the procedure of Glasmann and Simonson (1985). These four samples were also analyzed using scanning electron microscopy (SEM) performed with Dr. Glasmann using a KEVEX analyzer under the direction of Mr. Al Soeldner in the Botany Department at Oregon State University.

ARKOSIC-LITHIC SANDSTONES OF THE MCINTOSH AND COWLITZ FORMATIONS

The moderately well-sorted, friable, micaceous, fine- to medium-grained sandstones of the McIntosh and Cowlitz formations are petrographically similar micaceous lithic arkose based on classification of Folk (1974) and therefore, will be discussed together (Figure 36). Mineralogical grains identified during point counting included plagioclase, potassium feldspar, monocrystalline and polycrystalline quartz, biotite, muscovite, hornblende, and epidote. Rock fragments observed included: (1) metamorphic clasts of schist, gneiss, and quartzite; (2) microgranitic plutonic clasts; (3) sedimentary clasts of mudstone, siltstone, sedimentary quartzite, and carbonaceous plant material; and (4) basaltic clasts with intersertal, pilotaxitic, randomly oriented, and amygdaloidal textures.

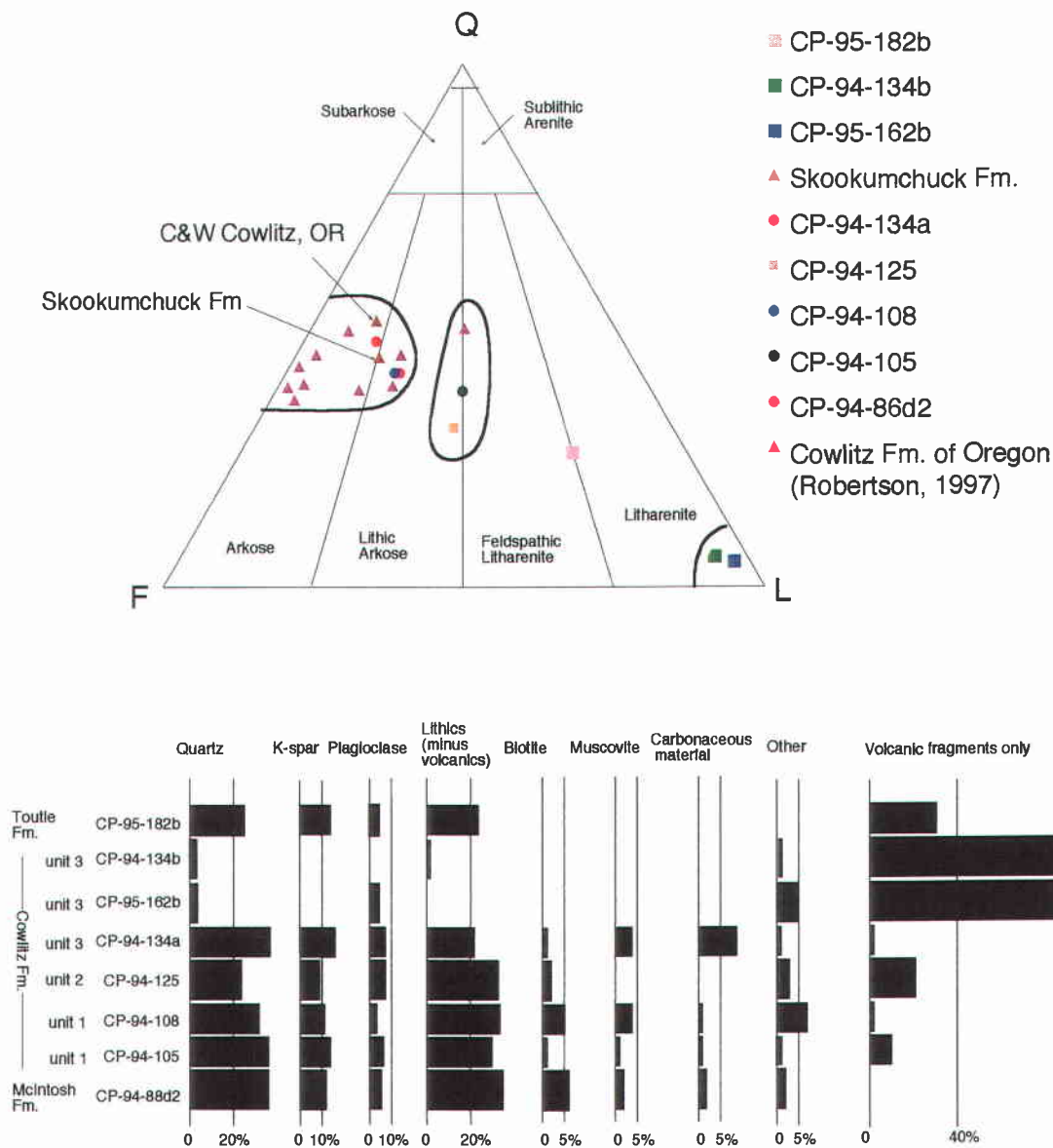


Figure 36. QFL ternary classification diagram (after Folk, 1974) (upper diagram) and more detailed framework grain composition bar graph (lower diagram) of the McIntosh, Cowlitz and Toutle sandstones in the study area.

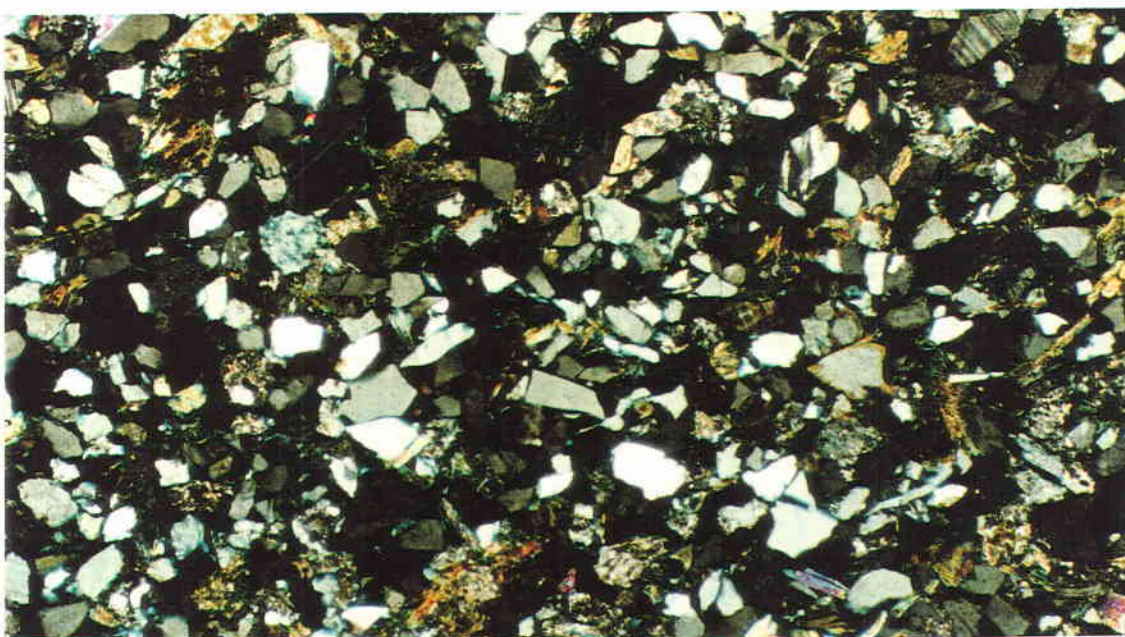
The four micaceous, lithic arkosic sandstone samples point-counted in this study are from the upper McIntosh sandstone and the informal units 1 and 3 of the Cowlitz Formation (Plates I and II). Sandstone sample CP-94-86d2 is from a hummocky cross-stratified, upper to middle shoreface succession of the upper McIntosh sandstone (measured section 3D, Plate II). Samples CP-94-105 and CP-94-108 were collected from two upper shoreface sandstone sequences in unit 1 of the Cowlitz Formation (measured sections 7A and 7D, Plate II). The shoreface sandstones from the McIntosh and lower part of Cowlitz formations are all moderately sorted and fine- to medium-grained. Sample CP-94-134a is from a moderately well-sorted, fine-grained tidal-channel sandstone from unit 3 of the Cowlitz Formation (measured section 11B, Plate II).

Framework grains in these micaceous lithic arkoses are typically subangular and composed of mostly quartz and feldspar (Figures 36, 37 and 38). The lack of detrital clay suggests these sandstones would classify as arenites. Quartz is twice as abundant as feldspar and mainly monocrystalline, although minor polycrystalline quartz is present. The ratio of potassium feldspar to albite-twinned plagioclase feldspar is 2:1 (Figure 36). Untwinned orthoclase feldspar is more abundant than gridiron twinned microcline. Additionally, these sandstones contain carbonaceous plant debris, muscovite and biotite, plagioclase, hornblende, and epidote grains (Figure 36 and Appendix III). Hornblende and epidote grains decrease in abundance higher in the measured section. Some quartz grains contain inclusions of rod-shaped rutile crystals that display a characteristic high birefringence. Lithic fragments are dominantly metamorphic, plutonic, and sedimentary and comprise about 30% of the framework grains in these samples. Minor volcanic fragments are also present. Some ductile metamorphic schist, volcanic, and mudstone clasts have been deformed into the interstices between more resistant brittle grains of quartz and feldspar during compaction. These plastically deformed clasts form the characteristic pseudomatrix of Dickinson (1970).

A.



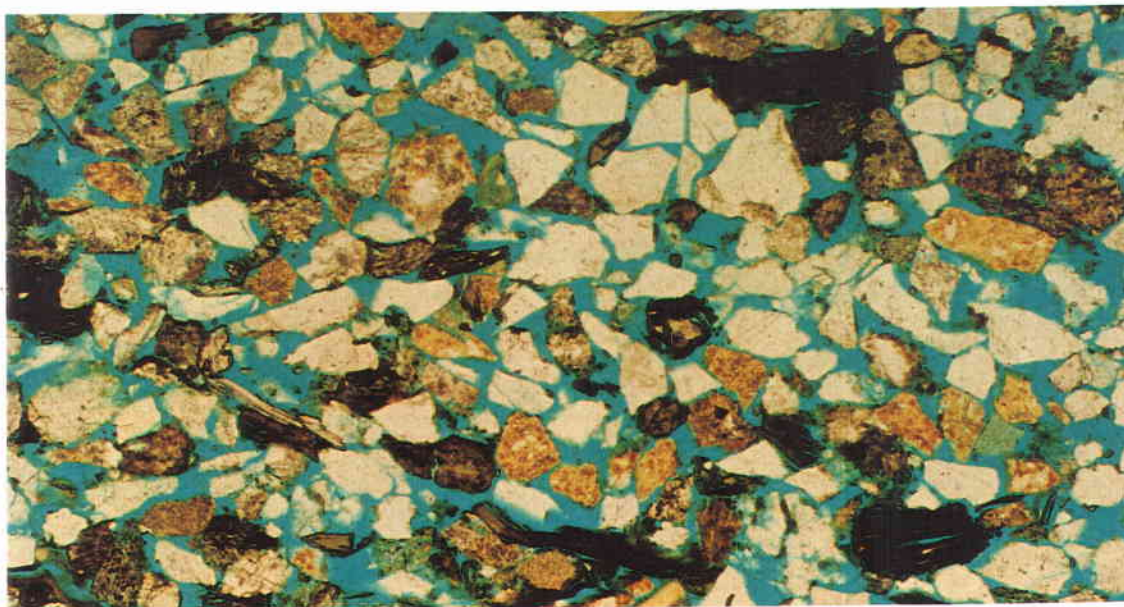
B.



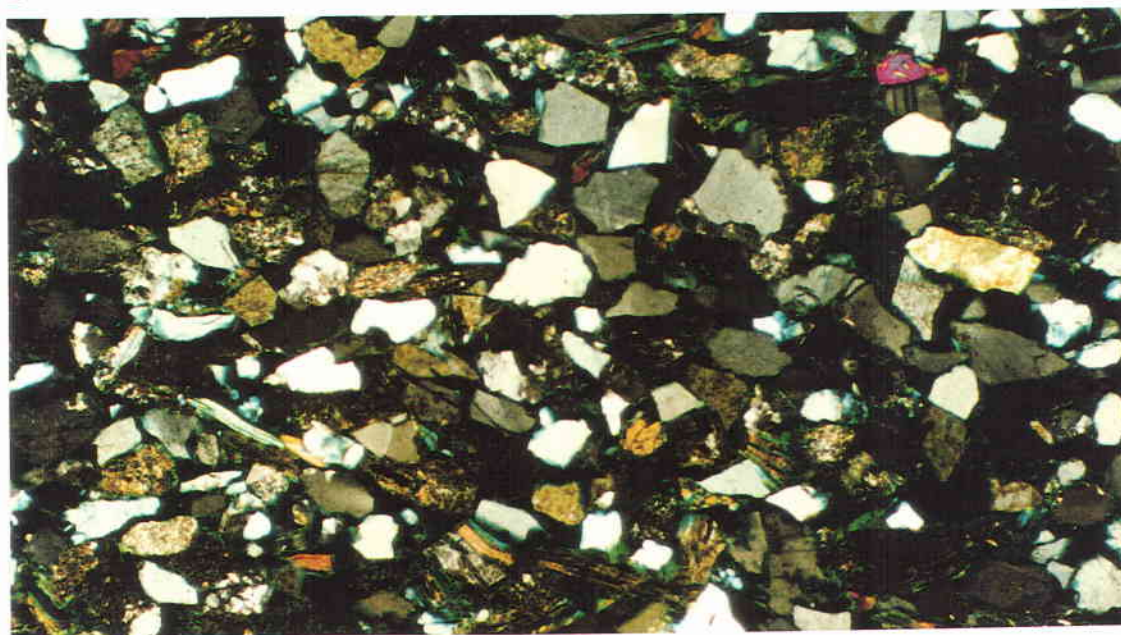
4x |-----| 1mm

Figure 37. Photomicrograph of micaceous, lithic arkose from the upper McIntosh Formation sandstone (sample CP-94-86d2, Plates I and II). Note dominant angular to subangular quartz and feldspar grains (yellow-stained potassium feldspar and plagioclase) and interconnectivity of intergranular pore spaces (blue dye). (A. Plane-polarized light, B. Crossed nichols)

A



B



4x ————— 1mm

Figure 38. Photomicrograph of the micaceous, lithic-arkosic sandstone of unit 1A of the Cowlitz Formation (CP-94-108, Plates I and II). Note slightly aligned, elongate, and uncompressed mica flakes between subangular quartz and feldspar grains (lower part of thin section) and minor grain-rimming clay cement (upper left corner). (A. Plane-polarized light, B. Crossed nicols)

Basaltic fragments with pilotaxitic, intersertal, and amygdaloidal textures become more abundant in the lithic arkose of unit 2, where one sample consists of approximately 20% basaltic clasts (sample CP-94-125, Plate II and Figure 36). Some basaltic clasts have been partially altered to smectite and greenish celadonite, although many display an unaltered delicate scoriaceous texture and, thus, were probably not transported over a long distance. The ratio of locally derived basaltic volcanic fragments to extrabasinal lithic plutonic and metamorphic clasts varies from 3:1 to 10:1 in the lithic arkosic sandstones of the Cowlitz Formation (Appendix III).

Lithic arkosic sandstones of the McIntosh and Cowlitz formations are highly micaceous and carbonaceous. There is a minor decrease in biotite abundance up section along Stillwater Creek, whereas the percentage of muscovite appears to be relatively consistent. The sample from the McIntosh Formation contains 9% mica and samples from unit 1 contain 2 to 9% mica. Mica is finer grained in the McIntosh sandstone than mica in unit 3 of the Cowlitz Formation (Figures 37 and 38). The sample from the subtidal sandstone facies (unit 3) contains 9% black carbonized plant fragments in thin section, which is more abundant than the 1 to 2% found in other Cowlitz sandstone samples. On the basis on porosity and friability characteristics, the reservoir potential of the lithic arkoses from the upper McIntosh sandstone and Cowlitz Formation is good to excellent. Framework grain contacts are commonly tangential indicating that these sandstones have not undergone much compaction by burial. Both carbonaceous plant debris and mica slightly bend ductily between brittle subangular quartz and feldspar grains as a result of minor burial compaction, although many muscovite grains are not compressed (Figure 38). These sandstones have 20% to 25% porosity as determined by visual estimation and point counting of grains vs. void spaces. Porosity is dominantly large sand size primary intergranular pores with minor secondary porosity (<5%) formed by partial dissolution of volcanic rock fragments. Primary depositional porosity is open and shows good

interconnection, suggesting good horizontal effective porosity and probably permeability. Pore throats are wide between intergranular pores and are not clogged by diagenetic clay minerals. Minor discontinuous grain-rimming clay cements are the only authigenic cementing material present. Vertical permeability is, however, decreased by long impermeable aligned laminae composed of carbonized plant debris and micas. On the basis of on clay mineral XRD and SEM analysis, smectite is the dominant clay-sized component of these lithic arkosic sandstones (Figure 39). Zeolites (clinoptilolite) are a second subordinate cementing constituent. Primary intergranular sand-size pores are open except for thin grain-rimming, wormy and cornflake-shaped smectite (Figure 39). Minor authigenic smectite clay cement rims entire framework grain surfaces in sample CP-94-86d2 (upper McIntosh Formation sandstone, Plate II). Some later forming zeolite crystals rise above this pervasive grain-rimming smectite clay. The later stage zeolites (clinoptilolite) were probably formed under low temperature conditions, indicating shallow burial for all these sandstones (Glasmann, personal communications, 1996). Sample CP-94-105 (unit 1 of the Cowlitz Formation, Plate II) is not cemented. No sparry calcite or quartz overgrowths were observed in these loosely packed sandstones unlike some Cowlitz sandstones in the Mist Gas Field of northwest Oregon (Berkman, 1990; Farr, 1989; Robertson, 1997). Fine flakes of biotite or muscovite were identified in clay mineral analysis of shoreface sandstone sample CP-94-108 (unit 1 of the Cowlitz Formation, Plate II). Minor potassium feldspar overgrowths were observed on some grains. The explosive basaltic volcanic events of the Grays River volcanics during Cowlitz sand deposition may have produced fine weathered ash that was deposited in these sandstones and subsequently altered and remobilized by pore water solution to form this authigenic pore-lining smectite cement. Partial dissolution of *in situ* glassy basaltic fragments in these lithic (volcanic) arkoses may have been another source of this early diagenetic smectite clay.

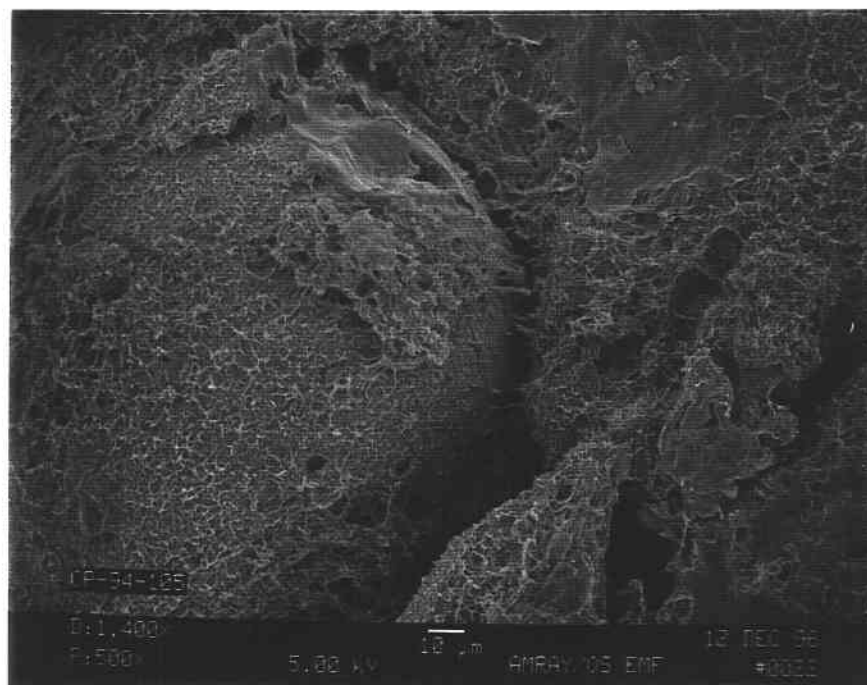
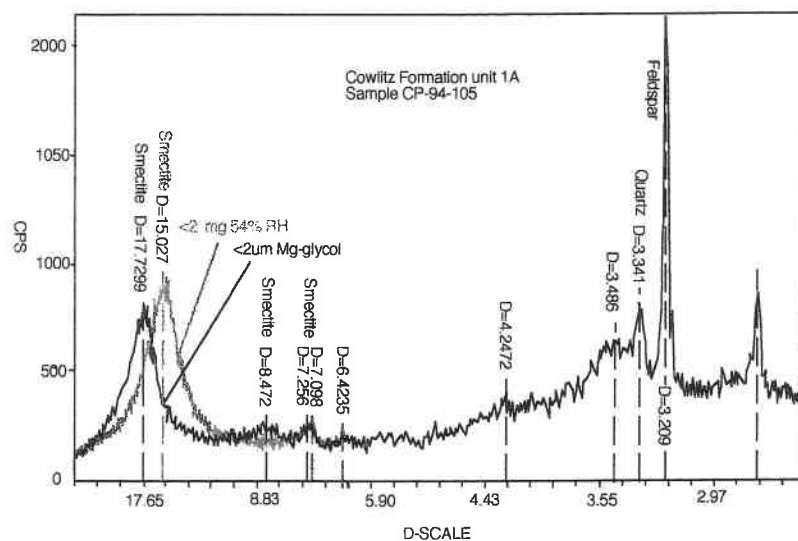


Figure 39. X-ray diffraction pattern and scanning electron (SEM) photograph of sample CP-94-105 from the upper shoreface lithic-arkosic sandstone of unit 1 of the Cowlitz Formation (Plates I and II). Note corn-flake texture of minor authigenic, grain-rimming smectite clay on sand size framework grains. Bar scale at bottom of SEM photograph is 10 microns.

VOLCANIC SANDSTONE OF THE COWLITZ FORMATION

Volcanic sandstones of the Cowlitz Formation are dominantly basaltic in composition and are predominant found in units 2 and 3 of the Cowlitz Formation (Plates I and II). Rock fragments identified during point counting included volcanic clasts with intersertal, pilotaxitic, randomly oriented, and amygdaloidal to vesicular igneous textures (MacKenzie et al., 1982). Minor amounts of mineralogical grains consisting of albite twinned plagioclase, potassium feldspar (orthoclase and some microcline), monocrystalline quartz, and clinopyroxene were identified in some of these sandstones (Appendix III). Some pumice, andesite, and unidentified microcrystalline (altered volcanics) clasts were observed in some volcanic sandstones.

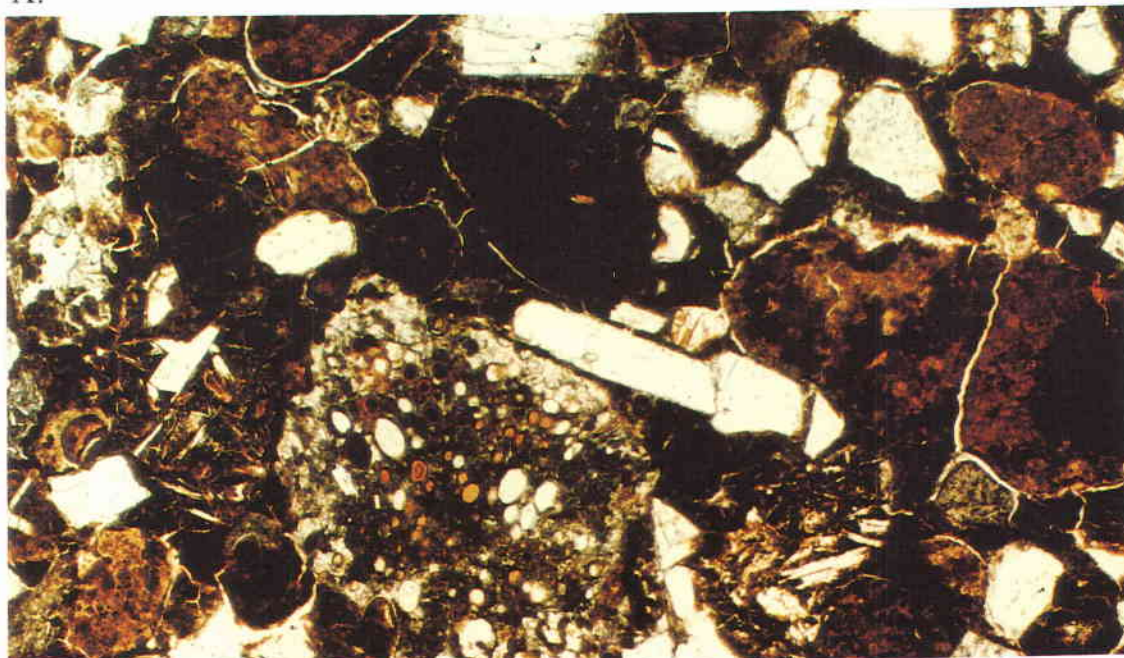
The basaltic sandstones in units 2 and 3 of the Cowlitz Formation can be categorized into four types: (1) hyperconcentrated flood-flow deposits consisting of thin beds of scoriaceous basalt, (2) thick beds of wave-reworked sandstone composed of basaltic lava fragments, (3) a mixed-source epiclastic volcanic conglomerate, distributary-channel? deposit, and (4) thick-bedded, subaqueous debris flow deposits. These thick beds consist mainly of subangular, scoriaceous and pilotaxitic basaltic clasts. The delicate highly vesiculated or scoriaceous clasts were most likely derived from a local basaltic source (Grays River volcanics to the southwest or Northcraft Volcanics to the northeast and western Cascade Goble and basalts to the east). Other volcanoclastic beds include a pumice lapilli tuff in unit 3 and numerous light tan air-fall tuffs (these fine-grained tuff beds are discussed in the following section Geochemistry of Tuff Beds from the Cowlitz and Toutle Formations). The pumice and more siliceous clasts probably were derived from the newly forming calc-alkaline volcanic arc (e.g., Northcraft Formation to the northeast or other early Cascade volcanoes to the east).

Thin hyperconcentrated flood-flow beds composed of scoriaceous basaltic sandstone are numerous in the lower shallow marine siltstone of unit 2 and in the

supratidal coastal swamp/marsh of unit 3. These beds can be correlated across the field area and form marker beds used in measured section correlation of unit 2 (marker beds U2A to L, Figure 10). In unit 3, this volcanoclastic-rich interval is also correlated between measured sections, though some beds are discontinuous (above coal seam A, Plates I and III). These sharp-bottomed beds are medium-grained and massive to normally graded. Samples CP-94-127 from unit 2, CP-94-134b (Figure 36) and CP-94-163a from unit 3 are compositionally very similar. They are calcite cemented and consist of 86% amygdaloidal basaltic clasts, 5% clinopyroxene (augite), 5% plagioclase, and 4% monocrystalline quartz grains as determined by thin section point counting and visual estimation. The subangular scoriaceous clasts may have formed during an explosive fountain eruption of basaltic magma (e.g., cinder cones or phreatomagmatic eruptions). The minor quartz and subrounded plagioclase constituents were incorporated into these flows as they moved across the delta-coastal plain. The planar laminated, largely monolithic composition, and graded nature of these beds indicate they are hyperconcentrated flood-flow deposits (as defined by Smith and Lowe, 1991) that spread across the low-lying marsh/swamp of unit 3. These flood-flow deposits had sufficient energy to enter the shallow marine environment of unit 2.

Thick beds of epiclastic basaltic sandstone and volcanic conglomerate are more compositionally varied than the thinner scoriaceous basaltic sandstones. The mollusc shell-rich, volcanic, silty sandstone (lithofacies 2a) in unit 2 consists of scoriaceous, pilotaxitic, and altered glassy basaltic volcanic clasts (Figure 40). Additionally, some clasts have an intersertal texture of randomly oriented plagioclase and augite. A few flattened long tube pumice fragments are also present. Minor plagioclase, monocrystalline quartz, and a few clinopyroxene (augite) grains are also observed. A sparry calcite cement bounding these clasts was most likely derived from dissolution of large former aragonite mollusc fragments contained in the sandstone (sample CP-94-121, measured

A.



B.



4x |-----| 1mm

Figure 40. Photomicrograph of shallow marine basaltic sandstone (sample CP-94-121) from the epiclastic (lithofacies 2a) storm-dominated middle to inner shelf sequence in unit 2. Note large amygdaloidal basalt clast (middle), altered basaltic glass fragments (right side), and monocrystalline quartz and plagioclase feldspar grains. (A. Plane-polarized light, B. Crossed nichols)

section 9C). These basaltic fragments may have originally been transported from volcanic highland areas by normal fluvial processes or as hyperconcentrated flood-flows or debris flows, but were later reworked by storm waves, tidal, and longshore currents and mixed with broken mollusc fragments and quartz and potassium feldspar.

An 2-m thick epiclastic, graded, sandy, granular to pebble volcanic conglomerate from measured section O7 was studied in thin section (sample CP-94-159, Plate II). Volcanic clasts in the conglomerate include plagioclase-phyric basalt with intersertal, randomly oriented to pilotaxitic flow textures. The pilotaxitic basalt clasts have aligned plagioclase microlites, opaques, ilmenite and green augite in an opaque-rich (5% to 10%) groundmass that is very similar in appearance to the Grays Rivers volcanics (see Grays River Petrology section). Albite twinned plagioclase phenocryst composition from a variety of these pebble-sized volcanic clasts range from 60An to 88An (Labradorite) (with an average of 73An) as determined using the Michel-Levy technique. Amygdaloidal, scoriaceous basaltic clasts and altered basaltic glass are also present. Dacite fragments with Carlsbad-twinned and oscillatory zoned plagioclase and quartz phenocrysts in a microcrystalline chert matrix, and pumiceous non-welded tuff clasts filled with calcite cement also occur. These more siliceous clasts may have be derived from an explosive western Cascade calc-alkaline source. The fine-grained matrix is dominantly composed of fine sand-sized subangular quartz and feldspar with subordinate muscovite and biotite flakes and large detrital albite twinned plagioclase feldspar grains. This deposit may be a distributary-channel sandstone containing mixed volcanic clasts derived from local basaltic Grays River terrain and distal more silicic calc-alkaline western Cascade source.

A 2.5-m thick basaltic debris flow deposit that occurs in measured sections 10C to 10D (sample CP-94-130a) is interbedded with an upper shoreface Cowlitz arkosic sandstone. This poorly sorted, matrix-supported, coarse-grained to granular, pebbly sandstone bed is composed of irregularly shaped scoriaceous and amygdaloidal basalt

clasts (70-80% of the total sample). The spheroidal amygdules are filled with sparry calcite and chlorophaeite, a yellowish brown concentrically-ringed mineraloid. Some plagioclase-phyric basalt clasts display intersertal, intergranular, and subophitic textures. Monocrystalline quartz and albite twinned plagioclase feldspar grains (2 to 5%) occur. Fine-grained, clay-altered scoria forms the abundant matrix between framework clasts. A poorly sorted, coarse-grained, scoriaceous basaltic sandstone that is interpreted to be a debris flow deposit in a subtidal channel forms the base of unit 3 and is in sharp, unconformable contact (sequence boundary) with the underlying shelfal, muddy siltstone at the top of unit 2 (measured section O10, Plate II). A sample collected (CP-95-162b) from this 6-m thick basaltic sandstone consists of amygdaloidal (69%), intersertal (12%), pilotaxitic (3%), and altered glassy (6%) basaltic clasts. Some scoriaceous clasts have been fragmented, with only small green celadonite clay-filled amygdules preserved. These amygdules are surrounded by sparry calcite cement. Large clinopyroxene (5%) crystals, monocrystalline quartz (5%), plagioclase (2%), and potassium feldspar (1%) grains were observed in this sample (Figure 36). Broken molluscan shell fragments are also present and some, are partially dissolved. The re-mobilized Ca^{+2} and CO_3^{-2} ions were then likely precipitated from pore water solution to form local calcite-cemented concretionary layers. In outcrop this sandstone-dominated debris flow deposit crumbles easily and has a dark muddy appearance.

A 1.8-m thick, ledge-forming, subangular, pumice lapilli tuff bed (marker bed U3-A, unit 3, Plates II and II) is parallel-laminated to massive and both normal and reversely graded (petrology sample CP-94-163b, Figure 21A). This sample is composed of altered pumice lapilli (75%), cryptocrystalline to glassy clasts (10%), amygdaloidal basalt (10%), and some pilotaxitic basaltic clasts (5%). Some of the long-tube pumice clasts are partially welded or compacted. This bed may have formed as a base surge or ash flow and subsequent air-fall volcanoclastic deposit as suggested by the mixed basaltic and silicic

pumice clasts in the basal portion (base surge) and graded upper part of the unit (air-fall). According to Irving et al. (1996) microprobe study, this pumiceous bed (location 11D, Plates I, II, and III) contains oligoclase feldspar crystals that indicate a dacitic composition from a western Cascade source. The $^{39}\text{Ar}/^{40}\text{Ar}$ date of 38.9 ± 0.1 Ma from these crystals (Irving et al., 1996) indicates a possible connection with the contemporaneous silicic explosive pyroclastic activity of the Northcraft Formation in the developing western Cascades to the northeast (Figure 2).

In summary, basalt clasts in all these volcanic sandstones are interpreted to have been derived from recycling of an intrabasinal volcanic source based on lithology, proximity to contemporaneous basaltic volcanism, and their subangular scoriaceous and pilotaxitic texture. These clasts were most likely derived from a local basaltic source (probably the Grays River volcanics to the southwest). Mark McCutcheon (personal communications, 1998) reports interbedded basaltic lavas, debris flows, and thicker basaltic pebbly sandstone in the Cowlitz Formation in the Coal Creek and Mt. Solo area near Longview, Washington along the Columbia River to the south of this study area. The presence of abundant delicate scoria clasts indicates that explosive basaltic volcanism (e.g., cinder cones and glassy vesicular tops of basalt flows) was occurring in the basin during deposition of units 2 and 3 of the Cowlitz Formation. Scoriaceous volcanic detritus typically would not survive extensive transport in a tractive fluvial environment from a distant source (i.e., continental volcanic source terrane to the east). Also, quartz and potassium feldspar grains are not abundant in these beds which indicates these pyroclastic and epiclastic deposits were subjected to very little reworking by tidal or wave processes. Additionally, chemical composition of plagioclase phenocrysts from basaltic clasts in sample CP-95-159 from unit 2 are typical of an oceanic basaltic source. This supports the interpretation that some of these scoriaceous basalt clasts were derived from erosion of the tholeiitic basalts of the Grays River volcanics. Some intersertal and randomly oriented

basaltic clasts may have had a possible Northcraft calc-alkaline basaltic and andesitic source to the northeast, and Crescent Formation source to the west (where not overlain by the McIntosh Formation). Some of these thicker beds contain pumice and dacitic clasts derived from an explosive early western Cascade calc-alkaline volcanic arc (e.g., Northcraft Formation) source to the east. Thus, the dominant source for these volcanic clasts was an oceanic type forearc terrane, with a secondary component derived from the nearby explosive western Cascade calc-alkaline arc.

SANDSTONE OF THE TOUTLE FORMATION

The feldspathic litharenite, volcanic sandstone, and reworked pumiceous lapilli tuff beds from the Toutle Formation (in this study area) are distinctively different from the lithic arkose and basaltic sandstones of the Cowlitz Formation (Figure 36). The volcanic component of these sandstones consists of subequal proportions of both basaltic-andesite and siliceous volcanic rock fragments, contains very little mica, and has a much lower porosity than sandstones of the Cowlitz Formation. Additionally, they lack the scoriaceous and pilotaxitic basalt that was common in the Cowlitz basaltic sandstones.

The lower fluvial feldspathic litharenite at the base of the Toutle fluvial unit A (sample CP-95-182b, measured section O38, Plate II) (Figure 36) consists of subrounded to subangular, moderately sorted, monocrystalline quartz (27%), potassium feldspar (both orthoclase and gridiron twinned microcline) (14%), and albite twinned plagioclase (7%) grains (Figure 36). The lithic components are polycrystalline quartz (13%), schist (7%), plutonics (2%), siliceous volcanics (15%), and altered basalt (15%). This sandstone may be recycled from erosion of the Cowlitz Formation sandstone and older volcanic units.

The hornblende-bearing pumiceous lapilli tuff (sample CP-95-182b, measured section O40), consists of very small plagioclase microlites in a glassy matrix. This reworked tuff also contains subordinate and distinctive rounded pilotaxitic basalt clasts

and albite twinned, large plagioclase grains in a glassy pyroclastic tuffaceous matrix. These fresh hornblende crystals ($^{39}\text{Ar}/^{40}\text{Ar}$ dated at 31.9 ± 0.4 Ma in this study), are green, brown, and orange; some may be iron-rich oxyhornblende. Whole-rock XRF chemistry indicates this tuff has a basaltic-andesite composition (Hammond, personal communications, 1996).

The fluvial volcanic sandstone that forms the upper part of the Toutle Formation (CP-95-186b, measured section O42, Plate II) consists of about 80% altered intersertal basalt, andesite, and siliceous volcanic clasts. The Hatchet Mountain basalt to the east and possible uplifted Crescent Volcanics to the west may have been the source for these basaltic clasts. Subordinate amounts of sedimentary and metamorphic quartzite, hornblende, monocrystalline quartz, plagioclase, clinopyroxene, and carbonaceous plant debris comprise the sandstone. The predominance of silicic volcanic clasts is evidence that the main source for sediment during Toutle time was the western Cascade calc-alkaline volcanic arc just east of the study area.

Reservoir potential of the volcanic and lithic arkosic sandstones of the Toutle Formation is moderate to poor. Grain contacts are generally tangential, indicating that these sandstones have not experienced significant burial compaction. However, carbonaceous plant debris and some altered basaltic clasts in the upper fluvial sandstone bend ductily between brittle subangular quartz and feldspar grains as a result of some burial compaction. The two sandstone samples have 5% to 10% porosity estimated by visual inspection. However, other volcanic arkosic sandstones from the lower part of the Toutle Formation may be much more porous, but they were too friable for thin section examination. Porosity is dominantly primary intergranular and shows partially open pore throats with moderately good interconnection between the intergranular porosity in sample CP-95-186b. Some basalt and siliceous volcanic clasts have undergone extensive dissolution forming secondary intragranular porosity. Vertical permeability is reduced by

abundant laminae composed of long impermeable aligned pieces of carbonized plant debris. One sample is well cemented by sparry calcite cement (CP-95-182b, Plate II). The dominant authigenic minerals in the upper volcanic sandstone sample (CP-95-186b, Plate II) are 8.9 Å zeolites (clinoptilolite) and early stage smectite grain-rimming cements (Figure 41). The late stage zeolites have grown above the thin rims of smectite and have also grown into the intergranular pore spaces between some volcanic grains.

GEOCHEMISTRY OF TUFF BEDS FROM THE COWLITZ AND TOUTLE FORMATIONS

A total of 25 geochemistry samples from tuff beds from throughout the Cowlitz and Toutle formations were submitted to professor Paul Hammond of Portland State University (Figure 42). These samples were then analyzed for major and trace elements using a Rigaku sequential x-ray fluorescence (XRF) unit by Dr. Peter Hooper of Washington State University, Pullman (Appendix IV). Most samples collected from the Cowlitz Formation came from fine-grained, light-colored tuff beds in coal seams from units 1 and 3. One sample from a light buff tuff interbedded with the Grays River volcanics was analyzed. Samples from the Toutle Formation were from the thick fine-grained tuffs interbedded with the upper fluvial strata in sections O42 to O43 (Plate II).

Most tuffs in the Cowlitz and Toutle formations of southwest Washington are fine-grained and clay-rich. Many are calc-alkaline volcanic arc in composition although some basalts and basaltic andesites (mafic in composition) may be tholeiitic (Hammond, written communications, 1996). The initial glassy chemical composition of most tuffs has been modified by weathering and diagenesis after burial in the sedimentary environment. This includes contamination by addition of terrigenous clay, fine clastic particles of quartz, and diagenetic alteration by permeating ground waters of varying compositions (Hammond, written communications, 1996). Tuffs with $\geq 20\%$ Al_2O_3 , as well as $\geq 2.0\%$

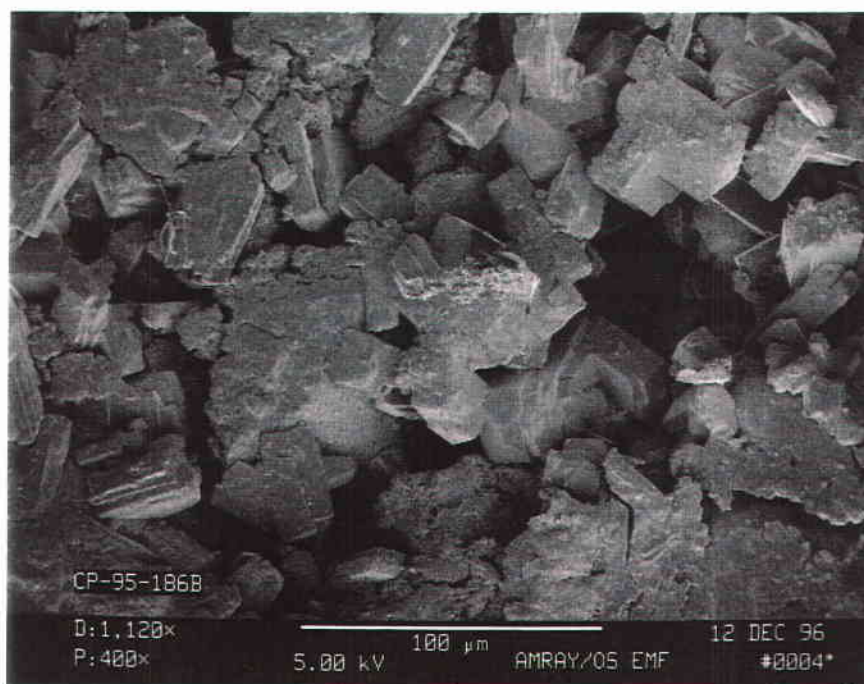
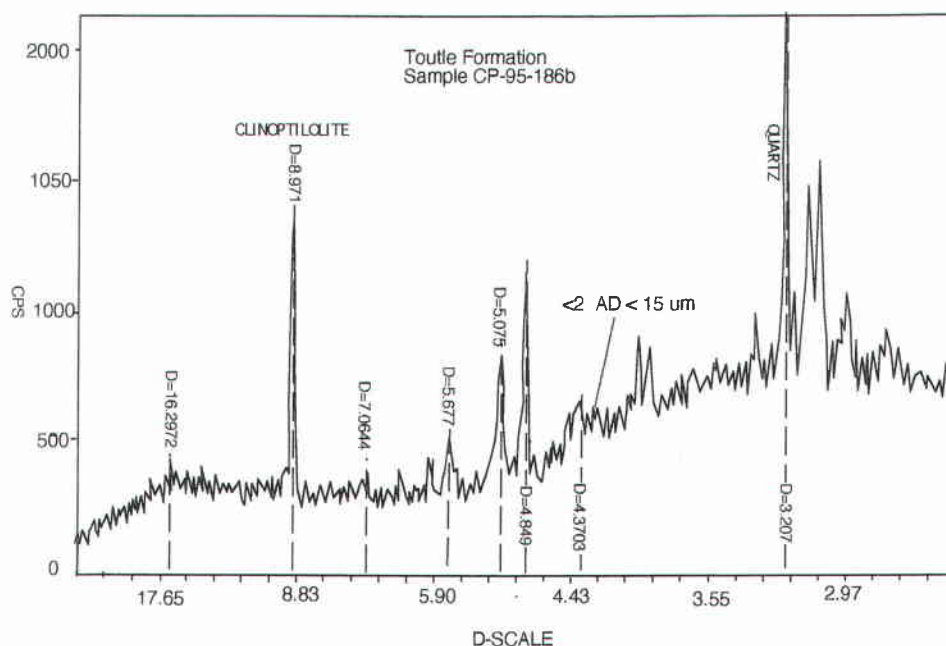


Figure 41. X-ray diffraction pattern and scanning electron (SEM) photomicrograph of sample CP-95-186b from the upper fluvial sandstone unit of the Toutle Formation (Plates I and II). Note large platy authigenic 8.9 Å zeolite (clinoptilolite) and thin grain-rimming smectite clays. These zeolites have grown into the pore spaces between volcanic rock fragments. Bar scale at bottom of SEM photograph is 100 microns.

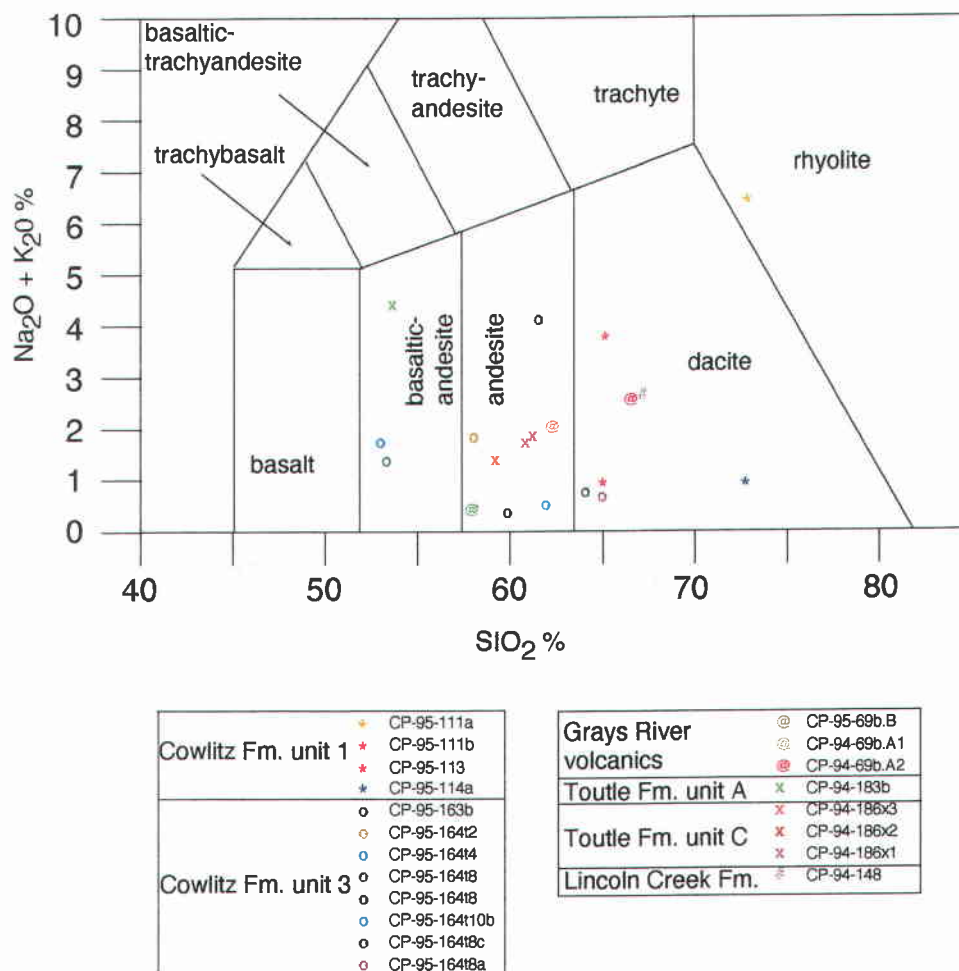


Figure 42. Tuffs of the Cowlitz, Toutle, and Lincoln Creek formations and the Grays River volcanics from the thesis area plotted on a total alkali vs. SiO₂ (TAS) diagram. This is based on the IUGS classification scheme of Le Bas and others (1986).

Ti_2O , $\leq 0.5\%$ K_2O , $\leq 1.0\%$ Na_2O , and others with $>10.0\%$ CaO , are considered chemically suspicious (Hammond, written communications, 1996).

The fine-grained and light colored tuffs from the Cowlitz and Toutle formations are generally andesitic to dacitic in composition, although many analyzed tuffs are enriched in secondary hygroscopic clay and show more than 20% alumina oxides and 2% titanium oxide by weight. These tuffs were leached of alkalis, some silica, possibly trace elements, and enriched in alumina and titania and thus may not have representative chemistries (Hammond, written communications, 1995). Only a few samples had Al_2O_3 weight percents $< 20\%$. These included a sample from the upper coal seams of Cowlitz unit 1 and a pumice lapilli tuff from unit 3. Tuffs from unit 1 are generally andesitic in composition (Appendix IV). One relatively unaltered tuff (sample CP-94-111a) from the lower thick 11.6-m thick coal seam in unit 1B (section 6H, Plates I and II) appears to be rhyolitic (73% SiO_2) in composition and is low in TiO_2 (0.26%) which indicates it may have had a western Cascade silicic volcanic-arc source (Appendix IV). Five tuffs in the upper coal seam in unit 3 are andesitic to dacitic in composition, though these tuffs are composed of $\geq 20\%$ alumina and may be diagenetically modified and do not reflect the initial composition (CP-95-164t2, -164t4, -164t6, -164t8b, and -164t10b, Figure 23, Plate II). The possible western Cascades source for these tuffs is the Northcraft Formation. Three tuffs from the upper fluvial unit of the Toutle Formation are andesitic in composition (CP-95-186x1, -186x2, and -186x3; Appendix IV and Plate II) (Hammond, written communication, 1996).

SUMMARY

A general paragenetic sequence of diagenesis can be described for the McIntosh and Cowlitz formations based on petrographic analysis of sandstone samples (Figure 43). The earliest diagenetic event was development of scattered sparry calcite cement in some samples. This cement was derived from dissolution of aragonite of the molluscan shells and is associated with mollusc-rich concretionary layers. With increasing burial depth, compaction of mica and carbonaceous plant fragments in the lithic arkoses reduced some primary intergranular porosity. Some schist and mudstone fragments also have been squeezed between more brittle quartz and feldspar grains indicating burial compaction was sufficient enough to distort these grains. Minor grain rotation also occurred. However, most micas are not bent and quartz and feldspar grains have large tangential point contacts, suggesting only minor burial effects under shallow burial depth conditions. Some early stage potassium feldspar (orthoclase) overgrowths are present but are not very widespread. Early stage authigenic smectite clay rims many framework grains, but has not filled much of the primary intergranular pores in these lithic arkosic micaceous sandstones. The later stage 8.9 Å zeolite (clinoptilolite) is formed under shallow burial conditions and indicates that the McIntosh Formation sandstone and lower part of the Cowlitz Formation were not buried deeper than approximately 5,000 to 7,000 feet.

This shallow burial of the sedimentary strata in this area, even though a thick sequence of Oligocene marine strata (Lincoln Creek Formation) filled this basin to the northwest, may be due to a local unconformity event that was formed at the end of deposition of the Cowlitz Formation in the study area (see Grays River volcanics section). This period of uplift and erosion may have created an upland or highland that prevented deposition of a thick sequence of Lincoln Creek strata in this area. The main center of basin subsidence was to the north, where the Lincoln Creek and overlying Miocene








EVENT	DIAGENETIC STAGE	Early-shallow subsurface	Late-Deep burial
Compaction			
Calcite cementation			
Lithic framework grain alteration			
Pore-lining clays			
Zeolite cementation			
Dissolution of feldspars			
K-spar overgrowths			

Figure 43. Paragenetic sequence of the diagenetic events in outcrop sample of sandstones in the McIntosh and Cowlitz formations. In general, time and depth of burial both increase towards the right. Note the late-stage dissolution of feldspars and earlier stage pore-lining clay (Modified from Robertson, 1997).

Astoria Formation sediment and volcanics were deposited, and thus this uplifted area took longer to subside and these strata in this area experienced only a shallow depth of burial.

A comparison of these fine- to medium-grained, lithic arkosic sandstone compositions from the type section of the Cowlitz Formation in southwestern Washington to the arkosic micaceous sandstones of the Cowlitz Formation in the subsurface in northwestern Oregon analyzed by C. Robertson (1997) indicates there is a minor increase in volcanic rock fragments in the type locality (Figure 36). This difference could be a result of one or a combination of the following factors (1) sampling bias, (2) differing point counting techniques, (3) the type Cowlitz was more proximal to a basaltic provenance, (4) storm wave-dominated depositional processes broke down and winnowed out volcanic clasts in northwest Oregon, (5) this formation consists of two disconnected delta lobes in Oregon and Washington derived from different volcanic and extrabasinal plutonic-metamorphic sources. Scoriaceous basaltic sandstones are more abundant in the type Cowlitz Formation than in the Mist Gas Field of northwest Oregon. Petrology and field studies of these sandstones indicate a mixed extrabasinal acidic plutonic-metamorphic provenance and an intrabasinal basaltic source (Appendix III). The predominant constituents of Cowlitz Formation arkosic sands were transported from a dissected arc (the Idaho Batholith and metamorphic core complexes of northeast Washington) through an ancestral Columbia River fluvial system. The basaltic clasts from the volcanic sandstones of the Cowlitz Formation have textural characteristics very similar to the Grays River volcanic and Tillamook Volcanics of northwest Oregon. A local basaltic source (Grays River volcanics and possibly Goble Volcanics) supplied basaltic sand to the shallow marine and marginal marine environments that form units 2 and 3 of the Cowlitz Formation. Explosive silicic calc-alkaline volcanic activity (e.g., Northcraft Formation and Goble) is also evident in the fine-grained andesite to silicic pumiceous tuff beds interbedded in units 1 and 3. A change in provenance accompanied the structural and

erosional event (unconformity) that occurred near the end of deposition of upper unit 5 of the Cowlitz Formation and before deposition of the Toutle Formation. The provenance of the Toutle and Lincoln Creek formations is of an active silicic volcanic arc (Goble and Hatchet Mountain volcanics of the western Cascade arc).

STRATIGRAPHY, PETROLOGY, AND GEOCHEMISTRY OF THE GRAYS RIVER VOLCANICS AND UNDERLYING GRAYS RIVER SEDIMENTARY SEQUENCE

NOMENCLATURE AND CORRELATION

Forearc and arc magmatism are temporally correlated with changes in plate motion and a significant decrease in Farallon-North America convergence rates between 44 and 28 Ma (Wells et al., 1984). Forearc extension occurred during the middle and late Eocene along a broad zone of right-lateral shear with the resulting eruptions of alkalic to tholeiitic basaltic magmas at several volcanic centers (e.g., Tillamook Volcanics in northwestern Oregon and Grays River volcanics in southwestern Washington). These oceanic-island volcanics are mainly subaerial flows, however, the lower part of the Tillamook Volcanics consists of submarine pillow lavas, breccia, and feeder dikes (Snively, 1987). Some volcanic rock units in southwest Washington mapped as the Goble Volcanics (arc derived) by Wells (1981) were renamed Grays River volcanics (forearc derived) by Phillips (1987). This change in nomenclature is due to major petrographic and geochemical differences (mainly FeO, TiO₂, and SiO₂) between these late middle and late Eocene volcanic units. The Grays River volcanics is located in this study area (i.e., Bebe Mtn. and Abernathy Mtn.), on the southern flank of the Willapa Hills (Crescent Fm. core) in southwestern Washington, and in the subsurface in northwestern Oregon (Plate I, Figures 3 and 44). The Goble Volcanics crops out farther east in the type area of northwest Oregon and in the western Cascade volcanic arc of southwest Washington.

Lavas in both the middle Eocene Tillamook and middle to late Eocene Grays River volcanics display a similar pilotaxitic (flow) texture of aligned plagioclase microlites with opaque ilmenite and colorful titanite in thin section. The lavas of the Grays River are

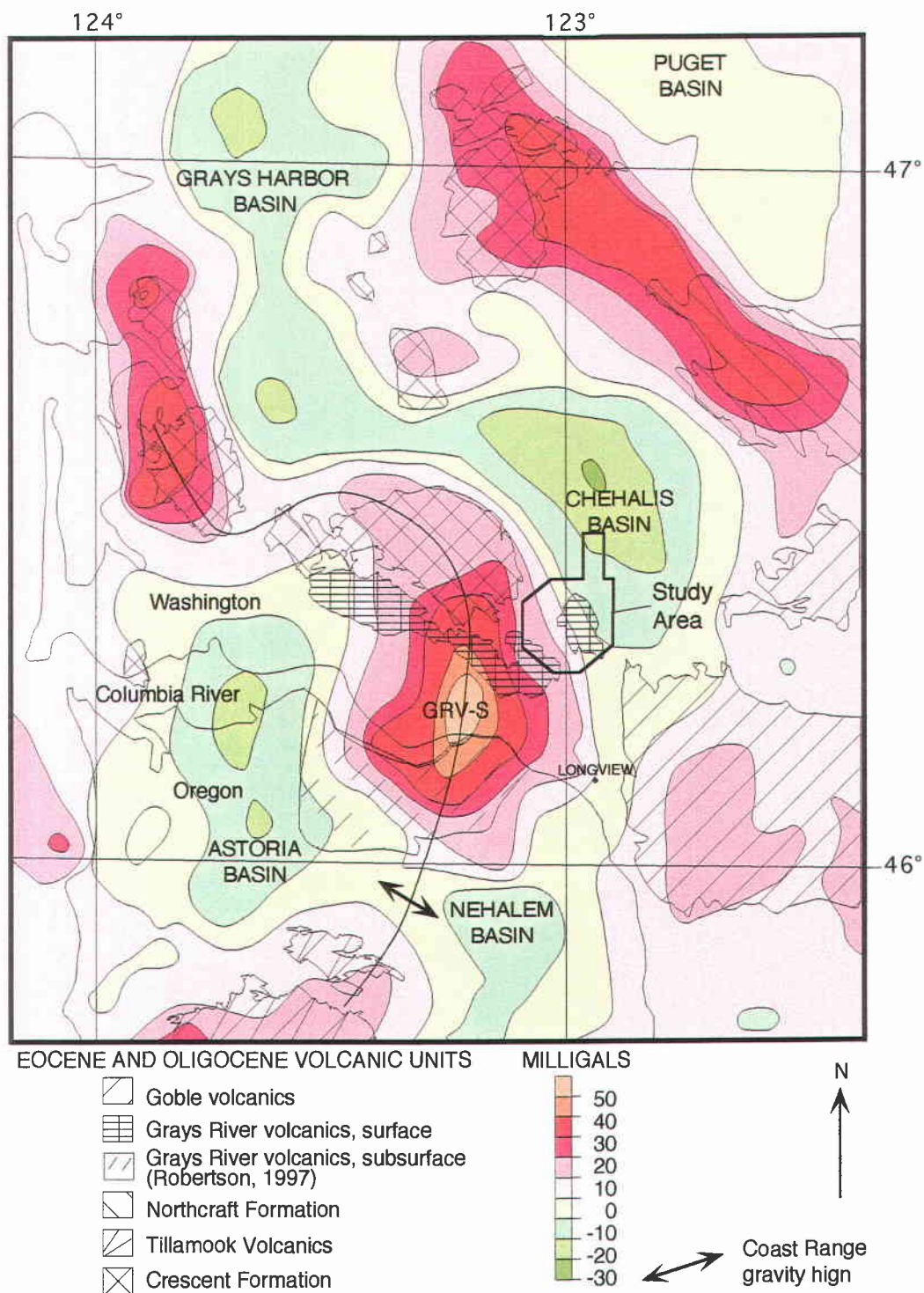


Figure 44. Residual wavelength-filtered gravity anomaly map and volcanic geology map superimposed to show relationship of shallow crustal features with mapped surface volcanic units. Large anomaly south of Grays River volcanics (GRV-S) outcrop may be the main eruptive center for the GRV (modified from Finn et al., 1991; Walsh et al., 1987; and Robertson, 1997).

mainly basaltic in composition with the Tillamook Volcanics containing some overlying feldspar-phyric andesite and dacite flows that suggest differentiation of tholeiitic basaltic magma in the upper crust before extrusion (Rarey, 1986; Safley, 1989). These volcanics are high-titanium oxide (3 to 4% TiO_2), high-iron oxide (FeO) basalts and are chemically distinct from the underlying lower TiO_2 and FeO Siletz-Crescent oceanic basalts and from the slightly younger calc-alkaline late Eocene to Oligocene Goble Volcanics to the east (Rarey, 1986). The 45 to 40 Ma Tillamook and 41 to 37 Ma Grays River volcanics appear to be chemically, petrographically, and be partially age equivalent (Rarey, 1986).

The widely separated outcrops of Tillamook Volcanics in northwestern Oregon and Grays River volcanics in southwestern Washington appear to be connected in the subsurface by the northern Coast Range gravity high (Armentrout and Suek, 1985; Snively, 1987). However, a more detailed gravity study by the U. S. Geological Survey (Finn et al., 1991) reveals a large gravity anomaly centered just north of the Columbia River that may be associated with the main eruptive center of the Grays River volcanics (GRV) (Figure 44). Steve Kennitz (personal communications, 1996) has found the Cowlitz of northwest Oregon to be interbedded with Grays River flows and the GRV to be over 5,100 feet thick in the subsurface in the Champlin Puckett well 13-36-85 (Sec. 36, T8N, R5W). He also found that each of these subsurface flows averages 35 to 60 feet in thickness and one 60 ft-thick volcanic breccia, 650 feet above the C and W sandstone of the Cowlitz Formation in Oregon (Sec. 34, T7N, R5W). This gravity high is distinctive and separates the Astoria and Nehalem basins which contain up to 10,000 feet of middle Eocene to Miocene sedimentary rocks (Niem and others, 1992; Niem and Niem, 1985).

Additional work by Steve Kennitz (personal communications, 1997) has determined that the Grays River volcanics and the Tillamook Volcanics are two separate volcanic centers. Both Kennitz and Christy Robertson (1997) in subsurface studies of well logs of the Cowlitz Formation and related formations of northwest Oregon,

concluded that the Tillamook Volcanics underlies the Cowlitz and Hamlet formations and the overlying Grays River volcanics is interbedded with the C and W sandstone of the Cowlitz Formation in northwest Oregon (Figure 3).

In this study, the Grays River volcanics can be further separated into two distinct volcanic piles or subunits based on its stratigraphic relationship with sedimentary units and radiometric ages collected from across the Grays River's outcrop distribution in southwest Washington. The older and thickest volcanic pile crops out in the central and western part of the Willapa Hills uplift mapped by Wells (1981) (Figure 2). A second younger volcanic pile was mapped in this study area around Bebe and Abernathy mountains (Figures 2 and 44, Plate I). This Grays River volcanics in this study area unconformably overlies the Cowlitz Formation and is discussed in detail in the following sections.

AGE DETERMINATION

The following age ranges of the Grays River volcanics and Tillamook Volcanics demonstrates these volcanics are largely time separated units. A dike with Grays River geochemistry to the northwest of their outcrop distribution (Moothart, 1992) has been $^{39}\text{Ar}/^{40}\text{Ar}$ dated at 41.4 ± 0.7 Ma and a flow in the easternmost exposure in this study area was dated at 36.85 ± 0.46 Ma. Whole-rock K-Ar ages from subaerial flows at the top of the Grays River volcanics range from 37.3 ± 2.2 Ma to about 39 Ma (late Eocene) in the eastern Willapa Hills area (Phillips et al., 1986; Wells and Coe, 1985). K-Ar ages from pillow basalts of the lower Tillamook Volcanics range from 43 to 46 Ma (Magill et al., 1981). The subaerial upper part of the Tillamook ranges from 42 to 43 Ma based on more reliable $^{39}\text{Ar}/^{40}\text{Ar}$ dating by McElwee (in Berkman, 1990); an $^{39}\text{Ar}/^{40}\text{Ar}$ date of 42.4 ± 0.5 was reported by Niem and others (1992a) for a flow near the top of the Tillamook Volcanics. Middle Eocene sedimentary rocks that contain lower Narizian benthic

foraminifera are interbedded with the lower part of the Grays River Volcanics in the western Willapa Hills (Wolfe and McKee, 1972). This biostratigraphic and radiometric relationship may make the Grays River volcanics of southwest Oregon as old as 43 Ma (Walsh et al., 1987); thus, younger in age than the Tillamook Volcanics of northwestern Oregon.

The Grays River volcanics can be separated into two (not-so-distinct in mapping) volcanic outcrop areas in southwest Washington based on age dates and stratigraphic relationship (Figure 45). The older part or volcanic complex that forms the thickest pile crops out in the central and western part of the Willapa Hills uplift. A second younger part of the volcanic complex was mapped in this study area at Bebe and Abernathy mountains. A high TiO_2 basalt dike with Grays River geochemistry, 20 km to the west, was $^{39}\text{Ar}/^{40}\text{Ar}$ dated at 41.4 ± 0.7 Ma (Moothart, 1991). The Ordway Creek porphyritic quartz monzonite and granodiorite stock (Wells, 1986) intruded into the older pile of Grays River volcanics to the southwest of this study area. This stock contains inclusions of Grays River volcanics and has a zircon fission track age of around 41 Ma (Walsh, 1987) and suggests the Grays River volcanics are older in this area. To the south, near Coal Creek, the Cowlitz Formation is interbedded with a basalt flow of the Grays River volcanics that has a whole-rock plateau $^{39}\text{Ar}/^{40}\text{Ar}$ age of 40.3 ± 0.3 Ma (Irving et al., 1996).

The youngest age date for a Gray River volcanics sample is from the easternmost exposures of this unit in this study area. Three fresh subaerial Grays River basalt samples were prepared and submitted to Dr. Robert Duncan of the College of Oceanic and Atmospheric Sciences, Oregon State University, Corvallis for $^{39}\text{Ar}/^{40}\text{Ar}$ dating using a laser-fusion mass spectrometer. The age dates from southwest to northeast (Plate I) are as follows: (1) 38.64 ± 0.40 Ma for sample CP-94-196 from southern Abernathy Mountain in the lower part of the pile, (2) 37.44 ± 0.45 Ma from sample CP-94-68du from

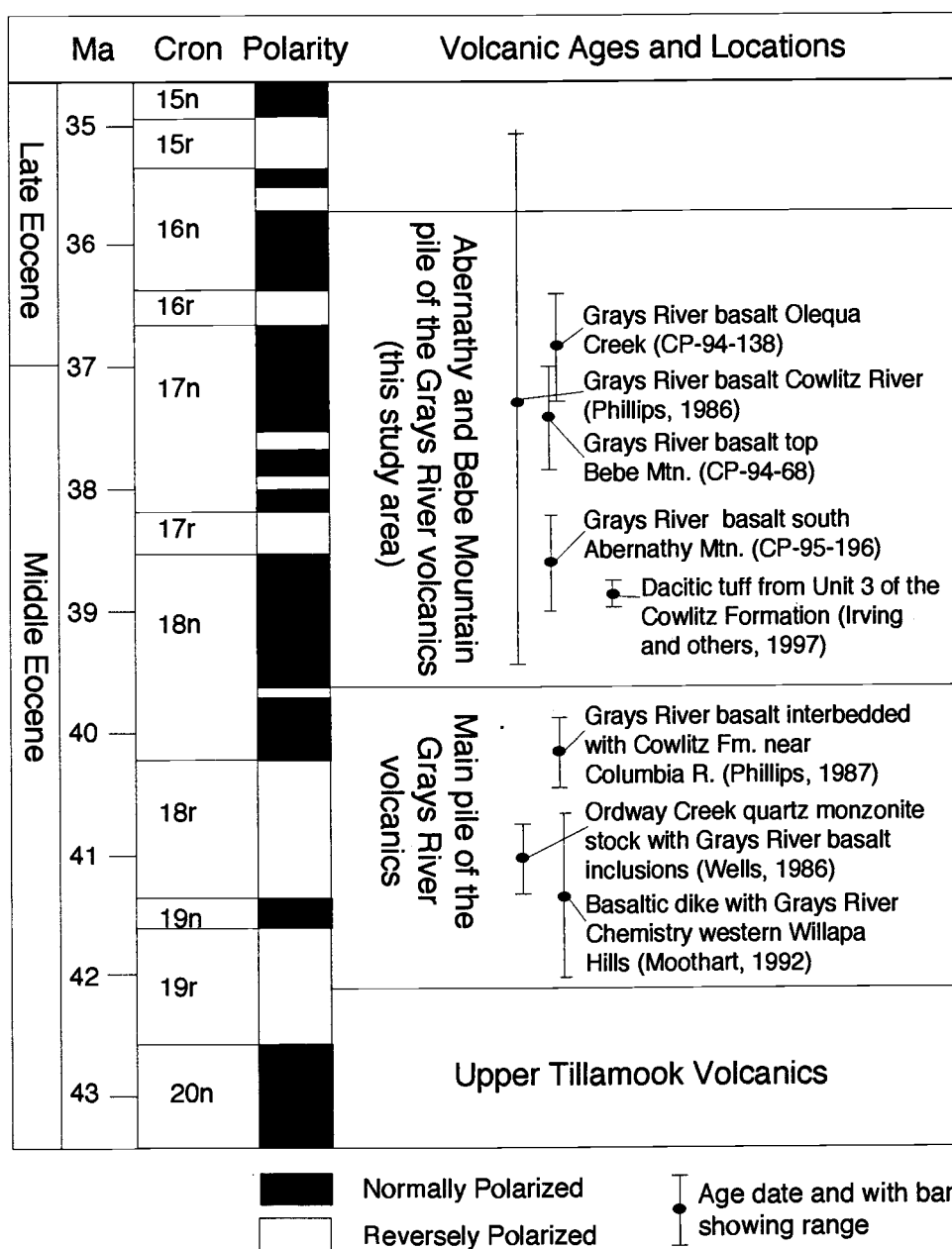


Figure 45. Magnetic polarity chart and volcanic age dates of the Grays River volcanics. Note disparate age of the two Grays River volcanic piles and their relationship to the magnetic time scale of Berggren and others (1995). According to Ray Wells (1985), the Grays River volcanics in the Willapa Hills formed during one reverse polarity episode (e.g., chron 18r). Locations and sources of age data are discussed in text.

northwestern Bebe Mountain, and (3) 36.85 ± 0.46 Ma for CP-94-138 from the upper part of the volcanic pile in lower Olequa Creek (Figure 45 and Plate I). This study has determined that this pile of Grays River volcanics and associated sedimentary sequence unconformably overlies the Cowlitz Formation (Figure 46). Marker A in Cowlitz Formation unit 3 has an age of 38.9 ± 0.1 Ma (Irving et al., 1996) and brackets the unconformity between the Bebe Mountain pile of the Grays River volcanics and the Cowlitz Formation to between 38 and 37 Ma.

MAGNETIC POLARITY

A portable fluxgate magnetometer was used in the lab to determine the magnetic polarity (normal or reversed) on 19 oriented igneous rock samples from the field area (Plate I). Three of these samples were $^{39}\text{Ar}/^{40}\text{Ar}$ dated and compared to the world-wide magneto-chronostratigraphic scale of Berggren et al. (1995) (Figure 45). All samples were oriented in the field for horizontal and north directions and structural data were recorded. The freshest samples were collected mainly in quarries (Plate I). These samples are stratigraphically from the lower, middle, and top of the Bebe Mountain pile.

The late Eocene basalts of the Grays River volcanics in the Bebe Mountain area are overwhelmingly normally polarized with only two reversely polarized samples at the base of the section, one of these from Abernathy Mountain (Plate I). Two samples were from basaltic intrusions with the rest from subaerial flows throughout the field area. The main pile of Grays River volcanics to the west is predominantly reversely polarized (Wells, 1985). Steve Moothart (1992) collected four intrusive basalt samples in the older part of the Eocene section (i.e., intruding lower Narizian strata) with Grays River volcanics geochemistry; all show reversed polarities and correlated with the mainly reverse-polarized pile mapped by Wells (1981) (i.e., older part of the Gray River volcanics).

These reversely polarized samples from the lower Grays River volcanics pile (from 41.4 ± 0.7 to 40.3 ± 0.3 Ma) fit within the 41.3 to 40.2 Ma age range of the 18r magnetochronologic interval. Additionally, one of these volcanic samples is interbedded with the Cowlitz Formation; indicating contemporaneous Cowlitz sedimentation and lower Grays River volcanism. The Bebe Mountain part of the Grays River pile in the east has an age range of 37.44 ± 0.45 to 36.85 ± 0.46 Ma and best fits into magnetochronologic interval 17n (Figure 45). Only two samples (CP-94-67 from the lower part of Bebe Mountain and CP-95-204 from Abernathy Mountain, Plate I) are reversed. These samples are from the base of the volcanic section but lie above sample CP-95-196 (normally polarized and age dated at 38.64 ± 0.40 Ma, Plate I). The reversely polarized samples thus fit into magnetochronologic interval 17r or the minor reversals at the base of 17n (Figure 45). The Abernathy Mountain pile ties with the mapped outcrop pattern of the Grays River volcanics in the Willapa Hills, but the slightly younger normally polarized Bebe Mountain pile is an isolated outcrop pattern (Plate I and Figure 45). Additionally, one Grays River volcanic dike is normally polarized (CP-94-34, Plate I).

GRAYS RIVER SEDIMENTARY SEQUENCE UNDERLYING THE GRAYS RIVER VOLCANICS

A local, valley-fill sequence overlies and unconformity on the Cowlitz Formation and underlies the Grays River volcanics in the study area. The post-Cowlitz sedimentary sequence was also identified in the subsurface by Weyerhaeuser Co. geologist Dave Pauli using numerous shallow core holes drilled in this area (Figure 46). This sedimentary unit is mainly evident in the subsurface under the western part of Bebe Mountain and the southern part of Abernathy Mountain and ranges from 0 to over 200 m in thickness (Pauli, written communications, 1996). This sedimentary unit also crops out in a few locations along the western margin of Bebe Mountain and the eastern side of Abernathy Mountain (label Tgvs on Plate I). This unit was deposited after a significant tectonic and erosive

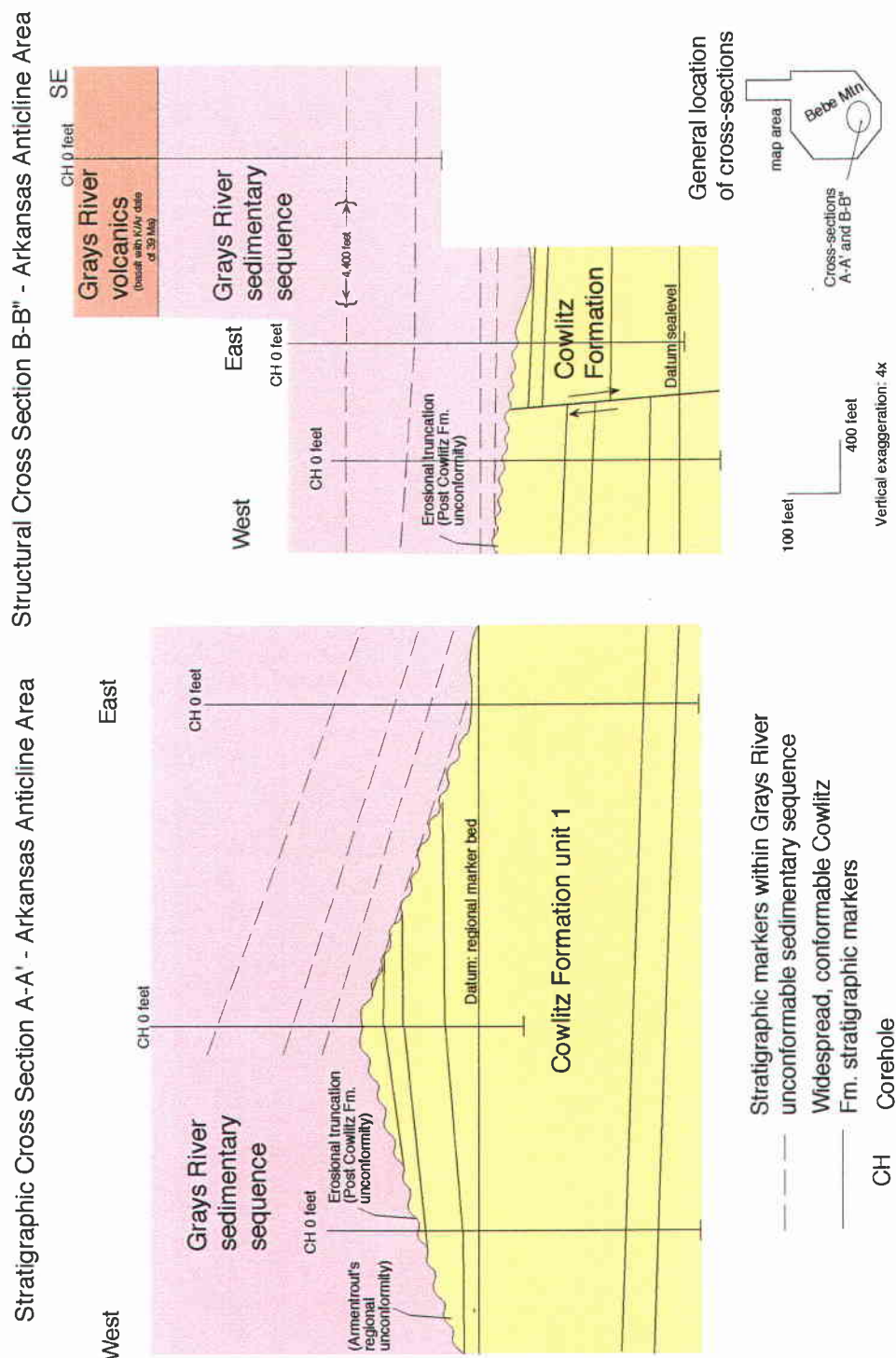


Figure 46. Stratigraphic and structural cross-sections from the Arkansas Creek area. Note angular unconformable relationship of the Cowlitz Formation and the (post Cowlitz) Grays River sedimentary sequence. This Grays River sedimentary sequence underlies the Grays River volcanics and post dates a major faulting event. (Slightly modified from Dave Pauli, written communications, 1994)

event and may have been deposited between down-dropped blocks of Cowlitz Formation (cross-sections B-B' and C-C' on Plate I). The tectonic and stratigraphic significance of this lower Grays River sedimentary unit will be discussed in the following Regional Correlation and Stratigraphic Relationships and Structural Geology chapters.

The lower part of this volcanic-arkosic sandstone sequence (informally referenced in this study as lower Grays River sedimentary sequence) is mainly composed of reworked strata of the Cowlitz Formation while the upper part is volcanic-rich. The arkosic sandstone and siltstone lithologic similarity of the lower part of the post-Cowlitz sequence and the arkosic sandstone-dominated units 1 to 3 of the Cowlitz Formation makes identification and mapping of the lower part of this post Cowlitz sedimentary unit difficult (Pauli, personal communications, 1995). However, tuffaceous siltstone from the lower interval lacks of mica, which is common in Cowlitz siltstone beds. Only the volcanic-dominated upper part of this unit was easily identifiable in the field, and, thus, the post-Cowlitz lower Grays River sequence may be more widespread than has been mapped in this study (Plate I).

The upper part of this sedimentary unit is composed of basaltic sandstone, lapilli tuff, basaltic breccia, and tuffaceous siltstone. The unit directly underlies the Grays River volcanics and has similar dip. A 5-m thick fining-upward sequence of poorly sorted and rounded volcanic pebble conglomerate overlain by a mollusc-bearing siltstone occurs directly underlying the Grays River volcanics at Abernathy Mountain location (CP-95-199, Plate I). The molluscs were identified as shallow marine *Tellina cowlitzensis* clams by Elizabeth Nesbitt (written communications, 1996). Stratigraphically higher strata, CP-95-202ts, Plate I), consist of planar-laminated, angular, basaltic sandstone. This sample was analyzed petrographically. Basaltic clasts in these strata display a pilotaxitic texture very similar to the overlying Grays River volcanics (i.e., probably derived from older Grays River volcanics to the west). At the southern end of Abernathy Mountain (SE 1/4,

NW 1/4, Sec. 1, T9N, R3W; Plate I) a 6-m thick, fining-upwards light brown basaltic lapilli tuff is a few meters from the contact with the overlying Grays River volcanic flows. Other locations along the southern part of Bebe Mountain consist of massive tuffaceous siltstone, maroon tuff, and volcanic sandstone beds. Some beds contain silicified stems and leaf imprints (location CP-94-68 and -69, Plate I). The depositional environment for this unit may be a volcanic-influenced fluvial system. However, shallow marine bivalves are anomalous and may indicate part of this unit was deposited subaqueously after a relative sea level rise. Erosion of older Grays River volcanics detritus to the west became more significant near the end of deposition of the unit. This large volcanic influx defines the beginning of a second Grays River eruptive event at Bebe Mountain.

GRAYS RIVER VOLCANIC STRATIGRAPHY

Multiple, large quarry pits used in extensive logging road construction provided excellent exposure of the Grays River volcanics throughout the field area (Plate I). Topography on some of these flows is that of bench-like questas on the western flank of Bebe Mountain. The Grays River volcanic lavas appear to be intracanyon on the eastern side of Bebe mountain where they are incised into the Cowlitz Formation sandstones (this will be discussed further later in this section). These flows were originally mapped as a separate intercalated volcanic unit, the Cowlitz volcanics by Henriksen (1956), but I mapped them as Grays River volcanics because they are younger (e.g., 36.85 ± 0.4 Ma) than the Cowlitz sedimentary units and much of the Grays River volcanics on Bebe Mountain. The Grays River volcanics in this area is up to 180 m thick and averages 70 m in thickness based on structural dip, well data (Pauli, written communications, 1995), and measured sections along Bebe Mountain (Plate I). Individual Grays River lava flows from both Abernathy and Bebe mountains are 3 to 30 m thick and dominantly subaerial (Figure 47A). The volcanics are dominantly aphyric to plagioclase-phyric with a basal section that

is pyroxene and olivine phenocryst bearing. The volcanic flows are interbedded with minor tuff and tuffaceous carbonaceous mudstone (5-10% of total Grays River volcanics) (Figure 47B). These sedimentary strata indicate there was some amount of time between flows to allow for formation of marshes and paleosols.

The following discussion is from field measurement, sampling and observations from the eastern part of the generally west-dipping Abernathy mountain section of the Gray River volcanics (Plate I). Sample location CP-94-196 located on the southern part of Abernathy Mountain consists of a grayish black, 8-m thick vertically jointed, pyroxene-olivine phyric to aphanitic basalt with a vesiculated top (see Volcanic Petrology Section, page 150) (Plate I). An $^{39}\text{Ar}/^{40}\text{Ar}$ date of 38.64 ± 0.40 Ma was calculated for sample CP-94-196. The vesiculated, scoriaceous, and brecciated base of this flow is pillowed. The outer carapace of these oblate pillows have altered glassy rinds. Some large vesicles are filled with calcite and zeolites. Other quarries from the southern part of Abernathy Mountain (W 1/2, Sec. 35, T10N, R3W; Plate I) exhibit 3-m- to 12-m-thick columnar-jointed aphyric basalt flows with 1m thick brecciated flow bottoms and vesiculated flow tops. These subaerial flows overlie the closely packed pillowed flow at sample location CP-95-196 (Plate I).

Quarry exposures on the northeastern part of Abernathy Mountain consist of aphyric microcrystalline basalt with scattered (0.5 to 1 mm) pyroxene phenocrysts (2% of total basalt). Vertical sheared and brecciated zones are present and large (1-2 m in diameter) colonnades are bounded by vesiculated flow tops and bottoms. One quarry (NE 1/4, SE 1/4, Sec. 20, T10N, R3W; Plate I) exposes a granular volcaniclastic and tuffaceous mudstone above a 12-m thick subaqueous pillow basalt flow. These interbedded strata occur at the base of the Abernathy volcanic pile. Sample location CP-95-204 (Plate I) is a large quarry that exposes a 30-m thick columnar-jointed subaerial basalt flow and is stratigraphically higher than the previously described outcrop exposure.

A.



B.



Figure 47. (A) Subaerial, columnar-jointed, basalt flow of the Grays River volcanics and (B) interbedded carbonaceous shale, finely laminated siltstone, and thin tuff beds from a quarry east of the Cowlitz River (1/4 SE, Sec. 16, T10, R2W; Plate I). Note basalt columns are 1 m wide and 3 m high and 25 cm rock hammer for scale.

Excellent exposures of tabular and columnar-jointed basaltic lava flows and subordinate interbedded tuffaceous sedimentary rocks provided by quarries on the southern part of Bebe Mountain (Plate I). In the quarry at location CP-94-3 (NW 1/4, Sec. 30, T10N, R2W). Four subaerial flows range from 3 to 12 m in thickness. The basal flow contains phenocrysts of (0.2 to .5 mm) pyroxene (5%-10%) and olivine and vesicles filled with white radiating zeolites. This flow is columnar-jointed and is vesiculated in the upper part. The second and thickest flow is a sparsely plagioclase-phyric basalt flow that was sampled for petrologic analysis (sample CP-94-3B). The top 3 m of this flow is extensively vesiculated and slightly brecciated. A 1-m thick, black, carbonaceous shale and lignite with interbedded altered fine-grained vitric tuff and tuffaceous siltstone overlie this flow. This marsh/swamp deposit is laterally discontinuous over 30 m due to loading of the overlying flow. Above, a thinner subaerial flow is overlain by another carbonaceous shale bed. The uppermost flow is extensively brecciated at the top and bottom. This upper flow contains vertical pipe vesicles that formed as this lava flowed over wet vegetation and flash-heated the water-saturated sediments, steam blasting the lava. Some paleo-weathered flow tops and bottoms contain smectite clay and reddish iron oxides alteration products. The flows in this quarry have a crude broad antiformal form that may have been formed when these flows mantled and over ran a paleotopographic hill or ridge. These intracanyon flows apparently blocked the paleostream drainage and formed a coal swamp or marsh where fine ash fall deposits accumulated. More flows capped these lignitic sediments and the cycle was repeated.

Subaerial lava flows from the northwestern part of the Bebe Mountain pile of the Grays River volcanics (western Pumphrey Mountain, Plate I) and are exposed in many quarries on the steep anti-dip slope of this mountain. On the upper part or steep west side the flows are exposed in a series of large landslide scarps (from south to north: locations CP-94-12 to 14, CP-94-69, CP-94-68, and CP-94-76; Plate I). An olivine- and

plagioclase-phyric basalt was sampled at location CP-94-76. This flow belongs to the regionally extensive basal sequence of the Grays River volcanics (petrology sample CP-94-76). Another quarry has exposed 20 m of basalt lava flows (three flows) and interbedded tuffaceous strata (SW 1/4, Sec. 1, T10N, R3E; location CP-94-69, Plate I). Stratigraphically overlying this, 1/4 of a mile to the north, another quarry contains over 50 m of flows and subordinate interbedded tuffaceous strata (location CP-94-68-lower and -upper sections, Plate I). These two quarries together expose at least five lava flows and three 1- to 3-m thick volcanoclastic and tuffaceous sedimentary interbeds. At locality CP-94-69 thin beds of finely laminated carbonaceous, tuff-rich siltstone are interbedded with yellow beds of sulfur-rich, medium-grained basaltic sandstone. Large (20 cm diameter and 50 cm long) silicified logs in this sedimentary interval are evidence that forests were present in this marsh/floodplain depositional environment. The overlying, massive and brecciated basaltic lava disrupted and loaded to 8 m into the underlying water-saturated strata. Baked, carbonaceous plant debris fills fractures in this hydrothermally altered plagioclase-phyric basaltic lava flow. A 1.5-m thick coarsening- and thickening-upward sequence of very light gray to white tuff, siltstone, and coarse-grained basaltic sandstone overlies the lower subaerial flow (base of location CP-94-68-lower section; NW 1/4, Sec. 1, T10N, R3E). A third, 6-m thick columnar-jointed flow is extensively brecciated in its upper part. Overlying the flows are reworked tuff, lapillistone, and a leaf impression-bearing siltstone that were deposited during re-establishment of a floodplain between volcanic flows. One tuff (western Cascades geochemistry) from this interval was sampled for geochemical analysis (CP-94-68t, CP-94-69b.A, -69b.A2, and -69b.B Plate I, Appendix V). The uppermost vesiculated aphanitic basalt flow has an extensively brecciated base (petrology sample CP-94-68du). An $^{39}\text{Ar}/^{40}\text{Ar}$ age of 37.44 ± 0.45 Ma

indicates this flow is from the upper part of the middle flows. Flow top autobreccia formed as rubble during cooling of the lava crust. The interior of the flow has vertical columnar joints.

Grays River volcanics along the more gently dipping east slope of the Bebe Mountain pile are generally aphyric and massive (lower Olequa Creek and Highway 411, Plate I). The stratigraphic relationship of the Grays River volcanics and the underlying Cowlitz Formation is exposed below a Burlington Northern Railroad trestle immediately south of the town of Vader (petrology sample CP-94-132; center, Sec. 32, T11N, R2W; Plate I). An intracanyon subaerial flow baked and sunk into an underlying tidal mudstone of Cowlitz Formation unit 3. This intracanyon flow does not crop out in Olequa Creek, which would be the case if it were interbedded with the Cowlitz Formation as Henriksen (1956) envisioned. A second subaerial flow that unconformably overlies the upper coal seam of unit 3 of the Cowlitz Formation incorporated large pods (1 to 3 m in diameter) of baked mudstone (petrology sample CP-94-138; SW 1/4, Sec. 32, T11N, R2W; Plate I). This flow becomes massive upwards and was $^{39}\text{Ar}/^{40}\text{Ar}$ age at 36.85 ± 0.46 Ma. Another basalt lava to the south is exposed along lower Olequa Creek. It totals over 30 m in thickness and is aphyric to sparsely plagioclase-phyric (petrology sample CP-94-140, Plate I). On top of this flow is a 15-m thick volcanic sequence consisting of massive flows with brecciated angular cobbles and vesiculated tops and bottoms. These autobrecciated intervals are composed of cobble-sized vesiculated fragments of basalt that formed as the lava cooled, fractured, and was re-incorporated into this flow as it moved. Along the Cowlitz River and lower Olequa Creek, several exposures of similar basalt flows were described and sampled for analysis (petrology samples CP-94-143 to -146, Plate I). These outcrops display a series of columnar-jointed aphyric subaerial basalt flows with brecciated bases.

A minor invasive relationship is evident at location 12C along the lower part of Olequa Creek (Plate I). The basal part of this subaerial lava flow is highly brecciated and vesiculated and has intruded as much as 2 m into the underlying tidal unit 3 of the Cowlitz Formation. Large mudstone and coal fragments were ripped up and incorporated into the flow. In the upper part of the exposure is a peperite dike composed of sandstone and altered basalt fragments. One coal bed was disrupted and truncated by this invasive dike and the underlying mudstone was baked and bleached. Disrupted and fragmented coal clast also are mixed with vesiculated basalt at the confluence of Olequa Creek with the Cowlitz River (Plate I).

Thin dikes of Grays River basalt occur throughout the field area. Generally, the dikes intruded sandstone-dominated units of the Cowlitz and McIntosh formations; however, some intruded siltstone-rich units (Plate I). These dikes generally followed pre-existing northwest-southeast trending faults. A "dike swarm" was mapped south of Ryderwood, between the Abernathy and Bebe mountain piles of the Grays River volcanics. These dikes are aphyric to plagioclase-phyric finely crystalline basalt and range from 1 to 5 m in width. Some dikes can be traced for a few kilometers, though some appear to be only tens of meters in length. These dikes can form ridges, although many do not have a distinctive topographic expression. Along Stillwater Creek four dikes were observed (Plate I). Basalt and peperite dikes that intruded the upper McIntosh sandstone are 0.9 to 6.1 m in width. Angular clasts in the largest peperite dike include McIntosh Formation mudstone, siltstone, sandstone, and altered basalt in a sandstone groundmass. Some sedimentary clasts are baked while others are unaltered. Dikes in Cowlitz unit 1 were observed along measured sections 7A and 7F (Plate I). One dike has a high TiO_2 Grays River geochemistry (measured section location 7F, Plate I) (Steve Kennitz, personal communications, 1996).

IGNEOUS GEOCHEMISTRY AND PETROLOGY

Data from twenty-one samples analyzed for major and trace element geochemistry by previous authors are used in this study to characterize the geochemical composition of the Grays River volcanics in the thesis area. Russ Evarts (written communications, 1995) of the U. S. Geological Survey supplied this author with unpublished XRF geochemical data from 10 basalt samples he collected in this area (Appendix V). Geochemical analysis of 11 other Grays River basalt samples collected by Phillips et al. (1989) from the thesis area were combined with Evarts' data to better characterize these volcanics (Figure 48). Phillips submitted samples for major oxides and trace element analysis to Peter Hooper at Washington State University; while Evarts' samples were analyzed by the U. S. Geological Survey geochemistry lab. All geochemical sample locations were plotted and compared to thin sectioned samples studied by this author (Plate I). Twenty-one thin sections of the Grays River volcanics in the thesis area were prepared for petrographic analysis. Thin sectioned samples were collected across the field area to characterize the texture and mineralogical variations of these flows. Three dikes were also studied petrographically to determine their compositional and textural relationship to the overlying subaerial flows.

Most samples collected by these previous researchers were from the southern and eastern part of Bebe Mountain. Other sample locations include the northwestern part of Bebe Mountain (Plate I). Most of Phillips et al. (1989) samples were from a 5-km stretch along Vader-Longview Highway 411, on the western flank of Bebe Mountain (Plate I) and reflect subaerial flows of the upper part of the Grays River volcanics. However, three samples (#38, #27 and #42; Phillips et al., 1989; Plate I) were from western Pumphrey Mountain and represent subaerial flows of the middle part of the Grays River volcanics that form Bebe Mountain (Plate I). Phillips et al. (1989) also sampled one subaerial flow

in the southern part of Bebe Mountain (#54, Plate 1) that came from the lower to middle flows that form Bebe Mountain (Appendix V). Russ Evarts also analyzed basalt samples from the southern Bebe Mountain area (F50, F51, and F53; Plate I and Appendix V). Both sets of data indicate the middle to upper flows of the Grays River volcanics in the thesis area have a similar geochemistry.

The 21 Grays River volcanics samples from the study area geochemically classify as subalkaline tholeiitic basalts. This classification was determined using the IUGS (International Union of Geologic Scientists) igneous rock classification scheme that plots total alkalies ($K_2O + Na_2O$) versus silica (Le Bas et al., 1986) (Figure 48A). Additionally, these subaerial flows all fall in the subalkaline basalt field of Irvine and Barager (1971); dashed line overlain on IUGS plot to delineate alkaline vs. subalkaline fields (Figure 48A). Finally, an iron enrichment diagram of Miyashiro (1974) was used to determine that these basalt flows are all tholeiitic in composition (Figure 48B).

All 21 Bebe Mountain samples from the map area are within the field outlined as Grays River volcanics by Phillips (1987) (Figure 48). This is based on geochemical analysis of the freshest samples from massive flow centers (Phillips, 1987; Evarts, personal communications, 1995). The geochemical data indicate that the Grays River basalts possess distinctive major oxide concentrations as compared to other volcanic units of the region (e.g., Goble, Northcraft, Siletz, Crescent Volcanics) (Phillips, 1987; Phillips et al., 1989; Rarey, 1985). Flows are enriched in P_2O_5 , total alkalies ($Na_2O + K_2O$), and especially TiO_2 (3.24 % average). The trace elements Rb, Nb, Sr, Ba, and Zr show enrichment of 2 to 10 times that of mid-ocean ridge basal (MORB) concentrations (Phillips et al., 1989). This distinctive enrichment of the Gray River basaltic lavas allows discrimination from other volcanic sequences. Additionally, the Grays River volcanics has a dramatically lower Cu concentration (59 ppm) than flows of

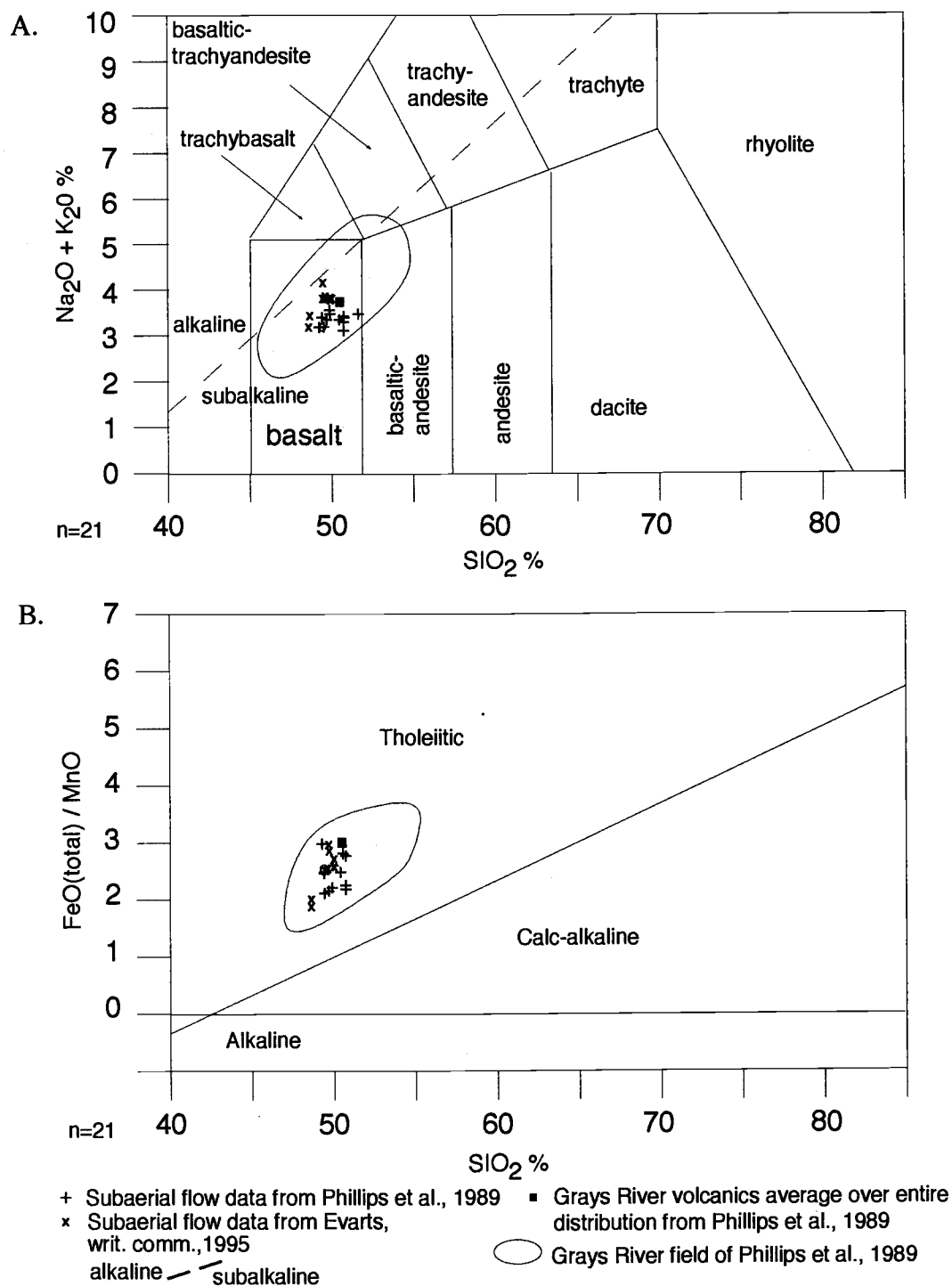


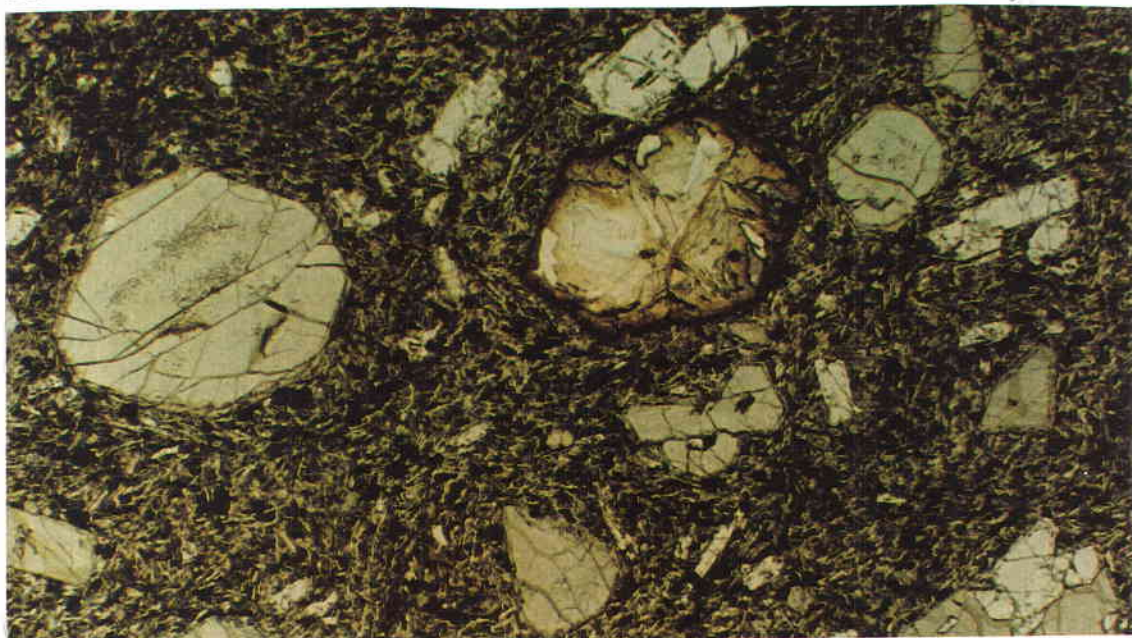
Figure 48. (A) Basalts of the Grays River volcanics from the thesis area plotted on a total alkali vs. SiO₂ (TAS) diagram. This is based on the IUGS classification scheme of Le Bas et al. (1986). Note dotted line separating alkaline vs. subalkaline volcanic rocks from Irvine and Barager's (1971) classification scheme. (B) Iron enrichment diagram of Miyashiro (1974). Note all samples plot as subalkaline tholeiitic basalt.

the Goble Volcanics (251 ppm) (Phillips et al., 1989). Finally, the Grays River volcanic flows are more mafic (lower SiO₂) than other early western Cascade arc volcanic units (e.g., Goble Volcanics or Northcraft Formation) of similar stratigraphic position (Phillips et al., 1989).

Petrologic analysis of the Grays River volcanics indicates that there are three petrographic basaltic textures from the subaerial flows in this area. These textures are: (1) a lower olivine-bearing (picritic) basalt, (2) a middle intersertal to plagioclase glomerophyric unit, and (3) an upper aphyric pilotaxitic intra-canyon flow unit. In general, all flows have phenocrysts (2%-5%) of olivine, plagioclase, and titaniferous augite, as well as, magnetite, ilmenite, and alteration products of olivine (e.g., iddingsite and chlorophaeite). The groundmass is typically intersertal to intergranular with abundant opaque ilmenite, microlites of plagioclase, clinopyroxene, and dark brown clay altered devitrified glass.

The lowermost flows from Bebe and Abernathy mountains are picritic, characterized by large olivine phenocrysts in an intersertal finely crystalline groundmass of plagioclase, clinopyroxene, and opaques (ilmenite and magnetite). Plagioclase microlites have a pilotaxitic flow texture. Sample CP-94-196 from southeastern Abernathy Mountain (dated at 38.6 Ma) contains large euhedral olivine phenocrysts which comprise 15% of the rock (Figure 49). Olivine composition ranges from Fo₇₈ to Fo₈₈ based on petrographic analysis using 2V and optical sign of ten phenocrysts in sample CP-95-196. This narrow composition range of olivine, restricted to relative magnesian compositions, is characteristic of tholeiitic basalts (Philpotts, 1990). Olivine phenocrysts average 1 mm in diameter but some are up to 3 mm and some contain plagioclase inclusions. Albite-twinned plagioclase phenocrysts are also present in subordinate amounts (3-5%) and are 1 mm to 0.5 mm in diameter. Alteration products include the yellow/green mineral chlorophaeite, green serpentine, and reddish-brown iddingsite; all derived from the

A.



B.



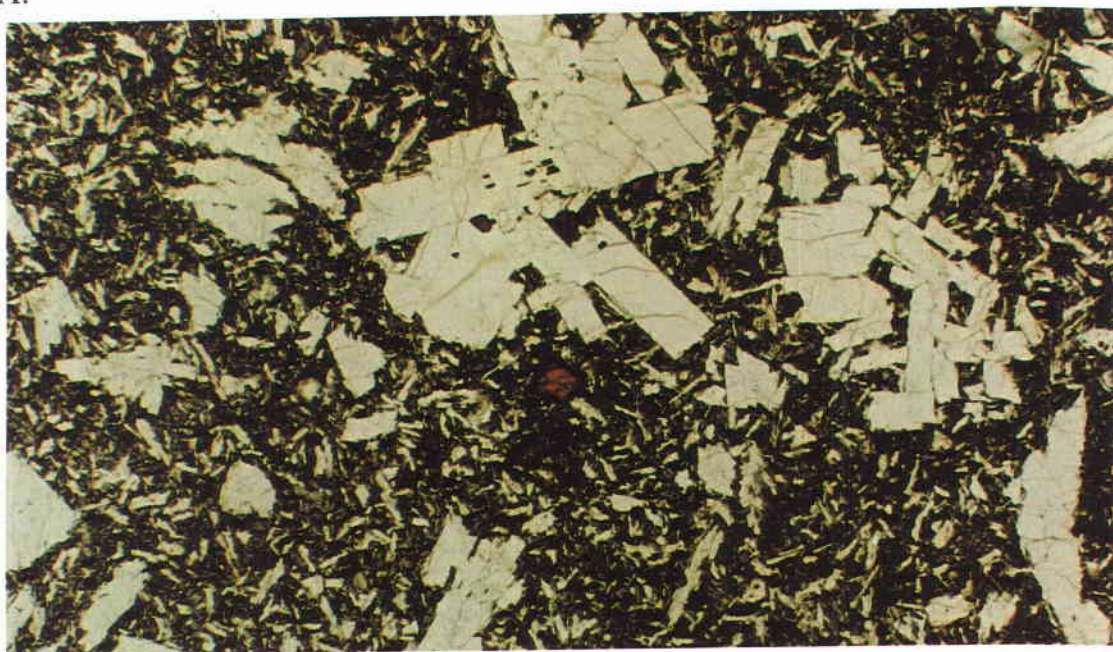
1mm 2mm

Figure 49. Photomicrograph of porphyritic olivine tholeiitic basalt flow from lower part of the Grays River volcanics (CP-95-196, Plate I). Note large olivine phenocrysts in an intersertal textured groundmass composed of plagioclase, clinopyroxene, and opaques. One olivine phenocryst has almost completely altered to iddingsite and chlorophaeite. (A. Plane-polarized light, B. Crossed nichols)

alteration of olivine. One other olivine-bearing tholeiitic basalt flow occurs in the lower part of the younger Grays River volcanics locality CP-94-76, northwestern Bebe Mountain (Plate I). Olivine phenocrysts in this lower flow are almost completely altered to iddingsite while the clinopyroxene is fresh and unaltered. Some plagioclase glomerocryst are present in minor amounts. Plagioclase microlites are surrounded by finely crystalline intergranular groundmass composed of titanomagnetite (deep purple), opaques including ilmenite (15% of groundmass), and the alteration product iddingsite.

Subaerial flows from the middle part of this volcanic unit are characterized by distinctive plagioclase glomerocrysts and olivine and plagioclase phenocrysts (Figure 50). Sample CP-94-14 from the lower middle part of the Grays River volcanics at Bebe Mountain contains 10% clinopyroxene (augite) and olivine phenocrysts in an intergranular to intersertal textured groundmass (Plate I). Some olivine and plagioclase cumulo-crysts are present and plagioclase microlites are flow aligned; displaying a pilotaxitic texture. Nearly 15% of basalt sample CP-94-68L is composed of plagioclase glomerocrysts in an intersertal groundmass of plagioclase microlites, brown devitrified glass, titaniferous augite, opaques, altered clinopyroxene, and iddingsite. A thick basalt dike intruding sandstone of Cowlitz unit 1 west of Bebe Mountain (sample CP-95-198, Plate I) contains similar plagioclase glomerocrysts (30%) in an intersertal plagioclase groundmass identical to that of a subaerial flow sample from locality CP-94-68L (Figure 50). From the southern part of Bebe Mountain, another basalt flow (sample CP-94-3) is composed of plagioclase glomerocrysts and altered olivine phenocrysts in a seriate to intersertal groundmass of plagioclase and clinopyroxene. Alteration products include iddingsite (10%) and sparry calcite. Basalt sample CP-94-68du is a finely crystalline and aphyric flow that displays a intergranular pilotaxitic flow texture of well-aligned plagioclase microlites surrounded by opaques (high TiO₂ ilmenite) and titanomagnetite. This flow from the upper middle part of the Grays River volcanics pile at Bebe Mountain was ³⁹Ar/⁴⁰Ar dated at 37.4 Ma. A similar

A.



B.



1mm 2mm

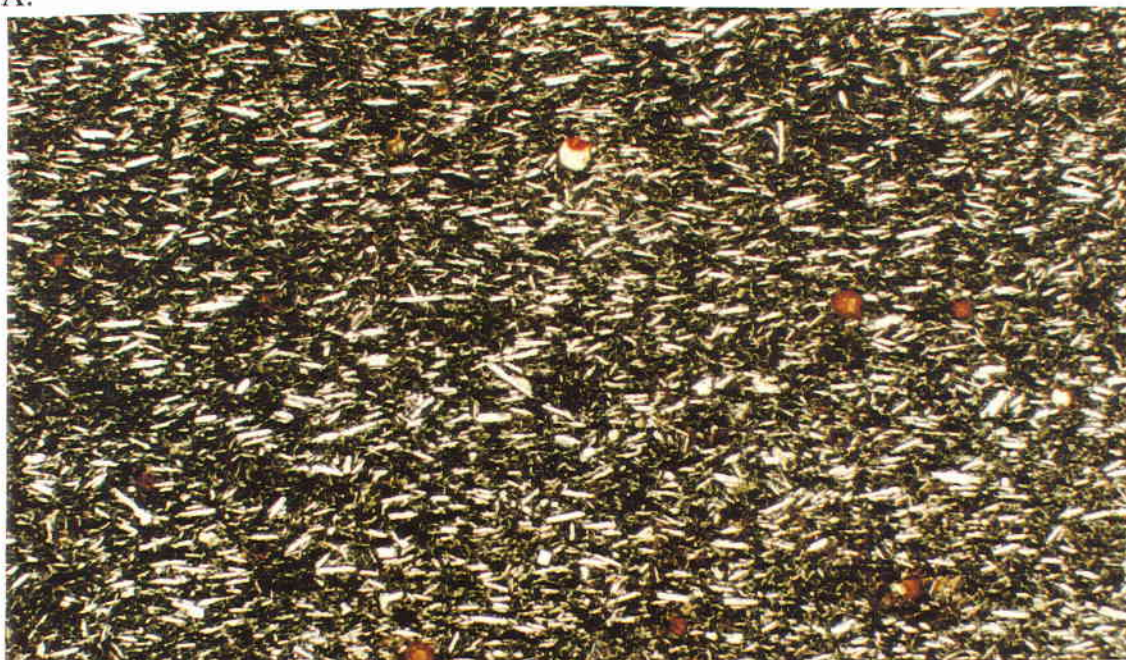
Figure 50. Photomicrograph of plagioclase glomerophyric basalt from a Grays River dike to the west of Bebe Mountain (CP-95-198, Plate I). This sample is very similar to the middle flows of the Grays River volcanics at Bebe Mountain. Note intersertal textured groundmass containing clinopyroxene, opaques magnetite/ilmenite, and iddingsite alteration and large randomly oriented glomerocrysts of plagioclase. (A. Plane-polarized light, B. Crossed nichols)

flow (sample CP-94-4, Plate I) contains a few scattered olivine phenocrysts and plagioclase glomerocrysts (3-5%). Sample CP-95-201 from Abernathy Mountain has an intersertal to micro-seriate texture and is compositionally and texturally similar to subaerial basalt flow samples collected from the top of Bebe Mountain (CP-94-12, -27, and -4; Plate I).

The uppermost flows of the Grays River volcanics at Bebe Mountain are dominantly aphyric and all display a distinctive pilotaxitic texture (Figure 51). These flows are visible along Olequa Creek and the Vader-Castle Rock Highway 411. One subaerial flow (sample CP-95-132) from south of the town of Vader is a finely crystalline intergranular olivine basalt similar to flows at the top of Bebe Mountain (e.g., samples CP-94-69 and CP-94-68du, Plate I). Up section, one subaerial basalt flow was $^{39}\text{Ar}/^{40}\text{Ar}$ dated at 36.8 Ma (sample CP-94-138) and has a pilotaxitic to micro-seriate texture with aligned plagioclase microlites surrounded by devitrified brown glass, plagioclase, clinopyroxene and small vesicles filled with calcite (Figure 51). The groundmass of a subaerial basalt (sample CP-94-140), along lower Olequa Creek, is identical with subaerial flows on the top of Bebe Mountain (e.g., sample CP-94-27) but lacks phenocrysts of olivine and plagioclase. Other subaerial basalt flows (e.g., samples CP-95-142 to -146) along the Cowlitz River, all have similar seriate intergranular and intersertal texture and composition. Titanogaugite, clinopyroxene, and opaque ilmenite surround aligned plagioclase microlites that are up to 1/4 mm in length. A few olivine and plagioclase phenocrysts are present.

Primary magma of intraplate volcanic provinces (i.e., hot spots) has a higher concentration of incompatible trace elements relative to MORB. This difference is the result of having a deeper mantle source that is not depleted as much as shallower mantle sources under mid-ocean ridges (Philpotts, 1990). This fact, when compared to the higher concentration of incompatible trace elements (Ti, K, Rb, Sr, Zr, and Ba) in the Grays

A.



B.

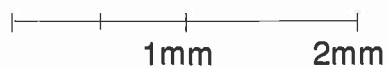
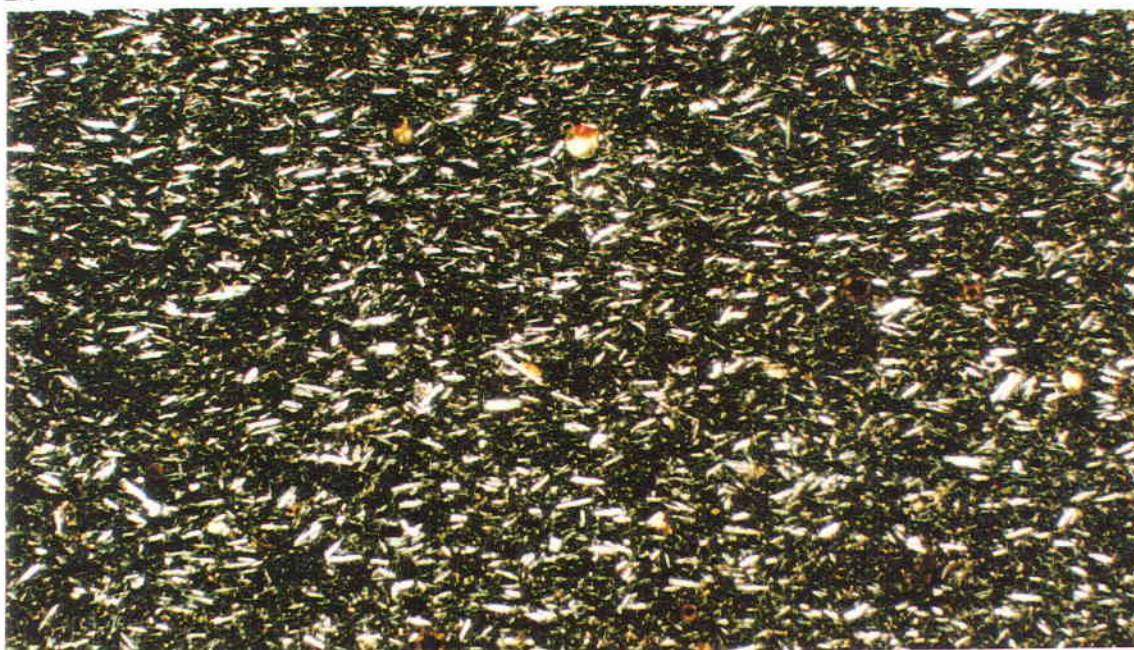


Figure 51. Photomicrograph of subaerial Grays River basalt displaying pilotaxitic flow texture (sample CP-94-138, $\text{Ar}^{39}/\text{Ar}^{40}$ dated at 36.8 Ma, Plate I) from the upper flows of the Grays River volcanics. Note aligned plagioclase microlites surrounded by an intersertal groundmass of dark devitrified glass, clinopyroxene, and opaque ilmenite. (A. Plane-polarized light, B. Crossed nichols)

River volcanics, indicates the Grays River volcanics are of an intraplate volcanic origin. The parental magma of intra-plate volcanic province is thought to be picritic basalt (Philpotts, 1990). The basal flows of the Grays River volcanics in this area are olivine-bearing tholeiites that may have been derived from just such a picritic basaltic parental magma. Additionally, tholeiitic basalts are formed first in the development of an intra-plate volcanic provenance and olivine is one of the earliest crystallizing minerals in these tholeiitic magmas (Philpotts, 1990). The Grays River volcanics of Bebe Mountain differ from the older Grays River volcanics to the west and the older Tillamook Volcanics to the south in that they are more olivine-rich and less fractionated than Tillamook volcanics that contain basaltic andesite and dacite (Mumford, 1988; Safley, 1989).

In conclusion, the flows in the lower part of the Grays River volcanics that form Bebe and Abernathy mountains may have been derived from primary mantle-derived magma injected into the southwest Washington rifted forearc initiating a younger Grays River volcanics eruptive episode that is separate from the older main pile of Grays River volcanics to the west (i.e., Willapa Hills of Wells, 1981). As this magmatic source fractionated and was tapped, plagioclase (labradorite) crystallizing in a magma chamber beneath Bebe Mountain formed glomerocrysts that were incorporated into the middle flows and dikes of Grays River volcanics at Bebe Mountain. The upper Grays River volcanics flows at Bebe Mountain are generally aphyric pilotaxitic tholeiitic high TiO_2 basalts with a primitive mantle-derived chemistry of an intra-plate volcanic provenance perhaps related to the waning phases of the Yellowstone Hot Spot that is thought to have formed the chemically similar high TiO_2 Tillamook Volcanics (Mumford, 1988; Duncan, 1982). These high TiO_2 tholeiitic basalt flows are from the early stage of magmatic differentiation. Later development of an intra-plate provenance results in formation of alkali basalt that is followed by differentiation resulting in more silicic products (e.g., rhyolite flows), all of which are absent in the Grays River flows of Bebe Mountain but

present in the upper Tillamook Volcanics and found as float in the older Grays River volcanics (Wells, personal communications, 1998). Perhaps the Grays River volcanics at Bebe and Abernathy mountains represent the last stage of tholeiitic subalkaline volcanism in this rifted forearc province, before the initial stages of calc-alkaline volcanism of the western Cascades (e. g., Goble Volcanics), as the subduction zone differentiated, generating magma farther east as the depth and angle of plate subduction changed (Niem, written communications, 1998).

MIDDLE EOCENE TO OLIGOCENE REGIONAL CORRELATION AND STRATIGRAPHIC RELATIONSHIPS IN SOUTHWEST WASHINGTON AND NORTHWEST OREGON

One of the goals of this study was to correlate regionally the Cowlitz Formation in the type area and associated middle to upper Eocene units to the Cowlitz Formation and associated units in northwest Oregon. The regional stratigraphic relationship of the middle to upper Eocene and lower Oligocene sedimentary and volcanic units in northwest Oregon and southwest Washington is complicated by complex sedimentary facies relationships and by subdivision of the basin by active basaltic volcanic edifices (lower Grays River volcanics). In northwest Oregon, delta-front sandstone, mapped as the upper Eocene Cowlitz Formation, unconformably overlies the middle Eocene Tillamook Volcanics and slope mudstone and shelf sandstone and volcanic conglomerate of the Hamlet formation (Niem et al., 1992; Niem and Niem, 1985; Robertson, 1997) (Figure 3). Foraminiferal assemblages from this study and Rau (1958) suggest the McIntosh Formation in this thesis area in southwest Washington is lower Narizian in age or about 44 Ma to at least 41 Ma (approximate age of the Tillamook Volcanics). Thus, the middle Eocene McIntosh Formation in southwest Washington is partially correlative with the Yamhill and Hamlet formations and Tillamook Volcanics of northwest Oregon (Figures 3 and 52). The upper McIntosh sandstone member unit in southwest Washington is a lithologic correlative of the arkosic micaceous shelfal sandstone of the Sunset Highway member of the Hamlet formation in northwest Oregon. This conclusion is based on biostratigraphic and lithostratigraphic correlation and stratigraphic position.

The type Cowlitz Formation in the thesis area ranges from approximately 41 to 38.5 Ma based on foram and molluscan biostratigraphic age determination (e.g., upper Narizian) and $^{39}\text{Ar}/^{40}\text{Ar}$ dates. The Grays River volcanics radiometrically dated as 38.6 Ma in southwest Washington unconformably overlies the type Cowlitz Formation in this

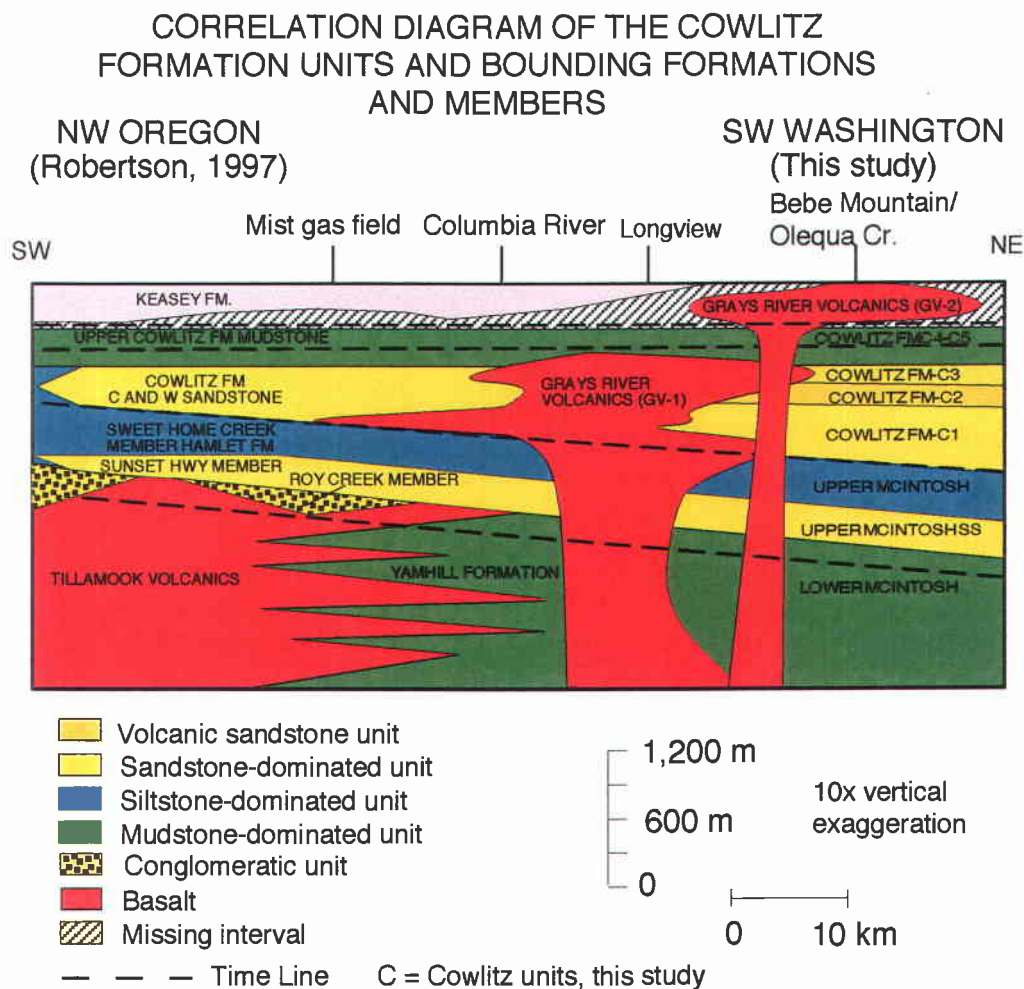


Figure 52. Correlation diagram of the Eocene Cowlitz Formation units and bounding formations between northwest Oregon and southwest Washington (from Robertson, 1997 and from this study).

study area. It is slightly older and interfingers with the Cowlitz Formation in the Longview area of southwest Washington (McCutcheon, personal communications, 1998) and in northwest Oregon in the subsurface at the Mist Gas Field (Robertson, 1997; Kennitz, personal communications, 1996) (Figure 52). The geochemically and petrologically identical high TiO₂ tholeiitic Tillamook Volcanics and Grays River volcanics formed at slightly different times and magneto-polarity events (Figure 41) and appear to be separate shield volcanoes (Kennitz, personal communications, 1996). The (late Narizian) Cowlitz Formation in Oregon and southwest Washington is probably the same correlative deltaic unit sandwiched between the Tillamook and upper Grays River volcanics (Figure 52). The Cowlitz is 1,240 m thick at the type area whereas the Cowlitz Formation in northwest Oregon is maximum of 700 m thick and not all subunits are lithologically correlative due to pinchout and facies changes.

The lowermost mudstone of the McIntosh Formation biostratigraphically correlates with the undifferentiated Yamhill Formation. This interpretation is based on bathyal to outer shelf foraminiferal assemblages identified by W. Rau (1958) from the lower McIntosh Formation (section locations 1B and 1D, on Plates I and II) that are assigned to the *Bulimina* cf. *Jacksonensis* zone of the upper Ulatisian to lower Narizian stages, the upper age of the zone is approximately 44 Ma based on Berggren's et al. (1995) time scale (McDougall, written communications, 1997). Additionally, in northwest Oregon, Niem and others (1992) reported a total-fusion ³⁹Ar/⁴⁰Ar radiometric age of 42.5 Ma for a flow near the top of the Tillamook Volcanics. Coccoliths collected from a mudstone interbedded with the lower subaqueous Tillamook Volcanics are assigned to the *Discoaster bifax* subzone CP 14a of Bukry (1973) (Snively and others, 1993), which ranges from 44 to 40.3 Ma (McDougall, 1997). Rarey (1985) reported CP14a zone coccolith assemblages identified by Bukry in the lower part of the Sweet Home Creek mudstone of the Hamlet Formation (lower Narizian). To the west, the lowermost part of the bathyal Fort Creek

member (Moothart, 1992) of the McIntosh Formation, contains Ulatisian to lower Narizian foraminifera. Moothart's overlying deep marine mudstone unit (Lebam member of the McIntosh) contains foraminifera that are mostly lower Narizian age, with upper Narizian foraminifera occurring only in the uppermost 150 m of the Lebam member Moothart (1992). This biostratigraphic age relationship indicates the lower McIntosh-Yamhill sea was a broad and connected outer shelf-slope system in southwest Washington and northwest Oregon during the middle Eocene.

The arkosic to lithic arkosic basal sandstone unit of the upper McIntosh member (informal) lithologically and stratigraphically correlates with the Sunset Highway member (informal) of the Hamlet formation in northwest Oregon (Figure 52). The shallow marine arkosic sandstone facies of the Sunset Highway Creek member have been correlated with a thin sequence of deep-water turbidite sandstone and mudstone facies in the Sweet Home Creek member farther west in northwestern Oregon (Mumford, 1988). Similarly, the upper McIntosh Formation arkosic sandstone unit of Wells (1981) may correlate with the arkosic turbidite sandstone of the Fort Creek member (informal) of the McIntosh Formation farther to the west in southwest Washington (Moothart, 1992). However, biostratigraphy and lithology indicate the quartzite and volcanic conglomerates of the Fort Creek member of the McIntosh Formation are older.

The upper McIntosh siltstone member in this study area, in part, correlates with the Sweet Home Creek member of the Hamlet formation of northwest Oregon (Figure 52). The Cowlitz C & W sandstone thins to the west into the upper Sweet Home Creek mudstone (Mumford, 1988). A 70-m thick sequence of thin-bedded deep-marine mudstone and micaceous, arkosic sandstone turbidites near the top of the Sweet Home Creek member (informal) of the Hamlet formation (Berkman, 1990, Robertson, 1997) may correlate to the coarsening-upwards outer shelfal sandstone-rich sequences near the top of the McIntosh Formation in this study area (Plate II). Planktonic coccolith

assemblages restrict the age for the Sweet Home Creek member of the Hamlet formation to subzone CP14a (Robertson, 1997) (Figure 3). Foraminiferal data indicate that the Sweet Home Creek was deposited during the upper Narizian. Weldon Rau (1958) also assigned strata of the Upper McIntosh Formation exposed along Stillwater Creek to the lower to middle Narizian stage. Rau restricted the upper 180 m of the formation to the upper Narizian. Additionally, Yett (1979) determined that the upper part of the upper McIntosh Formation (Stillwater Creek Member of Henriksen, 1956) and all the Cowlitz Formation (Olequa Creek Member) are late Narizian in age (late middle Eocene).

The lower and upper coal-bearing arkosic sandstone units 1 and 3 and the volcanic sandstone unit 2 of the deltaic Cowlitz Formation of the type section in Olequa and Stillwater creeks in southwest Washington (this study) appear to grade laterally into the largely wave-dominated, micaceous, arkosic shelf sandstone of the C and W sandstone of the Cowlitz Formation in northwest Oregon which also contains some thinner coal beds (Armentrout et al., 1983; Rarey, 1986; Berkman, 1990; Farr, 1989, Niem et. al., 1992). The overlying deep-water mudstone of the Cowlitz Formation (upper Cowlitz mudstone member) in northwestern Oregon in the subsurface in the Mist Gas Field (52 km to the south-southwest of the study area) probably correlates with outer shelfal glauconitic mudstones of unit 4 and deep-marine laminated micaceous siltstone unit 5 of the type Cowlitz Formation along Olequa Creek in southwest Washington (Robertson, 1997; this study) (Figure 52). The upper Cowlitz mudstone at Mist contains thin turbidites and slump zones, but large thicker chaotic mudstone conglomerate and sandstone channels (unit 5) are not present at Mist because this area was farther from incised channels formed during lowstand. In southwest Washington, near Coal Creek and the city of Longview, the Cowlitz Formation is interbedded with a basalt flow (Grays River volcanics) that has whole-rock plateau age of 40.3 ± 0.3 Ma (Irving et al., 1996). This basalt flow is, in part, correlative with the lower or older part of the Grays River volcanics (GV-1 on Figure 52)

interbedded with the Cowlitz Formation in the subsurface of northwest Oregon (Kennitz, 1996; Robertson, 1997) and is one chronostratigraphic marker for correlating the C and W sandstone of the Cowlitz Formation in Oregon with Cowlitz unit 1 in the type section in southwest Washington (Figures 2 and 3).

On the basis of stratigraphic position and lithologies elsewhere in southwest Washington, the coal-bearing, tide-influenced coastal plain and shallow-marine facies of the Skookumchuck Formation that crops out in the Centralia area (Flores and Johnson, 1995; Johnson, 1994; Snively et al., 1958), 40 km to the north, may be correlative with the tide-influenced, coal-bearing and delta front arkosic sandstone facies (units 1 to 3) of the type Cowlitz Formation described in this study (Figures 2 and 3). The middle Eocene Skookumchuck Formation attains a maximum thickness of 1,166 m in the Centralia-Chehalis area (Snively et al., 1958). An upper coal bed (11.6 m thick) in the tide-dominated marginal marine strata and arkosic, micaceous sandstone in the coal-rich 283-m thick unit 1B (section 7F to 8C) in the study area probably correlate to the 30-m thick lower coal zone of the Skookumchuck Formation of Flores and Johnson (1995). My interpretation of the stratigraphic sections from Flores and Johnson (1995) suggests the coal-bearing facies unit 1B of the type Cowlitz Formation and coal seams in the lower 113 m of the upper coal group of the Skookumchuck Formation are laterally equivalent based upon lithologic similarities and stratigraphic position. Also, marine unit 2 of the type Cowlitz Formation in Olequa Creek probably correlates with the middle siliciclastic interval in the Centralia mine of Flores and Johnson (1995). The 20- to 30-m thick middle coal zone and 15-m thick upper coal zone of the Skookumchuck Formation may correlate with the coal-bearing intervals in unit 3 of the type Cowlitz Formation in Olequa Creek. In addition, a zircon fission-track age of 39.2 ± 2.7 Ma determined by Brandon and Vance (1992) for a tuff within the coals of the Skookumchuck Formation and an $^{39}\text{Ar}/^{40}\text{Ar}$ age

of 38.9 ± 0.1 Ma for a 1.5-m thick tuff (Marker 3A) in unit 3 of the type Cowlitz Formation (Plate II) (Irving et al., 1996) further correlate these formations to almost the same time-stratigraphic interval.

The regional unconformity at the base of the Grays River volcanics (under Bebe Mountain) and the unconformity underlying the Toutle Formation (in Olequa Creek) may be two separate unconformities (Figure 53A). The uplift and erosional event that formed the older, late Eocene unconformity (regionally identified by Armentrout, 1987) was relatively short-lived and was followed by deposition of the upper Grays River volcanics and the basal Grays River sedimentary sequence in the Vader-Ryderwood-Bebe Mountain area. No record of deposition is preserved in the upper Olequa Creek area (Figure 53A) due to Oligocene uplift and erosion (e.g., the 2 unconformities merge in Olequa Creek). Up to six million years later, a second uplift and erosional event eroded down to the top of the Cowlitz Formation in the Olequa Creek area (e.g., down to unit 5) and was followed by deposition of the Toutle Formation in the Oligocene (e.g., based 32 Ma $^{39}\text{Ar}/^{40}\text{Ar}$ age date on hornblende lapilli tuff in basal Toutle Formation from this study). The regional extent of this unconformity and its precise age in Olequa Creek (e.g., date Cowlitz unit 5) is needed to determine whether this two unconformity hypothesis is correct.

The alternative hypothesis is that one unconformity formed at 38.5 Ma and was only locally covered and preserved by subaerial valley-filling flows of the Gray River volcanics in the Vader-Ryderwood-Bebe Mtn. area (Figure 53B). This unconformity was then exposed for six million years before it was covered by the 32 m. y. old Toutle Formation in the upper Olequa Creek area. The confirmation of this one unconformity hypothesis is difficult to determine because there would be no rock record to date. However, it is hard to imagine a six million-year period where no erosion or deposition took place in this active convergent margin and the two-erosional-events hypothesis is favored by this author.

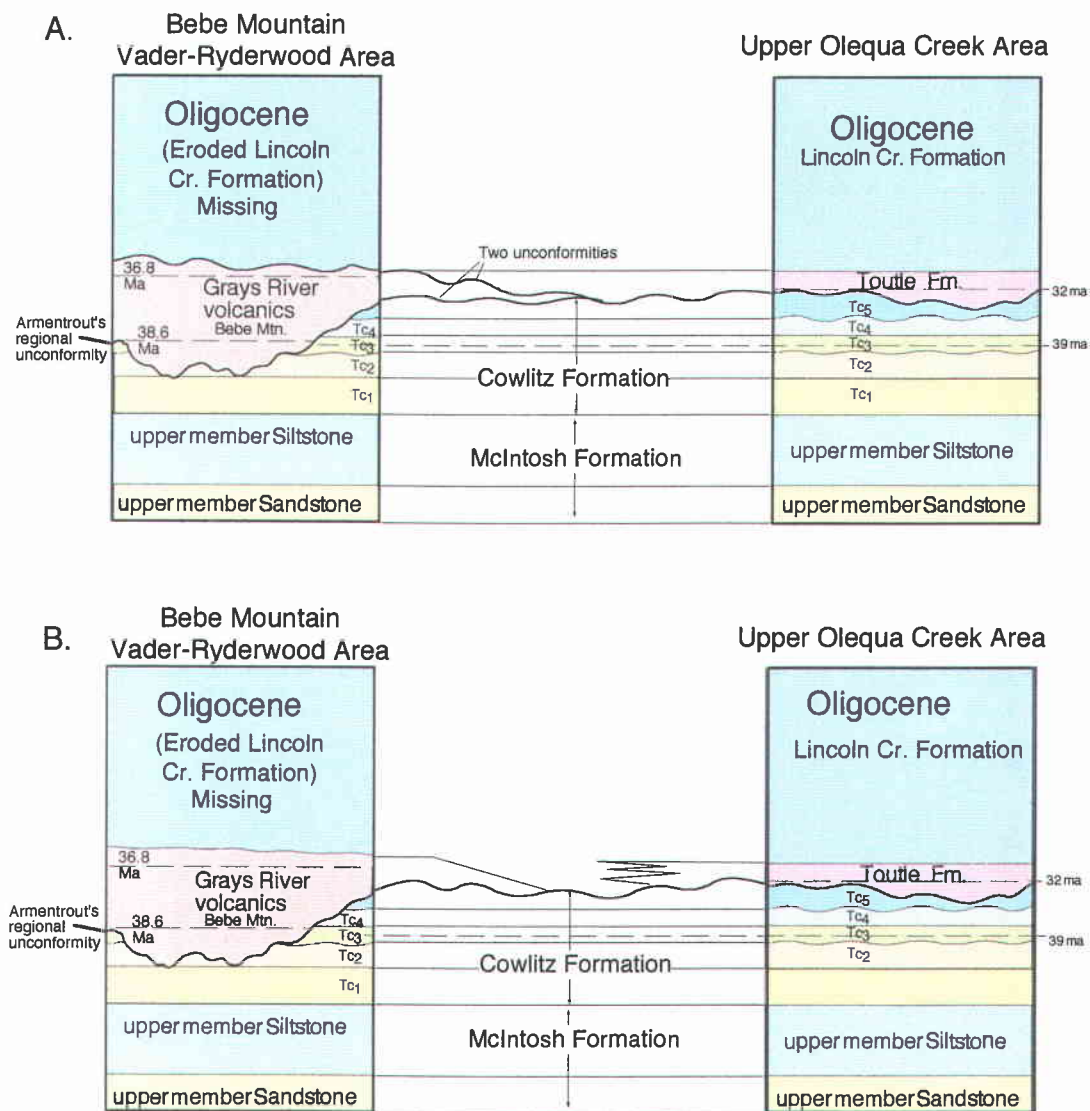


Figure 53. Two hypotheses for the unconformable relationship between the Cowlitz Formation and the Grays River volcanics and between the Cowlitz and Toutle formations in the Bebe Mountain area and in Olequa Creek. (A) two erosional events and (B) one erosional event.

STRUCTURAL GEOLOGY

REGIONAL STRUCTURE

The major tectonic feature of southwest Washington is the large volcanic basement high that forms the Willapa Hills uplift, located to the west and northwest of this study area (Figure 45). The oldest rock exposed in this uplift is oceanic crust of the lower to middle Eocene submarine basalts and basaltic breccias of the Crescent Formation. This volcanic high forms a gravity high distinguishable from the adjacent sediment-filled basinal lows to the southwest (Astoria basin) and northeast (Chehalis basin). This oceanic crust was effected during the lower middle Eocene by an episode of clockwise rotation of small fault-bounded blocks that occurred in a dextral transpressive regime. This tectonic episode initiated the Willapa Hills uplift (Wells and Coe, 1985). After this small block rotation, the rate of Farallon-North America plate convergence decreased and there was a westward migration of the subduction zone (Wells, 1984; Armentrout, 1987). This plate-boundary relocation and shear rotation event defines the first major sequence boundary unconformity preserved in the geologic record of southwest Washington (Armentrout, 1987).

During the middle Eocene, rapid subsidence of the volcanic basement created a 640-kilometer long forearc or marginal basin extending from the Klamath Mountains of southwestern Oregon to southern Vancouver Island, Canada (Niem and Niem, 1984; Niem et al., 1992b). Changes in plate motion resulted in strong oblique subduction that initiated development of a north-northwest and north-northeast striking conjugate fault system after deposition of the middle Eocene Cowlitz Formation in southwest Washington (Wells and Coe, 1985; Armentrout, 1987). North-northwest-trending right-lateral fault zones bordering early to middle Eocene oceanic crust basement blocks (Crescent Formation) in the Willapa Hills may have set up dextral shear couple with smaller

northwest-trending left-lateral faults accommodated the shear and thus, the clockwise rotation of small crustal blocks (Well and Coe, 1985). The driving force of this dextral shear resulted from the partial coupling of the subducting Farallon oceanic plate and the over riding North American plate (Wells, 1989).

LOCAL STRUCTURE

The thesis area is located on the eastern flank of the arcuate Willapa Hills uplift and on the southern part of the Chehalis basin (Figure 45). Most strata dip regionally 10° to 15° to the east, away from the Crescent Formation basement core of the Willapa Hills uplift. Anomalously steep (e.g., $>30^{\circ}$) attitudes generally reflect proximity to faults, drag along fault, local slumps, or large landslides. Faults in the Coast Range of Washington and Oregon are largely concealed by thick vegetation and extensive weathering. However, numerous faults were mapped in this study area (Plate I) based on (1) repetition or cutout of stratigraphic marker beds, (2) juxtaposition of differing stratigraphic units and abrupt lithology changes (e.g., sandstone to basalt along strike), (3) shear zones and fault planes exposed in stream beds, roadcuts, and quarries, (4) anomalous structural attitude of strata, and (5) grouping of consistent strikes and dips into domains. Motion on the faults was determined by measurement of slickensides on fault planes, by using dikes as piercing points (e.g., see fault IP and fault on Plate I), and continuation of regional thoroughgoing faults mapped by Wells (1981).

The fault pattern in the study area (Plate I) generally consists of a series of sub-parallel: (1) north-northwest trending right-lateral oblique-slip faults, (2) shorter northwest-trending left-lateral oblique and normal faults, (3) a few older north-northeast-trending right-lateral strike-slip faults, and (4) northeast-trending left-lateral faults. A broad south-southeast plunging anticline (Arkansas anticline) separates the outcrops of Gray Rivers volcanics on Bebe Mountain from Abernathy Mountain. This anticline folded

the McIntosh and Cowlitz formations, as well as, the overlying Grays River volcanics (Plate I). Wells (1981) defined this anticlinal axis in a U. S. Geological Survey open file map of the area. I found the anticline axis to be much more complexly faulted and difficult to define (Plate I).

North-northwest-trending right-lateral, oblique-slip faults are generally high-angle (60° to vertical) and are the most continuous faults in the field area (Plate I). The IP Land fault that was mapped along Stillwater Creek and in the surrounding area repeats > 240 m of stratigraphic section (locations 3D1 to 4A, Plate I). Many of these north-northwest trending faults have displaced the Grays River volcanics against the Cowlitz Formation. The west Pumphrey Mountain fault is one such major right-lateral strike-slip fault (Plate I). The Bebe Mountain fault has over 800 m of right-lateral displacement and 60 m of vertical offset (west side down). Oblique slip motion was determined by measuring slickensides ($\sim 10^\circ$ from horizontal) on fault planes in basalt quarries and displacement of sedimentary units and by using dikes as piercing points (e.g., see fault IP land fault on Plate I). Additionally, other north-northwest-trending faults, west and south outside of the study area, have displaced middle Miocene Columbia River Basalts (Wells, 1981). Therefore, many of these faults were active in the post-middle Miocene. However, an unsheared Grays River basalt dike intrudes a north-northwest trending fault along Stillwater Creek has indicates that some faults were active as early as latest middle Eocene (e. g., Cougar Flat fault, measured section location 7G, Plate I). Thus, the north-northwest-trending faults were active in the late Eocene and reactivated in the middle Miocene (e. g., Bebe Mountain, Baxter Cr., West Pumphrey Mtn., and the Abernathy Mtn. faults; Plate I).

Numerous sub-parallel, northwest-trending left-lateral and normal faults are bounded between the major north-northwest-trending right lateral faults. These northwest-trending faults are no longer than 2 km in length (Plate I). The strike slip component of

these faults appears not to exceed 1/2 km; for instance, the Farm fault along Stillwater Creek has a left-lateral displacement of 350 m based on displacement of the upper McIntosh sandstone. Four closely spaced northwest-trending faults along upper Olequa Creek have 10 to 65 m of throw as determined by stratigraphic repetition of Cowlitz Formation units 2 and 3 (e. g., Brim Cr. fault, Plate I). Many northwest-trending faults are intruded by Grays River basalt dikes. South of Ryderwood, a "dike swarm" was mapped (Plate I). A perpendicular extensional tectonic direction most likely allowed these dikes to intrude these fault zones. These intrusions indicate some of the northwest-trending faults were active after deposition of the Cowlitz Formation but before Grays River volcanics eruption (latest middle Eocene). These extensional faults are sub-parallel to the broad Arkansas anticline and most likely pre-date the compression event that formed the Arkansas anticline.

North-northeast and northeast-trending faults appear to be both older structures that are truncated by late Eocene north-northwest trending faults and reactivated younger faults that post-date the late Eocene Grays River volcanics. The Stillwater Creek fault is an older and possibly clockwise-rotated northeast-trending right-lateral oblique slip fault with many meters of vertical throw (Plate I). This fault, which juxtaposes upper McIntosh sandstone against Cowlitz unit, has been dismembered by numerous northwest- and north-northwest-trending faults. Additionally, one basalt dike (presumably Grays River volcanics) mapped by Wells (1981) intrudes this fault north of Stillwater Creek. Several other northeast-trending, right-lateral and normal faults were reactivated and have offset the Grays River volcanics with left-lateral displacement along the lower reaches of Olequa Creek (Plate I). One of these reactivated faults in the lower reaches of Olequa Creek has 50 m of throw and approximately 300 m of left-lateral displacement (Vader fault). Five hundred meters of left-lateral displacement on the Sewage Fault in Stillwater Creek resulted in 40 m of missing strata of McIntosh Formation in measured sections 4A to 5A

(Plate I). These northeast-trending faults could represent antithetic en echelon faults or Riedel shears formed in response to the northwest-trending strike-slip to oblique-slip faults in a wrench tectonic setting (Wilcox et al., 1973).

The broad, breached, northwest-trending Arkansas anticline trends between Bebe and Abernathy mountains (Plate I). This anticline is the eastward extension of the Willapa Hills uplift, the axis of the fold appears to be offset in a left-lateral sense by northeast-trending faults (Plate I). This compressional event deformed both the middle Eocene Cowlitz Formation and the overlying Grays River volcanics (Plate I). Regional structural analysis indicates this folding event deformed younger Oligocene to middle Miocene units as well and thus, is post-mid-Miocene event (Wells, 1981). The anticline mapped may have formed in a wrench tectonic setting (after Wilcox et al., 1973). Russ Evarts (personal communications, 1998) identified a possible extension of this anticline southeastward into the Washington Cascades where Miocene volcanics are involved.

SUMMARY

Two major periods of deformation are recognized in the Coast Range of Oregon and Washington: (1) oblique subduction in the latest middle Eocene resulted in latest normal and oblique-slip faulting and (2) post mid-Miocene oblique subduction formed dextral faults and broad regional folds throughout southwest Washington. These post-Eocene episodes of shear rotation effected the strata deposited in this basin and formed the major structural features in this study area (Wells and Coe, 1985).

In the subsurface at the Mist Gas Field in northwest Oregon, horst and graben style northwest- and northeast-trending normal faults offset the Eocene Cowlitz Formation and middle Eocene Tillamook Volcanics. Activity ceased prior to deposition of the upper Eocene to Oligocene Keasey Formation (Robertson, 1997). A similar conjugate set of normal faults involves strata older than the Grays River sedimentary sequence in this study

area based on subsurface correlation of drill holes of Cowlitz units (Pauli, personal communications, 1995). According to Pauli (written communications, 1994 and 1996) many of these faults do not displace the lower Grays River volcanics sedimentary sequence (Figure 46). Thus, this normal faulting episode may explain the unconformity at the base of the incised valley fill (Grays River sedimentary sequence) and the Grays River volcanics around and below Bebe Mountain (field evidence for this unconformity was discussed in the previous Grays River volcanics section). Additionally, the timing of this unconformable event is constrained by an age of 38.9 Ma (Irving et al., 1996) determined from a tuff in Cowlitz unit 3 in Olequa Creek and a 36.8 Ma age from an overlying Gray River basalt flow, 400 m to the south (Plate I). A late middle Eocene (~ 38 Ma) regional unconformity has been recognized by Armentrout (1987). He thinks that this unconformity is related to Farallon plate reorganization at the end of the Eocene which effected the whole North American Continent.

A second post-mid-Miocene episode of compression resulted in large folds, continued uplift of the Willapa Hills, and formation and reactivation of north-northwest and north-northeast trending dextral and sinistral strike-slip faults; overprinting the earlier (late Eocene) period of extensional deformation (Niem et al., 1992; this study). According to Niem et al. (1992), many northwest-trending Eocene normal faults were reactivated in post-late middle Miocene time (after emplacement of the middle Miocene Columbia River Basalt Group) with dominantly right-lateral oblique-slip displacement in a wrench tectonic setting. Eocene faults that underlie the Grays River volcanics also were reactivated in the late middle Miocene, offsetting the volcanics (e.g., Bebe Mtn. and other faults on Plate I). This post mid-Miocene deformation appears to have continued into the present as a result of northward translation of the Oregon Coast Range and Klamath Mountains into southwest Washington and Vancouver Island in Canada (Wells, personal communications, 1998).

OIL AND GAS POTENTIAL

At present, there is no oil or gas production in southwest Washington. However, the Cowlitz Formation is currently a gas producer (70 BCF) in the Mist area of northwest Oregon (Johnson et al., 1997; Armentrout and Suek, 1985) (Figures 2 and 3). Johnson et al. (1997) have defined a Cowlitz-Spencer gas play (407) that extends from the southern Puget basin to the Oregon-Washington border (this study area falls within this play) and used the Mist gas field as an analog for exploration. High quality source rock is the most important limiting factor in development of large oil or gas accumulations in Washington (Johnson et al., 1997). Natural gas in the Mist gas field was generated from Eocene marine shale (e.g., Hamlet Fm.) or non-marine Cowlitz carbonaceous mudstone and coal and migrated into intensely faulted reservoirs in overlying and interbedded Cowlitz shallow-marine sandstones (Robertson, 1997). Potential structural traps in this study area are conjugate normal and oblique-slip fault blocks and perhaps the Arkansas anticline (Plate I) where it is not breached by erosion to the southeast beneath the nearby western Cascades volcanic units. Smaller stratigraphic traps are also possible where subtidal channel sandstones are bounded by tidal-flat mudstone. Interbedded fine-grained rocks (tidal mudstone), overlying deep marine and outer shelf mudstone (unit 4 and 5), and the very thick tuffaceous siltstone of the Lincoln Creek Formation could form seals.

On the basis of porosity and friability of outcrop samples, the reservoir potential of lithic arkoses from in the upper McIntosh sandstone and Cowlitz Formation is good to excellent. These micaceous sandstones are generally clean and highly friable, although some shallow marine sandstones are tightly cemented by sparry calcite along discrete mollusc-bearing concretionary horizons. These sandstones have 20% to 25% porosity as determined by visual estimation and point counting of grains vs. void spaces. Porosity is dominantly large sand-sized primary intergranular pores with minor secondary porosity

(<5%) formed by partial dissolution of volcanic rock fragments. Primary depositional porosity is generally open and shows good interconnection, suggesting good horizontal effective porosity and permeability. Pore throats are wide between intergranular pores and are not clogged by diagenetic clay minerals. Minor discontinuous grain-rimming smectite clay cements are the only authigenic cementing material present. Vertical permeability is, however, decreased by long impermeable aligned laminae composed of carbonized plant debris and micas. The late stage zeolites (clinoptilolite) were probably formed under low temperature conditions, indicating shallow burial for all these sandstones (Glasmann, personal communications, 1996). Also shallow burial conditions are suggested by the lack of compaction or distortion of plastically deformable mica between quartz and feldspar grains. Correlative sandstones of the Skookumchuck Formation in the Jackson Prairie gas storage facility (15 km to the northeast) have porosities of 30 to 40 percent and permeabilities as high as seven darcies (Johnson et al., 1997).

The upper shoreface sandstone of the McIntosh Formation (potential reservoir) is 60 m thick and a thick overlying siltstone (upper McIntosh siltstone) forms an excellent seal (Plate II). The upper shoreface sandstones in the lowest unit of the Cowlitz Formation (unit 1A) are also potential reservoir bodies. These shallow marine micaceous arkosic sandstones are up to 40 m thick and are generally free of interbedded siltstone and mudstone (Plate II). Other potential reservoir sandstones include: a 50-m thick basaltic arkosic sandstone in unit 2, thin cross-bedded subtidal channel arkosic sandstone of unit 3, and discontinuous submarine channel sandstones in unit 5 (Plate I).

Potential source rock for natural gas includes carbonaceous mudstone and multiple coal seams (up to 11-m thick coals) in units 1B and 3 of the Cowlitz Formation. Organic matter in these Eocene mudstone and coal is terrestrial and gas-prone Type III variety (Johnson et al., 1997). These coals are lignite to subbituminous in rank with mean vitrinite reflectance values between 0.3 to 0.6 percent (Johnson et al., 1997). Enhanced

maturation could result from a high heat flow from the large basaltic intrusions of Grays River volcanics (e. g. feeders for the Bebe Mountain pile). The McIntosh Formation deep marine siltstone (upper McIntosh) and mudstone (lower McIntosh) are another possible source for natural gas in this area. A significant potential source rock, which may underlie the McIntosh and Cowlitz formations in this area, was penetrated by a few boreholes in the nearby Chehalis basin. This marine mudstone is up to 3,000 m thick (Johnson, 1997).

The structural style of the Mist field in Oregon is similar to the structure in this area (Figure 46). Gas is produced in the Mist gas field from pools in multiple, small, conjugate fault-block traps (Niem et al., 1992). The two episodes of faulting (late Eocene and post-middle Miocene) may have resulted in down-dropped blocks of coal-bearing strata (unit 1B and 3) allowing gas to migrate into adjacent reservoir arkosic sandstone of the upper McIntosh and lower Cowlitz unit 1A. The overlying siltstone of unit 5 and the Lincoln Creek Formation may act as a seal in the subsurface. Maximum burial and potential peak maturation occurred after deposition of the thick Oligocene Lincoln Creek Formation (Johnson et al., 1997). The normal fault blocks formed during the late Eocene structural event were available to trap potential, generated-gas in post-Lincoln Creek time.

GEOLOGIC HISTORY

During the middle Eocene, crustal subsidence of the volcanic basement created a 640-kilometer long forearc or marginal basin extending from the Klamath Mountains of southwestern Oregon to southern Vancouver Island, Canada (Niem and Niem, 1984; Niem et al., 1992b). In southwest Washington during this time, bathyal mudstone and shallow marine micaceous, arkosic sandstone of the lower McIntosh Formation, derived from erosion of Mesozoic Okanogan uplift, the North Cascades, and/or the Idaho Batholith (Heller et al., 1987), partially filled this forearc basin (Wells, 1981). The lower McIntosh Formation (>44 Ma to 42.5 Ma) was deposited near the shelf/slope break as a lowstand, transgressive and overlying highstand system tract of the first transgressive-regressive 3rd order cycle evident in this study area. Deposition of hemipelagic mud dominated these transgressive and highstand events, with distal turbidity currents depositing thin, graded micaceous, arkosic sandstone beds on the flank of this marginal-marine basin.

A relative sea-level fall of approximately 20 to 80 m resulted in development of a sequence boundary that separates the upper shoreface sandstone of the upper McIntosh Formation from the outer shelfal siltstone deposits of the lower McIntosh Formation (Plate II). The outer shelf-to-shoreface transitional strata, that may have existed between the two members, were eliminated during this lowstand event. As a result, 130 m of shoreface sandstone of the basal part of the upper McIntosh member was deposited on a wave-scoured erosional surface. A prograding middle shoreface to coal-bearing tidal-flat facies succession and an overlying aggradational upper to middle shoreface sandstone succession, formed as relative sea level began to rise. As this transgression continued, a 497-m thick bathyal siltstone of the upper member of the McIntosh Formation was deposited. This transgression ended after deposition of upper Narizian foram-bearing

siltstone at middle bathyal depth and reflects a maximum flooding surface. A highstand system tract of delta front sandstone formed the uppermost part of the upper McIntosh member and consists of several coarsening-up parasequences (Plate II). An abrupt change in water depth from the bathyal upper McIntosh mudstone to prograding inner shelf to littoral deposits of unit 1A of the Cowlitz Formation resulted in formation of a sequence boundary between the two formations and the end of 3rd order transgressive-regressive cycle II (Plate II).

In southwestern Washington, lithic-arkosic, micaceous sandstone of the Cowlitz delta prograded westward and buried the underlying deep-marine siltstone of the upper McIntosh Formation. The Cowlitz Formation was deposited as part of an extensive deltaic system of the Eocene Puget Group that drained granitic batholiths and metamorphic core complexes of the North American continent to the east (Buckovic, 1979; Berkman, 1990). These alternating shallow marine and tide-influenced marginal marine sandstone-mudstone-coal-bearing sequences were formed by three transgressive-regressive 3rd order cycles or relative sea level fluctuations.

Multiple prograding wave-dominated shoreface successions of the delta front/shoreface sandstone successions (lower part of unit 1A) were deposited during a regressive event or rapid decrease in water depth. This regression or progradation phase finally resulted in deposition of several coarsening- and thickening-upward marginal marine and coal-bearing delta plain-marsh/swamp parasequences that form an aggradational parasequence set of a highstand system tract (unit 1B). A transgression or onlap event occurred at the end of unit 1 deposition and the beginning of unit 2 of the Cowlitz Formation. This transgression resulted in deposition of five thickening- and coarsening-up storm-dominated shelf to delta-front hummocky bedded arkosic sandstone parasequences. Large amounts of locally derived basaltic scoria were mixed by wave and tidal currents with the lithic-arkosic sandstones in marine unit 2 as a result of active

explosive intrabasinal volcanism (lower Grays River volcanics southwest of the study area). A maximum flooding surface marks the deepest water depths (outer neritic to upper bathyal) of unit 2.

A sequence boundary between units 2 and 3 formed during a lowstand in which a river incised its valley into the older rocks. Subsequent marine flooding of the valley created a large estuary where sedimentation rate kept up with the rate of subsidence or accommodation space. Fining-upwards sandstone-mudstone-coal-bearing parasequences of subtidal, intertidal, supratidal, and nonmarine facies associations of the 170-m thick unit 3 were deposited in this large estuary. Nested subtidal channels, cross-bedded subtidal sand ridges with brackish water molluscs, sandy and muddy accretionary-bank deposits, thin volcanoclastic interbeds, and marsh-swamps developed interfingering facies within this rapid sediment-accumulating and subsiding tidal-flat estuary system of the Cowlitz Formation.

The granitic Idaho Batholith and Okanogan metamorphic core complex of northeast Washington were exposed at this time and contributed these sands via a Columbia River drainage system to the Cowlitz and McIntosh deltas. An intrabasinal explosive basaltic source (Grays River volcanics) supplied sediments to the shallow marine and nonmarine environments of units 2 and 3 of the Cowlitz Formation. Explosive calc-alkaline eruptions in the nearby early western Cascades (Northcraft Formation or Goble Volcanics) created glassy and pumice rich ash falls that fell over the coal-swamp of units 1 and 3. Unit 3 (tidal cross-bedded sands) migrated to north-northwest and south-southeast as a result of shore parallel transport up and this estuary and deflection around a growing volcanic edifice of Grays River volcanics to the south and southwest.

Minor shoaling-upward sea-level fluctuations in unit 4 resulted in deposition of coarsening- and thickening -upward parasequence of shelfal mudstone deposited below wave base to storm wave-dominated hummocky bedded shoreface sandstone and fair-

weather siltstone. Overall water depth increased in the upper 65 m of unit 4 from neritic to outer bathyal resulted in development of a maximum flooding surface near the top of the Big Bend locality and in the type section in Olequa Creek. This increase in water depth reflects the continued transgression or deepening event in the upper part of the Cowlitz Formation (Nesbitt, 1994).

Deeper marine laminated siltstone with subordinate fine-grained, thin-bedded turbidites, amalgamated and thick submarine-channel sandstone with chaotic mudstone breccia facies, and slump-folded and soft-sediment deformed intervals comprise the 150-m thick unit 5 of the Cowlitz Formation. This unit was deposited during a lowstand system tract of cycle V (Figure 35). During a relative sea level fall submarine channels were incised into the prodelta slope siltstone, arkosic sandstones were largely bypassed into the deeper marine environment via these channels but some channels were filled with grain flows, fluidized flows and high-concentration turbidity currents. This sequence boundary and lowstand system tract were tectonically control (out of phase with the world-wide eustatic sea level curve of Haq et al. (1987) during this time in the Eocene). Earthquakes in this tectonically active margin initiated large slump folds which slid downslope to the north.

In the latest Eocene, olivine tholeiitic basaltic magma derived from a picritic undepleted mantle migrated up into the Eocene crust in southwest Washington under Bebe Mountain and formed as a separate volcanic edifice composed of subaerial Grays River flows (Bebe Mtn. pile of the Grays River volcanics, this study area). This mafic magma inflated the crust and uplifted the Cowlitz strata, during a period of extension, creating an erosional unconformity (major Sequence Boundary II of Armentrout, 1987). This tectonically controlled unconformity marks a period of plate reorganization of the Farallon plate, which affected the western part of North America and part of South America (Armentrout, personal communications, 1997). A thick basal valley-fill sequence (Grays

River sedimentary sequence) that underlies the intracanyon Grays River flows was deposited in down-dropped blocks between normal-faulted Cowlitz strata. These normal faults cut the Cowlitz Formation and terminated against the Grays River sedimentary sequence and overlying volcanics.

The Cowlitz Formation in upper Olequa Creek is unconformably overlain by a younger Oligocene valley-fill unit (Toutle Formation). This 265-m fluvial to marginal marine incised valley-fill unit was deposited during a lowstand valley-fill event that graded, in the study area, upwards into the overlying deeper marine tuffaceous siltstone of the Lincoln Creek Formation. Unconformity-bounded tuffaceous strata of the Toutle and Lincoln Creek formations reflect a period of renewed tectonic instability and widespread distribution of volcanic ash in the forearc basin from the adjacent developing explosive calc-alkaline western Cascade volcanic arc.

CONCLUSIONS

The lithofacies, sequence stratigraphy, and structural geology of the middle to upper Eocene Cowlitz Formation and associated volcanic and sedimentary units in the western Willapa Hills area of southwest Washington were mapped and analyzed in this study. The main conclusions of this investigation are:

(1) The middle Eocene mudstone member of the lower McIntosh Formation is a minimum of 375 m thick (base not exposed) and was deposited near the shelf/slope break during lowstand, transgressive and highstand system tracts of a 3rd order cycle I.

Hemipelagic deep-marine micaceous mudstone deposition dominated with minor distal turbidity currents depositing thin, graded, micaceous, arkosic sandstone beds on the flank of this marginal-marine forearc basin.

(2) The 128-m thick, middle Eocene upper McIntosh member sandstone is a prograding middle shoreface lithic arkosic to coal-bearing, nonmarine facies succession and an overlying aggradational, upper to middle shoreface facies succession. A sequence boundary resulting from a relative sea-level fall of 20 to 80 m is defined by a rapid shoaling event between the upper and lower members of the McIntosh Formation.

(3) The 497-m thick tuffaceous micaceous siltstone unit of the upper McIntosh Formation underlies the Cowlitz Formation. Lithofacies of the lower part of the upper McIntosh siltstone unit include parallel-laminated and slump-folded delta-slope siltstone that formed as a transgressive system tract. The foram-bearing siltstone in the upper part of this McIntosh member was deposited in middle bathyal depths. The uppermost part of this member contains several coarsening-up delta front sandstone parasequences that form a highstand system tract.

(4) Stratigraphic measurement of the 1,238-m thick middle Eocene Cowlitz Formation in the type section along 43 km of Olequa and Stillwater creeks reveals

complex facies successions of wave- to tide-dominated deltaic and estuary-incised-valley sequences. The Cowlitz Formation can be informally divided into five mappable units consisting of alternating shallow marine and tidally influenced marginal marine sequences that are capped by a deep marine siltstone.

(5) The basal 558 m of the Cowlitz Formation consists of the following units: (1a) vertically stacked prograding wave-dominated shoreface facies of the micaceous lithic arkosic sandstone delta front parasequences and (1b) fining- and thinning-upwards coal-bearing coastal-delta-plain facies associations. A rapid change in water depth is evident in the basal part of unit 1A (a sequence boundary between the Cowlitz Formation and the deep marine mudstone of the underlying McIntosh Formation). The coarsening upwards parasequences of the lower part of unit 1A formed as a lowstand wedge system tract (LST) and an overlying transgressive system tract (TST). Unit 1B consists of coal-bearing, coarsening- and thickening-upwards parasequences that form an aggradational parasequence set of a highstand system tract (HST).

(6) The 205-m thick unit 2 is composed of five coarsening-up storm-dominated shelf to delta-front micaceous, lithic arkosic sandstone parasequences of a transgressive system tract (TST). Large amounts of scoriaceous basaltic volcanoclastic detritus began to mix with the extra basinal lithic-arkosic sandstones in this marine unit 2 as a result of local intrabasinal mafic volcanism (tholeiitic Grays River volcanics). The last parasequence overlies a maximum flooding surface that defines the greatest water depth (outer neritic to upper bathyal) in unit 2.

(8) A sequence boundary separates the shallow marine unit 2 of 3rd order sequence cycle III from the tide-dominated unit 3 of 3rd order sequence cycle IV. This sequence boundary formed during a lowstand that resulted in development of an incised valley cut into unit 2 that was followed by drowning of the valley by a relative sea level rise due to subsidence and formation of a large estuary. Irving and Nesbitt (1996)

determined an $^{39}\text{Ar}/^{40}\text{Ar}$ date of 38.9 ± 0.1 Ma for a thick tuff in unit 3 of the Cowlitz Formation. Several fining-upwards parasequences of subtidal, intertidal, and supratidal facies associations of the 170-m thick unit 3 were deposited in this large estuary as a lowstand system tract (LST). Nested subtidal micaceous lithic-arkosic sandstone channels with brackish water molluscan fauna, cross-bedded subtidal sandstone sand ridges, flaser-bedded sandy and muddy accretionary-tidal-bank deposits, thin volcanoclastic interbeds within supratidal coal-forming marsh-swamps developed complex interfingering geometries and facies within this estuary, a possible mouth of the ancestral Columbia River.

(9) The overlying, 155-m thick unit 4 of the Cowlitz Formation, consists of several offshore mudstone to thick, fossiliferous, hummocky bedded, wave-dominated shoreface micaceous arkosic sandstone facies successions in coarsening-upward parasequences. These vertically stacked parasequences form a retrogradational parasequence set of a transgressive system tract (TST) and an upper highstand system tract of the 3rd order sequence cycle IV. Strata in the upper part of unit 4 in Olequa Creek biostratigraphically correlate with a highstand, bioturbated mollusc-bearing sandy siltstone and glauconitic mudstone in the Big Bend type locality along the Cowlitz River. Water depth increases in the upper 65 m of unit 4 from neritic (e.g., shelf) to outer bathyal (maximum flooding event) based on shallow marine molluscan assemblages collected by Nesbitt (1995) at the Big Bend locality. This increase in water depth reflects the continuation of transgression or deepening event in the upper part of the Cowlitz Formation.

(10) The deep-marine facies of the 150-m thick unit 5, the uppermost unit of the type Cowlitz Formation, formed as a lowstand system tract of 3rd order cycle V. Deeper marine, laminated siltstone with subordinate fine-grained, thin-bedded turbidites, amalgamated and thick submarine-channel sandstone with a chaotic mudstone breccia

facies, and slump-folded and soft-sediment deformed intervals comprise unit 5. During a relative sea level fall submarine channels eroded into the prodelta slope siltstone. Arkosic sandstones were largely bypassed into the deeper marine environment via these channels, but some channels were filled with grain flows, fluidized flow and high-concentration turbidity currents. The sequence boundary and lowstand system tract of unit 4 appear to be tectonically controlled (i.e., local basin tectonics) because subsidence is out-of-phase with the world-wide eustatic sea level curve of Haq and others (1987) during this time). Earthquakes along this active subduction margin could have initiated large slump folds in this unit.

(11) Petrography (SEM, XRD, and thin section) and paleocurrent study of the lithic-arkosic sandstones indicates the predominant mineral and rock fragment constituents of McIntosh and Cowlitz formations micaceous lithic-arkosic sandstones and mudstones were transported from a distant, uplifted, and dissected arc (e.g., the granitic Idaho Batholith and North Cascade and Okanogan metamorphic core complexes to the northeast and east) by way of an ancestral Columbia River fluvial system. A subordinate intrabasinal explosive basaltic source (Grays River volcanics) supplied reworked scoriaceous, pyroclastic, and debris flow volcanic sand and pebble detritus to the shallow marine and nonmarine environments of the delta front unit 2 and tidal unit 3 of the Cowlitz Formation. Explosive calc-alkaline volcanic activity (Northcraft Formation and/or Goble Volcanics) is also evident in the pumiceous silicic tuff beds in the coal-bearing marsh/swamp deposits of units 1 and 3. Paleocurrent directions from tidal strata of unit 3 are to the north-northwest and south-southeast as a result of shore-parallel transport and deflection around a proposed growing volcanic edifice (Grays River volcanics located to the southwest and south, outside the study area).

(12) The type Cowlitz Formation in southwest Washington is correlated in this study to the Cowlitz Formation in northwest Oregon. In northwest Oregon, delta-front

sandstone, mapped as the upper Eocene Cowlitz Formation, unconformably overlies the middle Eocene Tillamook Volcanics and slope mudstone, shelf sandstone, and volcanic conglomerate of the Hamlet formation (Niem et al., 1992; Niem and Niem, 1985; Robertson, 1997) (Figure 3). The upper McIntosh Formation sandstone unit in southwest Washington is a lithologic correlative of the arkosic micaceous shelfal sandstone of the Sunset Highway member of the Hamlet formation in northwest Oregon. The Cowlitz is 1,200 m thick at the type area whereas the Cowlitz Formation in northwest Oregon is maximum of 400 m thick and not all subunits are lithologically correlative due to pinchout and facies changes.

(13) The Grays River volcanics is divided into two distinct volcanic complexes or subunits based on its stratigraphic relationship with sedimentary units, radiometric age dates, and magnetostratigraphy. An older (41 to 40 Ma) nearby reversely polarized volcanic pile crops out in the central and western part of the Willapa Hills uplift mapped by Wells (1981). A second younger intracanyon volcanic pile forms Bebe and Abernathy mountains and unconformably overlies the Cowlitz Formation. Intracanyon, largely normally polarized, olivine-bearing tholeiitic basaltic lavas of this upper Grays River volcanics package may have had a primary, undepleted picritic basaltic mantle source that defines a second renewal of Grays River forearc volcanism in southwest Washington. A 38.9 ± 0.1 Ma $^{39}\text{Ar}/^{40}\text{Ar}$ date from an oligoclase-bearing, pumiceous western Cascade arc derived tuff bed in unit 3 of the underlying Cowlitz Formation (Irving et al, 1996) and three $^{39}\text{Ar}/^{40}\text{Ar}$ dates of 38.64 ± 0.40 , 37.44 ± 0.45 , and 36.85 ± 0.46 Ma from the overlying normally polarized subaerial flows of Grays River volcanics bracket the timing of this short term unconformity. This tectonically controlled unconformity is marked by an extensive period of uplift and erosion during which normal or extensional faults which cut the Cowlitz Formation are truncated by an overlying basal Grays River non-marine volcanoclastic sedimentary incised-valley sequence and the overlying subaerial flows of the

Grays River volcanics of Bebe Mountain. Inflation of the forearc crust by this local basaltic volcanism may have contributed to this period of late Eocene uplift and erosion. However, John Armentrout (personal communications, 1997) believes this late Eocene unconformity may be more regional in extent and has effected the western U. S. to the Gulf Coast as a result of Farallon oceanic plate reorganization at this time.

(14) An angular unconformity between the upper Cowlitz Formation and the overlying Oligocene lowstand valley fill unit is a tectonically forced sequence boundary. This 265-m fluvial to marginal marine unit correlates with the shallow marine and fluvial upper Eocene to Oligocene Toutle Formation of May (1980) and the basal basaltic conglomerates of the Lincoln Creek Formation. A $31.9 \pm \text{Ma}$ $^{39}\text{Ar}/^{40}\text{Ar}$ date from a hornblende-bearing pumice lapilli tuff indicates that this valley-fill is a time correlative of the Toutle Formation of Roberts (1958) to the southeast. The lowstand valley-fill unit grades upward into the overlying deeper marine tuffaceous siltstone of the Lincoln Creek Formation.

(15) The rate of sedimentation for the Cowlitz Formation was calculated using $^{39}\text{Ar}/^{40}\text{Ar}$ age and measured thicknesses from the type section in Olequa Creek and from the overlying Grays River volcanics. The average sedimentation rate from the top of the lower McIntosh Formation to unit 3 (marker tuff bed) of the Cowlitz Formation is 39 cm/1,000 yrs. An average sedimentation rate of 1.6 m /1000 yrs. was determined from marker tuff bed 3A in unit 3 (38.9 Ma) of the Cowlitz Formation to the overlying Grays River volcanics (36.8 Ma) exposed near Olequa Creek. The average sedimentation rate calculated from the marker 3A tuff in unit 3 (Plates I and II) to the hornblende-bearing tuff (32 Ma) in the Toutle Formation is 7.2 cm/1,000 yrs. The lower value results from including up to 6 m. y. of nondeposition (i. e., presence of an unconformity) in the calculation.

(16) The structure in this area consists of one major fold, the Arkansas anticline, that is truncated by north-northwest and north-northeast trending faults and many subordinate northwest-trending faults. These structures formed as a result of two plate tectonic events: (1) highly oblique subduction that resulted in latest middle Eocene normal or extensional faulting and intrusion of some Eocene Grays River dikes along normal faults and (2) post mid-Miocene oblique subduction that formed dextral wrench faulting and broad regional folding throughout southwest Washington. The broad and open northwest-trending Arkansas anticline (an eastward extension of the Willapa Hills uplift) between Bebe and Abernathy mountains is highly truncated by northeast-trending sinistral and northwest dextral faults (Plate I). This post-middle Miocene transpressional event deformed both the Eocene Cowlitz Formation and the overlying Grays River volcanics (Plate I). This local faulting pattern which parallels the regional structure mapped by Wells (1981) indicates this folding and faulting event truncated mid-Miocene volcanic and sedimentary units.

(17) The oil and gas potential of the McIntosh and Cowlitz formations in this study area needs to be investigated in more detail but has promise. The thick (up to 50 m) lithic arkosic sandstones have a porosity of 25 to 35 % and are very friable. Numerous coal seams (up to 11 m thick) are potentially a source for gas. Additionally, the structure is similar to the gas-producing Mist gas field in northwest Oregon and can be considered an analog for exploration. The normal faults in this area may have formed traps and the overlying siltstone of unit 5 and the upper McIntosh siltstone form excellent seals. A potential maturation source is the Grays River volcanics, which could have locally brought these coal-bearing strata into the gas window.

REFERENCES

- Armentrout, J. M., 1977, Cenozoic stratigraphy of southwestern Washington, *in* Brown, E. H., and Ellis, R. C., eds., Geological Excursions in the Pacific Northwest: Geological Society of America 1977 Annual Meeting, p. 227-264.
- _____, Hull, D. A., and Beaulieu, J. D., 1983, Correlation of Cenozoic stratigraphic units of western Oregon and Washington: Oregon Department of Geology and Mineral Industries, Oil and Gas Investigation 7, 90 p. and 1 chart.
- _____, and Suek, D. H., 1985, Hydrocarbon exploration in western Oregon and Washington: American Association of Petroleum Geologists Bulletin, v. 69, p. 627-643.
- _____, 1987, Cenozoic stratigraphy, unconformity-bounded sequences, and tectonic history of southwestern Washington, *in* Schuster, J. E., ed., Selected papers on the geology of Washington: Washington Department Natural Resources, Division of Geology and Earth Resources Bulletin 77, p. 291-320.
- _____, 1996, Fundamentals of stratigraphic analysis, NWEA workshop.
- Berggren, W. A., Kent, D. V., Swisher, C. C., and Aubry, M. P., 1995, A revised Cenozoic geochronology and chronostratigraphy: *in* Berggren, W. A., Kent, Aubry, M. P., and Hardenbol, J., eds., Geochronology, time scales and global stratigraphic correlation: SEPM (Society for Sedimentary Geology) Special Publication No. 54, p. 129-212.
- Berkman, T. A., 1990, Surface-subsurface geology of the middle to upper Eocene sedimentary and volcanic rock units, western Columbia county, northwest Oregon: unpublished M. S. thesis, Oregon State University, Corvallis, 413 p.
- Bouma, A. H., 1962, Sedimentology of some flysch deposits: Amsterdam, Elsevier, 168 p.
- Bruer, W. G., 1980, Mist Gas Field, Columbia County Oregon: Technical Program Reprints, Pacific Section, AAPG-SEG-SEPM 55th Annual Meeting, Bakersfield, California, April 9-11, 10 p.
- Buckovic, W. A., 1979, The Eocene deltaic system of west-central Washington, *in* Armentrout, J. M., Cole, M. R., and TerBest, H., Jr., eds., Cenozoic paleogeography of the western United States: Pacific Coast Paleogeography Symposium 3, Society of Economic Paleontologists and Mineralogists, Pacific section, p. 147-163.
- Bukry, D., 1975, Coccolith and silicoflagellate stratigraphy, northwestern Pacific Ocean, Deep Sea Drilling Project Leg 32: Washington D. C., Initial reports of the Deep Sea Drilling Project, v. 32, p. 677-701.

- Cas, R. A. F., and Wright, J. V., 1988, Volcanic successions modern and ancient: New York, Chapman and Hall, 528 p.
- Clifton, H. E., 1983, Discrimination between subtidal and intertidal facies in Pleistocene deposits, Willapa Bay, Washington: *Journal of Sedimentary Petrology*, v. 53, p. 353-369.
- Dickinson, W. R., 1970, Interpreting detrital modes of graywacke and arkose: *Journal of Sedimentary Petrology*, v. 40, p. 695-707.
- Dott, R. H., Jr., and Bird K. J., 1979, Sand transport through channels across an Eocene shelf and slope in southwest Oregon, *in* *Geology of continental slopes: SEPM Special Publication No. 27*, p. 327-342.
- Dott, R. H. and Bourgeois, J., 1982, Hummocky stratification: significance of its variable bedding sequences: *Geological Society of America Bulletin*, v. 93, p. 663-680.
- Duncan, R. A., 1982, A captured island chain in the Coast Range of Oregon and Washington: *Journal of Geophysical Research*, v. 87, p. 10,827-10,837.
- Evarts, R., U. S. Geological Survey, Western Regional Branch, Menlo Park California, written and personal communication, 1994-1998.
- Farr, L. C., Jr., 1989, Stratigraphy, diagenesis, and depositional environments of the Cowlitz Formation (Eocene), northwest Oregon: , unpublished M. S. thesis, Portland State University, Portland, Oregon, 168 p.
- Finn, C., Phillips, W. M., and Williams, D. L., 1991, Gravity anomaly and terrain maps of Washington: U. S. Geological Survey Geophysical Investigations Map GP-988.
- Flores, R. M. and Johnson, S. Y., 1995, Sedimentology and lithofacies of the Eocene Skookumchuck Formation in the Centralia coal mine, southwest Washington, *in* Fritsch, A. E., ed., *Cenozoic paleogeography of the western United States-II: Pacific Section*, SEPM, book 75, p. 274-290.
- Folk, R. L., 1974, *Petrology of sedimentary rocks*: Austin, Texas, Hemphill, 182 p.
- Glasmann, J. R. and Simonson, G. H., 1985, Alteration of basalt in soils of western Oregon: *Soil Science Society of America Journal*, v. 59, no. 1, p. 262-273.
- _____, Professor of Geology, Oregon State University, personal communications, 1996-1998.
- Hammond, P. E., Emeritus Professor of Geology, Portland State University, written and personal communication, 1996-1997.
- Haq, B. U., Hardenbol, J., and Vail, P. R., 1987, Chronology of fluctuating sea levels since the Triassic: *Science*, v. 235, p. 1156-1167.

- Heller, P. L. and Ryberg, P. T., 1983, Sedimentary record of subduction forearc transition in the rotated Eocene basin of western Oregon: *Geology*, v. 11, p. 380-383.
- _____, Tabor, R. M., and Suczek, C. A., 1987, Paleogeographic evolution of the United States Pacific Northwest during the Paleogene time: *Canadian Journal of Earth Sciences*, v. 24, p. 1652-1667.
- Henriksen, D. A., 1956, Eocene stratigraphy of the lower Cowlitz River area, eastern Willapa Hills area, southwestern Washington: *Washington Division of Mines and Geology Bulletin* 43, 122 p.
- Irvine, T. N., and Barager W. R. A., 1971, A guide to the chemical classification of the common volcanic rocks: *Canadian Journal of Earth Sciences*, v. 8, p. 523-548.
- Irving, A. J., Nesbitt, E. A., and Renne, P. R., 1996, Age constraints on earliest Cascade arc volcanism and Eocene marine biozones from a feldspar-rich tuff in the Cowlitz Formation, southwest Washington: *EOS Transactions of the American Geophysical Union*, v. 77, no. 46, p. F-814.
- Kenitz, S., M. S. candidate, Portland State University, personal communication, 1996, 1997.
- Le Bas, M. J., Le Maitre, R. W., Streckeisen, A., and Zanettin, B., 1986, A chemical classification of volcanic rocks based on the total alkali-silica diagram: *Journal of Petrology*, v. 27, p. 745-750.
- Livingston, V. E., Jr., 1966, Geology and mineral resources of the Kelso-Cathlamet area, Cowlitz and Wahkiakum Counties, Washington: *Washington Division of Mines and Geology Bulletin* 54, 110 p.
- Johnson, S. Y., structural geologist and sedimentologist, United States Geological Survey, Branch of Sedimentary Processes, Denver Colorado, personal communications, 1994.
- _____, Tennyson, M. E., Lingley W. S., Jr., and Law, B. E., 1997, Petroleum geology of the state of Washington: U. S. Geological Survey Professional Paper 1582, 40 p.
- MacKenzie, W. S., Donaldson, C. H., and Guilford, C., 1982, *Atlas of igneous rocks and their textures*: Longman Scientific and Technical, New York, 148 p.
- Magill, J., Cox, A., and Duncan, R., 1981, Tillamook Volcanic Series: Further evidence for tectonic rotation of the Oregon Coast Range: *Journal of Geophysical Research*, v. 86, p. 2953-2970.
- May, D. J., 1980, The paleoecology and depositional environment of the late Eocene-early Oligocene Toutle Formation, southwest Washington: unpublished M. S. thesis, University of Washington, Seattle, 110 p.
- McDougall, K. M., Micropaleontologist, U. S. Geological Survey, written and personal communication, 1997.

- Miyashiro, A., 1974, Volcanic rock series in island arcs and active continental margins: *American Journal of Science*, v. 274, p. 321-355.
- Moothart, S. R., 1992, Geology of the middle and upper Eocene McIntosh Formation and adjacent volcanics and sedimentary rock units, Willapa Hills, Pacific County, southwestern Washington: unpublished M. S. Thesis, Oregon State University, Corvallis, 265 p.
- Mumford, D. F., 1988, Geology of the Elsie-lower Nehalem River area, south-central Clatsop and northern Tillamook counties, northwestern Oregon: unpublished M. S. thesis, Oregon State University, Corvallis, 392 p.
- Nesbitt, E. A., 1982, Paleocology and Biostratigraphy of Eocene Marine Assemblages from Western North America: unpublished Ph.D. thesis University of California, Berkeley, 213 p.
- _____, 1995, Paleocological analysis of molluscan assemblages from the middle Eocene Cowlitz Formation, southwest Washington: *Journal of Paleontology*, v. 69, no. 6, p. 1060-1073.
- _____, Research Associate, Thomas Burke Memorial Washington State Museum written and personal communication, 1996.
- Niem, A. R., and Niem, W. A., 1984, Cenozoic geology and geologic history of western Oregon, *in* Kulm, L. D., et al., eds., *Western North America continental margin and adjacent ocean floor off Oregon and Washington*: sheet 17.
- _____, MacLeod, N. S., Snavely, P. D., Jr., Huggins, D., Fortier, J. D., Meyer, H. J., Seeling, A., and Niem W. A., 1992, Onshore-offshore geologic cross section, northern Oregon Coast Range to continental slope: Oregon Department of Geology and Mineral Industries Continental Margin Transect OGI-26, 10 p., 1 plate.
- _____, Professor of Geology, Department of Geosciences, Oregon State University, Corvallis, written and personal communication, 1994-1998.
- Niem, W. A., Niem, A. R., and Snavely, P. D., Jr., 1992, Western Washington-Oregon coastal sequence, *in* Christiansen, R. L. and Yeats, R. S., eds., *Post-Laramide geology of the Cordilleran region: Geological Society of America, Geology of the North America (DNAG) volume*, v. G-3, p. 314-319.
- _____, Niem, A. R., and Snavely, P. D. Jr., 1992, Sedimentary embayments of the Washington-Oregon coast, *in* Christiansen, R. L., and Yeats, R. S., eds., *Post-Laramide geology of the Cordilleran region: Geological Society of America, Geology of the North America (DNAG) volume*, v. G-3, p. 265-270.
- Nio, S., and Yang, C., 1991, Diagnostic attributes of clastic tidal deposits: a review, *in* Smith, D. G., Reinson, G. E., Zaitlin, B. A., and Rahmani, R. A., eds., *Clastic tidal sedimentology: Canadian Society of Petroleum Geologists, Memoir 16*, p. 3-28.

- Pauli, D., Exploration Geologist, Weyerhaeuser Minerals Division, Tacoma, Washington, written and personal communication, 1994-1997.
- Pease, M. H., and Hoover, L., 1957, Geology of the Doty-Minot Peak area, Washington: United States Geological Survey Oil and Gas Investigations Map OM-188, scale 1:62,500.
- Pemberton, S. G. and MacEachern, J. A., 1992, Trace fossil facies models: Environmental and allostratigraphic significance; *in* Walker, R. G. and James, N. P., eds., *Facies Models: Response to sea level change*: Geological Association of Canada, p. 47-72.
- Phillips, W. M., Korosec, M. A., Schasse, H. W., Anderson, J. L., and Hagen, R. A., 1986, K-Ar ages of volcanic rocks in southwest Washington: *Isochron/West*, v. 47, p. 18-24.
- _____, 1987, Geologic map of the Mount St. Helens quadrangle, Washington: Washington Division of Geology and Earth Resources Open File Report 87-4, 63 p., 1 plate, scale 1:100,000.
- _____, Walsh, T. J., and Hagen, R. A., 1989, Eocene transition from oceanic to arc volcanism, southwest Washington: United States Geological Survey Open File Report, 89-178, p. 199-256.
- Philpotts, A. R., 1990, *Principles of igneous and metamorphic petrology*: Englewood, New Jersey, Prentice Hall, p. 275-297.
- Prothero D. R., and Armentrout, J. M., 1985, Magnetostratigraphic correlation of the Lincoln Creek Formation, Washington: Implications for the age of the Eocene/Oligocene boundary: *Geology*, v. 13, p. 208-211.
- Rarey, P. J., 1985, Geology of the Hamlet-North Fork of the Nehalem River area, southern Clatsop and northernmost Tillamook counties, northwest Oregon: unpublished M. S. thesis, Oregon State University, Corvallis, 457 p.
- Rau, W. W., 1958, Stratigraphy and foraminiferal zonation in some Tertiary rocks of southwest Washington: U. S. Geological Survey, Oil and Gas Investigation, Chart O. C. 57, 2 sheets.
- Roberts, A. E., 1958, Geology and coal resources of the Toledo-Castle Rock district, Cowlitz and Lewis Counties, Washington: United States Geological Survey Bulletin 1062, 71p., 6 plates.
- Robertson, C. L., 1997, Subsurface-surface facies distribution of the Eocene Cowlitz and Hamlet formations, northwest Oregon: unpublished M. S. thesis, Oregon State University, Corvallis, 143 p.
- Ryu, I.-C., Niem, A. R., and Niem, W. A., 1992, Schematic fence diagram of the southern Tyee basin, Oregon Coast Range, Oregon Department of Geology and Mineral Industries Oil and Gas Investigation 18, Portland, Oregon, 28 p., 1 plate.

- Ryu, I.-C., 1995, Stratigraphy, sedimentology, and hydrocarbon potential of Eocene forearc and subduction zone strata in the southern Tyee Basin, Oregon Coast Range: unpublished Ph.D. thesis, Oregon State University, Corvallis, 409 p.
- Safley, L. E., 1989, Geology of the Rock Creek-Green Mountain area, southeast Clatsop and northernmost Tillamook counties, northwestern Oregon: unpublished M. S. thesis, Oregon State University, Corvallis, 245 p.
- Schasse, H. W., 1987, Geologic map of the Centralia quadrangle, Washington: Washington Division of Geology and Earth Resources Open File Report 87-11, 28 p., 1 plate, scale 1:100,000.
- Smith, G. A., and Lowe, D. R., 1991, Lahars: volcano-hydrologic events and deposition in the debris flow-hyperconcentrated flow continuum *in* Fisher, R. V., and Smith, G. A., *Sedimentation in Volcanic Settings: SEPM Special Publications No. 45*, p. 59-70.
- Snavely, P. D., Jr., Brown, R. D., Jr., Roberts, A. E., and Rau W. W., 1958, Geology and coal resources of the Centralia-Chehalis district, Washington: U. S. Geological Survey Bulletin 1053, 159 p.
- _____, 1987, Tertiary geologic framework, neotectonics, and petroleum potential of the Oregon-Washington continental margin, *in* Scholl, D. W., Grantz, A., Vedder, J. G., eds., *Geology and resource potential of the continental margin of western North America and adjacent ocean basins- Beaufort Sea to Baja California: Circum-Pacific Council for Energy and Mineral Resources, Earth Sciences Series*, v. 6, p. 305-335.
- Van Wagoner, J. C., Mitchum, R. M., Campion, K. M., and Rahmanian, V. D., 1990, Siliciclastic sequence stratigraphy in well logs, cores, and outcrops: American Association of Petroleum Geologists Methods in Exploration Series 7, 55 p.
- Wagner H. C., 1967, Preliminary geologic map of the Raymond Quadrangle, Pacific County, Washington: United States Geological Survey Open-File Report 67-265, scale 1:62,500.
- Walker, R. G., 1992, Facies, Facies Models and Modern Stratigraphic Concepts, *in* Walker R. G., and James, N. P., *Facies models response to sea level change: Geological Association of Canada*, p.1-25.
- _____, and Plint, A. G., 1992, Wave- and storm-dominated shallow marine systems, *in* Walker R. G., and James, N. P., eds., *Facies models response to sea level change; Geological Association of Canada*, p. 219-238.
- Walsh, T. B., Korosec, M. A., Phillips, W. M., Logan, R. L., and Schasse, H. W., 1987, Geologic map of Washington - southwest quadrant: Washington Division of Geology and Earth Resources Geologic Map GM-34, 2 pl., 28 p.
- _____, 1987, Geologic map of Astoria and Ilwaco Quadrangles, Washington and Oregon: Washington Division of Geology and Earth Resources Open File Report 87-7, 32 p., 1 plate, scale 1:100,000.

- Weaver, C. E., 1912, A preliminary report on the Tertiary paleontology of western Washington: Washington Geological Survey Bulletin 15, 80 p.
- _____, 1937, Tertiary stratigraphy of western Washington and northwestern Oregon: University of Washington publications V. 4, Seattle, 166 p., 15 Pls.
- Wells, R. E., 1981, Geologic map of the eastern Willapa Hills, Cowlitz, Lewis, Pacific, and Wahkiakum Counties, Washington: United States Geological Survey Open-File report 81-674, scale 1:62,500.
- _____, Engebretson, D. C., Snavely, P. D., Jr., and Coe, R. S., 1984, Cenozoic plate motions and the volcano-tectonic evolution of western Oregon and Washington: *Tectonics*, v. 3, no. 2, p. 275-294.
- _____, 1984, Paleomagnetic constraints on the interpretation of early Cenozoic Pacific Northwest paleogeography, in Nilsen, T. H., ed., *Geology of the upper Cretaceous Hornbrook Formation, Oregon and California: Pacific Section Society of Economic Paleontologists and Mineralogists*, v. 42, p. 231-237.
- _____, and Coe, R. S., 1985, Paleomagnetism and geology of Eocene volcanic rocks of southwest Washington, implications for mechanisms of tectonic rotation: *Journal of Geophysical Research*, v. 90, no. B2, p. 1925-1947.
- _____, U. S. Geological Survey, Western Regional Branch, Menlo Park California, personal communication, 1994-1998.
- Wilcox, R. E., Harding, T. P., and Seely, D. R., 1973, Basic wrench tectonics: *American Association of Petroleum Geologists Bulletin*, v. 57, p. 74-96.
- Wolfe, E. W., and McKee, E. H., 1972, Sedimentary and igneous rocks of the Grays River quadrangle, Washington: United States Geological Survey Bulletin 1335, 70 p.
- _____, and McKee, E. H., 1972, Geology of the Grays River Quadrangle, Wahkiakum and Pacific counties, Washington: Washington Division of Geology and Earth Resources Geologic Map GM-4, scale 1:62,500.
- Yett, J. R., 1979, Eocene Foraminifera from the Olequa Creek Member of the Cowlitz Formation, southwestern Washington: M. S. thesis University of Washington, Seattle, 145 p.

APPENDICES

APPENDIX I: FORAMINIFERA IDENTIFICATIONFORM 9-1861
(JULY 1986)Page 1 of 7U.S. DEPARTMENT OF THE INTERIOR
GEOLOGICAL SURVEY

REPORT ON REFERRED FOSSILS

Stratigraphic Range lower Tertiary	Shipment Number WNGM-97-1
General Locality (state, country, ocean, etc.) Washington	Number of Samples 49
Quadrangle or Area Wildwood and Winlock 7.5' quadrangles	Region (county, province, sea, etc.) Lewis and Cowlitz Counties
Fossil Type(s) Foraminifers	Referred By Charles Payne, Oregon State University
Formation MacIntosh and Cowlitz Formations	Report By Kristin McDougall <i>Kristin McDougall</i>
Latitude (see map) Longitude	Report Date March 6, 1997

Project: Pacific Northwest Project

The following samples were submitted by Charles Payne, Oregon State University, for foraminiferal analysis. Samples were taken from the McIntosh and Cowlitz Formations as exposed along the Olequa and Stillwater Creeks in southwestern Washington.

Mf 8847 (Field number CP94-79) Lower McIntosh Formation
 Benthic foraminifers
Bathysiphon eocenicus Cushman and Hanna
Bulimina spp.
Karreriella spp.
Nodosaria spp. (fragment)
Trochammina spp.

Diatoms
 Radiolarians

AGE: Tertiary
 ECOLOGY: outer neritic to bathyal (> 50 m)

Mf8848 (Field number CP94-80A) Lower McIntosh Formation
 Sample is barren of foraminifers; pyritized diatoms are present.

**REPORT NOT TO BE QUOTED OR PARAPHRASED IN PUBLICATION
 WITHOUT A FINAL RECHECK BY THE PALEONTOLOGIST**

Mf 8849 (Field number CP94-84a) Lower McIntosh Formation

Benthic foraminifers

Cibicides elemaensis Rau
Cibicides natlandi Beck
Eponides mexicanus (Cushman)
Lenticulina inornata (d'Orbigny)
Nodosaria spp. (fragments)
Quinqueloculina weaveri Rau

Radiolarians

Sponge spicules

AGE: late Eocene, late Narizian to earliest Refugian Stage

ECOLOGY: outer neritic (50 - 150 m)

Mf 8850 (Field number CP94-84B) Lower McIntosh Formation

Sample is barren of foraminifers; megafossil fragments are present.

Mf 8851 (Field Number CP94-85B) Upper McIntosh Formation

Sample is barren of microfossils.

Mf 8852 (Field number CP94-86C) Upper McIntosh Formation

Sample barren of foraminifers. Plant remains abundant.

Mf 8853 (Field number CP94-86D) Lower McIntosh Formation

Benthic foraminifers

Bathysiphon eocenicus Cushman and Hanna
Praeglobobulimina spp (siliceous molds)

Radiolarians

AGE: Tertiary

ECOLOGY: at least outer neritic, probably near shelf slope break (± 150 m)

Mf 8854 (Field number CP94-87B) Lower McIntosh Formation

Benthic foraminifers

Bathysiphon eocenicus Cushman and Hanna
Bulimina spp.
Gyroidina spp.
?Lenticulina inornata (d'Orbigny)
?Praeglobobulimina pupoides (d'Orbigny)
?Valvulineria jacksonensis welcomensis Mallory

Diatoms (pyritized)

Radiolarians

AGE: late Eocene, probably late Narizian Stage

ECOLOGY: outer neritic or deeper (>150 m)

COMMENTS: Specimens are either siliceous or pyrite molds; very little original shell material remains.

Mf 8855 (Field number CP94-90) Upper McIntosh Formation
Sample barren of foraminifers. Fish tooth present.

Mf 8856 (Field Number CP94-92) Upper McIntosh Formation
Sample is barren of microfossils.

Mf 8857 (Field number CP94-93) Upper McIntosh Formation
Benthic foraminifers

Bulimina spp.
? *Ceratobulimina* spp.
Cyclamina pacifica Beck
Lenticulina spp.
Globobulimina pacifica Cushman
? *Pyrulina* spp.

Radiolarians

Megafossil fragments

AGE: late Eocene

ECOLOGY: Indeterminate

COMMENTS: Specimens are either siliceous or pyrite molds; very little original shell material remains.

Mf 8858 (Field number CP94-94) Upper McIntosh Formation
Benthic foraminifers

Globobulimina pacifica Cushman
Nodosaria spp.

Molluscan shell fragments

? Echinoid spines

AGE: Tertiary

ECOLOGY: at least outer neritic, probably near shelf slope break (± 150 m)

Mf 8859 (Field Number CP94-95) Upper McIntosh Formation
Benthic foraminifers

? *Bulimina* spp.
? *Cibicides* spp.
? *Lenticulina* spp.
? *Valvulinaria* spp.

AGE: Indeterminate

COMMENTS: Sample contains fragments of foraminifers

Mf 8860 (Field number CP94-100b) Cowlitz Formation - unit 1
Benthic foraminifers

Bolivina spp.

Mf 8861 (Field number CP94-102) Cowlitz Formation - unit 1
Sample is barren of microfossils.

Mf8862 (Field Number CP94-109B) Cowlitz Formation - unit 1
Sample is barren of microfossils.

Mf 8863 (Field number CP94-110a) Cowlitz Formation - unit 1
Sample barren of foraminifers.

Mf8864 (Field number CP94-119) Cowlitz Formation - unit 2
Sample is barren of microfossils.

Mf8865 (Field number CP94-121) Cowlitz Formation - unit 2
Sample is barren of microfossils.

Mf8866 (Field number CP94-122) Cowlitz Formation - unit 2
Sample is barren of microfossils.

Mf 8867 (Field number CP94-123) Cowlitz Formation - unit 2
Sample is barren of foraminifers. Plant remains abundant.

Mf8868 (Field number CP94-127) Cowlitz Formation - unit 2
Sample is barren of foraminifers but contains ?fish debris and SPORBO-like objects which are probably fecal pellets.

Mf8869 (Field number CP94-129) Cowlitz Formation - unit 2
Sample is barren of foraminifers but contains megafossil shell fragments and SPORBO-like objects (fecal pellets?).

Mf8870 (Field number CP94-130) Cowlitz Formation - unit 2
Benthic foraminifers

Dentalina consobrina d'Orbigny

Elphidium californicum Cook

Nonionellina applini (Howe and Wallace)

Ostracods

Megafossil shell fragments

AGE: lower Tertiary

ECOLOGY: inner neritic (0-50 m)

Mf8871 (Field number CP95-158) Cowlitz Formation - unit 2
Benthic foraminifers

?*Cibicides* spp.

Elphidium californicum Cook

Quinqueloculina imperialis Hanna and Hanna

Diatoms (pyrite)
Radiolarians
Ostracods (fragments only)
Megafossil shell fragments
Fish debris

AGE: lower Tertiary, probably late Eocene
ECOLOGY: inner neritic depths (0-50 m)
COMMENTS: Shell material very weathered.

Mf8872 (Field number CP95-159) Cowlitz Formation - unit 2
Sample is barren of foraminifers but contains megafossil shell fragments and SPORBO-like objects (fecal pellets?).

Mf8873 (Field number CP95-161A) Cowlitz Formation - unit 2
Sample is barren of foraminifers but contains megafossil shell fragments.

Mf8874 (Field number CP95-168) Cowlitz Formation - unit 3
Sample is barren of microfossils.

Mf8875 (Field number CP95-170) Cowlitz Formation - unit 3
Sample is barren of foraminifers but contains megafossil shell fragments.

Mf8876 (Field number CP95-171) Cowlitz Formation - unit 3
Sample is barren of foraminifers but contains ostracod molds.

Mf8877 (Field number CP95-173) Cowlitz Formation - unit 4
Sample is barren of microfossils, but contains radiolarians (Spumellarians), ostracod fragments, megafossil shell fragments, and fish debris.

Mf8878 (Field number CP95-174) Cowlitz Formation - unit 4
Sample is barren of foraminifers but contains plant material.

Mf 8879 (Field number 94CP-178) Cowlitz Formation - unit 4
Sample is barren of foraminifers. Plant remains abundant.

Mf8880 (Field number CP94-179x) Cowlitz Formation - unit 5
Sample is barren of microfossils.

Mf 8881 (Field number 94CP-180) Cowlitz Formation - unit 5
Sample is barren of foraminifers. Plant remains abundant.

Mf8882 (Field number CP95-181A) Cowlitz Formation - unit 5
Sample is barren of microfossils.

Mf8883 (Field number CP95-181B1) Cowlitz Formation - unit 5
Sample is barren of microfossils.

Mf8884 (Field number CP95-181B2)
Sample is barren of microfossils.

Mf8885 (Field number CP95-185) Lincoln Creek Formation (valley fill)
Sample is barren of microfossils.

Mf8886 (Field number CP95-183a) valley fill
Sample is barren of foraminifers but contains tubes and a shell fragment. The latter fragment is probably recent.

Mf8887 (Field number CP95-185)
Sample is barren of microfossils.

Mf8888 (Field number CP95-186a) valley fill
Sample is barren of microfossils.

Mf8889 (Field number CP95-186x) Lincoln Creek Formation
Sample is barren of foraminifers.

Mf8901 (Field number CP-156 0₃) Cowlitz Formation - unit 2
Benthic foraminifers

Dentalina consobrina (d'Orbigny)
Elphidium californicum Cook
Lenticulina mornata (d'Orbigny)
Lenticulina spp.
Nonionellina applini (Howe and Wallace)

Diatoms (pyrite)

Ostracods

Megafossil shell fragments

Fish debris

AGE: lower Tertiary

ECOLOGY: inner neritic (0-50 m)

Mf88902 (field number CP-155 0₃) Cowlitz Formation - unit 2
Benthic foraminifers

Elphidium californicum Cook
Lenticulina spp.
Nonionellina applini (Howe and Wallace)

AGE: lower Tertiary

ECOLOGY: inner neritic (0-50 m)

SUMMARY: Benthic foraminifers are scarce in the Olequa and Stillwater Creek sections sampled by Payne. Foraminifers were found in the McIntosh Formation and in units 1 and 2 of the Cowlitz Formation and associated microfossils (Diatoms, Radiolarians, or ostracodes), megafossil fragments, or fish debris were found in the units 3 and 4 of the Cowlitz Formation and in the Lincoln Creek Formation (valley fill) attesting to the marine origin of these units. Although unit 5 of the Cowlitz Formation contained no benthic foraminifers or associated microfossil, there is no evidence to suggest either a marine or nonmarine origin of this unit.

The only age diagnostic assemblages occurred in the lower McIntosh Formation (Mf8849 and Mf8854) and suggest a late Eocene age. These assemblages are assigned to the late Narizian through earliest Refugian Stages based on the presence of *Cibicides elemaensis*, *C. natlandi*, and *Valvulineria jacksonensis welcomensis*. The late Narizian to early Refugian interval is coeval with calcareous nannoplankton zone CP15 (see attached timescale). Benthic foraminifers found in the overlying McIntosh and Cowlitz Formations are not age diagnostic, they are commonly found in the late Eocene and therefore also support the late Eocene age. Samples collected by McDougall in 1981 from the Olequa and Stillwater Creek sections stratigraphically above Mf8870 (Payne sample 130) and below sample Mf8871 (Payne sample 158A) in unit 2 of the Cowlitz Formation contain a moderately diverse benthic foraminiferal assemblage including *Caucasina schencki*, *Sigmomorphina schencki*, *Quinqueloculina imperialis*, *Valvulineria willapaensis*, and assorted cibicides, elphidium, and anomalininids. These species are diagnostic of the base of the late Eocene, Refugian Stage. Unfortunately analysis of the McDougall samples is not complete but the more diverse assemblages may provide additional age data.

Despite the sparse foraminiferal assemblages, a minimum water depth can be estimated for the McIntosh Formation and units 1 and 2 of the Cowlitz Formation. The McIntosh Formation was deposited at outer neritic to upper bathyal depths (>50 to 500 m); the increased abundance of *Globobulimina* and *Praeglobobulimina* in the upper member suggests this member was probably deposited near the shelf/slope break and probably at upper bathyal depths (150-500 m) while the lower member was deposited at outer neritic depths. Units 1 and 2 of the Cowlitz Formation were deposited at inner neritic depths (0 to 50 m) based on the presence of species of *Elphidium*, *Cibicides*, *Nonionellina*, and *Quinqueloculina*. The more diverse assemblages in unit 2 of the Cowlitz Formation sampled by McDougall contain *Anomalina garzaensis*, *Pullenia salisburyi* and *Valvulineria tumeyensis* which indicate deposition occurred at outer neritic (50-150 m) rather inner neritic depths. Minimum water depths can not be estimated for the other units of the Cowlitz Formation or in the Lincoln Creek Formation because of the absence of foraminifers.

APPENDIX II: MACROFAUNAL IDENTIFICATION

THE THOMAS BURKE MEMORIAL WASHINGTON STATE MUSEUM
BOX 353010, UNIVERSITY OF WASHINGTON, SEATTLE WA 98195-3010

GEOLOGY AND PALEONTOLOGY DIVISION

Identification of fossils from the Cowlitz, Lincoln Creek and McIntosh Formations.
submitted by Chuck Payne, Department of Geosciences, Oregon State University.

Pelecypods listed first. * indicated beginning of gastropods list. ^ indicates scaphopod

	Taxonomic names (from C.E. Weaver, 1943, with some modification)	Inferred environment of deposition
CP 94-39 Cowlitz Fm	<i>Tellina cowlitzensis</i> Weaver <i>Nuculana washingtonensis</i> (Weaver) ? <i>Macoma</i> sp. ? <i>Tivolina</i> sp. <i>Corbula dickersoni</i> Weaver & Palmer * <i>Siphonalia sopenahensis</i> (Weaver) <i>Calyptrea diagoana</i> (Conrad) <i>Diodora stillwaterensis</i> (Weaver and Palmer) <i>Turritella uvasana</i> ? <i>olequahensis</i> ^ <i>Dentalium stramineum</i> Gabb <i>barnacles</i>	All these are molds, but many are in very good shape. I'll look at them again, when I have time. many are typical of <i>Turritella</i> - <i>Tivolina</i> shallow marine assemblage of Nesbitt, 1995 (see pp 1064-5) - but with some hard-ground species
CP 94-50	? <i>Crassatellites</i> ? <i>Veneridcardia</i> * <i>Calyptrea diagoana</i> (Conrad)	very badly weathered, but shallow marine genera
CP 94-51	<i>Glycymeris saggittata</i> (Gabb) most common <i>Acutostrea idriaensis</i> Gabb 2 nd most common <i>Venericardia homii clarki</i> Weaver & Palmer * <i>Calyptrea diagoana</i> (Conrad) one specimen	very shallow sand-dwelling clams and embayment oysters washed together
CP 94-53	<i>Acutostrea idriaensis</i> Gabb <i>Glycymeris saggittata</i> (Gabb) <i>Venericardia homii clarki</i> W&P <i>Corbicula willisi</i> White relatively very few * <i>Turritella uvasana olequahensis</i> W&P	mostly as above (94-51) but with the addition of the few brackish water <i>Corbicula</i>
CP 94-58	<i>Acutostrea idriaensis</i> Gabb <i>Corbicula cowlitzensis</i> Weaver	brackish embayment
CP 94-75	crab and clam material, unidentifiable	
CP 94-86 McIntosh F	? <i>Tivolina</i> or ? <i>Macrocallister</i>	molds only, but shallow marine. Needs more material
CP 94-109 Cowlitz	<i>Corbicula</i> or <i>Tellina</i> sp. very poorly preserved ? <i>Macrocallister</i> * <i>Siphonalia sopenahensis</i> Weaver	Shallow marine and ? brackish mixed together - ? storm deposited

CP 94-110	<i>Corbicula olequahensis</i> Weaver $\pm 95\%$ of sample <i>Acutostrea idriaensis</i> Gabb very few * <i>Siphonalia sopenahensis</i> Weaver one specimen	largely brackish water clams + a few intertidal specimens, storm/flood deposit
CP 94-111	<i>Corbicula willisi</i> White	Brackish with lots of organic matter, probably plant debris
CP 94-114a	<i>Corbicula willisi</i> White <i>Acutostrea idriaensis</i> Gabb most common	Brackish bay with tidal incursions of marine water
CP 94-114b	? <i>Tivelina</i> sp.	No information
CP 94-121a	<i>Acutostrea idriaensis</i> Gabb most of the material <i>Glycymeris sagittata</i> Gabb 2 nd most abundant <i>Thracia dilleri</i> Dall <i>Gari</i> sp. <i>Venericardia hornii clarki</i> W&P -most <i>Pitar (Lamelliconcha) eocenica</i> W&P <i>Tellina cowlitzensis</i> Weaver * <i>Calyptraea diagoana</i> (Conrad) <i>Turritella uvasana olequahensis</i> only 3 specimens barnacles and bryozoa as epibionts ¹ on inside of two of the oyster shells	Typical of Turritella-Tivelina shallow marine assemblage of Nesbitt, 1995, see pp 1064-5
CP 94-121b	<i>Acutostrea idriaensis</i> Gabb most common <i>Venericardia hornii clarki</i> Weaver & Palmer 2 <i>Corbicula willisi</i> White <i>Pitar californiana</i> (Conrad) rare	Mixed shallow marine with brackish - probably storm
CP 94-124	<i>Venericardia hornii clarki</i> W&P <i>Pteria clarki</i> Weaver & Palmer <i>Tellina</i> sp. ? <i>Pachydesma aragoensis</i> common in the Coaledo and Skookumchuck, but not previous record from Cowlitz * <i>Siphonalia sopenahensis</i> Weaver <i>Whitneyella oregonensis</i> Turner - this species has only been recorded in the Umqua Fm. previously <i>Calyptraea diagoana</i> (Conrad) * <i>Cadulus Gabbi</i> Sharp and Pilsbury -	Typical of Turritella-Tivelina shallow marine assemblage of Nesbitt, 1995, see pp 1064-5
CP 94-126	? <i>Venericardia hornii clarki</i> Weaver & Palmer * <i>Turritella uvasana stewarti</i> Merriam	Very weathered, but looks like remnants of the above
CP 94-131	<i>Pteria clarki</i> W&P	v shallow marine

¹ Epibionts are animals that live on the shells of other animals - as this was inside the oyster was dead

CP-95-157	<i>Acanthocardia (Schedocardia) brewerti</i> Gabb this is now the correct name for this clam * <i>Turritella uvasana stewarti</i> Merriam crab claws	v. shallow marine
CP95-161b	? <i>Corbicula willisi</i> White	very poorly preserved
CP95-163c	<i>Corbicula willisi</i> White * <i>Eulima lewisiana</i> Weaver <i>Potamides fettkei</i> Weaver	typical of brackish water assemblages - bay muds
CP95-166a	<i>Pteridaria clarki</i> W&P * <i>Viviparus washingtonianus</i> Arnold & Hannibal	mixed - freshwater snail with shallow marine clam
CP 95-166c	<i>Corbicula willisi</i> White	brackish bay muds
CP 95-170	Unionid clam * <i>Viviparus washingtonianus</i> Arnold & Hannibal	freshwater
CP95-189b	<i>Venericardia hornii clarki</i> Weaver & Palmer <i>Acutostrea idriaensis</i> Gabb <i>Septifer dichotomus</i> Gabb <i>Crassatellites washingtoniana</i> Weaver ? <i>Mytilus</i> <i>Nuculana washingtonensis</i> Weaver <i>Corbula dickersoni</i> W&P * <i>Turritella uvasana olequahensis</i> W&P <i>Siphonalia sopenahensis</i> (Weaver) <i>Polinices weaveri</i> (Dickerson) <i>Natica (Tectonatica) weaveri</i> Tegland <i>Colwellia brezzi</i> (Weaver) <i>Olivella mathewsoni</i> Gabb <i>Turricula cowhitzensis</i> (Weaver) <i>Gemmula fasteni</i> W&P <i>Mitra washingtoniana</i> Weaver	typical of <i>Turritella-Tivellina</i> assemblage of Nesbitt 1995 However most of these are micromollusks that I collected from dry sieving the sediment I'd like more!
CP95-177	<i>Pitar eocenica</i> W&P <i>Venericardia hornii clarki</i> Weaver & Palmer * <i>Turritella uvasana olequahensis</i> W&P <i>Calyptraea diagoana</i> (Conrad) <i>Polinices nuciformis</i> Gabb crab claw segments	v. shallow marine. part of <i>Turritella-Tivellina</i> assemblage of Nesbitt 1995
CP95-188a Lincoln Ck	<i>Crassatellites stillwaterensis</i> W&P	shallow marine
CP95-199a	<i>Tellina cowhitzensis</i> Weaver ? <i>Spisula</i> sp	clams are shallow marine but there is a leaf
CP95-202 McIntosh	all clam molds that may be <i>Corbicula</i>	brackish

APPENDIX IV: TUFF GEOCHEMISTRY

Sample no.	PHA 95407	PHA 95408	PHA 95406A	PHA 95404	PHA 95405	PHA 95399	PHA 95390	PHA 95391	PHA 95393	PHA 95396	PHA 95395
Lab no.	PHA 95407	PHA 95408	PHA 95406A	PHA 95404	PHA 95405	PHA 95399	PHA 95390	PHA 95391	PHA 95393	PHA 95396	PHA 95395
Analysis	WSU 1295	WSU 1295	WSU 1295	WSU 1295	WSU 1295	WSU 1295	WSU 1295	WSU 1295	WSU 1295	WSU 0696	WSU 1295
Batch						=91004-005					
Field no.	CP 94-111a	CP 94-111b	CP 94-113	CP 94-114a	CP 94-114b	CP 95-163b	CP 95-164t2	CP 95-164t4	CP 95-164t6	CP 95-164t8a	CP 95-164t8b
Lithology	tf	tf	m tf	lth lap tf	lth lap tf	pm lap tf	gry lth lap tf	clt pm lap tf	yel-grt tf	clt pm lap tf	pm lap tf
Source/tk, cm	oc/7	oc/7	oc/3	oc/100	oc/350	oc/150	oc/5	oc/6	oc/4	oc/5	oc/5
Strat position	mid Cowlitz	mid Cowlitz	mid Cowlitz	mid Cowlitz?	mid Cowlitz?	up Cowlitz	up Cowlitz	up Cowlitz	up Cowlitz	upper Cowlitz	up Cowlitz
Section/Well	in 11.6-m coal	in 11.6-m coal	bd				in 7.6-m coal b	in 7.6-m coal b	in 7.6-m coal b	in 7.6-m coal b	in 7.6-m coal b
1/4, 1/4, 1/4	Stillwater Cr	Stillwater Cr	Stillwater Cr	Stillwater Cr	Stillwater Cr	Olequa Cr	Olequa Cr	Olequa Cr	Olequa Cr	Olequa Cr	Olequa Cr
STR	NENWNE	NENWNE	NENWNE	NENWNE	NENWNE	NENWNE	NENWNE	NENWNE	NENWNE	NENWNE	NENWNE
7.5' quad	25-11N-3W	25-11N-3W	25-11N-3W	25-11N-3W	25-11N-3W	29-11N-2W	20-11N-2W	20-11N-2W	20-11N-2W	20-11N-2W	20-11N-2W
Lat N	46o24'58"	46o24'58"	46o24'59"	46o24'59"	46o24'59"	46o24'57"	46o25'30.5"	46o25'30.5"	46o25'30.5"	46o25'30.5"	46o25'30.5"
Long W	122o59'45.5"	122o59'45.5"	122o59'32"	122o59'27"	122o59'27"	122o57'55.5"	122o58'06"	122o58'06"	122o58'06"	122o58'06"	122o58'06"
Kelly/elev/ft	-135	-135	-135	-135	-135	-130	-150	-150	-150	-150	-150
Sample dep/ft	---	---	---	---	---	---	---	---	---	---	---
Major Elements (XRF, analyzed values, weight%)											
SiO2	69.01	61.87	59.12	65.57	62.74	58.37	52.46	54.51	53.45	55.98	55.92
Al2O3	15.53	18.91	19.51	12.71	14.94	14.81	20.34	17.72	19.06	18.13	17.65
TiO2	0.244	2.320	1.132	2.934	3.356	2.086	4.749	4.395	5.195	1.021	0.663
FeTO3	na	na	na	na	na	na	na	na	na	na	na
MnO	0.049	0.028	0.012	0.012	0.033	0.148	0.015	0.041	0.010	0.026	0.016
CaO	1.12	3.02	2.36	0.96	2.75	4.91	4.55	2.15	3.17	2.72	2.51
MgO	0.30	1.57	2.57	1.42	1.48	2.24	1.54	2.15	1.89	2.04	2.11
K2O	2.01	0.93	0.16	0.53	0.47	1.20	0.21	0.20	0.25	0.14	0.06
Na2O	4.14	2.74	0.88	0.43	0.79	2.81	1.55	0.35	1.01	0.69	0.42
P2O5	0.030	0.466	0.106	0.094	0.181	0.414	0.436	0.187	0.382	0.139	0.099
LOI @ 925C	nd	nd	nd	nd	nd	nd	nd	nd	nd	nd	nd
Total											
FeO*	2.20	2.23	3.96	5.09	5.97	7.39	4.34	5.32	4.47	6.63	6.65
Total w/o LOI	94.63	94.08	89.81	89.75	92.71	94.38	90.19	87.02	88.89	87.52	86.10
Major Elements (XRF, normalized values, weight%)											
SiO2	72.92	65.76	65.83	73.06	67.67	61.85	58.17	62.64	60.13	63.97	64.95
Al2O3	16.41	20.10	121.72	14.16	16.11	15.69	122.55	20.36	121.44	20.72	20.50
TiO2	0.258	2.466	1.260	13.27	13.62	2.210	15.27	15.05	15.84	1.167	0.770
FeO*	2.32	2.37	4.41	5.67	6.44	7.83	4.81	6.11	5.03	7.58	7.72
MnO	0.052	0.030	0.013	0.013	0.036	0.157	0.017	0.047	0.011	0.030	0.019
CaO	1.18	3.21	2.63	1.07	2.97	5.20	5.04	2.47	3.57	3.11	2.92
MgO	0.32	1.67	2.86	1.58	1.60	2.37	1.71	2.47	2.13	2.33	2.45
K2O	2.12	0.99	0.18	0.59	0.51	1.27	0.23	0.23	0.28	0.16	0.07
Na2O	4.37	2.91	0.98	0.48	0.85	2.98	1.72	0.40	1.14	0.79	0.49
P2O5	0.032	0.495	0.118	0.105	0.195	0.439	0.483	0.215	0.430	0.159	0.115
Total	100.00	100.00	100.00	100.00	100.00	100.00	100.00	100.00	100.00	100.00	100.00
Trace Elements (XRF, ppm)											
Ni	16	9	11	8	7	13	129	78	36	115	34
Cr	6	16	11	50	64	15	1052	122	28	3	0
Sc	2	9	16	17	18	19	37	21	22	11	3
V	0	92	26	239	291	141	413	323	307	44	28
Ba	730	457	61	284	338	581	349	242	376	109	44
Rb	89	19	4	41	29	39	3	8	8	4	3
Sr	112	718	146	118	323	371	404	150	334	174	152
Zr	1613	398	317	259	265	529	165	303	310	1785	1885
Y	188	41	25	10	12	152	158	30	181	146	42
Nb	1115	1102	29.2	151	155	195	160	175	196	191	1102
Ga	138	134	26	22	27	27	132	132	133	140	134
Cu	10	12	37	72	103	15	1239	75	71	11	5
Zn	1134	93	59	42	44	1144	1219	1217	1236	1168	1173
Pb	7	2	9	1	1	4	0	4	6	3	6
Li	---	---	---	---	---	---	---	---	---	141	---
Ce	---	---	---	---	---	---	---	---	---	230	---
Th	13	10	9	5	3	10	6	7	8	16	17
K2O+Na2O (bot)	6.50	3.90	1.16	1.07	1.36	4.25	1.95	0.63	1.42	0.95	0.56
Zr/Y (bottom)	6.97	9.71	12.68	25.90	22.08	10.17	2.84	10.10	3.83	17.07	21.07
Zr/Nb (bottom)	5.35	3.91	10.86	5.09	4.80	5.55	2.77	4.04	3.23	8.59	8.67

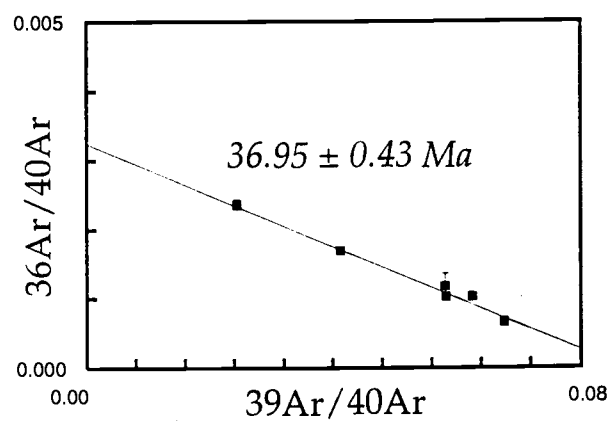
Sample no.	PHA 95394	PHA 95398	PHA 95397	PHA 95416	PHA 95417	PHA 95415	PHA 95389	PHA 95388	PHA 95387	PHA 95386	PHA 95383
Lab no.	PHA 95394	PHA 95398	PHA 95397	PHA 95416	PHA 95417	PHA 95415	PHA 95389	PHA 95388	PHA 95387	PHA 95386	PHA 95383
Analysis	WSU 0696	WSU 1295	WSU 1295	WSU 0696	WSU 0696	WSU 0696	WSU 1295	WSU 1295	WSU 1295	WSU 1295	WSU 1295
Batch	CP 95-16410	CP 95-16410	CP 95-16410	CP 94-69bA1	CP 94-69bA2	CP 94-69bB	CP 95-183b	CP 95-186x1	CP 95-186x2	CP 95-186x3	CP 95-148
Lithology	clt pm lap tf	blu-wh lith lap	brn-bk th lap	pale brn cly tf	pale red cly tf	yel-brn lap tf	hb lap-tf	tf w/ twigs	pale ol tf	lt gry tf	sty tf
Source/tk, cm	oc/7	oc/150	oc/150	oc/7	oc/7	oc/7	oc/74	oc/60	oc/150	oc/50-150	oc/7
Strat position	upper Cowitz	up Cowitz	up Cowitz	?up Cowitz	?up Cowitz	?up Cowitz	lo "Tautle" Fm	up "Tautle" Fm	up "Tautle" Fm	up "Tautle" Fm	lo Lincoln Cr
Section/Well	in 7.6-m coal bd	in 7.6-m coal bd	in 7.6-m coal bd	?	?	?	Olequa Cr	Olequa Cr	Olequa Cr	Olequa Cr	Olequa Cr
1/4, 1/4, 1/4	NWSWNW	NWSWNW	NWSWNW				NESENE	SWSWSW	SWSWSW	SWSWSW	NWNENE
STR	20-11N-2W	20-11N-2W	20-11N-2W	Winlock	Winlock	Winlock	5-11N-2W	37-12N-2W	37-12N-2W	37-12N-2W	33-12N-2W
7.5' quad	Winlock	Winlock	Winlock	Winlock	Winlock	Winlock	Winlock	Winlock	Winlock	Winlock	Winlock
Lat N	46o25'30.5"	46o25'30.5"	46o25'30.5"				46o28'08"	46o28'25.5"	46o28'25.5"	46o28'25.5"	46o29'05.5"
Long W	122o58'06"	122o58'06"	122o58'06"				122o57'13"	122o56'58"	122o56'58"	122o56'58"	122o56'28"
Kelly/elev/ft	-150	-150	-150				-230	-235	-235	-235	-270
Sample dep/ft											
Major Elements (XRF, analyzed values, weight%)											
SiO2	56.35	17.39	53.16	55.13	57.35	50.70	48.85	54.11	53.14	54.84	58.58
Al2O3	18.34	6.11	18.82	23.17	18.50	18.60	21.48	20.66	17.96	18.28	16.75
TiO2	1.622	1.678	4.452	2.759	2.006	1.183	1.930	1.980	1.482	1.832	1.746
Fe2O3	na	na	na	na	na	na	na	na	na	na	na
MnO	0.017	2.187	0.030	0.019	0.004	0.053	0.048	0.007	0.005	0.011	0.032
CaO	2.65	43.05	3.44	1.27	1.74	1.65	6.32	2.04	2.81	3.37	2.64
MgO	1.98	0.78	1.74	1.13	1.27	2.67	2.46	1.51	2.85	2.55	0.74
K2O	0.19	0.07	0.43	1.28	1.78	0.11	1.28	0.64	0.23	0.45	0.78
Na2O	0.93	0.07	1.17	0.50	0.53	0.32	2.80	1.10	1.10	1.22	1.62
P2O5	0.192	0.488	0.225	0.083	0.062	0.119	0.177	0.200	0.541	0.179	0.137
LOI @ 925C	nd	nd	nd	nd	nd	nd	nd	nd	nd	nd	nd
Total											
FeO*	6.21	3.34	5.78	3.40	3.59	11.25	5.47	5.99	9.38	7.37	3.92
Total w/o LOI	88.48	75.16	89.25	88.74	86.83	86.66	90.82	88.24	89.50	90.10	86.95
Major Elements (XRF, normalized values, weight%)											
SiO2	63.69	23.14	59.57	62.12	66.05	58.51	53.79	61.32	59.38	60.86	67.38
Al2O3	20.73	8.13	21.09	126.11	121.31	121.46	123.65	123.41	20.07	20.29	19.27
TiO2	1.833	2.232	14.99	13.11	2.310	1.365	2.125	2.244	1.656	2.033	2.008
FeO*	7.02	4.44	6.48	3.83	4.13	12.98	6.02	6.79	10.48	8.18	4.51
MnO	0.019	12.91	0.034	0.021	0.005	0.061	0.053	0.008	0.006	0.012	0.037
CaO	2.99	157.28	3.85	1.43	2.00	1.90	6.96	2.31	3.14	3.74	3.04
MgO	2.24	1.04	1.95	1.27	1.46	3.08	2.71	1.71	3.18	2.83	0.85
K2O	0.21	0.09	0.48	1.44	2.05	0.13	1.41	0.73	0.26	0.50	0.90
Na2O	1.05	0.09	1.31	0.56	0.61	0.37	3.08	1.25	1.23	1.35	1.86
P2O5	0.217	10.65	0.252	0.094	0.071	0.137	0.195	0.227	10.60	0.199	0.158
Total	100.00	100.00	100.00	100.00	100.00	100.00	100.00	100.00	100.00	100.00	100.00
Trace Elements (XRF, ppm)											
Ni	29	8	95	28	35	47	47	11	0	4	14
Cr	3	34	119	74	134	9	123	15	20	22	23
Sc	12	156	24	17	22	12	26	26	18	16	22
V	91	127	395	1748	11184	92	308	159	143	176	175
Ba	185	52	428	12499	14344	289	679	254	223	252	311
Rb	4	3	13	53	93	5	20	14	5	10	40
Sr	203	137	307	673	11088	150	473	258	250	347	263
Zr	1692	136	306	519	394	1853	180	366	323	289	254
Y	147	30	38	158	1207	34	21	147	172	162	150
Nb	1133	25.2	164	1118	155	1119	13.6	33.4	23.6	21.4	22.7
Ga	136	12	134	148	159	138	26	128	24	24	24
Cu	13	32	115	52	1155	11	92	108	49	80	76
Zn	1184	64	1189	88	88	1216	107	1250	104	1129	81
Pb	4	0	2	11	13	2	2	3	4	3	3
La	125	---	---	59	133	101	---	---	---	---	---
Ce	182	---	---	362	186	97	---	---	---	---	---
Th	11	2	4	12	10	13	4	10	4	6	6
K2O+Na2O (bot)	1.27	0.19	1.79	2.01	2.66	0.50	4.49	1.97	1.49	1.85	2.76
Zr/Y (bottom)	14.72	4.53	8.05	8.95	1.90	25.09	8.57	7.79	4.49	4.66	5.08
Zr/Nb (bottom)	5.20	5.40	4.80	4.42	7.22	7.17	13.24	10.96	13.69	13.50	11.19

APPENDIX V: GRAYS RIVER GEOCHEMISTRY

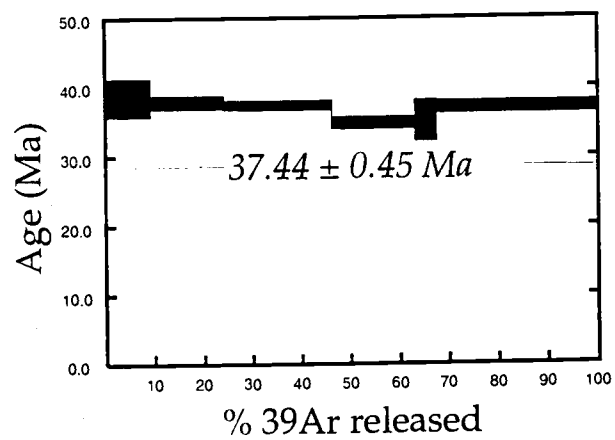
petrology sample #	°K/Ar 37 Ma	CP-94-145	CP-94-142	CP-94-143	CP-94-144	CP-94-4	CP-94-7L
USGS sample #	93CR-F01	93CR-F02	93CR-F46	93CR-F47	93CR-F48	93CR-F50	93CR-F51
<i>Major Elements (normalized values, weight%)</i>							
SiO ₂	49.64	50.02	49.64	49.71	49.99	49.56	48.69
TiO ₂	3.89	3.39	3.79	3.39	3.36	3.6	3.08
Al ₂ O ₃	14.07	14.77	14.17	14.06	14.18	13.82	13.23
FeO*	13.41	12.75	13.52	13.22	12.93	13.76	13.09
MnO	0.24	0.2	0.2	0.19	0.19	0.19	0.21
MgO	4.59	4.71	4.71	5.16	4.95	5.75	6.94
CaO	9.8	9.77	9.77	9.83	9.9	9.01	10.75
Na ₂ O	3.21	3.08	3.08	3.1	3.11	2.98	2.67
K ₂ O	0.63	0.66	0.66	0.62	0.67	0.79	0.75
P ₂ O ₅	0.51	0.64	0.64	0.71	0.71	0.52	0.59
Total	100	100	100	100	100	100	100
FeO*/MgO	2.92	2.71	2.86	2.56	2.61	2.39	1.89
Na ₂ O+K ₂ O	3.84	3.74	4.16	3.72	3.79	3.77	3.42
<i>Trace Elements (ppm)</i>							
Rb	11	<10	18	<10	15	17	<10
Ba	210	186	178	180	184	166	174
Nb	42	37	37	40	36	36	43
Sr	455	465	475	470	475	435	410
Zr	265	260	265	240	250	250	240
Y	33	37	32	33	38	30	31
Ni	28	25	40	35	46	45	124
Cr	28	50	50	50	53	52	196
V	320	280	320	290	290	310	300
Cu	30	47	24	55	53	43	89
Zn	92	86	86	94	93	91	96
Rb/Sr	0.024		0.038		0.032	0.039	
Ba/Nb	5	5	4.8	4.5	5.2	4.6	4
Zr/Nb	6.3	7	7.2	6	6.9	6.9	5.6
Y/Nb	0.79	1	0.86	0.83	1.06	0.83	0.72
Zr/Y	8	7	8.3	7.3	6.6	8.3	7.7
Ti/V	73	72.6	71	70.1	69.4	69.7	61.6
Ba/Zr	0.79	0.72	0.67	0.75	0.74	0.66	0.73
*Fe total							0.8

APPENDIX VI: $^{39}\text{Ar}/^{40}\text{Ar}$ AGE DATES

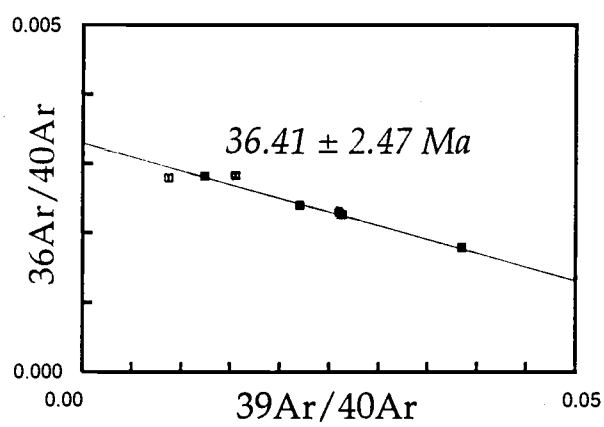
CP94-68du Coast Range basalt



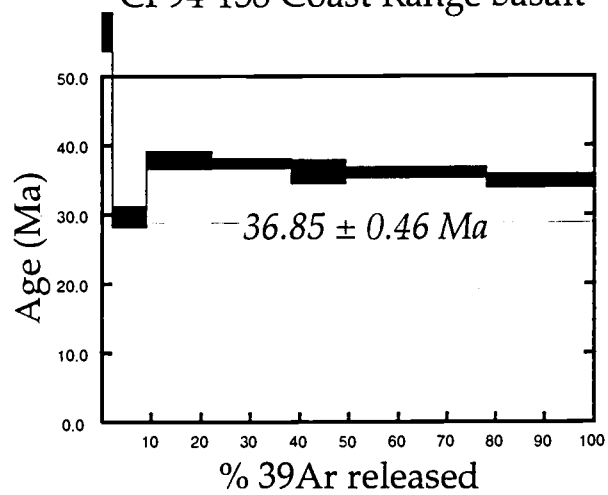
CP94-68du Coast Range basalt



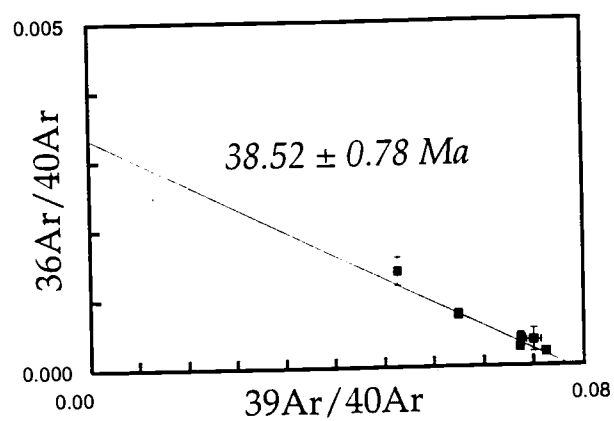
CP94-138 Coast Range basalt



CP94-138 Coast Range basalt



CP95-196 Coast Range basalt



CP95-196 Coast Range basalt

